STUDIES OF $GABA_A$ RECEPTOR SUBUNIT PROCESSING AND ASSEMBLY

By

Miriam Jane Smith

A Thesis Submitted for the Degree of Doctor of Philosophy of the University of London

Department of Biological and Pharmaceutical Chemistry

School of Pharmacy

University of London

29-39 Brunswick Square

London

WC1N 1AX

June 2004

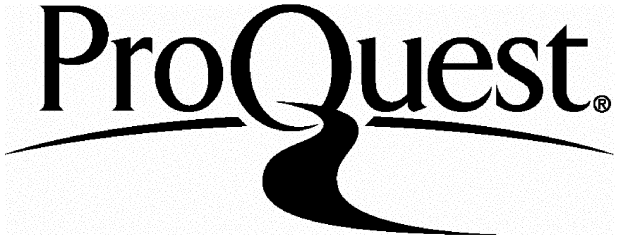

ABSTRACT

γ-Aminobutyric acid type A ($GABA_A$) receptors are the most abundant inhibitory neurotransmitter receptors in the mammalian central nervous system. They are ligand-gated chloride ion channels. Each receptor is composed from 5 of the 16 known subunits α1-6, β1-3, γ1-3, δ, π, θ and ε. Each subunit type confers different properties to the fully assembled receptor, leading to a diverse range of possible receptor subtypes. However, very few of the theoretically possible subtypes are actually observed *in vivo*. Here, a series of studies has been undertaken, using the yeast two-hybrid system, to investigate various aspects of $GABA_A$ receptor assembly and trafficking, to understand the molecular basis of the observed receptor diversity. Firstly, since $GABA_A$ receptor N-terminal domains have been implicated in subunit associations, α1 and β2 subunit N-termini were studied to identify assembly motifs, using 3 different yeast two-hybrid systems, the GAL4, modified LexA and CytoTrap® systems. Secondly, trafficking of receptors and the development and stabilisation of GABAergic synapses were investigated by screening a rat brain cDNA library using the $GABA_A$ receptor β3 subunit intracellular loop (β3-IL) and β2 N-terminal domain, respectively, to identify novel interacting proteins. The β2 N-terminus was found to interact with a DnaJ-domain-containing sequence, TID1L. Thirdly, receptor trafficking was investigated by further characterisation of the previously identified novel protein, $GABA_A$ receptor interacting factor (GRIF-1). The binding specificity of GRIF-1 with the $GABA_A$ receptor β2-IL was analysed. Structural and functional similarities between GRIF-1 and other members of the novel coiled-coil domain-containing gene family of proteins were investigated. GRIF-1 and a human homologue, KIAA1042, were compared for interactions with the $GABA_A$ receptor β2-IL and with kinesin heavy chain (KHC), KIF5C, as a KHC has been shown to associate with Milton, the *Drosophila melanogaster* orthologue of GRIF-1. Despite the high degree of amino acid homology between GRIF-1 and KIAA1042, only GRIF-1 was found to bind to the $GABA_A$ receptor β2-IL and to KIF5C, suggesting that the subtle differences between GRIF-1 and KIAA1042 lead to differences in functional specificity.

CONTENTS

Chapter 1: Introduction

Chapter 2: Materials and Methods

Chapter 3: Results 1

Chapter 4: Results 2

Chapter 5: Results 3

Chapter 6: General Discussion

List of Figures

List of Tables

ABBREVIATIONS

ACh	Acetylcholine
AChBP	Acetylcholine binding protein
AD	Activation domain
Ade	Adenine
ADH	Antidiuretic hormone
AMPA	α-Amino-3-hydroxy-5-methyl-isoxazole-4-propionic acid
Amp^R	Ampicillin resistance
APS	Ammonium persulphate
ATP	Adenosine triphosphate
BD	Binding domain
Bgt	Bungarotoxin
BiP	Immunoglobulin heavy chain binding protein
bp	Base pairs
CaMKII	Ca^{2+}-calmodulin type 2 dependent protein kinase
Cam^R	Chloramphenicol resistance
β-CCM	Methyl β-carboline-3-carboxylate
cDNA	Complementary deoxyribonucleic acid
CNS	Central nervous system
D1, 5	Dopamine receptor types 1 and 5
DMF	Dimethylformamide
DMSO	Dimethyl sulphoxide
DNA	Deoxyribonucleic acid
DNA-BD	DNA-binding domain
dNTPs	Deoxyribonucleotide triphosphates
ds	Double stranded
DTT	Dithiothreitol
EDTA	Ethylenediaminetetraacetic acid
ER	Endoplasmic reticulum
g	Gram
γ2L	γ2 Subunit long form
γ2S	γ2 Subunit short form

GABA	γ-Amino butyric acid
$GABA_{A, B, C}$	γ-Amino butyric acid receptor types A, B and C
GABARAP	GABA receptor associated protein
GAD	Glutamic acid decarboxylase
GAT	GABA transporters
GEF	GDP/GTP exchange factor
GluR	Glutamate receptor subunit type
GRIF-1	GABA receptor interacting factor 1
GRIP	Glutamate receptor interacting protein
GST	Glutathione-S-transferase
GTAP	$GABA_A$ receptor-tubulin complex-associated protein
h	Hour
HAP	Huntingtin-associated protein
HEK 293	Human embryonic kidney 293 cells
$5\text{-}HT_3$	5-Hydroxytryptophan type 3
IL	Intracellular loop
IPTG	Isopropyl-β-D-thiogalactopyranoside
Kan^R	Kanamycin resistance
KCC1	K^+/Cl^- co-transporter 1
KCC2	K^+/Cl^- co-transporter 2
KIF5A, B, C	Kinesin heavy chain protein types A, B and C
LB	Luria-Bertani
LGIC	Ligand-gated ion channel
M	Membrane
min	Minute
MOPS	3-N-morpholino propane-sulphonic acid
mRNA	Messenger ribonucleic acid
nACh	Nicotinic acetylcholine
NF-L	Neuronal intermediate filament subunit
NLS	Nuclear localisation signal
NMDA	N-methyl-D-aspartate
NR1	NMDA receptor subunit type 1
NR2	NMDA receptor subunit type 2
NSF	N-ethylmaleimide-sensitive fusion protein

OD	Optical density
OGT	β-O-linked N-acetylglucosamine transferase
PCR	Polymerase chain reaction
PDI	Protein disulphide isomerase
PDZ	PSD-95/Discs large/zonula occludens-1
PEG	Polyethylene glycol
P2X	Adenosine tri-phosphate (ATP)-gated receptors
PICK	Protein interacting with C Kinase
PKA	Protein kinase A
PKC	Protein kinase C
PMSF	Phenylmethylsulphonylfluoride
PSD	Post-synaptic density
^{1}SAP	Shrimp alkaline phosphate
^{2}SAP	Synapse associated protein
SCAM	Substituted cysteine accessibility method
SD	Selection dropout
SDS	Sodium dodecyl sulphate
SDS-PAGE	Sodium dodecyl sulphate-polyacrylamide gel electrophoresis
SMART	Simple Modular Architecture Research Tool
ss	Single stranded
TBE	Tris-buffered EDTA
TBPS	t-Butylbicyclophosphorothionate
TM	Transmembrane
UV	Ultra violet
v/v	volume/volume
w/v	weight/volume
X-GAL	5-Bromo-4-chloro-3-indolyl-β-D-galactopyranoside
X-α-GAL	5-Bromo-4-chloro-3-indolyl-α -D-galactopyranoside
YPAD	Yeast peptone adenine dextrose

ACKNOWLEDGEMENTS

Firstly, I would like to thank my supervisor, Professor Anne Stephenson, for giving me the opportunity to work in her lab and for all her help and support throughout my PhD.

Many thanks go to Dr Mike Beck for his invaluable supervision during my first year and for teaching me how to use the yeast two-hybrid system. I would also like to thank Dr Kieran Brickley for his help, especially for mammalian cell transfections and for preparation of the in-house antibodies.

Thank you to everyone else I've worked with in lab 437, Michalis Papadakis, Gurmail Ojla, Dr Lynda Hawkins, Karine Pozo and Sarah Cousins, for their advice and encouragement.

Finally, I acknowledge Vernalis for my PhD studentship grant.

CHAPTER 1: INTRODUCTION

1.1. THE LIGAND-GATED ION CHANNEL FAMILY OF NEUROTRANSMITTER RECEPTORS

The ligand-gated ion channels (LGICs) include three main superfamilies of proteins, grouped according to their evolutionary history (Le Novere and Changeux, 1999). These families are:

(i) the cationic, excitatory glutamate receptors, including N-methyl D-aspartate (NMDA), α-amino-3-hydroxy-5-methyl-isoxazole-4-propionic acid (AMPA) and kainate receptors.

(ii) the adenosine tri-phosphate (ATP)-gated receptors, which include the P2X receptors.

(iii) the nicotinic acetylcholine (nACh) receptor superfamily, which includes the excitatory nACh and 5-hydroxytryptophan type 3 (5-HT_3), and the inhibitory γ-aminobutyric acid (GABA) and glycine neurotransmitter receptors.

This thesis focuses on the nACh receptor family and in particular on the $GABA_A$ receptors. Members of the nACh receptor superfamily all share a common ancestral protein and significant amino acid sequence homology. Figure 1.1 is a diagram of an evolutionary tree showing the diversity of the nACh receptor family of proteins. Analyses of the DNA and amino acid sequences of the nACh receptor superfamily suggest that the common ancestor diverged early on into cationic and anionic receptors, the most ancient subtypes being the 5-HT_3 receptor subunits and GABA type A ($GABA_A$) receptor δ subunits (Ortells and Lunt, 1995). The cationic receptors then diverged to form the 5-HT_3 and nACh receptors, while the anionic receptors formed the GABA and glycine receptors. The close evolutionary relationship between these receptors is shown by their structural similarity and allows structural and functional information deduced from one receptor type to be applied to studies on other members of the superfamily. The muscle type nACh receptors, found at the neuromuscular junction, are the first and best characterised of the ligand-gated ion channels and are commonly used as a model for the study of other members of this superfamily.

1.1.1. THE NICOTINIC ACETYLCHOLINE RECEPTORS AS A MODEL FOR LGIC STRUCTURAL AND FUNCTIONAL STUDIES

The electric organ of *Torpedo* electric rays contains a high concentration of nACh receptors. The isolation of these receptors from *Torpedo*, through the use of α-

neurotoxin binding, has provided a source of protein in large enough quantities to allow investigation of their structure and function (Changeux *et al.*, 1970). The nACh receptors were the first LGIC receptors to be cloned and sequenced. The cDNA and protein sequences for all subunits have been compiled into an LGIC database (Le Novere and Changeux, 1999) which can be found online at http://www.pasteur.fr/units/neubiomol/LGIC.html. The nACh receptors are pentameric proteins, as determined by electron microscopy (Kistler and Stroud, 1981; Brisson and Unwin, 1985). Each subunit contains a large extracellular N-terminal domain that includes a disulphide bonded loop, four membrane spanning domains, a large intracellular loop between transmembrane (TM) domains 3 and 4 that contains regulatory sites, e.g. phosphorylation sites, and a short extracellular C-terminal domain. Muscle-type nACh receptors are composed of α, β, γ (or ε) and δ subunits. Each receptor is composed of 2α, 1β, 1δ and either a γ (embryonic) or an ε (adult) subunit. These subunits are arranged in a quasi-symmetrical pentamer around a central cationic pore. Figure 1.2 is a diagram showing the general topology of a typical nACh receptor subunit and the arrangement of subunits in a receptor. When activated by ligand binding, the channel conformation is altered to an 'open' state, which is permeable to Na^+ and K^+ ions. This allows a net influx of Na^+ ions and a net efflux of K^+ ions, giving rise to an overall depolarisation of the post-synaptic cell and transmission of an electrical signal through the neurone.

Nicotinic ACh receptor channels play an important role in the control of voluntary movement by providing a link between motor neurones and skeletal muscle. They are activated by binding of the endogenous neurotransmitter, ACh, at two ACh binding sites which are found at the α-γ and α-δ subunit interfaces. Simultaneous binding of ACh at both sites is necessary for channel opening. Residues involved in ligand binding have been identified at both sites, using photo-affinity methods (reviewed by Corringer *et al.*, 2000). For the α subunit, residues W86 and Y93, W149 and Y151, Y190, C192, C193 and Y198 were found to be involved in agonist binding (Middleton and Cohen, 1991; Chiara *et al.*, 2003). For the γ/δ subunits, homologous residues for each subunit have been identified corresponding to the γ subunit domains 55-59, 109-119 and 161-180 (reviewed by Corringer *et al.*, 2000; Karlin, 2002). The distribution of amino acids involved in agonist binding suggested that 6 distinct interacting domains, 3 from each subunit, are brought together to form a binding pocket. Further resolution of the

structure of nACh receptors was aided greatly by the discovery of an ACh binding protein that is homologous to the extracellular N-termini of nACh receptor subunits (Brejc *et al.*, 2001; Smit *et al.*, 2001).

1.1.2. THE NICOTINIC ACETYLCHOLINE BINDING PROTEIN

The acetylcholine binding protein (AChBP), released from glia in the CNS of *Lymnea Stagnalis* molluscs, was identified as a novel protein that inhibits neurotransmission by sequestering ACh at the synaptic cleft (Smit *et al.*, 2001). The crystal structure of the AChBP was also determined (Brejc *et al.*, 2001) showing it to be a homopentamer formed from subunits that are each 210 amino acids in length and lack transmembrane and intracellular domains. The deduced structure of the AChBP is shown in Figure 1.3. Each AChBP subunit contains an α-helix followed by two 3_{10} helices and ten β-strands which are folded into an immunoglobulin-like sandwich topology (Brejc *et al.*, 2001). The overall structure of the AChBP is equivalent to the extracellular N-terminal domains of the nicotinic acetylcholine receptor superfamily of proteins, sharing ~20% amino acid identity with the nAChR subunits. Since its discovery, the AChBP has been used as a molecular model for nAChRs and other members of the nAChR family of receptors to elucidate their structure and function.

Each AChBP monomer forms two contact interfaces with neighbouring subunits, one on either side. The crystal structure produced by Brejc *et al.* (2001) showed the positions of amino acids found at these interfaces on an AChBP subunit. These residues are not well conserved across the nAChR subunits and native nACh receptors contain non-identical subunits, however, at homologous positions on the nAChR α subunit, residues 16, 18, 20, 47, 89, 97, 98, 99, 127, 128, 129, 150, 151, 152, 155, 191 are shown to be present at the first, '+', interface and the residues 4, 5, 8, 9, 39, 41, 55, 79, 81, 101, 103, 104, 105, 107, 119, 123, 168, 169, 173 and 175 are found at the second, '-', interface (Brejc *et al.*, 2001; reviewed by Karlin, 2002).

1.2. THE GABA RECEPTORS

1.2.1. γ-AMINOBUTYRIC ACID

γ-Aminobutyric acid (GABA) was first isolated from brain in 1950 by paper chromatography (Awapara *et al.*, 1950; Roberts and Frankel, 1950; Udenfriend, 1950). It was shown to be a major fraction of the total amino acids in brain. Later, a previously unidentified extract, known as factor I, with an inhibitory effect in crayfish stretch receptor neurones was identified as GABA, thus demonstrating the role of GABA as an inhibitory transmitter (Bazemore *et al.*, 1957). GABA is now known to be the most abundant inhibitory neurotransmitter in the adult mammalian central nervous system (CNS), being present in 30% of all neurones in the brain (Bloom and Iversen, 1971). GABA is synthesised from glutamic acid by α-decarboxylation using the enzyme glutamic acid decarboxylase (GAD) and the co-enzyme, pyridoxal 5'-phosphate. The mechanism by which GABA exerts its effects involves binding of GABA to specific chloride (Cl^-) ion channel proteins in the post-synaptic membrane. GABA binding causes a conformational change in these channel proteins, opening a central ionic pore that allows an influx of Cl^- anions into the post-synaptic neurone. This hyperpolarises the neurone and inhibits action potentials, thus preventing signal transmission. Once used, GABA is removed from the synapse by high affinity sodium (Na^+)-dependent GABA transporters (GATs) that are present in the pre-synaptic terminal and surrounding glial cells. GABA is metabolised by GABA transaminase to form succinic acid semialdehyde which is then oxidised to form succinic acid and re-cycled via the citric acid cycle.

In addition to its role in inhibitory neurotransmission in the adult brain, GABA also acts as a trophic factor during neural development. During the early stages of neural development, the effects of GABA are excitatory (Cherubini *et al.*, 1991). This may be due to a reversed transmembrane Cl^- gradient, resulting in a higher intracellular than extracellular concentration of Cl^- ions and the net efflux of Cl^- ions upon opening of $GABA_A$ receptor channels, thus depolarising the post-synaptic neurone (Misgeld *et al.*, 1986). The shift in Cl^- ion gradient during early postnatal development that leads to the switch from excitatory to inhibitory effects of GABA activation, is due to an increase in expression levels of the Cl^- ion-extruding neuronal K^+/Cl^- co-transporter 2 (KCC2) (Rivera *et al.*, 1999). KCC2 counters the effects of the Cl^--accumulating KCC1, which

is strongly expressed from birth. GABA neurotransmission thus begins to display its characteristic inhibitory effects.

Some evidence has also been found for an excitatory response to GABA in adult neurones, although the mechanisms of action are not always clear. Neurones in the rat hippocampus were excited by a GABA induced efflux of bicarbonate ions (Staley *et al.*, 1995). GABA also had a Na^+-dependent excitatory effect on neurones in the rat accessory olfactory bulb (Goldmaker and Moss, 2000). Hilar cells of the Guinea pig hippocampus showed a GABA receptor mediated excitatory response to GABA, leading to an overall inhibitory response by hippocampal interneurones (Michelson and Wong, 1991). In the nematode worm, *Caenorhabditis elegans*, a cation selective GABA receptor, EXP-1, has been identified (Beg and Jorgensen, 2003). This receptor contains a pattern of charged residues in its pore-forming TM2 region necessary for cation selectivity (Imoto *et al.*, 1988; Beg and Jorgensen, 2003).

1.2.2. CLASSIFICATION OF THE GABA RECEPTORS

There are three receptor subtypes activated by GABA. These are designated $GABA_A$, $GABA_B$ and $GABA_C$. $GABA_A$ and $GABA_C$ receptors are fast acting, ionotropic, ligand-gated chloride ion channels, whereas $GABA_B$ receptors are slower acting G protein-coupled metabotropic receptors.

$GABA_A$ receptors represent the majority of GABA activated receptors. They are activated by GABA and the receptor agonist, muscimol. The receptor competitive and non-competitive antagonists, bicuculline and picrotoxin, respectively, are allosterically regulated by the cage convulsant, t-butylbicyclophosphorothionate (TBPS). Most $GABA_A$ receptors are also sensitive to the classical anxiolytic benzodiazepines, valium and librium. They are modulated further by a range of other compounds including barbiturates and neurosteroids. This makes the $GABA_A$ receptors important targets for the treatment of neurological conditions such as epilepsy and anxiety (reviewed by Stephenson, 1995).

The $GABA_B$ receptors are G protein-coupled receptors. Activation of $GABA_B$ receptors leads to a slow-acting inhibition of neurones by inhibition of voltage-gated Ca^{2+} channels and stimulation of G protein-coupled K^+ channels. $GABA_B$ receptors are insensitive to bicuculline, but are sensitive to the $GABA_B$ receptor agonist, baclofen, and the antagonists, phaclofen and saclofen. There are 3 $GABA_B$ receptor subunits, $GABA_BR1a$, $GABA_BR1b$ and $GABA_BR2$. These are heptahelical membrane proteins

which function as heterodimers at both pre- and post-synaptic sites (Kaupmann *et al.*, 1997; 1998). There are several effects of $GABA_B$ receptors including the suppression of neurotransmitter release by closing voltage-gated Ca^{2+} channels, hyperpolarisation of the post-synaptic neurone by opening K^+ channels and regulation of adenylate cyclase by activation of G-proteins (Bettler *et al.*, 1998). $GABA_B$ receptors are involved in the induction of long term potentiation (LTP) (Davies *et al.*, 1991). It has been suggested that control of gene expression leading to LTP may be regulated by direct interactions between $GABA_B$ receptors and transcription factors (Nehring *et al.*, 2000).

$GABA_C$ receptors are a separate sub-class of ionotropic GABA receptor channel. They are composed of the subunits ρ1-3 which have not been shown to associate with $GABA_A$ receptor subunits (Hackman *et al.*, 1998; Enz and Cutting, 1998). $GABA_C$ receptors also have a distinct pharmacological profile to the $GABA_A$ receptors (Bormann, 2000). For example, unlike $GABA_A$ receptors $GABA_C$ receptors are insensitive to benzodiazepines, bicuculline and baclofen. There are five GABA binding sites per $GABA_C$ receptor and it is thought that three GABA molecules are required for activation of these channels (Amin and Weiss, 1996). The remaining two sites may be involved in regulation of channel sensitivity or stabilisation of the open state of the receptor. $GABA_C$ receptors are mainly found in the retina, where they are expressed 10-fold higher than $GABA_A$ receptors and do not desensitise on prolonged activation. It was suggested that $GABA_C$ receptors are involved in the regulation of graded potentials in retinal neurones as they mediate smaller currents at lower concetrations of GABA compared to the $GABA_A$ class of receptors (Enz and Cutting, 1998). The focus of this thesis is on the $GABA_A$ receptors and these are discussed in more detail below.

1.2.3. THE $GABA_A$ RECEPTOR FAMILY OF PROTEINS

1.2.3.1. THE $GABA_A$ RECEPTOR SUBUNITS

There are 16 known $GABA_A$ receptor subunits in mammals. These are α1-6, β1-3, γ1-3, δ, ε, θ and π. A fourth β subunit and a fourth γ subunit exist only in chicks (Bateson *et al.*, 1991; Harvey *et al.*, 1993). Each $GABA_A$ receptor subunit shares a conserved topology. A typical $GABA_A$ receptor subunit is represented in Figure 1.4. From the diagram, it can be seen that approximately half of each subunit comprises a large extracellular N-terminus, which contains 2-3 N-glycosylation motifs, a conserved 15 residue disulphide-bonded loop and residues important for ligand binding. This is

followed by 4 TM domains of approximately 20 amino acids each and a large intracellular loop of ~120-150 residues between TM domains 3 and 4. The loop domain contains several regulatory sequences, including phosphorylation sites for protein kinase A (PKA), protein kinase C (PKC) and tyrosine kinase. $GABA_A$ receptors have a very short extracellular C-terminus with few or no residues protruding from the outer face of the membrane. The subunits share ~30-40% amino acid sequence identity between subunit subclasses and ~70-80% amino acid identity between subunits of the same class (Macdonald and Olsen, 1994). The large intracellular loop of each subunit is the most divergent region with little or no identity between subunits of the same or different classes. Three of the $GABA_A$ receptor subunits are known to exist as splice variants. The α6 subunit has an alternative splice form lacking amino acids 57-66 from the N-terminal domain; however, this short form of α6 produces non-functional receptors (Korpi *et al.*, 1994). The β3 subunit gene encodes 2 alternative transcripts, differing in their signal peptide, which may be indicative of regulatory control of β3 subunit expression (Kirkness and Fraser, 1993). The γ2 subunit exists as a short (γ2S) and a long (γ2L) form (Whiting *et al.*, 1990). γ2L differs from γ2S by 8 additional amino acids which are found at the beginning of the cytoplasmic loop region and which encode a phosphorylation site for PKC. The ε subunit may be substituted for a γ subunit or a δ subunit and confers insensitivity to anaesthetics (Davies *et al.*, 1997). The π and θ subunits show greatest amino acid sequence identity with the β subunits. The π subunit is only found outside of the CNS (Hedblom and Kirkness, 1997), while θ will assemble with α, β and γ subunits in the brain to form receptors with a 4-fold reduction in sensitivity to GABA (Bonnert *et al.*, 1999). Combinations of these $GABA_A$ receptor subunits associate to form pentameric integral membrane proteins, arranged to form a central ionic pore. Each subunit confers particular molecular and pharmacological properties to the fully assembled receptor. This allows for the formation of a range of receptor subtypes (McKernan and Whiting, 1996).

1.2.3.2. THE QUARTERNARY STRUCTURE, SUBUNIT COMPOSITION AND SUBUNIT STOICHIOMETRY OF $GABA_A$ RECEPTORS

The pentameric nature of the $GABA_A$ receptor has been demonstrated by electron microscopy (Nayeem *et al.*, 1994), co-expression of monomeric and tandem subunit constructs (Im *et al.*, 1995) and by sucrose density gradient centrifugation (Klausberger

et al., 2001a). The α1β2/3γ2 pentamer is by far the most common $GABA_A$ receptor subtype in adult brain tissue (Wisden *et al.*, 1992; Laurie *et al.*, 1992a; Fritschy *et al.*, 1992; Benke *et al.*, 1994; Pirker *et al.*, 2000). The subunit composition of this receptor subtype was determined by quantitative Western blotting (Tretter *et al.*, 1997). For this technique, chimeric α1-β3, α1-γ2 and β3-γ2 subunits were constructed to contain pairs of subunit-specific antibody epitopes, which could be compared for their relative strengths of detection. These antibodies were then used to detect receptors produced by co-transfected, wild-type α1, β3 and γ2 subunits in HEK 293 cells and the subunit ratios were then calculated. A ratio of 2:2:1 was calculated for co-expressed α:β:γ subunits. The same ratio was also found by comparing the relative fluorescence energy transfer of tagged α1, β2 and γ2 subunits co-transfected into HEK 293 cells (Farrar *et al.*, 1999).

The subunits of αβγ subunit-containing $GABA_A$ receptors are arranged in the order γαβαβ clockwise when viewed from the outer surface of the synaptic membrane. This stoichiometry and arrangement is represented in Figure 1.4. It was determined by molecular modelling (Trudell, 2002) using the acetylcholine binding protein (Smit *et al.*, 2001; Brejc *et al.*, 2001) as a model (Section 1.1.2.) and by expression of tandem and triplet linked subunit cDNA constructs (Baumann *et al.*, 2002). The αβγ pentamer contains the subunit requirements to represent the pharmacological profile of a classical native $GABA_A$ receptor i.e. shows potentiation by benzodiazepines. It has been shown, using subunit specific antibodies, that a single αβγ pentamer may contain two different α subunits and two different β subunits (Duggan *et al.*, 1991; Pollard *et al.*, 1993; Pollard *et al.*, 1995; Li and De Blas, 1997; Jechlinger *et al.*, 1998). This allows for additional receptor diversity. This variation in α and β subunit combinations, together with receptors that include the δ, ε, θ or π subunits, provides a range of receptor subtypes with alternative pharmacological profiles. $GABA_A$ receptor heterogeneity will be discussed further in Section 1.2.4.

1.2.3.3. LIGAND BINDING SITES OF THE $GABA_A$ RECEPTORS

As mentioned in Section 1.2.2, the $GABA_A$ receptors are sensitive to a variety of ligands, such as benzodiazepines, barbiturates and neurosteroids. This makes them important targets for the treatment of neurological disorders including epilepsy and anxiety. The effects of receptor activation by each of these compounds is dependent on the particular combination of subunit subtypes in the receptor. Studies showed that

cloned $GABA_A$ receptors composed of α and β subunits are responsive to GABA, but not to benzodiazepines and that the presence of the γ subunit is a requirement for the formation of the benzodiazepine binding site (Pritchett *et al.*, 1989; Stephenson *et al.*, 1990). Studies undertaken to reveal the locations of the binding domains for these ligands are discussed below.

1.2.3.3.1. The GABA Binding Domain

GABA, the endogenous ligand for $GABA_A$ receptors, causes inhibition of post-synaptic action potentials by binding to specific interaction sites on $GABA_A$ receptors. There are two low affinity binding sites for GABA located at the interfaces between the α and β subunits. These sites are activated by μM concentrations of GABA and are important for channel gating. Studies using photoaffinity labelling, site-directed mutagenesis, or the substituted cysteine accessibility method (SCAM) have been used to locate residues involved in the GABA binding domain on α1 and β2 subunits (Amin and Weiss, 1993; Smith and Olsen, 1994; Boileau *et al.*, 1999; Wagner and Czajkowski, 2001). The two homologous domains of the β subunit, Y157/T160 and T202/Y205, were found to be involved in GABA binding (Smith and Olsen, 1994). The distance between the Y157/T160 and the T202/Y205 binding domains suggested that a loop structure may be necessary to bring these domains together. The α1 subunit residues F64, R66 and S68 (Boileau *et al.*, 1999) and the β2 subunit residues S204, Y205, R207 and S209 (Wagner and Czajkowski, 2001) were all shown to line the GABA binding pocket, while β2 F200, S201, T202 and G203 do not line the binding pocket, but affect the affinity of GABA binding. The high affinity binding sites for GABA are thought to be formed from conformational variants of the low-affinity binding sites (Baur and Sigel, 2003) and to be involved in stabilisation of the desensitised state of the $GABA_A$ receptor (Newell and Dunn, 2002). δ Subunit-containing $GABA_A$ receptor subtypes have a higher affinity for GABA than those containing a γ subunit. They do not show desensitisation on prolonged activation (Nusser *et al.*, 1998). This suits them to tonic inhibition. These receptors are found mainly in cerebellar granule cells on extra-synaptic somatic and dendritic membranes, where GABA is found in low, but constant, concentrations. γ Subunit-containing receptors have a lower sensitivity to GABA than δ-subunit containing receptors and are desensitised on prolongued activation, therefore they are more suited to phasic inhibition (Nusser *et al.*, 1998). These receptors are

mainly localised to synaptic sites where GABA is found at higher concentrations but for short periods of time.

1.2.3.3.2. The Benzodiazepine Binding Domain

The benzodiazepine drugs are central nervous system (CNS) depressants that act on $GABA_A$ receptors to allosterically modulate the effects of GABA. These drugs are commonly used to treat anxiety. Benzodiazepine drugs are variously anxiolytic, anti-convulsive, sedative/hypnotic, amnesic and muscle-relaxing. The binding site for the benzodiazepines is found at the α-γ interface. It is the γ subunit that confers benzodiazepine sensitivity to the receptor, while the particular effects of a benzodiazepine are modulated by the α subunit subtype associated with the $GABA_A$ receptor. There are 3 γ subtypes. The γ2 and γ3 subunits confer benzodiazepine sensitivity to fully assembled αβγ receptors. γ2 Subunits are widespread throughout the brain and mediate most of the effects of benzodiazepines, while γ3 is only weakly distributed throughout the brain (Pirker *et al.*, 2000). The γ1 subunit is widely distributed throughout the brain, but confers a benzodiazepine sensitivity 10 times weaker than that of the γ2 subunit (Ymer *et al.*, 1990). The α subunit variant receptor subtypes α1βγ2, α2βγ2, α3βγ2 and α5βγ2 are benzodiazepine-sensitive. The α1 subunit confers benzodiazepine type I pharmacology in that it displays a high affinity for the non-benzodiazepine agonist, CL 218 872, 2-oxoquazepam and the inverse agonist, methyl β-carboline-3-carboxylate (β-CCM) (Pritchett *et al.*, 1989). α Variant receptor subtypes α2βγ2, α3βγ2 and α5βγ2 are relatively insensitive to these compounds, i.e. display benzodiazepine type II pharmacology. These subunits mediate the anxiolytic effects of benzodiazepines. In particular, α5 is thought to be involved in regulating the amnesic effects as it is found mainly in the hippocampus, as detected by radioligand binding (Sur *et al.* 1999a). Knockout mice for the α5 gene have been shown to possess an enhanced ability to remember the location of a hidden platform in a water maze test (Collinson *et al.*, 2002). The α4βγ2 and α6βγ2 receptor subtypes are benzodiazepine-insensitive.

Studies have been carried out to identify amino acids that are important for the binding of benzodiazepines. Site-directed mutagenesis of amino acids in the γ2 subunit have implicated M57, M58, M130 (Kucken *et al.*, 2000; Buhr and Sigel, 1997), F77, A79 and T81 (Teissere and Czajkowski, 2001) as components of the benzodiazepine binding

pocket. Further, it is thought that the involvement of alternating residues between γ2 F77 and T81 are due to the presence of a β-sheet structure in this region (Teissere and Czajkowski, 2001). The β-sheets are indicated in Figure 1.5 which shows a homology model of the N-terminal domains of the $GABA_A$ receptor, based on the AChBP.

A number of studies have also been carried out on the α subunits, again using site-directed mutagenesis of particular residues to assess their effects on benzodiazepine binding. Mutation of the α3 subunit glutamate, at residue 225, to the glycine of the α1 subunit in the same position, increased the displacement of the benzodiazepine antagonist [^{3}H] Ro 15-1788 by CL 218 872. Thus, the benzodiazepine type II properties of the α3 subunit were converted to the benzodiazepine type I properties of an α1 subunit (Pritchett and Seeburg, 1991). Conversion of the α1 subunit histidine at position 101 to an arginine as that of the α6, benzodiazepine-insensitive, subunit. The displacement of the benzodiazepine antagonist [^{3}H] Ro 15-4513 binding by diazepam was decreased by this mutant (Wieland *et al.*, 1992). In the reciprocal assay, conversion of the α1 subunit arginine at position 100 of the α6 subunit to a histidine (Wieland and Luddens, 1994) or a glutamine (Korpi *et al.*, 1993) induces benzodiazepine sensitivity, indicating the importance of this residue in benzodiazepine sensitivity. Mutations in the α6 subunit of P161 to T and V211 to I both caused selective sensitivity to benzodiazepines (Wieland and Luddens, 1994). The widespread distribution of residues found to be involved in benzodiazepine binding suggests that a specific conformation of the N-terminal domains is required to bring these residues together to form a binding pocket (Wieland and Luddens, 1994).

The CNS depressant class of drugs also include the barbiturates. The effects of barbiturate drugs are again modulated by α subunits, although, unlike the benzodiazepines, barbiturates act on α4βγ and α6βγ receptors as well as α1βγ, α2βγ, α3βγ, and α5βγ. Another difference between benzodiazepines and barbiturates is that barbiturates are capable of directly activating α4βγ receptors in addition to their GABA potentiating effects (Akk *et al.*, 2004).

1.2.4. REGULATION OF $GABA_A$ RECEPTOR HETEROGENEITY

1.2.4.1. EXPRESSION OF $GABA_A$ RECEPTOR SUBUNITS

As mentioned earlier, the 16 known $GABA_A$ receptor subunits (α1-6, β1-3, γ1-3, δ, π, ε and θ) provide the potential for a large number of distinct receptor subtypes. However,

not all possible combinations have been found experimentally *in vivo* and the total number of different receptors that actually exist is unknown. Table 1.1 lists the most common $GABA_A$ receptor subtypes found in the brain. From the table it can be seen that a very few receptor subtypes account for the vast majority of total $GABA_A$ receptors. The common $\alpha1\beta2/3\gamma2$ receptor combination incorporates the γ subunit which is less sensitive to GABA than the δ subunit, but which has a higher amplitude response (Saxena and MacDonald, 1996) and shows the phasic response to GABA at synaptic sites (Nusser *et al.*, 1998). The $\alpha1$ subunit has the second highest sensitivity to GABA of the α subunits i.e. it does not significantly reduce the GABA sensitivity of the $\gamma2$ subunit as other α subunits may e.g. $\alpha3$ (Bohme *et al.*, 2004). The β subunits do not affect the receptor sensitivity to GABA (Bohme *et al.*, 2004), but show specific targeting of receptors compared to the non-specific targeting by the $\beta1$ subunit (Connolly *et al.*, 1996a). Other receptor subtypes may act to modulate the effects of GABA in different brain regions by allowing a range of responses to the same GABAergic signal.

Various regulatory mechanisms are employed to limit receptor diversity. The first limiting factor is the differential expression of $GABA_A$ receptor subunit mRNAs in different neurones i.e. not all subunits are expressed in all types of neurone. A number of studies have been carried out to determine which subunits are expressed in different areas of the brain. The results are outlined below.

The distribution of the $GABA_A$ receptor subunits has been studied using *in situ* hybridisation (Wisden *et al.*, 1992; Laurie *et al.*, 1992a; Davies *et al.*, 1997; Hedblom and Kirkness, 1997) and by detecting subunit immunoreactivities in particular neurones (Fritschy and Mohler, 1995; Pirker *et al.*, 2000; Bonnert *et al.*, 1999). The $\alpha1$ subunit is by far the most widely expressed of the α subunits. The $\alpha2$ and $\alpha3$ subunits show a more localised distribution i.e. $\alpha2$ is found mainly in the forebrain and cerebellum and $\alpha3$ subunits are mainly found in the olfactory bulb and layers V and VI of the cerebral cortex (Wisden *et al.*, 1992). The $\alpha4$ subunit shows the weakest expression of the α subunits, followed by $\alpha5$, which also shows a low overall distribution. The $\alpha6$ subunit is localised almost exclusively to cerebellar granule cells. There are 3 β subunits. The $\beta2$ subunit is the most abundantly expressed β isoform in the brain, closely followed by $\beta3$. $\beta1$ is less common. The β subunits have also been implicated in targeting of receptors to distinct subcellular locations (Connolly *et al.*, 1996b). The $\gamma2$ subunit is the most

abundantly expressed γ isoform, followed by γ1. The γ3 subunit has a low overall distribution in adult brain. Expression of the δ subunit is mainly restricted to the cerebellum and frequently co-localises with the α4 and α6 subunits. The ε subunit is found in the amygdala, thalamus and subthalamic nucleus (Davies *et al.*, 1997). The θ subunit is distributed through the striatum, hypothalamus, amygdala, hippocampus, substantia nigra and regions of the hindbrain (Bonnert *et al.*, 1999). The π subunit is only found outside of the brain, in lung, prostate, thymus and showing most prominent expression in the uterus (Hedblom and Kirkness, 1997).

1.2.4.1.1. Developmental Changes in the Expression of $GABA_A$ Receptors

A developmental shift in subunit expression may contribute towards subunit availability and therefore $GABA_A$ receptor subunit composition. Studies of $GABA_A$ receptor subunit mRNA expression show a change in subunit composition between embryonic and adult receptors (Araki *et al.*, 1992; Laurie *at al.*, 1992). In these studies the α1 subunit showed an expression pattern consistent with an adult form of subunit, being expressed in neonatal neurones, but not during any stage of embryonic development. The α2, α3 and α5 subunits were shown to be expressed strongly during embryonic and early postnatal development, but to decrease in strength at later stages. This pattern was particularly pronounced for the α5 subunit. α4 was found in both differentiated and undifferentiated cells. The α6 and δ subunits showed no mRNA expression during embryonic development, appearing in early postnatal brain. The β1 subunit was present in the undifferentiated neuroepithelium and expression increased during development and postnatally. β2 and β3 subunits both appeared during cortical development. β3 expression was strongest perinatally, while β2 expression was highest in adult brain. Expression of γ1 and γ3 subunits showed stronger expression at earlier stages of development, but neither was widely expressed at any stage. The γ2 subunit showed strong expression at all stages of development and adulthood. These changes in subunit subtype expression reflect the change in function of $GABA_A$ receptors during neuronal development.

1.2.4.1.2. Induced Changes in $GABA_A$ Receptor Subunit Expression

In adult brain, changes in receptor subunit composition may be induced by neuronal activity or by neurological conditions e.g. epilepsy (Schwarzer *et al.*, 1997). For

example, in the pilocarpine-induced temporal lobe epilepsy model in rat brain, an altered $GABA_A$ receptor pharmacology has been observed in the dentate gyrus (Cohen *et al.*, 2003). Using this model, a decrease in receptor sensitivity to the non-benzodiazepine sedative, zolpidem, and an increase in sensitivity to zinc blockade was observed, resulting from a pilocarpine-induced down-regulation of α1 subunits and their replacement with α4 subunits.

1.2.4.2. RESTRICTED ASSOCIATION OF $GABA_A$ RECEPTOR SUBUNITS

As described above, some neurones express multiple subunit subtypes simultaneously (Wisden *et al.*, 1992; Laurie *et al.*, 1992a, b; Fritschy and Mohler, 1995; Pirker *et al.*, 2000). This allows for the formation of a range of receptor subtypes within a single cell type, not all of which are observed. Therefore, further mechanisms must reduce the number of receptor subtypes formed.

Preferential binding of certain subunits over others is one regulatory mechanism that limits the total number of receptor subtypes. For example, α4 subunit containing receptors account for ~20% of all $GABA_A$ receptors in the thalamus and are found in both α4βγ2 and α4βδ receptors, but the latter are approximately twice as abundant (Sur *et al.*, 1999b). The lack of functional homomeric $GABA_A$ receptors at the cell surface shows another limiting factor in receptor diversity, indicating that particular subunit compositions are favoured over others. Expression of individual $GABA_A$ receptor subunits does not result in surface expressed receptors, except in the case of β3 subunits which have been shown to form homo-oligomeric, but GABA-insensitive receptors that are capable of reaching the cell surface (Taylor *et al.*, 1999). The amino acid motif 'GKER', (G171, K173, E179, R180) is necessary for this homo-oligomerisation (Taylor *et al.*, 1999) and introduction of these residues into the β2 subunit produces β3-like homo-oligomerisation of β2 subunits (Bollan *et al.*, 2003). This shows that particular amino acid sequences are important for determining which subunits will coassemble.

1.2.5. ASSEMBLY OF THE LIGAND-GATED ION CHANNELS

Expressed receptor subunit mRNAs are targeted to and translated by ribosomes on the endoplasmic reticulum (ER). As the subunit polypeptides are manufactured they are targeted through the membrane of the ER by an N-terminal signal peptide. They are then exposed to modifying factors within the ER lumen and undergo protein folding and

processing, including post-translational modifications, such as disulphide bridge formation and N-linked glycosylation. Folding events are mediated by chaperone proteins and folding enzymes, such as immunoglobulin heavy chain binding protein (BiP), calnexin and protein disulphide isomerase (PDI) (reviewed by Kleizen and Braakman, 2004). Proper folding of subunits is essential for exit from the ER. The correct conformation ensures masking of ER retention signals within subunits, as demonstrated for the 5-HT_{3B} subunits which contains the 'CRAR' motif that promotes ER retention of 5-HT_{3B} homomers, but which is masked by assembly with 5-HT_{3A} subunits, leading to ER exit of assembled 5-HT_{3A}:5-HT_{3B} heteromers (Boyd *et al.*, 2003). Those subunits that are not properly folded are also retained in the ER by binding of chaperone proteins and the mis-folded subunits are subsequently degraded. The chaperone proteins, BiP and calnexin, have both been shown to bind $GABA_A$ receptor subunits that have been retained in the ER (Connolly *et al.*, 1996a). The $GABA_A$ receptor assembly process was inefficient, such that only ~30% of all subunits synthesised in baby hamster kidney cells were finally assembled into functional receptors (Gorrie *et al.*, 1997). This low assembly efficiency is similar to that found for the nACh receptors in mouse muscle cells and fibroblasts (Merlie and Lindstrom, 1983; Ross, *et al.*, 1991).

1.2.5.1 NICOTINIC ACETYLCHOLINE RECEPTOR ASSEMBLY AS A MODEL FOR ASSEMBLY OF THE LIGAND-GATED ION CHANNEL RECEPTOR SUPERFAMILY

The order of subunit assembly of the nicotinic acetylcholine (nACh) receptors is thought to be determined by one of two mechanisms: the 'heterodimer' mechanism or the 'sequential' mechanism. The heterodimer mechanism was proposed after studies involving transfection of combinations of *Torpedo californica* nACh receptor subunits into *Xenopus* oocytes (Saedi *et al.*, 1991). The results suggested that the first stage in assembly was the rapid formation of αγ and αδ dimers. These dimers subsequently combine to form $\alpha_2\gamma\delta$ tetramers, before the β subunit binds.

The sequential mechanism was also determined using *Torpedo* nACh receptor subunits (Green and Claudio, 1993). *Torpedo* nACh receptor subunit assembly does not occur at 37°C, but occurs at 20°C 10 x slower than mammalian subunit assembly. The subunits were synthesised at 37°C, then the temperature decreased to 20°C to induce assembly. ^{35}S-labelled subunits were tracked at intervals over 48 h. The results showed that αβγ

trimers are formed rapidly within 5 minutes after synthesis. A δ subunit is then slowly incorporated into this complex to form a tetramer, before the second α subunit binds. Experiments favouring the sequential formation of receptors disagree with those for the heterodimer in the order of subunit binding. The methods of studying receptor assembly for each proposed mechanism may explain these differences. Results favouring the heterodimer mechanism were based on the final compositions of fully assembled receptors observed after co-expression of 2, 3 or 4 nAChR subunits (Saedi *et al.*, 1991). Subunit associations occurring in the absence of 1 or more subunits may not be representative of native receptor assembly intermediates. The sequential mechanism was determined by observing the intermediate stages of receptor assembly on co-expression of all 4 subunits simultaneously (Green and Claudio, 1993). Therefore, this method is more likely to represent accurately the intermediate stages of receptor assembly.

Experiments based on the method used to determine the sequential formation of nACh receptors, were used to show ligand binding site formation on nACh receptors after particular subunit rearrangements during assembly (Green and Claudio, 1993; Green and Wanamaker, 1998; Mitra *et al.*, 2001). The ACh and α-bungarotoxin (Bgt) binding sites are found at the α-γ and α-δ subunit interfaces. The α-bungarotoxin (Bgt) binding site was found to form on αβγ trimers, before the binding of the δ subunit. The first ACh binding site, found at the α-γ interface, was formed on αβγδ tetramers and the second ACh binding site, found at the α-δ interface, was formed on αβγδα pentamers after the binding of the second α subunit. The requirement of the formation of the disulphide-bonded loops of the α and β subunit N-terminal domains for efficient receptor assembly was also studied and found to be essential for completion of assembly (Green and Wanamaker, 1998; Mitra *et al.*, 2001). This is thought to be due to cysteine loop-dependent conformational rearrangements that produce recognition sites for subunits incorporated at the later stages of assembly. The general mechanism of nACh receptor assembly is thought to be similar for all members of the receptor superfamily. However, there are a greater number of possible receptor subunit combinations for the $GABA_A$ receptors than for muscle type nACh receptors, therefore additional motifs may exist to allow alternative subunit binding.

1.2.5.2. $GABA_A$ RECEPTOR ASSEMBLY

Several recent studies have identified sequences in $GABA_A$ receptor subunit N-terminal domains that play an important role in subunit oligomerisation. The results of these studies are summarised in Table 1.2. Mutation of the α1 subunit tryptophans, W69 and W94, and co-expression of the resulting mutant subunit with wild-type β2 and γ2 subunits, showed both α1W69 and α1W94 residues to be important for interactions with the β2 and γ2 subunits (Srinivasan *et al.*, 1999). Further analyses of α1β3γ2-type receptors were carried out using co-expression of combinations of full-length wild-type, truncated, chimeric and/or mutated subunits in mammalian cells. The α1 subunit sequence 54-68 was identified as important for assembly with the β3 subunit and in particular the glutamine at position 67 and the serine at position 68 were key residues (Taylor *et al.*, 2000; Sarto *et al.*, 2002a). The sequence α1(80-100) was found to be important for assembly with γ2(1-104) (Klausberger *et al.*, 2001b). The results show evidence for distinct binding domains on each subunit N-terminus that mediate interactions with particular subunits. Furthermore, in a comparative study of binding between the α1 subunit and the various β subunits, the α1 subunit arginine residue, R66, was found to be necessary for oligomerisation with β2, but not β1 or β3 subunits (Bollan *et al.*, 2003), indicating selective binding motifs. It has also been shown that homologous domains on each subunit are responsible for oligomerisation. For example, the domains β3(52-66) and γ2(67-81), which are in a homologous position to α1(54-68), were each shown to be involved in oligomerisation with the α subunit (Sarto *et al.*, 2002a). In addition, homologous domains between γ3 and γ2 subunits were shown to be important for interactions with α and β subunits (Sarto *et al.*, 2002b).

1.2.6. REGULATION OF LIGAND-GATED ION CHANNELS BY INTERACTING PROTEINS

1.2.6.1. NMDA RECEPTOR REGULATORY PROTEINS

The assembly, processing, trafficking, surface expression, recycling and activity of ligand-gated ion channels are all regulated by a range of interacting proteins. Table 1.3 shows a list of proteins that have been identified as interacting with various members of the ligand-gated ion channel superfamily. The functions of these proteins are discussed below.

The majority of identified NMDA receptor-associated proteins have been found to interact with subunit isoform specific regions of the C-terminal domains. NMDA receptor subunits have a different topology from the nACh receptor superfamily. Each subunit contains a large extracellular N-terminal domain, 4 membrane (M) domains and a large intracellular C-terminal domain. Domains M1, M3 and M4 span the membrane, while M2 forms a re-entrant loop. Assembled NMDA receptors are composed of NR1 and NR2 subunits in adult brain. In the developing brain an NR3A subunit is also expressed (Das *et al.*, 1998). The NR1 subunit exists in 8 distinct spice variants (1a, 1b-4a, 4b) and there are 4 NR2 subunits (A-D) (reviewed by Stephenson, 2001). The a and b forms of NR1 subunit differ in the absence or presence of the N-terminal sequence encoded by exon 5 of the NMDA receptor gene, respectively. The NR1 splice forms 1-4 differ in the presence or absence of the exon 21 encoded sequence, C1, which is present in NR1-1a, b and NR1-3a, b, but not NR1-2a, b or NR1-4a, b, and in the presence of alternative forms of the exon 22 product, C2 and C2'. NR1-1a, b and NR1-2a, b contain C2, while NR-3a, b and NR1-4a, b contain C2'.

1.2.6.1.1. Proteins Involved in Anchoring and Localisation of NMDA Receptors

NMDA receptors are found at asymmetrical synapses. At these synapses the post-synaptic density (PSD) is much thicker than the pre-synaptic density. A large number of PSD proteins have been identified and found to be involved in clustering of glutamate receptors at the post-synaptic membrane. The members of this protein family are PDZ domain-containing proteins. PDZ domains were named for the first 3 proteins found to contain them, i.e. PSD of 95 kDa mwt (PSD-95), Discs large and ZO-1. PSD-95, also known as synapse associated protein (SAP), SAP90, was the first of these proteins to be discovered. It contains 3 PDZ domains, which are important for mediating protein-protein interactions (Saras and Heldin, 1996). PSD-95 was shown to interact with the NMDA receptor NR2A subunit C-terminus via the PSD-95 PDZ2 domain (Kornau *et al.*, 1996). Later, SAP102 and channel associated protein of the synapse of 110 kDa (chapsyn-110)/PSD-93 were identified and were also found to interact with NMDA receptors (Lau *et al.*, 1996; Kim *et al.*, 1996). Thus, members of the PDZ protein family, are involved with localisation and stabilisation of NMDA receptors at the synapse. In addition, association of PSD-95 with NMDA receptors has also been shown to mediate NMDA subunit expression and channel activity (Yamada *et al.*, 1999; Rutter and Stephenson, 2000).

Yeast two-hybrid cDNA library screening was used to identify several proteins that interact with the intracellular C-terminal tail of NMDA receptor subunits. α-Actinin-2 is a member of the spectrin/dystrophin family and was found to interact with both the NR1 and NR2B subunits and actin (Wyzynski *et al.*, 1998). It localised to asymmetrical, but not symmetrical synapses and is thought to anchor NMDA receptors at the synapse by providing a link to actin filaments. The novel coiled-coil protein, Yotiao, was isolated from another yeast two-hybrid screen (Lin *et al.*, 1998). It is a 1640 amino acid protein which interacts with a 37 amino acid sequence of the NR1 C-terminus via the yotiao sequence (970-1241). This protein is also involved in receptor clustering, by linking NMDA receptors to the cytoskeleton.

Another link from the NMDA receptor NR1 subunits to the cytoskeleton is by interaction with the neuronal intermediate filament subunit, NF-L (Ehlers *et al.*, 1998). NR1 subunits containing a C-terminal C1 cassette bind the ends of NF-L subunits and inhibit NF-L assembly. NR1 and NF-L were also found to co-localise in growth cones (Ehlers *et al.*, 1998). This, in addition to the interaction with EphB receptors, which are known to be involved in axon guidance (Dalva *et al.*, 2000), also implicates NMDA receptors in axonal outgrowth and the development of synapses.

1.2.6.1.2. Proteins Modulating NMDA Receptor Function

Once anchored at the synaptic membrane further protein interactions are responsible for modulating receptor function. The calcium sensor protein, calmodulin (CaM), was found by co-immunoprecipitation to associate with, and inactivate, NMDA receptors (Ehlers *et al.*, 1996). The C-terminus of the NR1 subunit was found to contain two CaM binding sites, one mediating high affinity and the other mediating low affinity binding. In addition, CaM was found to have two binding sites for NR1 subunits (Akyol *et al.*, 2004). The C-terminal domain binds in a Ca^{2+}-independent manner, while the N-terminal site requires Ca^{2+} for interaction. CaM was also found to bind at the same location as α-actinin. Therefore, it is possible that CaM regulates NMDA function by displacement of α-actinin (Akyol *et al.*, 2004).

The dopamine D1 receptor also modulates the function of NMDA receptors by a direct interaction between the C-terminus of D1 with the C-terminus of NMDA NR1-1a or NR2A subunits (Lee *et al.*, 2002). The D1 (387-416) interaction with NR1-1a causes a phosphatidyl inositol-3 (PI-3) kinase dependent reduction in NMDA receptor-mediated cytotoxicity, while the D1 (417-446) interaction with NR2A leads to a PI-3 kinase

independent reduction in NMDA receptor-mediated currents. The interaction between D1 and NMDA receptors also allows the regulation of D1 activity on stimulation of NMDA receptors which causes an increase in D1 receptor number at the plasma membrane (Pei *et al.*, 2004). These interactions allow cross-regulation between the two receptor types.

As mentioned in Section 1.2.6.1.1. the extracellular domain of EphB tyrosine kinase receptors has also been shown to interact with the extracellular N-terminus of NMDA NR1 subunits on activation of EphB by its ligand, EphrinB (Dalva *et al.*, 2000). There is, thus the potential for extensive regulatory cross-talk between the various receptor signalling pathways.

1.2.6.2. AMPA RECEPTOR REGULATORY PROTEINS

1.2.6.2.1. Proteins Involved in AMPA Receptor Trafficking and Clustering

AMPA receptors are composed of the subunits GluR1-GluR4, which have a similar topology to the NMDA receptor subunits (Section 1.2.6.1). The intracellular C-terminal domains of these receptors are also responsible for interactions with regulatory proteins. SAP97 is another member of the PDZ domain protein family. It was shown by immunoprecipitation and chemical cross-linking that SAP97 interacts with the AMPA receptor GluR1 subunit C-terminus (Leonard *et al.*, 1998).

Yeast two-hybrid screening of the GluR2 C-terminal 50 amino acids isolated the proteins glutamate receptor interacting protein (GRIP1) and protein interacting with C kinase (PICK1) (Dong *et al.* 1997; Xia *et al.*, 1999). GRIP1 is a ~120 kDa protein that contains seven PDZ domains. The domains PDZ4 and PDZ5, along with 30 amino acids found C-terminally to PDZ5 are required for the interaction with GluR2 (Dong *et al.* 1997). A homologue, GRIP2, has also been identified (Dong *et al.*, 1999). Both proteins showed widespread expression in rat brain with specific antibodies, with a subcellular localisation to dendritic spines, although GRIP2 expression began later in development than GRIP1 (Dong *et al.*, 1999). GRIP1 is an adaptor protein that interacts directly with the kinesin heavy chain proteins, KIF5(A-C), and AMPA receptors to guide transport of the receptors to dendrites (Setou *et al.*, 2002). PICK1 is also a PDZ domain-containing protein that is involved in clustering of AMPA receptors at the synapse. As PICK1 is also a phosphorylation substrate for PKCα (Staudinger *et al.*, 1995) it may have a second function in the modulation of AMPA receptor activity. In addition, both GRIP1 and PICK1 have been found to interact with the EphB receptors, which, in turn, interact

with NMDA receptors (Torres *et al.*, 1998; Dalva *et al.*, 2000). This is another potential mechanism for cross-talk between ion channel subtypes.

1.2.6.2.2. Proteins Regulating AMPA Receptor Function

N-ethylmaleimide-sensitive fusion protein (NSF) is an ATPase involved in fusion of synaptic vesicles to the pre-synaptic membrane. NSF has 3 domains; an N-terminal domain and two ATP binding domains. All 3 domains are required for interactions with the AMPA receptor GluR2 subunit. This association plays a role in the regulation of AMPA receptor mediated synaptic transmission (Nishimune *et al.*, 1998).

1.2.6.3. NICOTINIC ACETYLCHOLINE RECEPTORS AND RAPSYN

The first protein shown to interact directly with one of the ligand-gated ion channels was the 43 kDa protein, rapsyn (Phillips *et al.*, 1991). Rapsyn was found to play a role in aggregation of nACh receptors at the plasma membrane. Three separate domains mediate the different functions of rapsyn (Ramarao and Cohen, 1998). Myristylation of the N-terminus is involved in membrane targeting of the protein. The amino acid domain 1-90 contains 2 tetratricopeptide (TPR) domains, which are thought to be involved in protein-protein interactions, and this region mediates the association of rapsyn with itself. Amino acids 298-331 form a predicted coiled-coil domain and are involved in the clustering of nACh receptors. Rapsyn was also shown to stabilise nACh receptor clusters at the synaptic membrane, slowing the turnover of receptors at the cell surface compared to receptors expressed in the absence of rapsyn (Wang *et al.*, 1999).

1.2.6.4. GLYCINE RECEPTORS AND GEPHYRIN

The glycine receptor interacting protein, gephyrin, has a similar function to rapsyn as it is involved in receptor clustering and anchoring (Kirsch *et al.*, 1991; 1993). Purification of glycine receptors by affinity chromatography co-purified a 93 kDa protein (Pfeiffer *et al.*, 1982). This protein was found to bind both glycine receptors and tubulin (Kirsch *et al.*, 1991) and was thus shown to form a bridge between glycine receptors and the cytoplasmic matrix. The clustering of glycine receptors by gephyrin is induced by interaction with the novel GDP/GTP exchange factor (GEF), collybistin, possibly by activation of a member of the Rho/Rac family of GTPases (Kins *et al.*, 2000). Gephyrin is expressed widely throughout the brain at synaptic sites and is not always co-associated with glycine receptors (Kirsch *et al.*, 1993). This suggested that gephyrin

may be involved at synapses for other LGICs. In wild-type mouse brain gephyrin was found to colocalise with γ2 subunit-containing $GABA_A$ receptors (Esserich *et al.*, 1998). γ2 Subunit knockout mice resulted in decreased gephyrin immunoreactivity at GABAergic synapses. In a reciprocal assay, antisense oligonucleotides blocking expression of gephyrin lead to an equivalent reduction in γ2 subunit punctate staining. This suggested that gephyrin also plays a role in receptor clustering at GABAergic synapses. However, a direct interaction between gephyrin and $GABA_A$ receptors has not been shown. Therefore, other $GABA_A$ receptor interacting proteins may provide a link between $GABA_A$ receptors and gephyrin.

1.2.6.5. $GABA_A$ RECEPTOR INTERACTING PROTEINS

Table 1.4 shows a list of $GABA_A$ receptor interacting proteins. Some of these proteins are described below.

1.2.6.5.1. The $GABA_A$ Receptor-Tubulin Complex-Associated Proteins (GTAPs)

In 1997, Kannenberg *et al.* (1997) carried out an initial study to identify proteins associated with mature $GABA_A$ receptors. In this study, actin, tubulin and several unidentified $GABA_A$ receptor-tubulin complex-associated proteins (GTAPs) were isolated by co-immunoprecipitation with the receptor α1 subunit. One of these, GTAP-34 (GTAP of molecular weight 34 kDa), was subsequently found to be a serine kinase that interacts directly and specifically with, and phosphorylates, the $GABA_A$ receptor β3 subunit IL (Kannenberg *et al.*, 1999). In an attempt to identify this GTAP, a 34 kDa protein was purified from bovine brain by immunoaffinity chromatography using an α1 subunit antibody (Schaerer *et al.*, 2001). This protein was identified as the multi-functional protein, gC1q-R, which is mainly localised in mitochondria. However, while it was found to interact strongly with the $GABA_A$ receptor β subunits, gC1q-R did not phosphorylate the β3 subunit IL, making it unlikely to be the previously isolated, GTAP-34. It was proposed that gC1q-R may be involved in receptor biosynthesis or may interfere with receptor phosphorylation, modulating receptor function (Schaerer *et al.*, 2001).

1.2.6.5.2. Proteins Involved in $GABA_A$ Receptor Trafficking and Clustering

The $GABA_A$ receptor associated protein, GABARAP, was identified from a yeast two-hybrid cDNA library screen using the $GABA_A$ receptor γ2S intracellular loop as a bait (Wang *et al.*, 1999). GABARAP is a 13.9 kDa protein. It is similar to microtubule-associated proteins, MAP-1A, MAP-1B and MAP-light chain 3 (LC3) and contains a tubulin binding domain at its N-terminus (Wang *et al.*, 1999). Affinity chromatography studies showed that GABARAP binds to tubulin and $GABA_A$ receptors at the same time (Wang *et al.*, 2000). This suggests that GABARAP provides a link between $GABA_A$ receptors and the cytoplasmic matrix. Further, yeast two-hybrid studies demonstrated an interaction between GABARAP and the glycine receptor anchoring protein, gephyrin (Kneussel *et al.*, 2000). However, immunofluorescence labelling of GABARAP demonstrated localisation to the ER and Golgi, rather than gephyrin-rich post synaptic densities, indicating that a role in targeting of receptors was more likely than anchoring. While roles in both targeting and clustering of $GABA_A$ receptors have been proposed, the precise function of GABARAP remains unknown.

The ubiquitin-related protein, Plic-1, was also identified from a yeast two-hybrid cDNA library screen, but using a $GABA_A$ receptor α1 subunit IL as a bait (Bedford *et al.*, 2001). Immunofluorescence labelling of Plic-1 showed co-localisation with $GABA_A$ receptors both at the post-synaptic plasma membrane and within intracellular compartments such as the Golgi body and clathrin-coated pits. This implies that Plic-1 is involved in regulating the trafficking and recycling of $GABA_A$ receptors.

In another yeast two-hybrid cDNA library screen, the novel $GABA_A$ receptor interacting factor, GRIF-1, was discovered, using the $GABA_A$ receptor β2 subunit IL as a bait (Beck *et al.*, 2002 and see Section 5.1.1). This protein was proposed to function as a $GABA_A$ receptor trafficking factor due to its amino acid sequence homology with the Huntingtin-associated protein (HAP-1), which is involved in cellular trafficking (Li *et al.*, 2002) and to its *Drosophila melanogaster* orthologue, Milton, which was shown to be a kinesin-associated adaptor protein (Stowers *et al.*, 2002). GRIF-1 may therefore have a similar role to the AMPA receptor interacting protein, GRIP1. The function of GRIF-1 is discussed further in Chapter 5.

1.2.6.5.3. Cross-Inhibition Between $GABA_A$ and Dopamine D5 Receptors

Dopamine D5 receptors are G-protein-coupled receptors that effect neurotransmission via activation of the adenylate cyclase pathway. These receptors have been shown to co-localise with $GABA_A$ receptors in hippocampal neurones (Liu *et al.*, 2000). A direct interaction was ascertained between the C-terminal tail of D5 receptors and the $GABA_A$ receptor γ2 subunit IL. This interaction requires agonist stimulation of both D5 and $GABA_A$ receptors and leads to the cross-inhibition of receptor activity on subsequent stimulation with reciprocal agonists.

1.2.6.5.4. $GABA_A$ Receptor Phosphorylation and Endocytosis

Recycling of $GABA_A$ receptors by endocytosis and reinsertion into the membrane provides a mechanism of controlling receptor activity at the cell surface. There is evidence that two separate mechanisms are involved in $GABA_A$ receptor endocytosis, one clathrin-dependent and one clathrin-independent (Herring *et al.*, 2003). The clathrin-mediated pathway was shown to regulate constitutive endocytosis of $GABA_A$ receptors. The adaptor protein, AP2, which is involved in recruitment of cargoes into clathrin-coated pits, was shown to bind specifically to $GABA_A$ receptor β1, β3, γ2S and γ2L subunits (Kittler *et al.*, 2000). In addition, the dileucine motif at residues 343 and 344 of β2 subunits has been identified as an AP2 binding site that is critical for clathrin-mediated endocytosis (Herring *et al.*, 2003). This mechanism regulates receptor number at the cell surface.

A study of mammalian cells containing immunofluorescently labelled $GABA_A$ receptors demonstrated that PKC reduces the number of $GABA_A$ receptors at the cell surface (Connolly *et al.*, 1999). This reduction was achieved by preventing recycling of γ2 subunit-containing receptors to the surface from intracellular pools, rather than by blocking endocytosis. Receptor internalisation continued in the absence of PKC. Receptor degradation did not occur, but reinsertion of receptors into the plasma membrane was reduced, thus resulting in decreased cell surface expression.

It has been shown that $GABA_A$ receptor β and γ2 subunits are phosphorylated by various kinases (e.g. PKA, PKC, tyrosine kinase, CamKII). Glutathione-S-transferase (GST) pull-down assays have identified a direct interaction between PKC and $GABA_A$ receptor β1 and β3 subunits (Brandon *et al.*, 1999). In the same study the receptor for activated kinase (RACK-1) was found to associate directly with β1 and α1 subunit ILs,

although the presence of RACK-1 was not found to be necessary for the interaction of PKC to take place.

1.2.7. AIMS OF THE THESIS

As has been discussed in this introduction, various mechanisms are employed within neurones to regulate of the assembly and activity of $GABA_A$ receptors. These mechanisms may be intrinsic to the $GABA_A$ receptor subunits, as in the case of assembly motifs, or via interactions with other proteins. The overall objective of this thesis was to elucidate further aspects of $GABA_A$ receptor subunit processing, assembly and trafficking. The first aim was to validate the use of the yeast two-hybrid system for identification of sequences within the $GABA_A$ receptor α1 and β2 subunits that are important for receptor assembly. The second aim was to identify proteins interacting with $GABA_A$ receptors that may play important roles in (i) trafficking and functional regulation of receptors and (ii) in the formation, stabilisation and plasticity of GABAergic synapses. The third aim of the study was to characterise further the function of the $GABA_A$ receptor interacting protein, GRIF-1, family of proteins and to investigate the possible role of GRIF-1 as a kinesin adaptor protein. All of these aspects were addressed using the yeast two-hybrid methodology.

FIGURE 1.1. EVOLUTIONARY TREE REPRESENTING THE NICOTINIC ACETYLCHOLINE RECEPTOR SUPERFAMILY OF PROTEINS

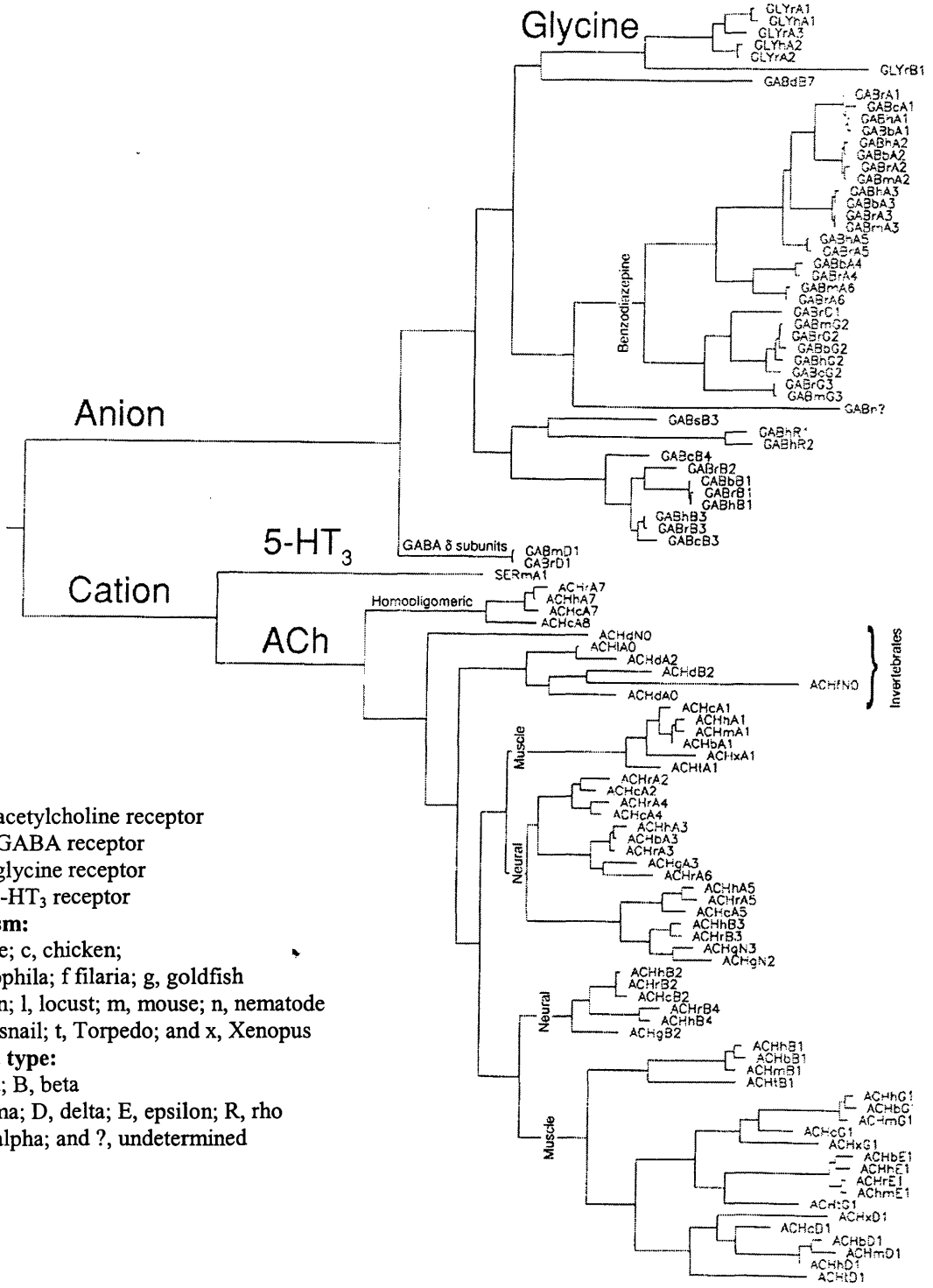

Key:
ACH = acetylcholine receptor
GAB = GABA receptor
GLY = glycine receptor
SER = 5-HT_3 receptor
Organism:
b, bovine; c, chicken;
d, Drosophila; f filaria; g, goldfish
h, human; l, locust; m, mouse; n, nematode
r, rat; s, snail; t, Torpedo; and x, Xenopus
Subunit type:
A, alpha; B, beta
G, gamma; D, delta; E, epsilon; R, rho
N, non-alpha; and ?, undetermined

The diagram shows an evolutionary tree for the nicotinic acetylcholine receptor superfamily, based on the maximum likelihood method. Taken from Ortells and Lunt (1995).

FIGURE 1.2. STRUCTURAL MEMBRANE TOPOLOGY OF A NICOTINIC ACETYLCHOLINE RECEPTOR SUBUNIT

A

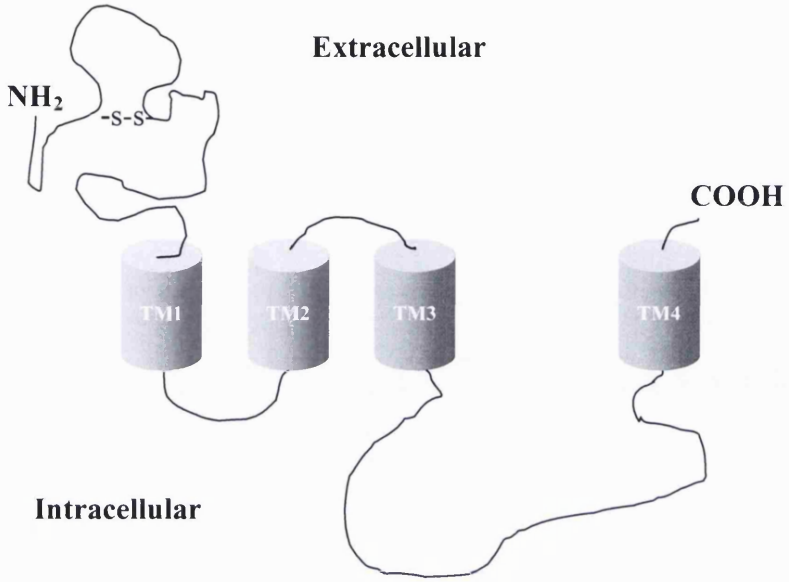

B

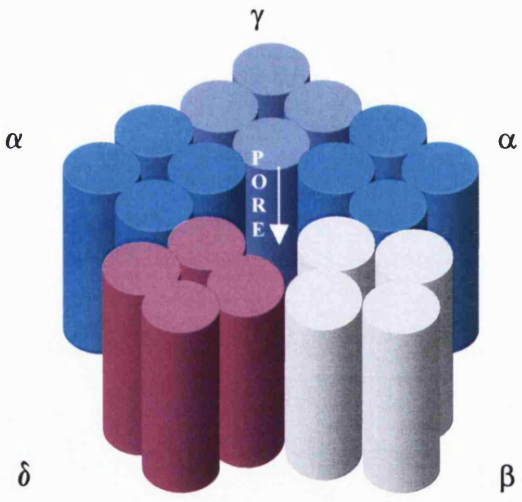

A shows the general subunit membrane topology of a typical nicotinic acetylcholine receptor subunit and B shows the arrangement of subunits around the ion channel pore.

FIGURE 1.3 SUBUNIT STRUCTURE AND ARRANGEMENT OF THE ACETYLCHOLINE BINDING PROTEIN

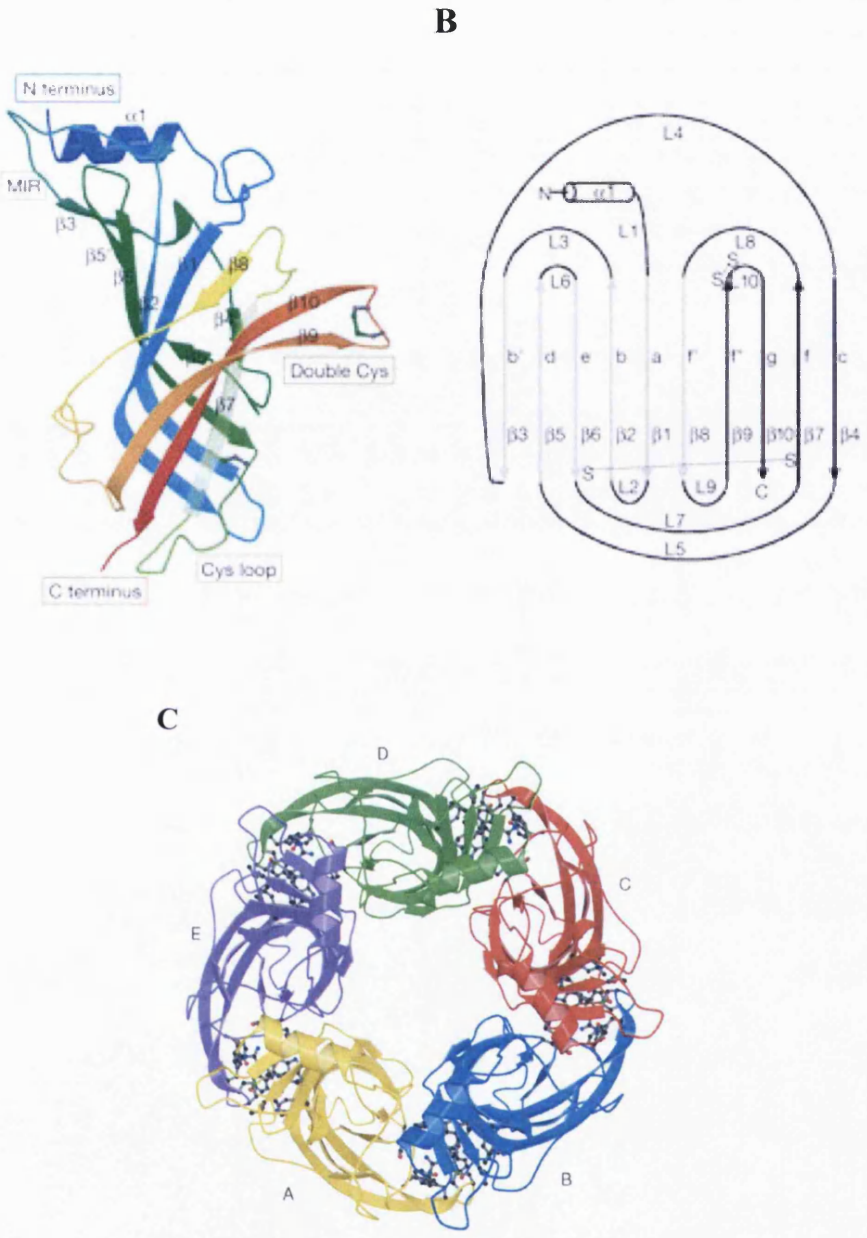

A is a ribbon representation of a single subunit of the acetylcholine binding protein, using graded colouring from blue (N-terminus) to red (C-terminus), with an α-helix indicated in purple. The disulphide bridge is indicated as a ball-and-stick loop. B is a diagrammatic representation of the subunit topology, indicating β-strands, loops, the α-helix and the disulphide bridge structure. C shows a ribbon representation of subunit arrangement. Ligand-binding domains are shown as ball-and-stick structures. Taken from Brejc *et al.* (2001).

FIGURE 1.4. STRUCTURAL MEMBRANE TOPOLOGY OF A TYPICAL $GABA_A$ RECEPTOR SUBUNIT

A

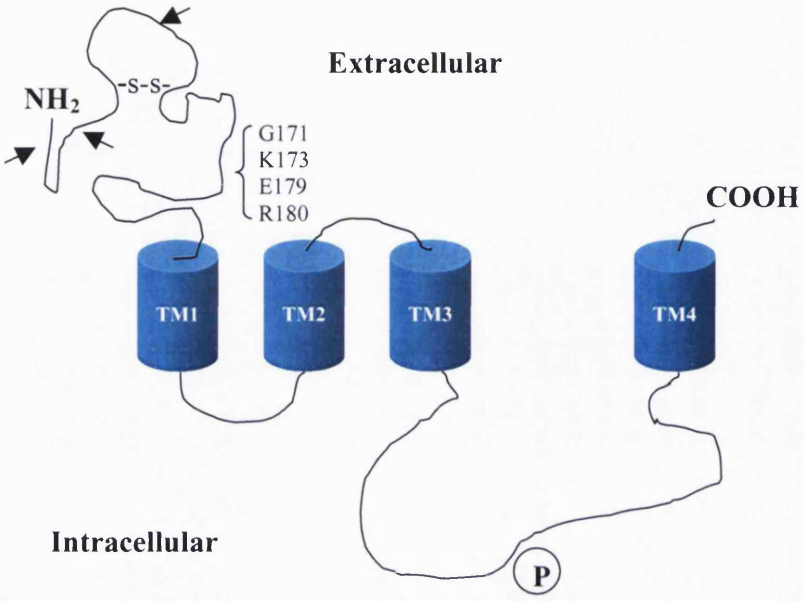

B

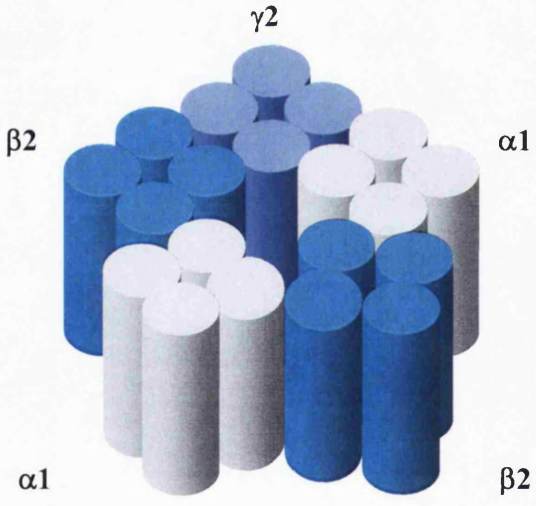

A shows a typical $GABA_A$ receptor subunit indicating potential N-linked glycosylation sites (➘), extracellular N- and C-termini, the disulphide bonded loop -s-s- and the transmembrane (TM) domains. B shows the arrangement of subunits around the ion channel pore (Trudell, 2002, Baumann *et al.*, 2002).

FIGURE 1.5. HOMOLOGY MODEL OF THE $GABA_A$ RECEPTOR N-TERMINAL DOMAINS BASED ON THE ACHBP

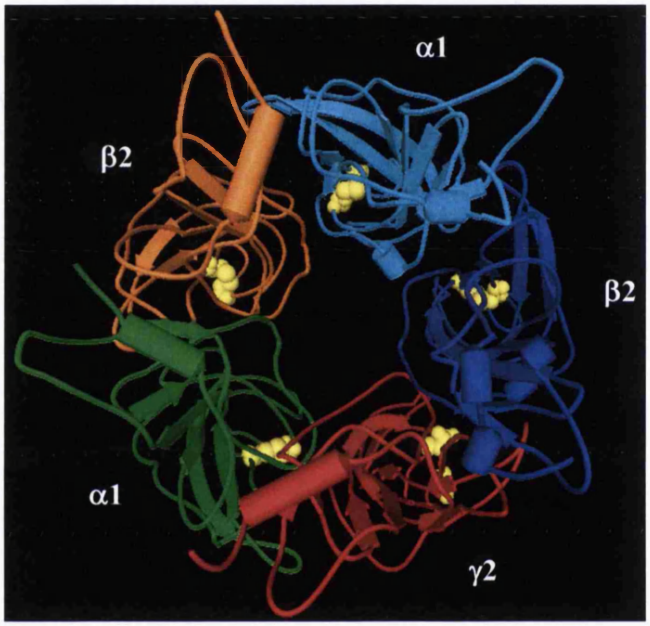

The diagram shows a ribbon representation of the pentameric structure of the $GABA_A$ receptor extracellular N-terminal domains modelled on the structure determined for the acetylcholine binding protein and viewed from above. Disulphide bridges are indicated in yellow. This diagram was created by Dr Mire Zloh, School of Pharmacy, University of London.

TABLE 1.1. MOST ABUNDANT $GABA_A$ RECEPTOR SUBTYPES IN RAT BRAIN

$GABA_A$ Receptor Subtype	Relative Abundance in Rat Brain (%)
α1β2γ2	43
α2β2/3γ2	18
α3β*γ2/3	17
α2β*γ1	8
α5β3γ2/3	4
α6β*γ2	2
α6β*δ	2
α4β*δ	3
Minor Subtypes	3

Table 1.1 shows a list of the most common $GABA_A$ receptor subtypes found in the rat brain and their respective percentage abundances. * The β subunit isoform is not known in all cases due to the lack of β subunit subtype-selective antibodies. The table is modified from Table 1 of McKernan and Whiting (1996).

TABLE 1.2. SUMMARY OF $GABA_A$ RECEPTOR SUBUNIT ASSEMBLY CONTACT SITES WITHIN THE N-TERMINAL DOMAIN

Subunit	Important Residues	Interaction	Reference
α1	58-67, Q67 +S68	β3	Taylor *et al.* (2000)
	80-100	γ2(91-104)	Klausberger *et al.* (2000; 2001b)
	54-68	β3	Sarto *et al.* (2002a)
	W69 + W94	β2→α1 +/or α1→γ2 interface	Srinivasan *et al.* (1999)
	R66	β2	Bollan *et al.* (2003)
γ2	91-104	α1(80-100)	Klausberger *et al.* (2001b)
	83-92	α1 + β2	Klausberger *et al.* (2000)
	67-81	α1	Sarto *et al.* (2002a)
γ3	70-84	α1 + β3	Sarto *et al.* (2002b)
	86-95	α1 + β3	Sarto *et al.* (2002b)
	94-107	α1	Sarto *et al.* (2002b)
β3	52-66	α1 binding	Sarto *et al.* (2002a)
	GKER	homooligomerisation	Taylor *et al.* (1999)

Table 1.2 shows a list of the sequences within $GABA_A$ receptor subunit N-terminal domains that are found to be important for receptor oligomerisation.

TABLE 1.3. PROTEINS INTERACTING WITH LIGAND-GATED ION CHANNEL RECEPTORS

Receptor	Interacting Protein	Reference	Function
NMDA	PSD95/SAP90	Kornau *et al.* (1996)	Receptor clustering.
	PSD93/ Chapsyn110	Kim *et al.* (1996)	Receptor clustering.
	SAP102	Lau *et al.* (1996)	Receptor clustering and immobilisation at the synapse.
	α-actinin-2	Wyszynski *et al.* (1997)	NMDA receptor anchoring protein.
	Calmodulin	Ehlers *et al.* (1996)	Inactivation of NMDA receptors.
	Yotiao	Lin *et al.* (1998)	Links NMDA receptors to the cytoskeleton.
	D1	Lee *et al.* (2002)	Receptor cross-talk.
	EphB	Dalva *et al.* (2000)	Receptor cross-talk.
	Neuronal Intermediate Filaments	Ehlers *et al.* (1998)	Anchoring and localisation of receptors.
AMPA	NSF	Nishimune *et al.* (1998)	Binds GluR2 and regulates synaptic transmission.
	PICK1	Xia *et al.* (1999)	AMPA receptor clustering.
	GRIP1	Dong *et al.* (1997)	Adaptor protein for AMPA receptor trafficking.
	SAP97	Leonard *et al.* (1998)	Receptor clustering.
nACh	Rapsyn	Phillips *et al.* (1991); Wang *et al.* (1999)	Clustering and metabolic stabilisation of nACh receptors.
Glycine	Gephyrin	Kirsch *et al.* (1991); Kirsch *et al.* (1993)	Clustering and anchoring of glycine receptors.

Table 1.3 shows a list of proteins identified as interacting with various members of the ligand-gated ion channel receptor superfamily and their functions.

TABLE 1.4. A TABLE OF THE KNOWN $GABA_A$ RECEPTOR INTERACTING PROTEINS

Interacting Protein	Subunit Specificity	Reference	Function
Gephyrin	Indirect interaction with γ2	Esserich *et al.*, (1998); Giustetto *et al.* (1998)	Clustering $GABA_A$ receptors by indirect association.
GABARAP	γ2 394-411	Wang *et al.* (1999)	Links $GABA_A$ receptors to the cytoskeleton.
Plic-1	α1-α3 (346-355), α6,β1-β3	Bedford *et al.* (2001)	$GABA_A$ receptor trafficking factor.
GRIF-1	β2 324-394	Beck *et al.* (2002)	$GABA_A$ receptor trafficking factor.
gClq-R (34 kDa)	β1-β3 (399-413)	Shaerer *et al.* (2001)	Multi-functional protein.
Protein Kinase C RACK-1 (Receptor for Activated C Kinase)	β1 β3 (PK-C); α1, β1 (RACK)	Brandon *et al.* (1999)	Down-regulation of GABA receptors at the cell surface.
AP2	β3 and γ2s, γ2L, β2-IL (aa 343/344)	Kittler *et al.* (2000); Herring *et al.* (2003)	Recruitment to clathrin-coated pits for receptor endocytosis.
D5 Dopamine receptors	γ2-IL	Liu *et al.* (2000)	Receptor cross-inhibition.
GTAP-34	α1 subunit-containing receptors	Kannenberg *et al.* (1997; 1999)	Phosphorylation of β3 subunit.

The table shows a list of $GABA_A$ receptor-interacting proteins and their regulatory functions.

CHAPTER 2:
MATERIALS AND METHODS

2.1. MATERIALS

Agar, peptone, yeast extract and yeast nitrogen base without amino acids were purchased from GibcoBRL (Paisley, UK). Agarose, ammonium sulphate, ethanol, ethylenediaminetetraacetic acid disodium salt (EDTA), D(+)-galactose, D(+)-glucose, glycine, glycerol, hydrochloric acid, hydrogen peroxide, isopropyl alcohol, magnesium chloride, magnesium sulphate, methanol, potassium chloride, potassium dihydrogen phosphate, D(+)-raffinose, sodium acetate, sodium chloride, sodium hydrogen phosphate, disodium hydrogen phosphate, sodium dihydrogen phosphate, and tris(hydroxymethyl)methylamine (Tris-base) were purchased from Merck (Dorset, UK). Adenine hemisulphate, ampicillin, boric acid, bromophenol blue, chloramphenicol, 4-hydroxycinnamic acid (p-coumaric acid), dimethyl formamide (DMF), dimethyl sulphoxide (DMSO), DNA sodium salt from salmon testes, dithiothreitol (DTT), ethidium bromide, kanamycin, lauryl sulphate (SDS; sodium dodecyl sulphate), lithium acetate, 5-amino-2, 3-dihydro-1, 4-phthalazinedione (luminol), lyticase, β-mercaptoethanol, mineral oil, 3-N-morpholino propane-sulphonic acid (MOPS), pepstatin A, polyethylene glycol (PEG) molecular weight (mwt) 3350, D-sorbitol, Tween®-20 and p-xylene cyanole were purchased from Sigma Chemicals (Dorset, UK). All DNA molecular weight markers, dNTPs, restriction enzymes and T4 DNA ligase were purchased from either Roche (East Sussex, UK) or Helena Biosciences (Tyne and Weir, UK). *Pfu* DNA polymerase was purchased from Promega (Southampton, UK), *Taq* polymerase from HT Biotechnologies Ltd (Cambridge, UK) or Invitrogen (Groningen, Netherlands) and shrimp alkaline phosphatase (SAP) from Amersham Pharmacia Biotech (Bucks, UK). The SeeBlue pre-stained protein marker and dual promoter TOPO TA cloning kit were purchased from Invitrogen (Groningen, Netherlands). Qiaprep mini-, midi- and maxiprep kits, Qiaquick PCR purification kit and Qiaex II gel purification kit were all purchased from Qiagen Ltd (West Sussex, UK). Isopropyl-β-D-thiogalactopyranoside (IPTG), 5-bromo-4-chloro-3-indolyl-β-D-galactopyranoside (X-GAL) and 5-bromo-4-chloro-3-indolyl-α-D-galactopyranoside (X-α-GAL) were purchased from Melford Laboratories Ltd. (Cambridge, UK). Selective dropout supplements, the Matchmaker™ 2 and 3 yeast two-hybrid systems and Marathon™-ready rat brain cDNA were purchased from Clontech Laboratories UK Ltd. (Hants, UK). The CytoTrap® yeast two-hybrid system was purchased from Stratagene Europe (Amsterdam, Netherlands). DNA sequencing reagents and

equipment, such as POP6 (performance optimised polymer 6), BigDye™ terminator ready reaction mix, template suppression solution, 10 x buffer with EDTA, capillaries, glass syringes and 0.5 ml septa, were purchased from Perkin Elmer Applied Biosystems (Warrington, UK). Oligonucleotide primers were purchased from Proligo (Paris, France). Commercial antibodies were purchased from Amersham International plc. (Buckinghamshire, UK), Upstate (New York, USA) or Roche (East Sussex, UK). The anti-$GABA_A$ receptor α1-IL (324-341) antibody, PEKPKKVKDPLIKKNNT-Tyr coupled to keyhole limpet hemocyanin (KLH), characterised by Duggan and Stephenson (1990), anti-$GABA_A$ receptor β2-IL (381-395) antibody, KAGLPRHSFGRNALE-Cys coupled to thyroglobulin, characterised by Pollard and Stephenson (1997) and anti-His-tagged GRIF-1(8-633) were produced in-house and affinity-purified by Dr. Kieran Brickley. Protogel (30% [w/v] acrylamide: 0.8% [w/v] bis-acrylamide (37.5:1) was purchased from National Diagnostics (Yorkshire, UK). The pBluescript II SK^+KIAA1042 and pBluescript II SK^+KIAA0531 (KIF5C) plasmid constructs were a kind gift from Professor T. Nagase of the Kazusa DNA Research Institute, Chiba, Japan.

2.1.1. YEAST TWO-HYBRID SYSTEM COMPONENTS

2.1.1.1. GAL4 System Cloning Vectors and Control Vectors

Vector	Description	Selection Genotype	Size (kb)
pAS2-1 (DNA-BD)	ADH1 promoter, *GAL4* DNA-BD, *TRP1*, Amp^r, CYH^S2	-Trp, Amp^r	8.4
pGAD10 (AD)	ADH1 promoter, *GAL4* AD, *LEU2*, Amp^r	-Leu, Amp^r	6.6
pGBKT7 (DNA-BD)	ADH1 promoter, *GAL4* DNA-BD, *TRP1*, Kan^r	-Trp, Kan^r	7.3
pGADT7 (AD)	ADH1 promoter, *GAL4* DNA AD, *LEU2*, Amp^r	-Leu, Amp^r	8.0
pVA3-1 (DNA-BD)	ADH1 promoter, murine $p53_{(72-390)}$ in pGBT9, *TRP1*, Amp^r	-Trp, Amp^r	9.4
pTD1-1 (AD)	ADH1 promoter, SV40 large T-antigen$_{(84-708)}$ in pACT2, *LEU2*, Amp^r	-Leu, Amp^r	10.0

2.1.1.2. GAL4 System Yeast Strain Genotype

Yeast Strain	Genotype
AH109	*MATa, trp1-901, leu2-3, 112, ura3-52, his3-200, gal4Δ, gal80Δ, LYS2 : : $GAL1_{UAS}$-$GAL1_{TATA}$-HIS3, $GAL2_{UAS}$-$GAL2_{TATA}$-ADE2, URA : : $MEL1_{UAS}$-$MEL1_{TATA}$-lacZ*

2.1.1.3. Modified Lex A System Cloning Vectors

Vector	Description	Selection Genotype	Size (kb)
pMBL33 (DNA-BD)	ADH promoter, *LexA* DNA-BD with SV40 NLS, *TRP1*, Kan^r	-Trp, Kan^r	7.3
pGADT7 (AD)	ADH1 promoter, *GAL4* DNA AD, *LEU2*, Amp^r	-Leu, Amp^r	8.0

2.1.1.4. Modified Lex A Yeast Strain Genotype

Strain	Genotype
L40	*MATa his3Δ200 trp1-901 leu2-3, 112 ade2 LYS2::* (4lexAop-*HIS3*) *URA3::* (8lexAop-*lacZ*) *GAL4*

2.1.1.5. CytoTrap® System Vectors

Vector	Description	Selection Genotype	Size (kb)
pMyr	GAL1 promoter, myristylation signal anchor protein, *CYC1* teminator, *2* micron ori, f1 ori, *URA3*, Cam^r	-Ura, Cam^r	5.6
pSos	ADH1 promoter, hSOS Ras activator, ADH1 terminator, pUC ori, 2 micron ori, *LEU2*, Amp^r	-Leu, Amp^r	11.3
pSos MafB	ADH1 promoter, hSOS Ras activator, ADH1 terminator, pUC ori, 2 micron ori, *LEU2*, Amp^r, full length MafB	-Leu, Amp^r	12
pMyr MafB	GAL1 promoter, myristylation signal anchor protein, *CYC1* teminator, *2* micron ori, f1 ori, *URA3*, Cam^r, full length MafB	-Ura, Cam^r	6.9
pSos Col 1	ADH1 promoter, hSOS Ras activator, ADH1 terminator, pUC ori, 2 micron ori, *LEU2*, Amp^r, Murine 72 kDa type IV collagenase (aa 148-357)	-Leu, Amp^r	11.9
pMyr Lamin C	GAL1 promoter, myristylation signal anchor protein, *CYC1* teminator, *2* micron ori, f1 ori, *URA3*, Cam^r, human lamin C (aa 67-230)	-Ura, Cam^r	6.5
pMyr SB	GAL1 promoter, myristylation signal anchor protein, *CYC1* teminator, *2* micron ori, f1 ori, *URA3*, Cam^r, Sos-binding protein	-Ura, Cam^r	7.2

2.1.1.6. CytoTrap® Yeast Strain Genotype

Strain	Genotype
cdc25H	*MATα, ura3-52, his3-200, ade2-101, lys2-801, trp1-901, leu2-3, 112, cdc25-2* Gal^+

2.1.2. BACTERIAL STRAIN FOR MOLECULAR CLONING

Strain	Genotype
DH5α	F^-, ϕ80*lac*ZΔM15, Δ(*lac*ZYA-*arg*F)U169, *deo*R, *rec*A1, *end*A1, *hsd*R17(r_k^-, m_k^+), *pho*A, *sup*E44, *thi*-1, *gyr*A96, *rel*A1, λ^-.

2.1.3. OLIGODEOXYRIBONUCLEOTIDE PRIMER SEQUENCES FOR POLYMERASE CHAIN REACTION AMPLIFICATION

Description	Primer Sequence*
TM3/β2-IL/TM4 (282-450) 5' cloning primer	5'-AT**GAATTC**GACATGTACCTAATGGGGTGC-3'
TM3/β2-IL/TM4 (282-450) 3' cloning primer	5'-AT**GGATCC**GGAGGCTGGAGTTTAGTTCAC-3'
β2-IL/TM4 (303-450) 5' cloning primer	5'-CG**GGATCC**AACTACATCTTCTTTGGG-3'
β2-IL/TM4 (303-450) 3' cloning primer	5'-AT**GGATCC**GGAGGCTGGAGTTTAGTTCAC-3'
α1-IL (304-384) 5' cloning primer	5'-AT**GAATTC**GCCACAGTAAACTATTTCAAC-3'
α1-IL (304-384) 3' cloning primer	5'-AT**GGATCC**GGTTTTCTTGGGTTCTGGCGG-3'
α1-N (1-224) 5' cloning primer	5'-AT**GAATTC**CAGCCCTCCCAAGATGAAC-3'
α1-N (1-224) 3' cloning primer	5'-AT**GGATCC**GTAGCCGATTTTTCTCTTC-3'
β2-N (1-220) 5' cloning primer	5'-AT**GAATTC**CAGAGTGTCAATGACCCTAG-3'
β2-N (1-220) 3' cloning primer	5'-AT**GGATCC**GTAGCCAATGTTTCTTTTC-3'
pSOS α1-N (1-224) 5' cloning primer	5'-TATT**GGATCC**GACAGCCCTCCCAAGAT-3'
pSOS α1-N (1-224) 3' cloning primer	5'-CG**GCGGCCGC**GTAGCCGATTTTTCTCTTC-3'
pSOS β2-N (1-220) 5' cloning primer	5'-TATT**GGATCC**CTCAGATGGTCAATGACC-3'
pSOS β2-N (1-220) 3' cloning primer	5'-CG**GCGGCCGC**GTAGCCATGTTTCTTTTC-3'
pMYRα1-N (1-224) 5' cloning primer	5'-TATT**GAATTC**CAGCCCTCCCAAGATGAAC-3'
pMYRα1-N (1-224) 3' cloning primer	5'-TATT**CTCGAG**GTAGCCGATTTTTCTCTTC-3'
pMYRβ2-N (1-220) 5' cloning primer	5'-AT**GAATTC**CAGAGTGTCAATGACCCTAG-3'
pMYRβ2-N (1-220) 3' cloning primer	5'-AT**GTCGAC**GTAGCCAATGTTTCTTTTC-3'
β3-IL (306-425) 5' cloning primer	5'-TATT**GGATCC**TTTTCTTTGGACGAGGCT-3'

β3-IL (306-425) 3' cloning primer	5'-TATT**CTGCAG**TCTGTCTATGGCATTCAC-3'
KIAA0531(1-957)	5'-TTAT**GAATTC**ATGGCGGATCCAGCCGAAT-3'
KIAA0531(1-957)	5'-TTAT**GTCGAC**TTATTTCTGGTAGTGAGTGG-3'
KIAA1042 (1-953) 5' cloning primer	5'-TATT**GAATTC**CACATGGCATTGGTT-3'
KIAA1042 (1-953) 3' cloning primer	5'-TATT**GGATCC**TCACCGTAAGCTAGT-3'
KIAA1042(124-283) 5' cloning primer	5'-TTAT**GAATTC**CGGGATTTAGAATTGGCC-3'
KIAA1042(124-283) 3' cloning primer	5'-TTAT**CTCGAG**TTACTCCTCTTGCTGG-3'
pAS2-1 5' sequencing primer	5'-GACTGTATCGCCGGTATTGC-3'
pGADT7 5' sequencing primer	5'-TATTCGATGATGAAGAAGATACCCCACCAAACC-3'
pGBKT7 5' sequencing primer	5'-TCATCGGAAGAGAGTAG-3'
DnaJ end sequencing primer	5'-CCTCAGGAGTACATCATGC-3'

*Bold sequences show restriction enzyme recognition sites.

2.1.4. PARAMETERS FOR POLYMERASE CHAIN REACTION AMPLIFICATION PROGRAM

PCR was carried out following the general program described in Section 2.2.2.6. Specific parameters for each sequence are detailed below.

Sequence	**Annealing Temperature (30 s per cycle)**	**Extension Time Per Cycle at 72°C**
α1(1-224)	55°C, decreasing by 0.5°C per cycle for 10 cycles, then 50°C for 15 cycles.	2 min
β2(1-220)		2 min
β3(306-425)		1 min
β2(282-450)	52°C	1 min
β2(303-450)	52°C	1 min
KIAA0531(1-957)	52°C	8 min
α1(304-384)	53°C	1 min
KIAA1042(1-953)	53°C	8 min
KIAA1042(124-283)	53°C	1 min

2.2. METHODS

2.2.1. BACTERIAL METHODS

2.2.1.1. MAINTENANCE OF BACTERIAL CELLS

Bacterial cells were streaked onto LB (Luria-Bertani medium: 1% (w/v) peptone, 0.5% (w/v) yeast extract, 0.5% (w/v) NaCl, 2% (w/v) agar, pH 7.0) agar and incubated overnight inverted at 37°C. Liquid cultures of bacteria were prepared by inoculation of 1 ml or 5 ml LB liquid medium (as above, but without agar) with a single colony from a plate culture and incubated overnight with shaking at 37°C. Stock cultures were stored in 15% (v/v) glycerol at -80°C.

2.2.1.2. PREPARATION OF CHEMICALLY COMPETENT BACTERIAL CELLS

Competent cells were prepared by growth in medium containing magnesium and a carbon source (glucose) and stored in a glycerol-polyethylene glycol (PEG) solution (Nishimura *et al.*, 1990). Bacterial cells from a glycerol stock were streaked onto LB agar using a sterile loop and incubated overnight at 37°C. A 5 ml LB culture was inoculated with a single colony from the overnight plate culture and incubated overnight at 37°C with shaking. A 1 ml aliquot of overnight bacterial culture (e.g. DH5α *E. coli*) was transferred to 100 ml sterile LB medium, containing 10 mM $MgSO_4$ and 0.2% (w/v) glucose in a 500 ml flask. The culture was incubated at 37°C with shaking for 2 h. After this the $OD_{\lambda = 600\ nm}$ was checked approximately every 30 min on a spectrophotometer until OD = 0.7-0.9. The cells were chilled on ice for 10 min and kept cold for all subsequent steps.

The cells were harvested by centrifugation at 2500 g for 10 min at 4°C in pre-cooled centrifuge tubes. The supernatant was discarded and the pellets were pooled by resuspension in 1 ml chilled resuspension solution (LB with 0.2% (w/v) glucose and 10 mM $MgSO_4$). The cells were added to 5 ml storage solution (LB containing 36% (v/v) glycerol, 12% (w/v) PEG and 12 mM $MgSO_4$), mixed thoroughly and 100 µl aliquots dispensed into chilled 0.5 ml tubes. Cells were stored immediately at -80°C.

2.2.1.3. PREPARATION OF ELECTROCOMPETENT BACTERIAL CELLS

Electrocompetent bacterial cells were used for electroporation transformations of the plasmid DNA recovered from yeast cells since they are more efficient in the uptake of

DNA. The protocol was carried out as described in the Clontech Yeast Protocols Handbook. A 5 ml LB starter culture was prepared by inoculation with a single bacterial colony. The culture was incubated overnight at 37°C with shaking. A 250 ml LB culture was inoculated with 250 µl of the overnight culture. This was incubated at 37°C with shaking until the $OD_{\lambda = 600\ nm}$ reached 0.6. The culture was poured into 5 x pre-chilled 50 ml centrifuge tubes and incubated on ice for 15 min. Cells were harvested by centrifugation at 4,000 g and 4°C for 15 min. The supernatants were decanted and each pellet resuspended in 50 ml 10% (v/v) glycerol. The tubes were centrifuged as before. The supernatants were removed and each pellet resuspended in 25 ml 10% (v/v) glycerol, centrifuged as before and the supernatants discarded. The pellets were pooled and resuspended in 5 ml 10% glycerol. The suspension was centrifuged once more. The glycerol was removed and the pellet resuspended in 0.5 ml 10% (v/v) glycerol. The cells were dispensed in 50 µl aliquots into 0.5 ml tubes. These were stored immediately at -80°C.

2.2.1.4. CHEMICAL TRANSFORMATION OF COMPETENT BACTERIAL CELLS

Chemically competent bacterial cells were transformed using a 42°C heat-shock. DNA (200-400 ng DNA [1-5 µl ligation mix]) was added to 100 µl competent cells (e.g. DH5α *E. coli*) and incubated on ice for 10 min. The cells were heat-shocked at 42°C for 1 min, then immediately returned to ice and chilled for a further 10 min. Each reaction was added to a 1 ml aliquot of SOC (1% (w/v) peptone, 0.5% (w/v) yeast extract, 0.5% (w/v) NaCl, 2% (w/v) agar, pH 7.0, 0.2% (w/v) glucose, 25 mM KCl, 10 mM $MgCl_2$ and 10 mM $MgSO_4$) in a 1.5 ml centrifuge tube. This was incubated at 37°C with shaking for 1 h. After the incubation, 100 µl of each reaction was spread onto LB agar containing the appropriate antibiotic (e.g. 50 µg/ml ampicillin). The plates were incubated at 37°C overnight.

2.2.1.5. ELECTROPORATION TRANSFORMATION OF COMPETENT BACTERIAL CELLS

Electrocompetent bacterial cells were transformed with plasmid DNA isolated from yeast as described in the Clontech Yeast Protocols Handbook. This method was used, because it yielded a higher transformation efficiency compared to chemical

transformation. This increased efficiency is necessary, because the large amount of yeast genomic DNA, isolated along with the plasmid DNA, reduces transformation efficiency. A 50 µl aliquot of electrocompetent DH5α cells was thawed and transferred to a pre-chilled electroporation cuvette with a 0.1 cm gap between electrodes. Plasmid DNA was added to the sample and the cuvette placed in a Flowgen EasyjecT Plus electroporator. Cells were shocked at 2500 V for 5 msec. The electroporator was set at 25 µF capacitance and 201 Ohms shunt resistance. The cells were immediately suspended in 1 ml SOC solution and transferred to a 1.5 ml tube. The suspension was incubated at 37°C for 1 h with shaking. Cells were harvested by centrifugation at 9000 rpm for 2 min. The pellet was resuspended in 100 µl residual SOC solution and plated onto LB agar containing an appropriate antibiotic. Agar plates were incubated at 37°C overnight until colonies appeared.

2.2.1.6. SMALL-SCALE PREPARATION OF PLASMID DNA

Up to 20 µg plasmid DNA were purified from bacterial cells using the Qiagen miniprep system following manufacturer's guidelines. In this procedure the bacteria are lysed in alkaline conditions then DNA is isolated by adsorption to a silica-gel membrane at a high salt concentration. DNA is eluted from the silica membrane by reducing the concentration of salt.

Cells from an overnight bacterial culture of 5 ml were harvested by centrifugation for 10 min at 4000g at 4°C. The supernatant was removed and the pellet resuspended in 250 µl resuspension buffer P1 (50 mM Tris-HCl, pH 8.0, 10 mM EDTA, 100 µg/ml RNase). The suspension was transferred to a 1.5 ml microcentrifuge tube and 250 µl lysis buffer P2 (200 mM NaOH, 1% (w/v) SDS) were added. The tube was inverted 4-6 times to mix and the lysis reaction was allowed to continue for no more than 5 min. Next, 350 µl neutralisation buffer, N3 (contains acetic acid), was added and the tube was inverted 4-6 times to mix. The cell debris was separated from the suspension by centrifugation at 15000 g for 10 min, producing a compact white pellet. The supernatant containing the DNA was transferred to a miniprep column in a 2 ml collection tube. This was centrifuged at 15000 g for 30-60 sec at room temperature and the flow-through discarded. The column was washed by adding 500 µl buffer PB (contains isopropanol) and centrifuging for 30-60 sec. The flow-through was again discarded. The spin column was washed a second time by adding 750 µl buffer PE (contains ethanol) and

centrifuging for 30-60 sec. The flow-through was discarded and the tube centrifuged for an additional 60 sec to remove any residual wash buffer. The spin column was placed in a clean 1.5 ml tube and the DNA eluted by addition of 50 µl buffer EB (10 mM Tris·HCl, pH 8.5) to the centre of the spin column. This was left to stand for 1 min at room temperature and the eluted DNA collected by centrifugation for 1 min.

2.2.1.7. MEDIUM-SCALE PREPARATION OF PLASMID DNA

Qiagen midi prep kits were used for medium scale (up to 100 µg DNA) preparations of plasmid DNA following manufacturer's guidelines.

Cells from an overnight bacterial culture of 50 ml were harvested by centrifugation for 30 min at 4°C and 6000 g. The supernatant was removed and the pellet resuspended in 4 ml resuspension buffer P1. The cells were lysed by addition of 4 ml lysis buffer P2. The tube was inverted gently 4-6 times and the lysis reaction allowed to continue for no more than 5 min. The reaction was stopped by addition of 4 ml pre-chilled neutralisation buffer P3 (3.0 M potassium acetate, pH 5.5). This was inverted 4-6 times to mix and incubated on ice for 15-20 min. The tube was then centrifuged at 20000 g for 30 min at 4°C. During the centrifugation, a Qiagen Tip-100 was equilibrated by adding 4 ml buffer QBT (750 mM NaCl; 50 mM MOPS, pH 7.0; 15% (v/v) isopropanol; 0.15% (v/v) Triton®X-100). After the centrifugation step, the supernatant was added to the column and allowed to flow through by gravity. The column was washed with 2 x 10 ml buffer QC (1.0 M NaCl, 50 mM MOPS, pH 7.0, 15% (v/v) isopropanol) and the DNA eluted into a new centrifuge tube using 5 ml buffer QF (1.25 M NaCl, 50 mM Tris-HCl, pH 8.5, 15% isopropanol). The DNA was precipitated by addition of 3.5 ml isopropanol at room temperature and centrifugation for 30 min at 4°C and 20000 g. The supernatant was carefully decanted and 4 ml 70% (v/v) ethanol added to the tube. This was mixed briefly using a vortex mixer and the DNA harvested by centrifugation for 15 min at 4°C and 20000 g. The supernatant was decanted and the tube centrifuged again to remove any residual ethanol. The pellet was air-dried for 5-10 min and resuspended in 50-100 µl buffer EB by incubation at 37°C mixing occasionally. The recovered DNA concentration was determined on a spectrophotometer using $OD_{\lambda = 260\ nm}$ readings; an $OD_{\lambda = 260\ nm} = 1$ indicates approximately 50 µg/ml double stranded (ds) DNA.

2.2.1.8. LARGE-SCALE PREPARATION OF PLASMID DNA

Qiagen HiSpeed Plasmid Maxi preps were used to isolate large scale (up to 750 μg) preparations of plasmid DNA following manufacturer's guidelines.

A single colony from a selective bacterial culture on agar was used to inoculate a 5 ml liquid LB selective culture, which was incubated for approximately 8 h with shaking at 37°C. This culture was used to inoculate a second culture at a 1/1000 dilution in 250 ml selective LB, which was incubated for 12-16 h. The cells were harvested by centrifugation at 6000 g for 15 min at 4°C. The bacterial pellet was resuspended in 10 ml buffer P1. The cells were lysed by addition of 10 ml buffer P2, mixing gently and incubating at room temperature for 5 min. During the incubation, a cap was attached to a Qiafilter Maxi cartridge. After the 5 min incubation, 10 ml pre-chilled buffer P3 was added to neutralise the reaction. The lysate was poured into the Qiafilter cartridge and incubated at room temperature for 10 min to allow the protein precipitate to float to the surface. During this incubation a HiSpeed Maxitip was equilibrated by addition of 10 ml buffer QBT. After the incubation, the cap was removed from the Qiafilter cartridge, the plunger inserted and the lysate filtered through the cartridge into the HiSpeed tip. As the cleared lysate flowed through the tip, plasmid DNA bound to the resin. The tip was washed with 60 ml buffer QC and the DNA was eluted into a 50 ml tube using 15 ml buffer QC. DNA was precipitated from the eluate by adding 10.5 ml isopropanol and incubating at room temperature for 5 min. During the incubation, the plunger was removed from a 30 ml syringe and a QIAprecipitator Maxi module attached to the outlet. The precipitated eluate was poured into the syringe and filtered through the precipitator. The DNA in the precipitator was washed with 2 ml 70% ethanol and dried by pushing air through the precipitator twice, ensuring that the syringe was removed from the precipitator before removing the plunger each time. The DNA was collected in a 1.5 ml tube by eluting with 0.5 ml buffer EB.

2.2.2. DNA MANIPULATION

2.2.2.1. FLAT BED AGAROSE GEL ELECTROPHORESIS

Flat bed agarose gel electrophoresis was used to check for the presence and/or purity of DNA. A 1% (w/v) agarose gel was prepared in 1 x TBE (89 mM Tris, 89 mM boric acid, 2 mM EDTA, pH 8.5). The agarose was heated until dissolved and cooled slightly before adding 1 μl ethidium bromide per 50 ml of agarose and pouring it into a gel-

casting tank with assembled casting gates and a well comb. The gel was left to solidify at room temperature before removing the well comb and casting gates. The tank was filled with 1 x TBE until the wells were submerged. DNA samples were loaded onto the gel with 1 µl 6 x loading dye per 5 µl sample (6 x stock loading dye: 50% (v/v) glycerol, 20 mM EDTA, 100 mM Tris-HCl, pH 8.0, 0.1% (w/v) bromophenol blue and 0.1% (w/v) xylene cyanole). The tank lid was affixed and a constant voltage of 56 V was applied to the gel for approximately 1 h. The gel was lifted carefully from the tank and the DNA visualised over ultraviolet (UV) light. The Kodak EDAS 120 program (Electrophoresis Documentation and Analysis System) was used for gel analysis.

2.2.2.2. DNA EXTRACTION FROM AN AGAROSE GEL

The Qiaex II gel extraction procedure was used to purify DNA from agarose gel slices for subsequent use in molecular cloning. DNA bands were excised from an agarose gel using a scalpel. Exposure of DNA to UV light was minimised by holding the gel slightly away from the light source in a transparent plastic tray. The weight of the gel slice was determined by placing in a pre-weighed 1.5 ml tube (up to 250 mg agarose per tube). For DNA fragments 100-4000 bp, 3 volumes buffer QX1 (contains sodium perchlorate) to 1 volume of gel were added (e.g. 300 µl QX1 buffer per 100 mg gel). For fragments larger than 4 kb, 3 volumes buffer QX1 and 2 volumes H_2O were added. The Qiaex II was resuspended by vortex mixing for 30 sec, then added to the sample and mixed (add 10 µl Qiaex II to ≤2 µg DNA and 30 µl to 2-10 µg DNA). The agarose was solubilised by incubation in an Eppendorf thermomixer at 50°C for 10 min to allow the Qiaex II to bind the DNA with shaking to keep the Qiaex II in suspension. The Qiaex II was harvested by centrifugation at 15000 g for 30 sec and the supernatant removed. The pellet was washed with 500 µl buffer QX1 to remove residual agarose, washed twice with 500 µl buffer PE each time. The pellet was air-dried for 10-15 min (until the pellet became white). To elute the DNA, 20 µl 10 mM Tris-HCl, pH 8.5, was added and the pellet resuspended by vortex mixing. This suspension was incubated at room temperature for 5 min for fragments ≤4 kb or at 50°C for 5 min for fragments 4-10 kb. Qiaex II silica-gel was collected at the bottom of the tube by centrifugation at 15000 g for 30 sec and the supernatant, containing the eluted DNA, was carefully transferred to a clean tube.

2.2.2.3. ETHANOL PRECIPITATION OF DNA

This protocol is used for the recovery and purification of DNA. To the DNA sample, 0.1 volumes of 3 M sodium acetate and 2.5 volumes of 100% (v/v) ethanol were added. The sample was then incubated on ice for 15 min. The sample was centrifuged at 15000 g for 30 min at 4°C. The supernatant was removed and the pellet washed with 100 µl 70% (v/v) ethanol. This was centrifuged again at 15000 g for 1 min. The ethanol was removed and the DNA centrifuged again briefly. Any remaining ethanol was removed with a pipette and the pellet air-dried for approximately 10 min at room temperature. The pellet was then resuspended in 20 µl H_2O or 10 mM Tris-HCl, pH 8.5.

2.2.2.4. RESTRICTION ENZYME DIGESTIONS

Small scale (10 µl) restriction enzyme digestions containing ~ 0.5 µg DNA were used to analyse DNA samples and large scale (50 µl) restriction enzyme digestions containing ~2-5 µg DNA were used to prepare DNA for subsequent cloning. The reaction mixture contained 1 x enzyme buffer, 1-3 units of enzyme, the DNA sample to be digested and was made up to the final volume with sterile H_2O. Digestion reactions were incubated for 1-2 h at 37°C.

2.2.2.5. DESIGN OF OLIGONUCLEOTIDE PRIMERS FOR POLYMERASE CHAIN REACTION (PCR)

Oligodeoxyribonucleotide primers (see Section 2.1.3 for list of primers used) were designed and purchased from Proligo for use in amplification of specific DNA sequences by PCR. The amplified products were used for molecular cloning as outlined in Figures 2.1 and 2.2. The following criteria were used as guidelines for primer design:

1. Each primer should contain approximately 18-24 annealing bases.
2. The GC content should be 40-60% with minimal internal repeats or complementary sequences to avoid internal primer binding.
3. Ideally, a 3' GC 'clamp' is included to improve binding specificity at the 3' end.
4. Where restriction enzyme recognition sites were included in primer sequences, extra bases were added to aid enzyme cutting near the end of DNA sequences. The number of extra bases added to the primer were chosen following the enzyme manufacturer's recommendations.

5. Where a pair of primers was used, the melting temperatures (Tm) should be within 10°C of each other as mismatched Tms lead to mis-priming at different annealing temperatures. In general, the annealing temperature is assumed to be 5°C below the melting temperature.

Melting temperatures were calculated using the Wallace rule:

i.e. Melting Temperature = (4[G + C] + 2[A + T]) (Wallace *et al.*, 1979),

[G + C] = Nº of guanine + cytosine bases, [A + T] = Nº of adenine + thymine bases.

An NCBI BLAST search was always carried out on each primer against the Genbank database to check for homology to other sequences.

2.2.2.6. POLYMERASE CHAIN REACTION AMPLIFICATION

PCR reactions were used to amplify specific DNA sequences from either Clontech rat brain cDNA, or previously constructed plasmids, for use in subsequent cloning. A PCR reaction mix was prepared containing 200-500 ng template DNA, 0.2 mM dNTPs (0.2 mM each of adenine, thymine, guanine and cytosine deoxynucleotides in 10 mM Tris-HCl, pH 8.5), 0.2 μM forward primer, 0.2 μM reverse primer, 1 x Promega *Pfu* DNA polymerase buffer (20mM Tris-HCl, pH 8.8, 10mM KCl, 10mM $(NH_4)_2SO_4$, 2mM $MgSO_4$, 0.1% Triton® X-100 and 100 μg/ml nuclease-free BSA), 1.5 units Promega *Pfu* DNA polymerase enzyme and the volume made up to 100 μl with sterile H_2O. Samples were mixed briefly in thin-walled 0.5 ml tubes and PCR was carried out in a Hybaid PCR Express thermal cycler.

Typical PCR program:

Step 1: 1 cycle of 94°C* for 4 min.

Step 2: 30 cycles of 94°C for 30 sec.

50-55°C# for 30 sec.

72°C† for 2 min per 1 kb of DNA to be amplified.

Step 3: 1 cycle at 72°C for 7 min.

* Denaturation step.

Annealing temperature is calculated as 5°C below the melting temperature (Section 2.2.2.5.). This value varied depending on the primer sequence.

† DNA extension step.

Once finished, the temperature was held at 4°C. The products were analysed by restriction enzyme digestion (Section 2.2.2.4) and analysed by flat bed agarose gel electrophoresis (Section 2.2.2.1).

2.2.2.7. DNA PURIFICATION

The Qiagen PCR purification kit was used to remove enzymes and other impurities from DNA samples after reactions such as PCR (Section 2.2.2.6). In this protocol, filtration columns containing a silica-gel membrane binds DNA under high salt concentrations, but allows elution of DNA when salt conditions are reduced.

Buffer PB was added to the DNA reaction mix in a 5:1 ratio (e.g. 500 µl buffer to 100 µl reaction mix). The sample was transferred to a Qiaquick spin column and centrifuged at 15000 g for 1 min. The flow-through was discarded. The DNA was washed by adding 750 µl buffer PE and centrifuging as before. The sample was centrifuged again to ensure all residual buffer was removed. The Qiaquick spin column was inserted into a clean 1.5 ml centrifuge tube. DNA was eluted by adding 30-50 µl buffer EB and centrifuging as before.

2.2.2.8. LIGATION OF DNA SEQUENCES INTO CLONING VECTORS

Ligation reactions for insertion of a DNA fragment into a cloning vector were set up containing 1 x ligation buffer (66 mM Tris-HCl, pH 7.5, 5 mM $MgCl_2$, 1 mM dithiothreitol (DTT), 1 mM ATP), 1.5 units T4 DNA ligase and linearised vector and insert DNA in a ratio of approximately 1:1. Each reaction was incubated overnight either at 16°C or thermocycling between 10°C for 1 min and 30°C for 1 min (Lund *et al.*, 1996).

2.2.2.9. DEPHOSPHORYLATION OF 5' VECTOR DNA ENDS

For plasmids linearised using a single restriction enzyme, dephosphorylation of 5' ends was necessary to prevent recircularisation of the vector during the subsequent ligation reaction. If a plasmid had been cut with two different enzymes 5' dephosphorylation was not necessary, but was still used to reduce background recircularisation. This background is due to incomplete digestion, leaving some plasmids cut by only one enzyme. Dephosphorylation was carried out in 1 x shrimp alkaline phosphatase (SAP) buffer (20 mM Tris-HCl, pH 8.0, 10 mM $MgCl_2$) with 1 unit of SAP enzyme. The

mixture was made up to its final volume with H_2O and incubated at 37°C for 1 h. SAP was heat-inactivated by incubation at 65°C for 15 min.

2.2.2.10. TA CLONING OF PCR PRODUCTS USING THE INVITROGEN TOPO pCR II VECTOR

Invitrogen TOPO® TA cloning is a method for the non-directional insertion of *Taq* polymerase-amplified PCR products into the pCR®II-TOPO plasmid vector. This strategy uses topoisomerase I instead of DNA ligase. When combined with the pCRII cloning vector, topoisomerase I binds and activates duplex DNA leading to a fast and efficient ligation. PCR products amplified by *Pfu* polymerase were first supplemented with 3' A overhangs in order to facilitate TA cloning. A reaction mix was prepared containing 1 x *Taq* polymerase buffer (20 mM Tris-HCl, pH 8.4, 50 mM KCl and 1.5 mM $MgCl_2$), 0.2 mM dNTPs, 0.5 units *Taq* polymerase enzyme and made up to 30 µl with purified PCR product. The mixture was incubated at 72°C for 30 min then chilled on ice.

A second reaction mix, containing 4.5 µl PCR product (with 3' A overhangs), salt solution (200 mM NaCl and 10 mM $MgCl_2$) and 0.5 µl TOPO® TA cloning vector, was prepared in a 0.5 ml microfuge tube and mixed briefly. The reaction was incubated at room temperature for 5 min and the resultant construct was subsequently transformed into competent bacterial cells (Section 2.2.1.4).

2.2.2.11. PCR SCREENING OF RECOMBINANT BACTERIAL COLONIES

Bacterial colonies resulting from transformation of competent DH5α cells (Section 2.2.1.4.) with plasmid DNA were screened by PCR amplification to verify recombinants. A PCR reaction mixture containing 1 x *Taq* polymerase buffer, 0.2 mM dNTP stock, 0.2 µM forward (vector) oligonucleotide primer stock, 0.2 µM reverse (insert) oligonucleotide primer stock, 1 unit *Taq* polymerase enzyme, made up to 15 µl with sterile H_2O, was prepared for each recombinant bacterial colony to be tested. LB liquid medium containing an appropriate antibiotic was dispensed in 1 ml aliquots into 1.5 ml tubes. Sterile 10 µl pipette tips were used to pick recombinant colonies from the overnight plate cultures. Each tip containing a colony was swirled in a 15 µl aliquot of PCR mix to act as DNA template. An appropriate PCR screening program (see Section 2.2.2.6. for a typical PCR program) was used to amplify the recombinant vector

construct DNA in these tubes. The remainder of the colony on the pipette tip was ejected into a tube of LB to inoculate the pre-culture. Liquid LB cultures were incubated at 37°C for 6-8 h with shaking.

After PCR amplification, each screening product was analysed by 1% agarose flat bed gel electrophoresis (Section 2.2.2.1) to identify true recombinants. Overnight cultures were prepared for each verified recombinant colony in 15 ml tubes, using 100 µl of the pre-culture in 5 ml LB inoculated with the appropriate antibiotic.

2.2.2.12. AUTOMATED SEQUENCING OF DNA

2.2.2.12.1. PCR for Sequencing Samples

Automated DNA sequencing was carried out on the Perkin Elmer ABI PRISM® 310 Genetic Sequencer. Sequencing reactions were based on the dideoxy chain-termination method (Sanger *et al.*, 1977). Dideoxynucleoside triphosphate terminators tagged with fluorescent dyes were used for detection. PCR reactions for sequencing samples were prepared using the ABI PRISM® BigDye™ terminator cycle sequencing ready reaction kit version 2.0. The BigDye™ terminator ready reaction mix contained premixed dye terminators, deoxynucleoside triphosphates, AmpliTaq DNA polymerase, FS, r*Tth* pyrophosphatase and $MgCl_2$. PCR samples contained 0.5-1 µg DNA, 3.3 pmol forward (vector) primer, 2 µl BigDye™ terminator ready reaction mix, 2 µl 5 x sequencing buffer (400 mM Tris-HCl, pH 9.0 and 10 mM $MgCl_2$) and made up to 10 µl with H_2O. Sequences were amplified by PCR which added fluorescent labels to the ends of each sequence. Once amplified, ethanol precipitation was used to purify the DNA (Section 2.2.2.3) and each DNA pellet was resuspended in 20 µl template suppression solution.

2.2.2.12.2. Preparation of the ABI PRISM® 310 Genetic Sequencer

The sequencing block, buffer vials and polymer syringe of the Perkin Elmer ABI PRISM® 310 Genetic Sequencer were cleaned with warm sterile H_2O and dried thoroughly prior to sequencing. These were reassembled in the machine along with a sequencing capillary. The syringe was filled with performance optimised polymer (POP6) and attached to the block. The block was very slowly filled with polymer, opening each valve in turn, ensuring no air bubbles remained in the system. The capillary was filled with polymer using the Sequence Fill Capillary software function. Sample names were added to a Sample Sheet and used to prepare an Injection List for

the sequencing run. DNA samples in template suppression solution were heated to 95°C for 2 min, centrifuged briefly and added to the sample tray. The results were analysed using the ABI PRISM® 310 sequencing analysis program and visualised using the Chromas or vector NTI program.

2.2.2.13. DNA ANALYSIS PROGRAMS

The cDNA sequences for rat $GABA_A$ receptor subunits were found using the NCBI Genbank database (http://www.ncbi.nlm.nih.gov/). Sequences of positive clones, obtained from yeast two-hybrid library screening, were identified by performing a BLAST search of this database. Architectural domains of sequences were determined using the online Simple Modular Architecture Research Tools (S.M.A.R.T.) application from embl-heidelberg (http://smart.embl-heidelberg.de/) and previously published data.

2.2.3. YEAST PROTOCOLS

2.2.3.1. MAINTENANCE OF YEAST CELLS

GAL4 Yeast Strain

AH109 yeast cells were streaked onto yeast extract peptone dextrose with adenine (YPAD) agar (2% (w/v) peptone; 1% (w/v) yeast extract; 2% (w/v) glucose; 0.003% (w/v) adenine hemisulphate; 2% (w/v) agar; pH 5.8) and incubated at 30°C for 2-4 days. Once cells appeared, agar plates were stored at 4°C. Liquid cultures were inoculated by a single colony from the plate culture and incubated overnight at 30°C with shaking. Cells were stored in 15% (v/v) glycerol at -80°C.

Modified Lex A Yeast Strain

Carried out as for GAL4, except:

1. The yeast strain, L40, was used.

CytoTrap® Yeast Strain

Carried out as for GAL4, except:

1. The yeast strain, cdc25Hα, was used.
2. Incubation steps carried out at 30°C for the GAL4 system were carried out at 22-25°C for the CytoTrap® system.

2.2.3.2. PREPARATION OF COMPETENT YEAST CELLS

2.2.3.2.1. Method 1: Standard High Efficiency Yeast Transformation

The GAL4 System

This was carried out following the standard high efficiency yeast transformation protocol of Agatep *et al.* (1998). AH109 yeast cultures were grown in medium containing lithium acetate, single-stranded (ss) DNA and polyethylene glycol, to produce high efficiency competent cells. A 5 ml liquid culture of YPAD in a loose-lid 15 ml tube was inoculated with a single yeast colony from an agar plate culture and mixed thoroughly to resuspend the cells ensuring no clumps remained. The culture was incubated overnight at 30°C with shaking. The $OD_{\lambda = 600\ nm}$ was determined and the volume of culture containing $2.5x10^8$ cells was used to inoculate a 50 ml YPAD culture in a 250 ml flask to give a starting titre of $5x10^6$ cells/ml. This culture was incubated at 30°C with shaking for 3-4 h. The $OD_{\lambda = 600\ nm}$ was taken at intervals after 2-3 h until it reached >2. The cells were harvested by centrifugation in a 50 ml tube at 2500 g for 5 min. The supernatant was decanted and the pellet resuspended in 20 ml H_2O to wash the cells. This suspension was centrifuged again to pellet the cells and the supernatant removed. The pellet was resuspended in 900 µl H_2O and transferred to a 1.5 ml tube. The cells were harvested by centrifugation at 15000 g for 1 min, the supernatant removed and the cells resuspended in 700 µl 1M lithium acetate. The cell suspension was incubated at 30°C for 10 min. Aliquots of 50 µl 1M lithium acetate cell suspension were dispensed into 0.5 ml tubes. Cells were harvested by centrifugation at 5600 g for 1 min and the supernatant removed. The samples were then ready to proceed to the transformation reaction.

The Modified Lex A System

Carried out as for the GAL4 system, except:

1. The yeast strain, L40, was used.

The CytoTrap® System

Carried out as for the GAL4 system, except:

1. The yeast strain, cdc25Hα, was used.
2. Any incubations carried out at 30°C for the GAL4 system were carried out at 22-25°C for the CytoTrap® system.
3. The overnight culture was prepared in 20 ml.
4. The $OD_{\lambda = 600\ nm}$ of the overnight culture was ~1.

5. The starting $OD_{\lambda = 600\ nm}$ for the second culture was 0.2.
6. The second culture was grown until the $OD_{\lambda = 600\ nm}$ reached 0.7.
7.

2.2.3.2.2. Method 2: High Efficiency Transformation of Intact Yeast Cells Using Single Stranded Nucleic Acids as a Carrier

The GAL4 System

For some assays an alternative method for the preparation of competent cells was used to produce a higher transformation efficiency. This was carried out following the yeast transformation protocol of Schiestl and Gietz (1989). For this method, a 5 ml liquid YPAD culture in a loose-lid 15 ml tube was inoculated with a single AH109 yeast colony from an agar plate culture and was mixed thoroughly to resuspend the cells ensuring no clumps remained. The culture was incubated overnight at 30°C with shaking. The $OD_{\lambda = 600\ nm}$ was determined and a second culture of 50 ml was inoculated with the first to a starting $OD_{\lambda = 600\ nm}$ of 0.15. This culture was incubated at 30°C with shaking until the $OD_{\lambda = 600\ nm}$ reached 0.4. The cells were harvested by centrifugation at 2500 g for 5 min and the supernatant removed. The pellet was resuspended in 25 ml H_2O and centrifuged again as before. The H_2O was decanted and the pellet resuspended in 10 ml LiSorb solution (100 mM lithium acetate; 10 mM Tris, pH 8.0; 1 mM EDTA, pH 8.0; 1 M sorbitol). The cells were centrifuged again and the pellet resuspended in 300 ml LiSorb solution. To this suspension, 30 µl of 2 mg/ml pre-boiled single stranded salmon sperm DNA were added. The cells were dispensed into 0.5 ml tubes in 25 µl aliquots and were used immediately or stored at -80°C.

The Modified Lex A System

Carried out as for the GAL4 system, except:

1. The yeast strain, L40, was used.

The CytoTrap® System

Carried out as for the GAL4 system, except:

1. The yeast strain, cdc25Hα, was used.
2. Incubations carried out at 30°C for the GAL4 system were carried out at 22-25°C for the CytoTrap® system.
3. The $OD_{\lambda = 600\ nm}$ of the overnight culture was ~1.
4. The starting $OD_{\lambda = 600\ nm}$ of the second culture was 0.2.
5. The second culture was grown until the $OD_{\lambda = 600\ nm}$ reached <0.7.

2.2.3.3. TRANSFORMATION OF COMPETENT YEAST CELLS

2.2.3.3.1. Method 1: Standard High Efficiency Yeast Transformation

The GAL4 System

This was carried out following the standard high efficiency yeast transformation protocol of Agatep *et al.* (1998). The transformation mix contained 120 µl 50% (w/v) PEG, 18 µl 1M lithium acetate, 25 µl 2 mg/ml salmon sperm DNA in TE (10 mM Tris-HCl; 1 mM Na_2 EDTA, pH 8.0) and 16 µl sterile H_2O per transformation. This was mixed thoroughly and added to the competent AH109 cell pellets along with 0.2-0.5 µg of each appropriate plasmid vector. Each transformation was mixed again and incubated at 30°C for 30 min, then heat-shocked by incubation at 42°C for 30 min. The tubes were centrifuged at 5600 g for 1 min to pellet the cells and the transformation mix was removed. Each pellet was resuspended in 0.5 ml H_2O and 100 µl of the suspension plated out onto each appropriate type of dropout medium (plates lacking leucine and tryptophan [-leu/-trp] showed successful transformation and those lacking leucine, tryptophan, histidine and adenine [-leu/-trp/-his/-ade] showed a protein-protein interaction). The plates were incubated at 30°C for 4 days - 2 weeks for colonies to grow.

The Modified Lex A System

Carried out as for the GAL4 system, except:

1. The yeast strain, L40, was used.
2. Plates lacking only leucine, tryptophan and histidine (-leu/-trp/-his) were used to test for protein-protein interactions.

The CytoTrap® System

Carried out as for the GAL4 system, except:

1. The yeast strain, cdc25Hα, was used.
2. Incubations carried out at 30°C for the GAL4 system were carried out at 22-25°C for the CytoTrap® system.
3. Transformed cells were plated out only onto plates lacking leucine and uracil (-U/-L) at this stage.
4. Once colony growth was seen on plates lacking leucine and uracil they could be tested for protein-protein interactions. To do this, 3 x colonies were picked for each transformation and patched onto 2 x -U/-L plates containing glucose-based media and 2 x -U/-L plates containing galactose-based media. This was done by

resuspending each colony in 25 µl H_2O and dropping 2.5 µl of the suspension onto each plate. One of each type of plate was placed at 22-25°C and the two remaining plates placed at 37°C. Colony growth on -U/-L plates showed an interaction.

2.2.3.3.2. Method 2: High Efficiency Transformation of Intact Yeast Cells Using Single Stranded Nucleic Acids as a Carrier

The GAL4 System

This was carried out following the yeast transformation protocol of Schiestl and Gietz (1989).To each tube of competent AH109 yeast cells was added 5 µl pre-boiled 2 mg/ml salmon sperm DNA, 100 µl LiPEG (100 mM lithium acetate; 10 mM Tris, pH 8.0, 1 mM EDTA, pH 8.0, 40% (w/v) PEG [mwt 3350]) solution and 200-400 ng of each plasmid construct. Samples were vortex mixed and incubated at room temperature for 20 min. Next, dimethyl sulphoxide (DMSO) (12 µl) was added and each sample was heat-shocked at 42°C for 10 min. Transformations were centrifuged at 5600 g for 1 min to collect the cells and the transformation mix was removed. Each pellet was resuspended in 200 µl H_2O and 100 µl of transformation mix plated onto each appropriate dropout selection media. All plates were incubated at 30°C for 4 days - 2 weeks for colonies to appear.

The Modified Lex A System

Changes are as above for modified Lex A system, method 1.

The CytoTrap® System

Changes are as above for CytoTrap® system, method 1.

2.2.3.4. LIBRARY-SCALE SEQUENTIAL TRANSFORMATION OF YEAST USING THE GAL4 SYSTEM

Library screening of a rat brain cDNA library in the pGAD10 fish vector was carried out according to the 30 x scaled up sequential transformation of Agatep *et al.* (1998).

A bait plasmid containing the target protein fusion construct was initially transformed into the yeast strain, AH109, using the 1 x transformation protocol described in Section 2.2.3.3.1. The single transformant was selected for using -Trp dropout media. A single colony was picked from the selective plate and used to inoculate a 50 ml selective -Trp dropout culture. This was incubated overnight at 30°C with shaking. The $OD_{\lambda = 600\ nm}$ of

the overnight culture was determined and the volume of culture containing 7.5 x 10^8 cells calculated. The cells from this volume of culture were harvested by centrifugation at 3000 g for 5 min. The cell pellet was resuspended in 150 ml YPAD to give a starting cell titre of 5 x 10^6 cells/ml. This culture was incubated at 30°C with shaking until the cells had gone through 2 divisions; this corresponded to an $OD_{\lambda = 600\ nm}$ of 2.0. The cells were harvested by centrifugation as above. The supernatant was removed and the cells resuspended in H_2O. The centrifugation was repeated and the supernatant removed. The pellet was resuspended in 3 ml 100 mM lithium acetate and incubated in a water bath at 30°C for 15 min. The cells were harvested by centrifugation once more and the lithium acetate discarded. The pellet was resuspended by addition of the transformation mix. The transformation mix contained 7.20 ml 50% (w/v) PEG, 1.08 ml 1.0 M lithium acetate, 1.50 ml 2 mg/ml ssDNA, X* ml plasmid DNA and 1.02 - X ml H_2O. The resuspended cells were incubated at 30°C for 30 min rotating gently several times to keep the contents thoroughly mixed and to maintain even heat distribution. The cells were heat-shocked by incubation at 42°C for 45 min mixing the contents at intervals. The transformants were harvested by centrifugation at 3000 g for 5 min and the transformation mix removed. The pellet was resuspended in 20 ml H_2O and plated onto 50 x -Trp/-Leu/-His/-Ade 150 mm selective plates in 400 µl aliquots. All plates were incubated at 30°C for 4-7 days until colonies grew. Potential positive interactors were verified as described in Figure 2.3.

* The value of X depends on the amount of library DNA to be screened.

2.2.3.5. THE β-GALACTOSIDASE FILTER LIFT ASSAY

The β-galactosidase assay is a colorimetric assay used to verify positive yeast colonies, i.e. putative protein-protein interactions, from GAL4 or mLexA assays by detecting the presence of β-galactosidase reporter gene activity, induced by GAL4 activation. In this assay, 5-bromo-4-chloro-3-indolyl-β-D-galactopyranoside (X-GAL) is converted by β-galactosidase to indolyl-blue (dichloro-dibromo-indigo) and galactose, causing the formation of a blue, water insoluble precipitate.

Filter papers (#5 Whatman) were cut to fit a petri dish. One was soaked in Z buffer (60 mM Na_2HPO_4, 40 mM NaH_2PO_4, 10 mM KCl, 1 mM $MgSO_4$, pH 7.0) with 0.27 ml β-mercaptoethanol and 1.67 ml X-GAL (20 mg/ml stock solution) per 100 ml, while the other was placed over the plate of colonies to be tested. Once the filter paper was

completely wetted, it was removed from the plate and dipped in liquid nitrogen for at least 10 sec. Once frozen, the filter paper was thawed at room temperature and placed colony-side-up onto the filter pre-soaked in Z buffer. The filters were incubated at 30°C until the colonies turned blue (30 min-8 h).

2.2.3.6. THE α-GALACTOSIDASE OVERLAY ASSAY

The α-galactosidase assay is used to test for α-galactosidase activity in recombinant 2-4 day old colonies from GAL4 or mLexA assays, which is induced by GAL4 activation.
A Z-buffer/agarose solution was prepared (10 ml Z-buffer with 0.2% (w/v) agarose and 25 µl 5-bromo-4-chloro-3-indolyl-α-D-galactopyranoside (X-α-GAL) stock solution per 30 ml plate) and heated in the microwave to dissolve. The solution was then cooled slightly, poured over the yeast test plate and allowed to set. Once solid, the gel was incubated at 30°C until the colonies turned blue (30 min-8 h).

2.2.3.7. ISOLATION OF PLASMID DNA FROM YEAST

Plasmid DNA was isolated from yeast cells as described in the Clontech Yeast Protocols Handbook. A patch of cells was scraped from a selective agar plate and resuspended in 50 µl H_2O in a 1.5 ml microfuge tube. A 10 µl aliquot of 5 U/µl lyticase solution was added to each sample and mixed thoroughly. Tubes were incubated at 37°C with shaking for 1 h. A 10 µl aliquot of 20% (w/v) SDS was added to each tube and mixed thoroughly for 1 min. Samples were frozen at -20°C for 1 h, then thawed at room temperature to ensure complete lysis of the cells. The tubes were mixed vigorously and the sample volume was adjusted to 200 µl with TE buffer (200 mM Tris, 20 mM EDTA, pH 7.0). A 200 µl aliquot of phenol:chloroform:isoamyl alcohol (25:24:1) was added to each tube and the tube mixed vigorously for 5 min. All samples were centrifuged at 15000 g for 10 min. The upper (aqueous) phase was transferred to a new 1.5 ml tube. DNA was precipitated by addition of 8 µl 10 M ammonium acetate and 500 µl 100% ethanol. Tubes were incubated at -80°C for 1 h. Precipitated DNA was harvested by centrifugation at 15000 g for 10 min. The supernatant was removed and the tubes centrifuged for a further 1 min. Residual supernatant was removed and the pellets left to air-dry for 10 min. Each pellet was resuspended in 20 µl 10 mM Tris-HCl, pH 8.5 and stored at -20°C until needed.

2.2.3.8. PREPARATION OF YEAST CULTURES FOR PROTEIN EXTRACTION

Yeast protein extracts were prepared as described in the Stratagene CytoTrap® Vector Kit instruction manual. For each transformed yeast strain to be assayed a 5 ml culture was prepared, using a single colony dispersed in SD medium. A 10 ml culture of untransformed yeast in YPAD was also prepared for use as a negative control. Each culture was incubated at 30°C with shaking at 220-250 rpm until the $OD_{\lambda = 600\ nm}$ reached > 1.0. Each culture was centrifuged at 1000 g for 5 min at room temperature to pellet the cells and the supernatant was removed. Protein extracts were prepared for each cell pellet using the following method.

2.2.3.9. PREPARATION OF PROTEIN EXTRACTS FROM YEAST USING A UREA-/SDS METHOD

For each protein extraction a yeast cell pellet, prepared as described in Section 2.2.3.8, was resuspended in 1 ml pre-chilled H_2O. To each cell suspension, 150 µl freshly prepared NaOH/ β-mercaptoethanol (β-ME) buffer (1.85 M NaOH, 7.5% (v/v) β-ME) were added. Samples were vortex mixed for 30 s and incubated on ice for 15 min. Samples were vortex mixed again for 30 s and 150 µl 55% trichloroacetic acid (TCA) were added to each. Cells were vortex mixed as before and incubated on ice for 10 min. Protein extracts were harvested by centrifugation at 12 000 g for 10 min at 4°C. The supernatant was removed and each sample was centrifuged again to remove any residual supernatant. Each pellet was resuspended in 300 µl SU buffer (5% (w/v) SDS, 8 M Urea, 125 mM Tris-HCl, pH6.8, 0.1 mM EDTA, 0.005% (w/v) bromophenol blue) with 15 mg/ml dithiothreitol (DTT) added immediately prior to resuspension of the pellet. Tris-base (pH8.0) was used to neutralise the samples if the SU buffer turned yellow on resuspeding the pellet. All samples were heated to 65°C for 3 min and dispensed into 100 µl aliquots and stored at -80°C until needed.

2.2.3.10. YEAST TWO-HYBRID LIBRARY SCREENING

Yeast two-hybrid screening of a rat brain cDNA library was carried out in order to identify proteins interacting with $GABA_A$ receptor subunits. All screens were carried out in the GAL4 system, using the DNA-BD vector, pGBKT7, and the AD vector, pGAD10.

2.2.3.10.1. Construction of the Bait Plasmid

A fusion protein was constructed, comprising the DNA binding domain (BD) of the GAL4 transcription factor fused to the protein fragment to be screened. To do this, cDNA encoding the protein of interest was inserted into the multiple cloning site of the GAL4 yeast two-hybrid bait plasmid, pGBKT7, ensuring that it was in frame with the GAL4 BD. Figures 2.1 and 2.2 summarise the stages in molecular cloning.

2.2.3.10.2. Transformation of Yeast with the Bait Plasmid

In order to maximise the efficiency of library screening, a sequential transformation was used. The DNA-BD plasmid was first introduced into yeast by a single small-scale transformation (described in Sections 2.2.3.2 and 2.2.3.3) and selected on media lacking tryptophan (-W). The resulting yeast strain, containing the DNA-BD construct, was then amplified in a selective, -W, liquid culture and transformed with library cDNA in a subsequent reaction. This method was chosen to ensure that the amount of DNA-BD plasmid would not limit the potential number of interactions with library clones.

2.2.3.10.3. Small-Scale Library Screen

A small-scale test screen was carried out to determine the transformation efficiency of the library. Yeast, pre-transformed with DNA-BD plasmid, were transformed in a small-scale reaction with 1 μg of rat brain library cDNA and spread onto a large (140 mm diameter) plate containing media selective for both plasmids. The number of resulting colonies were counted and used to determine the amount of library DNA necessary for adequate coverage in a large-scale screen. As the library had a complexity of $>10^6$ independent clones, at least this number needed to be screened for adequate coverage.

2.2.3.10.4. Large-Scale Library Screen

To screen the library, a 30 x scaled up transformation was carried out on yeast pre-transformed with DNA-BD plasmid DNA as described in Section 2.2.3.4. Transformants from the large-scale library screen were selected for on growth media lacking tryptophan, leucine, histidine and adenine (-4 dropout media).

2.2.3.11. ANALYSIS OF PUTATIVE POSITIVE CLONES

2.2.3.11.1. Reporter Gene Activity

One week after the large-scale library screen a sterile loop was used to pick colonies from selective plates and re-streak them onto fresh media. It was possible that excess library clones (not interacting with the DNA-BD construct) could have become incorporated into a particular cell. These extra clones tend to be lost over time under selective conditions. Therefore, to ensure that only the plasmid causing reporter gene activity remained, cells were re-plated onto -4 dropout media every week during analysis. Selective liquid media was used to grow up colonies for use in preparation of glycerol stocks (Section 2.2.3.1). Yeast colonies containing putative positive interactors were assayed for β-galactosidase activity, as described in Section 2.2.3.5.

2.2.3.11.2. DNA analysis of positive clones

Plasmid DNA was extracted from yeast cells as described in Section 2.2.3.7 for clones which were found to be positive for β-galactosidase activity. Only very small amounts of DNA could be obtained using this method, therefore DH5α bacterial cells were transformed with plasmid DNA extracts by electroporation (see Sections 2.2.1.3 and 2.2.1.5) and amplified to increase the number of plasmids. Plasmid DNA was purified from bacteria as described in Section 2.2.1.6.

DNA encoding each positive clone was excised from its AD vector by restriction enzyme digestion (Section 2.2.2.4). Digestion products were electrophoresed on a 1% agarose gel and their size determined. DNA sequencing was also carried out for each construct. A BLAST search was performed against the NCBI GenBank database for each sequence in order to identify clones and subsequently to determine whether each clone was in frame with the GAL4 AD.

2.2.3.11.3. Yeast Analysis of Positive Clones

Interactions of clones which were positive for β-galactosidase activity and which were found to be in frame with the GAL4 AD were verified by co-transformation of yeast in small-scale reactions with the original DNA-BD construct. If the clones grew on selective media on re-transformation, they were then co-transformed with DNA-BD constructs containing other $GABA_A$ receptor sequences (see Chapter 4, Figure 4.3) to check for the specificity of interaction with the original DNA-BD.

2.2.4. PROTEIN METHODS

2.2.4.1. WESTERN BLOTTING

2.2.4.1.1. Preparation of Sodium Dodecyl Sulphate (SDS)-Polyacrylamide Gels

Sodium dodecyl sulphate (SDS) polyacrylamide gels were used for the electrophoresis of protein samples. Clean glass gel casting plates were assembled in a gel casting apparatus ensuring a water tight seal. The plates were separated using 0.75 mm plastic spacers. A 10% acrylamide separating gel solution was prepared (375 mM Tris, 2 mM EDTA, pH 8.8, 10% acrylamide:bisacrylamide [37:1], 0.1% (w/v) SDS and 0.2% (v/v) TEMED). The solution was degassed for 20 min in a vacuum. Once degassed, 165 µl 10% (v/v) ammonium persulphate solution (APS) were added and the mixture poured immediately between the gel casting plates (approximately 7 ml per gel), leaving enough space between the top of the gel and the top of the glass plates to fit the length of the well comb teeth. The gel was overlaid with butanol (60 µl per gel) and left to polymerise for 30 min. Once the gel had polymerised, the butanol was removed and the top of the separating gel was rinsed with water. Next, a stacking gel solution was prepared (125 mM Tris, 2 mM EDTA, pH 6.8, 0.1% (w/v) SDS, 6% (v/v) acrylamide:bisacrylamide [37:1], 0.125% (v/v) TEMED) and degassed for 20 min. Once the stacking gel solution was degassed, 0.2% APS was added and 1 ml of the solution was immediately overlaid onto the separating gel. A well comb was inserted and the stacking gel was left to polymerise for 30 min. Once the polymerisation was complete, the well comb was removed and the gel was ready for use in SDS-polyacrylamide gel electrophoresis (SDS-PAGE).

2.2.4.1.2. Sodium Dodecyl Sulphate Polyacrylamide Gel Electrophoresis (SDS-PAGE)

Protein extracts from yeast prepared as described in Section 2.2.3.9 were analysed by SDS-PAGE under reducing conditions prior to western blotting. Each gel was placed into a gel cassette and assembled in a gel tank. 1 x electrode buffer (50 mM Tris, 384 mM glycine, 3.6 mM EDTA, pH 8.8, SDS 1.8% (w/v)) was prepared and poured into the gel tank to cover the bottom of the gel and the reservoir between the gels. The well combs were removed from the gels and each well was rinsed with electrode buffer using a pipette. Samples were boiled at 80°C for 5 min. A Hamilton microlitre syringe was used to load 15 µl of sample to the base of each well, adding buffer alone to any unused

well. Electrophoresis was carried out at maximum voltage and 20 mAmp constant current for approximately 3 h, until the dye front reached the bottom of the gel.

2.2.4.1.3. Electrophoretic Transfer of Proteins From Polyacrylamide Gels to Nitrocellulose Membranes

Once protein samples had been separated on by SDS-PAGE, they were transferred to a nitrocellulose membrane. Four pieces of blotting paper slightly larger than the gel and one piece of nitrocellulose membrane about the same size as the gel were cut out per gel and each soaked in 1 x transfer buffer (12.5 mM Tris; 96 mM glycine; 20% (v/v) methanol). The SDS-PAGE apparatus was disassembled and the gel retrieved. A transfer cassette was assembled by placing a pre-soaked sponge onto one side of the cassette, followed by two pieces of pre-soaked blotting paper. The polyacrylamide gel was placed on top of this and the nitrocellulose membrane, pre-soaked in transfer buffer, arranged to cover it, being careful to exclude air bubbles. Two more pieces of blotting paper were added over the blot and covered by a second piece of sponge. The cassette was closed and placed in a Hoefer electro-transfer tank, containing 800 ml 1 x transfer buffer, with the nitrocellulose side of the assembly facing the positive electrode. Proteins were transferred from the gel to the nitrocellulose by applying a constant voltage of 50 V for 2.5 h or 14 V overnight.

2.2.4.1.4. Antibody Detection of Proteins

The transfer apparatus was disassembled and the nitrocellulose membrane was placed in phosphate buffered saline (PBS) (136.9 mM NaCl, 2.68 mM KCl, 10 mM Na_2HPO_4, 1.76 mM KH_2PO_4, pH 7.4) containing 5% (w/v) Marvel milk powder and 100 µl Tween®-20 per 100 ml to block non-specific sites on the nitrocellulose membrane. This was incubated at room temperature with gentle shaking for 1 h. The blot was incubated in a primary antibody solution at an appropriate dilution in PBS containing 2.5% (w/v) Marvel milk powder. The antibody solution was removed and the blot washed for 4 x 10 min each in PBS containing 2.5% Marvel milk powder and 0.1% (v/v) Tween®-20. The relevant horseradish peroxidase (HRP) conjugated secondary antibody was diluted to an appropriate concentration in PBS containing 2.5% Marvel milk powder. This was added to the blot and incubated for 1 h shaking gently at room temperature. As the secondary antibody was added, 10 ml 1.25 mM luminol and 100 µl p-coumaric acid were thawed

in the dark at room temperature. The secondary antibody solution was removed and the blot washed for 3 x 20 min in PBS containing 0.1% (v/v) Tween®-20. The 10 ml thawed luminol, 100 µl p-coumaric acid and 5 µl H_2O_2 were added to a tray and mixed. The blot was immediately incubated in this solution for 1 min. After 1 min, excess luminol was removed from the blot which was then placed between two sheets of plastic along with a strip of tracker tape to show the positions of molecular weight standards. The blot was developed and analysed on the Syngene GeneGnome chemiluminescence bio-imaging system.

FIGURE 2.1. SUMMARY OF THE STAGES IN DIRECT MOLECULAR CLONING

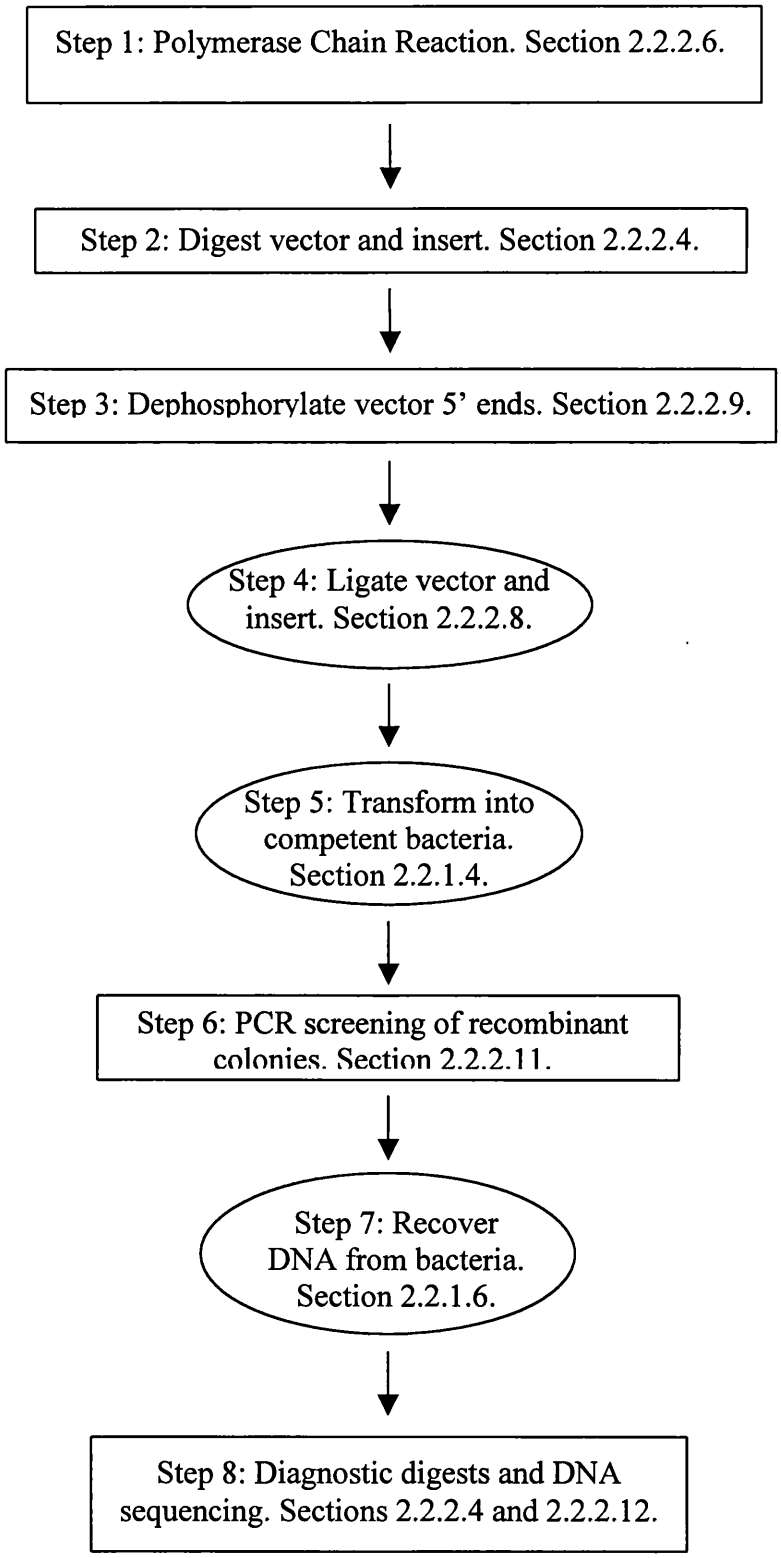

FIGURE 2.2. SUMMARY OF THE STAGES IN INDIRECT MOLECULAR CLONING

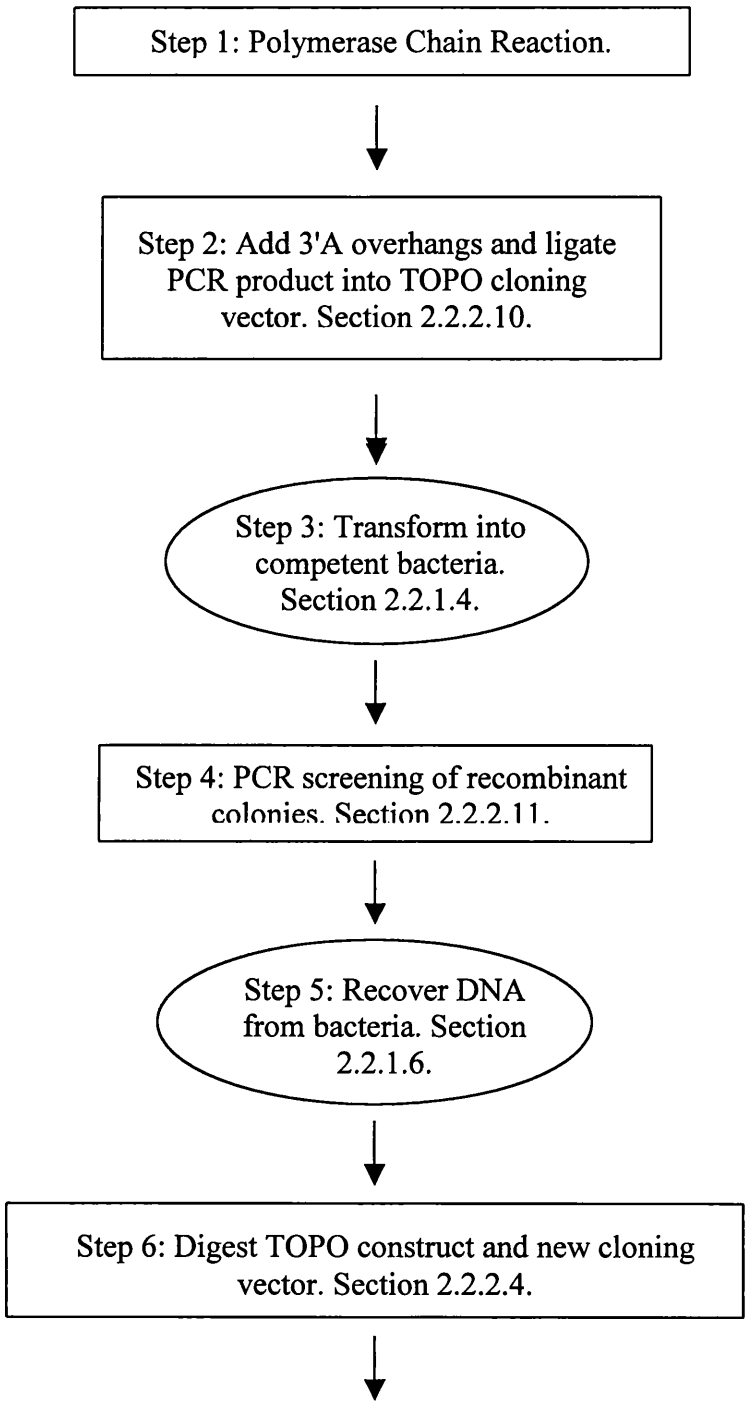

The rest of the cloning procedure then continues as for direct cloning from step 2, Figure 2.1.

FIGURE 2.3. SUMMARY OF THE STAGES IN YEAST TWO-HYBRID LIBRARY SCREENING AND VERIFICATION OF PUTATIVE INTERACTING cDNA CLONES

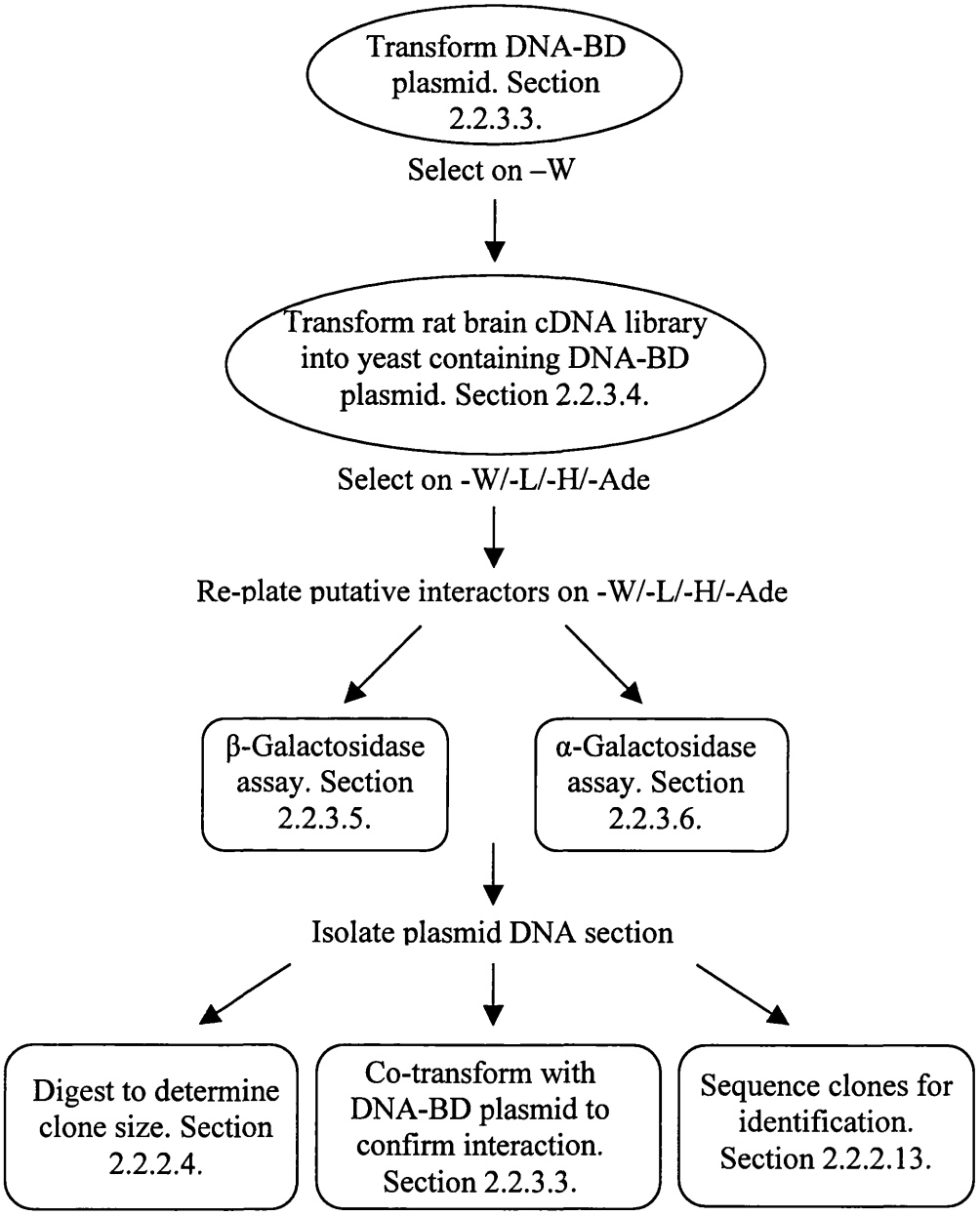

CHAPTER 3:
RESULTS 1

3.1. INTRODUCTION TO THE YEAST TWO-HYBRID SYSTEM

3.1.1. DETECTING PROTEIN-PROTEIN INTERACTIONS

Formation of protein complexes, regulation of protein activity and transmission of information through cellular signalling pathways are all dependent on protein-protein interactions. Identifying which proteins will interact and characterising how they interact is important for understanding how cell structure and function is maintained and how communication within and between cells is achieved. There are many biochemical and molecular techniques available for the study of these interactions.

Classical *in vitro* biochemical techniques include chemical cross-linking, in which protein interactions are studied by inducing covalent linkages between proteins, using chemicals chosen for their specific reactivity with certain functional side groups, under a particular set of conditions i.e. pH, temperature, chemical concentrations (reviewed by Golemis, 2002). Another example is affinity chromatography, in which a protein of interest is attached to a solid support matrix either directly or via a fusion protein linker, commonly glutathione-S-transferase (GST), and used to isolate associating proteins from a protein extract. The associated proteins are then harvested from the complex by elution with a competing ligand, a change in pH or by the addition of sodium dodecyl sulphate (SDS). The associated protein products obtained using either of these techniques may then be visualised by staining with Coomassie Brilliant Blue after SDS-polyacrylamide gel electrophoresis (SDS-PAGE). Interactions detected by these methods generally need to be substantiated using a second technique such as co-immunoprecipitation, to confirm that the interaction is likely to occur under physiological conditions. Co-immunoprecipitation is based on the premise that many protein associations formed *in vivo* are conserved after cell lysis under non-denaturing conditions. To determine whether two known proteins interact, the first protein of interest is precipitated by a specific antibody. A second protein, stably associated with the first, may be co-precipitated in this complex and detected by western blotting with a specific antibody against the second protein. A potential drawback of co-immunoprecipitation is that some interactions may not be stable enough to withstand the extraction process. Therefore weak or transient interactions may remain undetected. Another drawback of co-immunoprecipitation is the need for further analytical techniques, e.g. mass spectroscopy, for the identification of novel interactors. For mass spectroscopy, proteins are ionised by electrospray ionisation (ESI) or matrix assisted

laser desorption ionisation (MALDI). The mass/charge (m/z) ratio of the resulting ions is analysed and screened against a protein database to identify the protein. (reviewed by Yates III, 2000). The development of tandem mass spectroscopy (MS/MS) negates the need for protein separation by SDS-PAGE as particular proteins may be identified directly from samples of a protein complex (McCormack *et al.*, 1997).

Fluorescence resonance energy transfer (FRET) (Heim and Tsien, 1996; Mitra *et al.*, 1996) and, more recently, green fluorescent protein proximity imaging (GFP-PRIM) (De Angelis *et al.*, 1998), have been used to study associated proteins *in vivo*. FRET allows the detection of protein-protein interactions by light emission from one (acceptor) fluorophore upon excitation by another (donor) fluorophore (e.g. a GFP mutant producing. blue, yellow or cyan light emission) when the two fluorophores are brought within close enough proximity for energy transfer to occur. This technique is useful for detection of heterotypic protein interactions, but is insensitive for detecting homotypic interactions as two proteins carrying the same fluorophore will not cause FRET. GFP-PRIM was developed specifically for the detection of homotypic interactions, using a GFP mutant, thermotolerant GFP (ttGFP) which fluoresces at two spectral wavelengths. The ratio of light emission at these peaks is the same for a monomeric protein at constant temperature, but differs for the same protein in a homo-oligomeric state. The ratio between these spectral peaks can therefore be used to measure the extent of homotypic association for a particular tagged protein.

Another important *in vivo* technique is the yeast two-hybrid assay. This technique has been used extensively in this thesis and is discussed in detail below.

3.1.2. THE YEAST TWO-HYBRID SYSTEM AS A METHOD FOR DETECTING PROTEIN INTERACTIONS

The yeast two-hybrid system is a sensitive genetic technique for detecting protein-protein interactions *in vivo* (Fields and Song, 1989). The sensitivity of this assay enables the detection of weak or transient protein-protein interactions that may not be recognised by classical biochemical methods, such as co-immunoprecipitation (see Section 3.1.1). The yeast two-hybrid assay can be used to confirm an interaction between two known proteins, to characterise these interactions i.e. by determination of specific interaction domains, and for the detection of novel interactions of a known protein by screening of a yeast two-hybrid cDNA library. The simple library screening procedure is a high throughput technique which, once established, can be easily used to

screen large numbers of proteins and requires only small amounts of cDNA of full-length or even partial gene sequences, as opposed to the large amounts of purified protein required for some classical biochemical techniques (Criekinge and Beyaert, 1999). There are many cDNA libraries currently available for screening, obtained from various species and tissue types. This enables specific screening for interacting proteins that are expressed in the native tissue of a test protein, thus reducing the likelihood of identifying interactions that would not normally occur *in vivo* i.e. interactions between two proteins that are not expressed in the same tissues. Additionally, the assay is performed *in vivo* which may mean that test proteins are more likely to be found in their native conformation.

3.1.3. THE BASIS OF THE GAL4 YEAST TWO-HYBRID SYSTEM

The original, GAL4, yeast two-hybrid assay was developed by Fields and Song in 1989, following a series of studies on transcription factors (TFs) and the discovery that they are modular proteins, composed of separable, functional domains (reviewed by Fields and Sternglanz, 1994). The TF DNA binding domain (DNA-BD) binds the upstream activation sequence (UAS) of a gene promoter and the acidic activation domain (AD) initiates assembly of gene transcription apparatus. Characterisation of these domains showed that when separated, each TF domain retains its independent function, but is incapable of activating gene transcription alone (Keegan *et al.*, 1986). TF function may be restored if the two domains are brought within close proximity to each other, or to the complementary domain of another transcription factor. For example, the AD of the GAL4 TF activates transcription in yeast when fused to the DNA-binding LexA repressor if a LexA operator is present near the beginning of the transcription start site (Brent and Ptashne, 1985). These studies suggested a novel method for detection of protein-protein interactions, as demonstrated by Fields and Song (1989), using the known interactors SNF1 and SNF4.

In the GAL4 yeast two-hybrid system, the AD and the DNA-BD of the GAL4 TF are encoded separately by two yeast expression vectors. Each vector contains a series of unique restriction enzyme recognition sites (the multiple cloning site) at the C-terminal end of the encoded AD or DNA-BD domain. DNA encoding test proteins is cloned into the vectors, such that the C-terminus of each TF domain becomes fused to the N-terminus of a protein of interest to create an in frame gene fusion construct. Both the AD and DNA-BD fusion constructs are introduced into yeast cells containing an

inactivated GAL4 gene. A positive interaction between the two test proteins brings the AD and DNA-BD together, thus reconstituting transcription factor activity. The reconstituted GAL4 TF induces transcription of reporter genes under the control of the GAL4 promoter, leading to changes in the yeast reporter strain phenotype, which can be detected by growth selection and colorimetric assays. The genetic basis of the GAL4 yeast two-hybrid assay is represented schematically in Figure 3.1.1.

3.1.4. THE GAL4 YEAST TWO-HYBRID SYSTEM REPORTER GENES

The GAL4 transcription factor, along with its negative repressor, GAL80, is responsible for transcription of genes encoding the α- and β-galactosidase enzymes. In the yeast two-hybrid system, yeast strains have been engineered, such that nutritional selection genes have also been placed under the control of the GAL4 promoter. Figure 3.1.2 shows the four reporter genes used in the GAL4 yeast two-hybrid system. Screening for expression of these GAL4 dependent reporter genes provides a method for demonstrating protein-protein interactions between two-hybrid fusion constructs. The commonly used reporter genes *HIS3* and *ADE2* encode enzymes that are involved in the biosynthesis of histidine (H) and adenine (Ade), respectively. Colony growth on nutritional selective media lacking histidine and adenine (-H, -Ade) is a quick and simple assay for activation of *HIS3* and *ADE2* reporter genes. Colorimetric assays for the α- and β-galactosidase enzymes are commonly used as secondary screens for protein interactions. α- and β-Galactosidase enzymes are involved in facilitating proper digestion of carbohydrates. When expressed in yeast, β-galactosidase activity can be detected by a filter lift assay in which addition of 5-bromo-4-chloro-3-indolyl-β-D-galactopyranoside (X-GAL) is broken down into dichloro-dibromo-indigo (indolyl-blue) and galactose, causing the formation of a blue, water insoluble precipitate. α-Galactosidase activity is detected similarly to β-galactosidase, but uses 5-bromo-4-chloro-3-indolyl-α-D-galactopyranoside (X-α-GAL) as a substrate and, since α-galactosidase is a secretory protein, activity may be assayed directly on solid yeast media.

3.1.5. THE GAL4 YEAST TWO-HYBRID SYSTEM EXPRESSION VECTORS

In this thesis a combination of MATCHMAKER system 2 and system 3 plasmid vectors was used. Figure 3.1.3 shows plasmid maps for the GAL4 yeast two-hybrid vectors of

Clontech MATCHMAKER systems 2 and 3. The DNA-BD vector for MATCHMAKER GAL4 yeast two-hybrid system 2 is pAS2-1. This vector contains the GAL4 DNA-BD and replication origins for expression in bacteria and yeast. An ampicillin resistance gene provides antibiotic selection in bacteria and a tryptophan (W) marker allows nutritional selection in yeast. Unique restriction enzyme recognition sites in the multiple cloning site at the C-terminus of the TF domain facilitate insertion of DNA sequences into the vector. The AD vector used in this system was the MATCHMAKER library vector, pGAD10. This vector contains the GAL4 AD, replication origins for expression in bacteria and yeast, an ampicillin resistance gene for selection in bacteria, a leucine (L) marker for nutritional selection in yeast and a multiple cloning site for insertion of DNA encoding test proteins.

The MATCHMAKER 3 system vectors are pGADT7 and pGBKT7. These improved vectors are high copy number plasmids that include a hemagglutinin (HA) and a c-myc epitope tag, respectively. This makes specific antibodies unnecessary for detection of fusion proteins expressed in yeast. System 3 vectors also contain a nuclear localisation signal (NLS) which is incorporated into the N-terminus of the multiple cloning site. This enables test proteins that do not contain an intrinsic NLS to be directed to the nucleus. Compatible multiple cloning sites in pGADT7 and pGBKT7 aid direct transfer of inserts between these vectors. Incorporation of pGBKT7 into yeast allows increased transformation efficiency of AD vectors over yeast containing other DNA-BD vectors. This increases the likelihood of obtaining interacting proteins from a cDNA library. In the pGBKT7 vector the ampicillin resistance gene is replaced by a kanamycin resistance gene. This is useful for isolation of yeast AD plasmids from bacteria after library screening, as bacteria cannot accommodate more than one type of resistance marker at a time, leading to the expulsion of plasmids containing alternative resistance markers to those under selection.

The positive control plasmids for MATCHMAKER system 2 are pTD1-1 and pVA3-1. pVA3-1 is a DNA-BD vector, derived from pAS2-1, which contains a (W) yeast nutritional selection marker and encodes the murine oncogene, p53. pTD1-1 is the AD vector, derived from the AD plasmid, pACT2, which contains a (L) yeast selection marker and encodes the SV40 large T-antigen, respectively. As p53 and the large T-antigen are known to interact these fusion constructs are used to confirm the authenticity of the system. Empty AD and DNA-BD vectors, i.e. vectors containing no insert DNA, are used as negative controls to show that co-transformation of the AD and

DNA-BD domains alone does not lead to activation of reporter genes. The vectors for all MATCHMAKER systems are designed to be compatible, such that system 2 and system 3 vectors are interchangeable.

3.1.6. THE YEAST STRAIN, AH109

The yeast strain, AH109, was used for all GAL4 system assays. The genotype of AH109 yeast is shown in Section 2.1.1.2. Inactivation mutations in tryptophan and leucine genes ensure that yeast cannot grow on selective media lacking these amino acids unless transformed with plasmid vectors containing functional copies of these genes. Deletion mutations in the GAL4 and GAL80 genes prevent transcription activation of genes under their control. Histidine, adenine and *LacZ* genes have been placed under the control of the GAL4 responsive promoters *GAL1*, *GAL2* and *MEL1*, respectively. Functional transcription of the GAL4 responsive genes is only restored by interactions of exogenously introduced proteins fused to the separate GAL4 AD and DNA-BD TF domains. Introduction of two nutritional selection markers i.e. histidine and adenine, rather than histidine alone (as found in many other yeast strains), provides added stringency to the assay and reduces the occurrence of false positives due to leaky *HIS* activity. In these strains *HIS* activity must be regulated by addition of 3-amino-1, 2, 4,-triazole (3-AT), a selective inhibitor of the enzymatic activity of the *HIS3* gene product. The *MEL1* promoter controls the *MEL1*and *LacZ* reporter genes. These genes encode the α- and β-galactosidase enzymes, respectively.

3.1.7. THE LEXA AND MODIFIED LEXA YEAST TWO-HYBRID SYSTEMS

The LexA yeast two-hybrid system works on the same principle as the GAL4 system i.e. through reporter gene activation, but uses a prokaryotic rather than a eukaryotic TF. The DNA-BD fusion protein is the full-length LexA transcription factor, and the AD fusion protein is the blob 42 (B42) protein. These protein domains are used to activate transcription of the *E. coli* LacZ reporter gene. The LexA system reduces non-specific activation of reporter genes by protein-protein interactions between the TF fusion domains and endogenous yeast proteins since a prokaryotic TF is used in a eukaryotic system. It is not possible to tell prior to screening whether the GAL4 or the LexA system is more likely to identify a particular interactor for any given protein. Table

3.1.1 shows a comparison between reporter gene activation in the GAL4, LexA and mLexA yeast two-hybrid systems.

3.1.8. THE MODIFIED LEXA YEAST TWO-HYBRID SYSTEM EXPRESSION VECTORS

The modified (m) LexA yeast two-hybrid system is a hybrid-hybrid system between the GAL4 and LexA systems. The pGADT7 AD vector remains the same, but the pGBKT7 DNA-BD vector is replaced by pMBL33. Figure 3.1.4 shows the expression vectors used in the mLexA yeast two-hybrid system. The pMBL33 vector was constructed from the backbone of the GAL4 vector, pGBKT7, and the LexA DNA-BD of the LexA vector, pEG202-NLS, by homologous recombination (created by Dr Mike Beck). This gives the pMBL33 hybrid vector the same yeast nutritional selection marker (i.e. -W) and the same bacterial antibiotic selection marker (i.e. kanamycin) as the pGBKT7 vector, but the LexA transcription factor fusion protein and multiple cloning site of the LexA pEG202-NLS vector. Thus, reporter genes are activated by a LexA-GAL4 hybrid TF. Brent and Ptashne (1985) showed that this combination of TF domains is capable of activating reporter genes. Detection of reporter gene activation is by histidine nutritional selection (-His) and β-galactosidase activity only. Therefore, selection is less stringent than for the GAL4 system. The yeast strain, L40, is used for this assay as it contains LexA, rather than GAL4, activated reporter genes. In this assay the mLexA system was used in an attempt to study proteins which showed auto-activation in the presence of the eukaryotic GAL4 DNA-BD fusion protein while keeping similar selection criteria to the GAL4 assay (see Section 3.3).

3.1.9. THE YEAST STRAIN, L40

The yeast strain, L40, was used for all mLexA assays. The genotype of L40 yeast is shown in Section 2.1.1.4. This yeast strain contains deletion mutations in the tryptophan and leucine genes creating nutritional selection for expression of plasmid vectors containing functional copies of these genes. The *HIS3* and *lacZ* genes have been placed under the control of the LexA operator and transcription may only be induced by reactivation of the LexA transcription factor i.e. due to interactions between test proteins fused to the TF domains. Hence detection of protein-protein interactions is by

nutritional selection for histidine on solid yeast media and by β-galactosidase activity in filter lift assays.

3.1.10. THE CYTOTRAP® YEAST TWO-HYBRID SYSTEM

The CytoTrap® yeast two-hybrid system, originally the Sos recruitment system (Aronheim *et al.*, 1997), differs from both the GAL4 and the mLexA systems in that it is not dependent on transcription factor activation in the nucleus for detection of protein-protein interactions. Instead, interactions are detected in the cytoplasm of the temperature-sensitive yeast strain, cdc25H. Figure 3.1.5 shows a schematic representation of the basis of the CytoTrap® two-hybrid assay.

The CytoTrap® assay is based on a point mutation in the yeast *cdc25* gene which encodes a guanyl nucleotide exchange factor (GNF). Cdc25 is the yeast homologue of the human (h) *Sos* protein, responsible for activation of the Ras signalling pathway and regulation of cell growth. The mutation in the *cdc25* gene leads to a temperature-sensitive cdc25 protein, thus preventing cell growth at 37°C, but not at the permissive temperature of 25°C. It is possible to rescue the Ras signalling pathway with the hSos protein. However, a myristylation signal is required to target the hSos protein to the cell membrane where the interaction takes place. Expression vectors for this assay each contain a protein of interest fused to the N-terminus of either a myristylation signal, to carry the first protein to the cell membrane, or a functional copy of the human GNF, which activates Ras, but is not targeted to the membrane when expressed alone. A positive interaction between the two test proteins results in transport of hSos to the cell surface where it initiates the Ras signalling pathway, enabling cdc25H yeast cells to grow at 37°C. In this way, the CytoTrap® system allows the study of proteins that have an intrinsic transcription factor activity, or that require post-translational modifications, dependent on localisation to the cytoplasm, to be functional.

3.1.11. THE CYTOTRAP® YEAST TWO-HYBRID EXPRESSION VECTORS

The CytoTrap® expression vectors are pMyr and pSos. The pMyr vector encodes the v-Src myristylation signal under the control of the GAL1 promoter and contains origins of replication for bacteria and yeast. A chloramphenicol resistance gene allows antibiotic selection in bacteria and a uracil (U) marker allows nutritional selection for plasmid expression in yeast. The pSos vector encodes amino acids 1-1067 of the hSos

gene under the control of the ADH1 promoter and contains replication origins for both bacteria and yeast. Bacterial antibiotic selection is via an ampicillin resistance gene and nutritional selection in yeast is conferred by a leucine (L) marker. Plasmid maps for the pMyr and pSos vectors are shown in Figure 3.1.6.

There are five control plasmids for the CytoTrap® system. These are pSos-MafB, pSos-Col1, pMyr-MafB, pMyr-Lamin C and pMyr-SB. pSos-MafB and pMyr-MafB each encode the full-length v-maf musculoaponeurotic fibrosarcoma oncogene homologue B (MafB) protein which is known to form dimers *in vivo* and pMyr-SB encodes a Sos binding protein. Therefore the co-transformation of pSos-MafB with pMyr-MafB and pSos-MafB with pMyr-SB are used as positive control transformations that should result in cell growth at 37°C. pSos-Col1 encodes amino acids 148-357 of murine collagenase type IV and pMyr-Lamin C encodes amino acids 67-230 of human lamin C. Neither collagenase IV nor human lamin C interact with MafB, therefore the pairwise combinations pSos-MafB with pMyr-Lamin C and pSos-Col1 with pMyr-MafB are used as negative control reactions and should not allow cell growth at 37°C. Co-transformation of empty pMyr and pSos vectors is an additional negative control for this assay.

3.1.12. THE YEAST STRAIN, CDC25H

The yeast strain cdc25H was used for all CytoTrap® assays. The genotype of cdc25H yeast is shown in Section 2.1.1.6. Deletion mutations in this strain allow for nutritional selection of plasmid vectors expressing uracil and leucine marker genes. The point mutation in the cdc25 gene renders cell growth of this yeast strain temperature-sensitive. Introduction of expression vectors containing interacting proteins into yeast allows recruitment of hSos to the cell membrane and reconstitutes the Ras pathway to permit cell growth at 37°C.

All pSos vector fusion proteins are under the control of the ADH1 promoter which is constitutively expressed. However, the pMyr vector fusion proteins are under the control of the GAL1 promoter which is inhibited when yeast cells are grown on glucose-based media, but activated on galactose-based media. This means that cells containing interacting fusion proteins are able to grow on galactose-based, but not glucose-based media at 37°C. At 25°C cdc25H yeast do not require activation of the

Ras pathway by hSos. Therefore cells are able to grow on both glucose and galactose-based media, whether or not they contain interacting fusion proteins.

3.1.13. LIMITATIONS OF THE YEAST TWO-HYBRID SYSTEM

While the yeast two-hybrid assay provides a simple and convenient method for the rapid identification of protein-protein interactions, there are some limitations to this technique. The main drawback is the occurrence of false positives (MATCHMAKER GAL4 Two-Hybrid System 3 and Libraries User Manual). This is mainly due to activation of reporter genes by proteins with intrinsic transcription factor (TF) properties. It is also possible for a protein that does not normally function as a transcription factor to exhibit TF properties when localised to the nucleus in the yeast two-hybrid system (Ma and Ptashne, 1987). In addition to spurious TF properties, protein-protein interactions detected in the cytoplasm and/or nucleus may not represent actual interactions (reviewed by Fields and Sternglanz, 1994). In a yeast two-hybrid assay, proteins are overexpressed, making non-specific interactions more likely, due to the large quantities of protein present, although this does not seem to contribute significantly to the number of false positives detected. A list of the most common false positives identified using the yeast two-hybrid system is available at: http://www.fccc.edu/research/labs/golemis/main_false.html.

As well as the possible identification of false positives it is also possible that some true interactions may fail to be detected in the yeast two-hybrid system i.e. false negatives. This could be partially due to proteins that are not easily targeted to the nucleus, e.g. those containing particular localisation signals that target them to other subcellular locations. The incorporation of a nuclear localisation signal (NLS) into more recent yeast two-hybrid expression vectors was introduced to alleviate this problem. In addition, one reason for the smaller average size range of the MATCHMAKER library cDNAs, compared to those of other manufacturers, is that partial clones are less likely to include a competing localisation signal (Fields and Sternglanz, 1994). Post-translational modifications in yeast differ from those in mammalian cells and improper processing may prevent interactions dependent on these modifications, e.g. glycosylation and disulphide bond formation. However, it has been shown for some proteins that interactions dependent on these modifications are still possible (Ozenberger and Young, 1995). Attachment of the TF fusion domain may prevent interactions dependent on a free N-terminal domain. Test proteins are usually inserted at

the C-terminus of the TF fusion moiety for ease of cloning. However, for the LexA system, an expression vector has been created in which the test protein is inserted at the N-terminus of the TF domain. This has been shown to identify successfully interacting partners that were not found using the GAL4 system (Beranger *et al.*, 1997).

3.1.14. VARIATIONS OF THE YEAST TWO-HYBRID SYSTEM

Since the introduction of the original yeast two-hybrid system (Fields and Song, 1989), a number of modified versions of the assay have been created to allow the investigation of different types of protein interaction. The yeast one-hybrid assay was created to identify proteins that interact with DNA (Wang and Reed, 1993). In this assay the chosen target DNA element, together with specific reporter genes, is incorporated into the genome of a yeast reporter strain by homologous recombination. The resulting recombinant yeast strain is subsequently transformed with a plasmid encoding the AD of the GAL4 TF fused to a potential DNA-binding protein. Positive interactions are detected by the activation of inducible reporter genes which confer nutritional or enzymatic selection to recombinant yeast cells. Indirect protein-protein interactions or interactions dependent on the modification of one or both of the test proteins may be studied in another system, the yeast tribrid system (Osborne *et al.*, 1995). In this assay a third protein is transformed into a yeast reporter strain, together with the two test proteins. This protein may be a bridging protein that provides a link between two indirect interactors or may be required to stabilise a weak interaction. Alternatively, the third protein may be a modifying enzyme, required to activate one or both of the interactors, e.g. for interactions dependent on phosphorylation. These hybrid assays are all used to study positive interactions. However, proteins that dissociate interactions are also an important control mechanism in cells and these would not be detected in any of these systems. Thus, the reverse two-hybrid assay was created to enable identification of these inhibitory proteins through the use of a counter-selectable marker (Vidal *et al.*, 1996a; b). A positive interaction between proteins causes expression of a marker that is toxic to the cell. Inactivation mutations in proteins that normally interact, or addition of a third protein that blocks a known interaction prevents expression of the toxic marker, thus allowing cell growth on selective media.

The dependence of some protein interactions on post-translational modifications that only occur in mammalian cells is a particular problem in a yeast-based system. In an attempt to overcome this problem the mammalian two-hybrid system was developed

(Dang *et al.*, 1991; Vasavada *et al.*, 1991). Fusion proteins expressed in mammalian cells are more likely to fold into their native conformation and, therefore more likely to display their native function. Interactions may be assayed after 2-3 days, which is much faster than the 1-2 weeks for yeast. However, transfer of DNA is inefficient in this system and as a result screening of cDNA libraries for novel interactions is difficult. Therefore, this assay is generally used to confirm and characterise interactions already identified in yeast. Another variation on this assay is the bacterial two-hybrid system. The rapid growth-rate and high transformation efficiency of bacteria makes screening large cDNA libraries faster and increases the likelihood of identifying interactions with rare clones. Another advantage of using this prokaryotic system is that the number of false positives due to interactions with endogenous homologous proteins is reduced. The main drawback in this system is the inability to perform post-translational modifications. It has been shown here that there is a wide variety of hybrid systems, each developed with its own advantages and disadvantages. However, the original yeast two-hybrid assay remains the most widely used.

3.2. $GABA_A$ RECEPTOR SUBUNIT ASSEMBLY

3.2.1. RATIONALE FOR THE STUDY OF $GABA_A$ RECEPTOR α1 AND β2 SUBUNIT N-TERMINAL DOMAINS IN THE YEAST TWO-HYBRID SYSTEM

To understand the observed diversity of $GABA_A$ receptors, it is important to identify factors that are involved in determining which receptor subunits will co-assemble. Each $GABA_A$ receptor is composed of 5 from the 16 known subunits found in the adult mammalian central nervous system. These are α1-6, β1-3, γ1-3, δ, ε, θ and π. Each subunit confers distinct physiological and pharmacological attributes to the fully assembled receptor e.g. the γ2 subunit confers a benzodiazepine sensitivity (Pritchett *et al.*, 1989), which is modulated by the α subunit subtype associated with it (reviewed by Sieghart, 2000). The theoretical range of $GABA_A$ receptor subtypes with different properties, produced by all possible combinations and arrangements of the 16 subunits, is vastly greater than the number for which there is experimental evidence *in vivo* (Benke *et al.*, 1991, 1994; Duggan *et al.*, 1991; McKernan *et al.*, 1991; Fritschy *et al.*, 1992; Fritschy and Mohler, 1995; Jechlinger *et al.*, 1998). For example, the two most widely expressed $GABA_A$ receptors contain α1, β2 and γ2 or α2, β3 and γ2 subunits and these two subtypes alone account for 75-85% of all diazepam-sensitive $GABA_A$ receptors in rat brain, as determined by co-immunoprecipitation studies using subunit-specific antibodies (Benke *et al.*, 1991; Benke *et al.*, 1994). Other subunits are much less common. For example, the δ subunit is mainly found extrasynaptically in cerebellar granule cells and is most commonly associated with α1 and α6 subunits (Shivers *et al.*, 1989; Nusser *et al.*, 1998).

Multiple receptor subunits are often expressed at the same time in certain neurones, as determined by *in situ* hybridisation using antisense oligonucleotides to specific subunits (Wisden *et al.*, 1992; Laurie *et al.*, 1992a, b) and by the detection of subunit immunoreactivities in particular neurones (Fritschy and Mohler, 1995; Pirker *et al.*, 2000). However, not all subunits that are co-expressed in a particular cell type will co-assemble. For example, γ and δ subunits are both expressed in cerebellar granule cells, but form distinct receptor subpopulations i.e. γ2-containing receptors are found at synapses, while δ-containing receptors are found extrasynaptically (Nusser *et al.*, 1998). Therefore there must be mechanisms, other than transcriptional control, that regulate $GABA_A$ receptor subunit composition.

The N-terminal domains of $GABA_A$ receptor subunits have been implicated in receptor

assembly by studies involving the expression of full-length and truncated subunits in mammalian cells (Klausberger *et al.*, 2000; 2001; Sarto *et al.*, 2002a, b). Full-length α1, β3 and γ2 subunits were co-expressed in HEK 293 cells with or without truncated γ2 ($\gamma2_T$) subunits containing only the extracellular N-terminal domain. The $\gamma2_T$ fragments reduced the surface expression of $\alpha1\beta3\gamma2$ receptors, showing them to be competent for incorporation into the assembled receptor i.e. $\alpha1\beta3\gamma2_T$, but not for surface expression. Mutant and chimeric α1 and γ2 subunits were also used to identify specific sequences within the N-termini that are important for inter-subunit associations. For example, γ2 (91-104) and γ2 (83-90) are involved in binding to α1 and β3 subunits, respectively and α1(80-100) is involved in binding to γ2 subunits (Klausberger *et al.*, 2001). Factors regulating $GABA_A$ receptor heterogeneity are discussed further in Section 1.2.4.

3.2.2. AIM OF THE STUDY

The aim of this study was to test the validity of the yeast two-hybrid system in the identification of $GABA_A$ receptor α1 and β2 subunit extracellular N-terminal assembly motifs. The yeast two-hybrid system has been used successfully to study assembly domains in K^+ channel intracellular N-terminal domains (Xu *et al.*, 1995) and in extracellular regions of α and β Na^+/K^+ ATPase subunits (Colonna *et al.*, 1997). Further, the soluble acetylcholine binding protein (AChBP), which is structurally similar to the subunit N-terminal domains of the nicotinic acetylcholine receptor super-family of which the $GABA_A$ receptors are members, has been shown to form a pentameric homo-oligomer in yeast (Smit *et al.*, 2001) i.e., N-terminal regions are capable of co-association in the absence of transmembrane domains. Therefore, it should be possible to use the same methodology to study $GABA_A$ receptor subunit assembly. The α1 and β2 $GABA_A$ receptor subunit N-terminal regions were chosen for initial studies as they, together with the γ2 subunit, produce the most abundant $GABA_A$ receptor subtype expressed in adult brain.

3.3. RESULTS

3.3.1. PREPARATION OF THE GAL4 PLASMID $GABA_A$ RECEPTOR α1 AND β2 SUBUNIT N-TERMINAL FUSION CONSTRUCTS

$GABA_A$ receptor α1(1-224) and β2(1-220) subunit N-terminal domains were cloned in frame into the GAL4 yeast two-hybrid AD vector, pGADT7, to generate the fusion constructs GAL4 AD-α1(1-224) and GAL4 AD-β2(1-220). The direct cloning method was used and is outlined in Figure 2.1. PCR amplification was performed as described in section 2.2.2.6 and specific program parameters for amplification are detailed in Table 2.1.4. Oligonucleotide primers specific for each sequence are shown in Table 2.1.3. Figures 3.2.1-3.2.3 represent the different stages of construction i.e. amplified PCR product, diagnostic digestion of PCR products and diagnostic digestion of recombinant plasmids to confirm that the correct sequences had been inserted. Similar results were seen for all constructs generated in this chapter. α1(1-224) and β2(1-220) were then sub-cloned into the GAL4 pGBKT7 plasmid to produce the fusion constructs GAL4 DNA-BD-α1(1-224) and GAL4 DNA-BD-β2(1-220). Figure 3.2.4 shows the results of nucleotide sequencing for each plasmid construct, focussing on the restriction insertion site to demonstrate that each insert sequence is in-frame with the TF domain encoded in each vector. Figure 3.2.5 shows the plasmid maps representing α1(1-224) and β2(1-220) fusion constructs for the GAL4 system and figures 3.2.6 and 3.2.7 show the results of immunoblotting of protein extracts from yeast cells transformed with individual constructs GAL4 AD-α1(1-224), GAL4 AD-β2(1-220), GAL4 DNA-BD-α1(1-224) or GAL4 DNA-BD-β2(1-220) to confirm expression of each fusion protein in yeast. Each AD fusion protein contains an HA epitope tag and each DNA-BD fusion protein contains a c-myc epitope tag. A band corresponding to the predicted size of ~43 kDa was seen for each DNA-BD fusion protein and ~41 kDa for each AD fusion construct.

3.3.2. YEAST TWO-HYBRID RESULTS FOR THE CO-TRANSFORMATION OF $GABA_A$ RECEPTOR α1 AND β2 SUBUNIT N-TERMINAL DOMAINS IN THE GAL4 SYSTEM

Combinations of GAL4 AD and DNA-BD fusion constructs containing a $GABA_A$ receptor α1 or β2 subunit N-terminal domain were co-transformed into the GAL4 yeast strain AH109. N-terminal domain test transformations contained α1/β2, α1/α1 or β2/β2

combinations. The positive control plasmids, pTD1-1 and pVA3-1, contain the proteins p53 and the SV40 large T antigen, respectively. These proteins are known to interact and were co-transformed to ensure that known interactions could be detected. Single DNA-BD negative controls included pGADT7α1(1-224) or pGADT7β2(1-220) co-transformed with an empty pGBKT7 vector. Single AD negative controls contained pGBKT7α1(1-224) or pGBKT7β2(1-220) co-transformed with an empty pGADT7 vector. These were used to assess whether either of the N-terminal domains was capable of autonomous reporter gene activation. A double negative control contained both empty pGADT7 and empty pGBKT7. All co-transformants were plated onto -2 and -4 dropout media and assayed for β-galactosidase reporter gene activity. The results are summarised in Table 3.2.1. Figure 3.2.8 shows the results of the β-galactosidase assay for these co-transformations.

From Table 3.2.1, it can be seen that all plasmids were successfully transformed into yeast as all co-transformants were able to grow on -2 dropout media. The positive control plasmids pVA3-1 and pTD1-1 showed growth on -4 dropout media and were positive for β-galactosidase activity. The double negative control transformants showed no growth on -4 media and no β-galactosidase activity. pGADT7α1(1-224) co-transformed with pGBKT7β2(1-220) showed some growth on -4 media but this was very weak. The combination pGADT7β2(1-220)/pGBKT7α1(1-224) showed a higher degree of reporter gene activity. pGADT7α1(1-224) with pGBKT7α1(1-224) showed the same level of reporter gene activity as pGADT7α1(1-224)/pGBKT7β2(1-220). pGADT7β2(1-220) with pGBKT7β2(1-220) showed the highest degree of reporter gene activation of the double combinations. Single negative control combinations of pGBKT7α1(1-224) or pGBKT7β2(1-220) with an empty pGADT7 plasmid showed no reporter gene activation. However, single combinations of pGADT7α1(1-224) or pGADT7β2(1-220) co-transformed with an empty pGBKT7 vector did show both growth on -4 dropout media and were positive for β-galactosidase activity, indicating that both α1 and β2 N-termini are capable of auto-activating reporter genes. This meant that it was not possible to know whether the reporter gene activity seen for any of the N-terminal domain combinations α1/β2, β2/α1, α1/α1 or β2/β2 represented true interactions or were due to auto-activation by a single sequence in the AD vector.

3.3.3. THE MODIFIED LEX A YEAST TWO-HYBRID SYSTEM

Since the $GABA_A$ receptor α1 and β2 N-termini both showed auto-activation of reporter genes when co-transformed in the AD plasmid with an empty DNA-BD plasmid, a second yeast two-hybrid system was tested. The modified (m)LexA system is similar to the GAL4 system in that it uses re-constitution of transcription factor activity to detect protein-protein interactions. However, the DNA-BD plasmid, pMBL33 contains the prokaryotic LexA promoter rather than the eukaryotic GAL4 promoter (Section 3.1.8). If the auto-activity seen in the GAL4 system was due to the GAL4 DNA-BD protein then it should still be possible to test the N-terminal domain interactions in the mLexA system.

3.3.4. SUB-CLONING OF THE α1 AND β2 N-TERMINAL DOMAINS INTO THE mLEXA DNA-BD VECTOR

The $GABA_A$ receptor subunit sequences α1(1-224) and β2(1-220) were sub-cloned in-frame into the mLexA plasmid pMBL33 from the pGADT7α1(1-224) and β2(1-220) constructs. Creation of the fusion proteins was verified using nucleotide sequencing, as shown for the GAL4 AD and DNA-BD fusion constructs in Figure 3.2.4. Plasmid maps showing the α1(1-224) and β2(1-220) fusion constructs for the mlexA yeast two-hybrid system are shown in Figure 3.2.9.

3.3.5. YEAST TWO-HYBRID RESULTS FOR THE CO-TRANSFORMATION OF $GABA_A$ RECEPTOR α1 AND β2 SUBUNIT N-TERMINAL DOMAINS IN THE mLEXA SYSTEM

The yeast strain, L40, was co-transformed with the same combinations of α1 and β2 N-terminal domain fusion constructs as for the GAL4 system, but in pGADT7 and pMBL33 vectors (Table 3.2.2.). The interaction between GRIF-1(8-633) and the $GABA_A$ receptor β2-IL(303-427) was used as a positive control for this system.

As can be seen in Table 3.2.2, all plasmid combinations were successfully co-transformed, showing growth on -2 dropout media. The GRIF-1(8-633)/β2-IL(303-427) positive control showed reporter gene activity in this system on both -4 dropout media and for β-galactosidase activity. The double empty vector negative control showed no activity. Double N-terminal domain combinations showed a similar pattern of results to

those obtained in the GAL4 system. pGADT7α1(1-224) co-transformed with pMBL33β2(1-220) showed some growth on -4 media and was positive for β-galactosidase activity. pGADT7β2(1-220) with pMBL33α1(1-224) activated reporter genes more strongly. Negative controls containing α1(1-224) or β2(1-220) in the DNA-BD and an empty AD vector showed no reporter gene activity. However, as for the GAL4 system, when α1(1-224) or β2(1-220), fused to the GAL4 AD, were co-transformed with an empty DNA-BD, reporter genes were activated, leading to both growth on -4 media and to β-galactosidase reporter gene activity. This result indicates that altering the transcription factor used to activate reporter genes does not remove any intrinsic transcription factor activity of either α1(1-224) or β2(1-220). It is therefore not possible to show conclusively in either the GAL4 or the mLexA system, whether the $GABA_A$ receptor α1 and β2 subunit N-terminal domains interact.

3.3.6. THE CYTOTRAP® YEAST TWO-HYBRID SYSTEM

The CytoTrap® yeast two-hybrid assay differs from the GAL4 and the mLexA systems in that detection of protein-protein interactions is not dependent on transcription factor activity. (Section 3.1.10). Instead, the yeast strain, cdc25H, is employed, which contains a mutant Sos protein. Sos is a guanyl nucleotide exchange factor (GNEF) which is necessary for activation of the Ras signalling pathway. The mutant Sos renders the Ras pathway inactive making the cdc25H yeast strain temperature-sensitive, i.e. allowing growth at the permissive temperature of 25°C but preventing growth at the restrictive temperature of 37°C. Detection of protein-protein interactions is based on reconstitution of the Ras signalling pathway. The first protein of interest, cloned in frame into the pMyr vector, is fused to a myristylation signal that targets the construct to the plasma membrane. The second protein of interest, cloned into the pSos vector, is fused to the hSos protein and if the two test proteins interact, Sos is brought to the cell surface where it activates the Ras signalling pathway, allowing cells to grow at 37°C.

3.3.6.1. PREPARATION OF THE CYTOTRAP® YEAST TWO-HYBRID SYSTEM

As the CytoTrap® yeast two-hybrid system had not been previously established in our laboratory, it was important to verify this assay as a means of testing protein-protein interactions. Firstly the phenotype of the yeast strain, cdc25Hα, was tested for

temperature and nutritional revertants. Cells from a glycerol stock were streaked onto 2 YPAD agar plates. One plate was incubated at 25°C and the other at 37°C. Both plates were then observed daily for 4 days. Colonies were observed on the plate incubated at the permissive temperature of 25°C, but no colonies grew at the restrictive temperature of 37°C. This showed that the cells were not temperature revertant. Next, cdc25H cells were streaked onto a series of glucose-based dropout media plates, individually lacking uracil, leucine, histidine or tryptophan, to test their nutritional phenotype. Each plate was incubated at 25°C and observed daily for 4 days and no cell growth was seen on any plate. This showed that the yeast cells were not nutritionally revertant.

3.3.6.2. YEAST CO-TRANSFORMATIONS OF CYTOTRAP® POSITIVE AND NEGATIVE CONTROL PLASMIDS

Once the phenotype of the yeast strain, cdc25H, had been verified, control co-transformations were carried out to confirm that the system was working properly. The CytoTrap® control plasmids are described in Section 3.1.11. Double combinations of the positive control plasmids, pMyrMAFB/pSosMAFB and pMyrSB/pSosMAFB and of the negative control plasmids, pMyrMAFB/pSosCol1, pMyrLaminC/pSosMAFB and pMyr/pSos were used to co-transform cdc25H yeast cells. All control co-transformants were plated onto dropout media and any resulting colonies observed after 1 week were analysed as described in Section 2.2.3.3. The results are summarised in Table 3.2.3. Both pMyrMAFB/pSosMAFB and pMyrSB/pSosMAFB positive control co-transformants grew at 37°C on galactose-based media whereas pMyrMAFB/pSosCol1, pMyrLaminC/pSosMAFB and pMyr/pSos negative control combinations showed no growth. These results confirmed the authenticity of the CytoTrap® system.

3.3.7. SUB-CLONING OF THE $GABA_A$ RECEPTOR α1 AND β2 N-TERMINAL DOMAINS INTO pMYR AND pSOS VECTORS

Having established the CytoTrap® yeast two-hybrid system in the laboratory, this assay was used to test for associations between the $GABA_A$ receptor α1 and β2 subunit N-termini. Firstly, the α1(1-224) and β2(1-220) sequences were cloned into the pMyr and pSos expression vectors. The restriction enzyme recognition sequences in the multiple cloning sites of these vectors were not compatible for sub-cloning with any of the other yeast two-hybrid vectors used so far. Therefore, $GABA_A$ receptor N-terminal domain

sequences were each PCR amplified using a previously produced GAL4 α1(1-224) or β2(1-220) construct as a template. The specific PCR parameters are described in Table 2.1.4 and the specific oligonucleotide primers are shown in Table 2.1.3. The PCR products were cloned in frame into the pMyr and pSos vectors. Correct insertion of $GABA_A$ receptor α1(1-224) or β2(1-220) subunit N-termini was verified by nucleotide sequencing, as shown for the GAL4 AD and DNA-BD fusion constructs in Figure 3.2.4. Plasmid maps for the α1(1-224) and β2(1-220) sequences in the CytoTrap® vectors are shown in Figure 3.2.10.

3.3.8. YEAST TWO-HYBRID RESULTS FOR THE CO-TRANSFORMATION OF $GABA_A$ RECEPTOR α1 AND β2 SUBUNIT N-TERMINAL DOMAINS IN THE CYTOTRAP® SYSTEM

The yeast strain, cdc25Hα, was co-transformed with combinations of α1 and β2 N-terminal domain constructs in pMyr and pSos vectors. Transformants were grown on glucose-based media lacking uracil and leucine (-U/-L) to ensure that both constructs were present. After 3-6 days colonies were patched onto 2 x glucose-based and 2 x galactose-based -U/-L media agar plates. One of each type of plate was incubated at 25°C and the two remaining plates were incubated at 37°C. At 25°C all co-transformants should be able to grow. At 37°C glucose-based media inhibits the GAL1 promoter, preventing cell growth. Positive interactions are indicated by growth on galactose-based media at 37°C. The results are shown in Table 3.2.4. Figure 3.2.11 shows an example of the CytoTrap® yeast two-hybrid results seen for co-transformants on galactose-based -UL dropout media after incubation at 37°C.

The positive control co-transformations were pSos MAFB with pMyr MAFB and pSos MAFB with pMyr SB. Both of these combinations produced growth on galactose-based media at 37°C. The negative control combinations were pSos MAFB with pMyr lamin C, pSos Col1 with pMyr MAFB and empty pSos with empty pMyr. None of these combinations produced colony growth on galactose-based media at 37°C. No growth was seen for any of the single negative N-terminal domain control combinations. However, none of the double test combinations containing α1(1-224) and β2(1-220) produced growth on galactose-based media at 37°C. These results, therefore, do not show any interactions between the α1 and β2 $GABA_A$ receptor N-termini.

3.4. DISCUSSION

3.4.1. THE GAL4, MODIFIED LEXA AND CYTOTRAP® YEAST TWO-HYBRID SYSTEMS

In this chapter, three different yeast two-hybrid systems have been used to examine interactions between the $GABA_A$ receptor α1 and β2 subunit extracellular N-terminal domains. The first system to be tested was the GAL4 assay which relies on the activity of the eukaryotic GAL4 transcription factor (TF) to detect protein-protein interactions. In this system, although the N-terminal domain co-transformations produced reporter gene activity, single negative controls containing either an α1(1-224) or a β2(1-220) N-terminus fused to the GAL4 AD co-transformed with an empty DNA-BD plasmid also produced reporter gene activity, indicating that both the α1 and β2 subunit N-termini are capable of autonomous activation of reporter gene transcription. This suggests that both N-termini have some intrinsic TF activity or that they bind to other proteins in the nucleus that do. The auto-activation produced by both sequences meant that it was not possible to determine whether the N-terminal domains associated. Interestingly, reporter gene activity was stronger for the β2 than for the α1 subunit and for each subunit, activation was stronger when the N-terminus in the AD vector was co-transformed with an empty DNA-BD vector than when co-transformed with another N-terminus. This indicates that the presence of a second protein hindered the TF properties of each sequence.

Since it was not possible to study the N-terminal domains in the GAL4 system a second system was employed. The modified LexA system is also dependent on transcription factor activity, but in this case, uses the prokaryotic LexA TF DNA-BD rather than the eukaryotic GAL4 TF. The same experiments were carried out in this system to determine whether changing the TF apparatus would abolish the auto-activity seen in the GAL4 system. Unfortunately, a similar pattern of results was seen. Both the α1(1-224) and β2(1-220) sequences caused auto-activation of reporter genes when co-transformed into yeast in an AD vector with an empty DNA-BD vector, reporter gene activity was stronger for the β2 than for the α1 subunit and for each subunit, activation was stronger when the N-terminus in the AD vector was co-transformed with an empty DNA-BD vector than when co-transformed with another N-terminus. Therefore, neither of these systems could be used for further studies.

The TF properties of α1 and β2 subunit N-termini prevented their being studied in a system based on reconstitution of reporter gene activation. Interactions in the CytoTrap® system occur in the cytoplasm, therefore TF properties of test proteins do not affect the detection of two-hybrid interactions. As no reporter gene activity was detected in any of the N-terminal domain co-transformations, the results indicate that any reporter gene activity detected for these experiments in either the GAL4 or mLexA systems was due to auto-activation by individual α1(1-224) or β2(1-220) AD fusion constructs. Since $GABA_A$ receptor subunit N-termini have been shown to assemble in mammalian cells (Klausberger *et al.*, 2000; 2001; Sarto *et al.*, 2002a, b), the results described in this chapter suggest that the receptor fusion constructs studied here were not folded correctly in yeast cells and were, thus not competent for oligomerisation.

3.4.2. PROTEIN FUSION CONSTRUCTS USED IN THE YEAST TWO-HYBRID ASSAY

Figure 3.2.12 shows schematic diagrams representing the fusion proteins used in each yeast two-hybrid system. The relative sizes of each fusion protein domain can be seen. For the GAL4 system the AD and DNA-BD TF domains comprise approximately one third of the total fusion protein and for the LexA system, the DNA-BD TF domain is approximately half of the total fusion protein. For the CytoTrap® system the Myr signal is only 15 amino acids in length, whereas the hSOS protein is approximately 5 times larger than the N-terminal domains. It is possible that the attachment of a relatively large protein sequence to the test protein of interest could inhibit some interactions. For example, the N-terminus of each protein of interest to be studied in the yeast two-hybrid system is fused to the C-terminus of a hybrid construct protein encoded by the host vector. This order of sequences could potentially inhibit interactions between test proteins that require a free N-terminus for binding. The sequences identified so far in $GABA_A$ receptor N-termini that are in involved subunit assembly are located towards the N-terminal side of the sequences (see Figure 3.2.13), but may be close enough to the centre of the sequences that they are not restricted by the fusion conditions. In the LexA system, it is possible to construct fusion proteins in which the order of the hybrid domains is reversed, with the test protein fused to the N-terminus of the hybrid protein encoded by the vector (Beranger *et al.*, 1997). These constructs may be used to detect some interactions that are blocked by a restricted N-terminus.

3.4.3. PROTEIN PROCESSING IN THE YEAST TWO-HYBRID SYSTEM

To avoid counteracting the nuclear localisation signal (NLS) of the yeast two-hybrid vectors, the α1 and β2 subunit signal peptides were not included in the fusion constructs. These signals are normally responsible for targeting the proteins through the exocytic pathway i.e. endoplasmic reticulum (ER) and Golgi, to the membrane. TFs are nuclear proteins that are normally targeted to, and translated by, cytosolic ribosomes. Therefore, in the GAL4 and the mLexA systems, yeast two-hybrid fusion constructs, once incorporated into yeast cells, are transcribed in the nucleus and then exported directly into the cytoplasm where they are translated into protein. Once formed, the mature fusion proteins are targeted back to the nucleus and it is here that any interactions between test proteins cause the activation of reporter genes. In the CytoTrap® system, fusion proteins are not targeted back to the nucleus, but remain in the cytoplasm and any protein-protein interactions are detected at the cell membrane.

$GABA_A$ receptor subunits are normally processed through the ER (Connolly *et al.*, 1996) which contains particular enzymes and chaperone proteins that are important for proper protein folding. However, in all three yeast two-hybrid systems, (with the exception of the pMyr vector, which encodes a membrane protein and may therefore be targeted through the exocytic pathway) the fusion proteins bypass this stage of receptor assembly when directed to the cytoplasm. This means that they are not subjected to many of the post-translational modifications that occur during normal protein synthesis and folding, such as disulphide bond formation and N-linked glycosylation. $GABA_A$ receptor subunit N-termini contain sites for both N-linked glycosylation and for disulphide bridge linkages. N10 and N110 of the α1 N-terminus are potential N-linked glycosylation sites and C138 and C152 are involved in disulphide bonded loop formation. In the β2 N-terminus there are 3 potential N-linked glycosylation sites, N8, N80 and N135, where N135 occurs between residues C136 and C150, which are involved in the formation of the β2 subunit N-terminus disulphide bonded loop. It has been observed in immunoprecipitation studies that a lack of N-linked glycosylation does not prevent receptor subunit assembly, but rather that $GABA_A$ receptor subunits show a preferential binding to subunits with un-glycosylated or partially glycosylated N-termini (Connolly *et al.*, 1996). Mutation of cysteine rsidues in α and β subunits of the nACh receptors showed that subunits retained their ability to oligomerise in *Xenopus* oocytes, but at a greatly reduced efficiency (Sumikawa and Gehle, 1992). Since the mutant

subunits were cotransfected with wild type γ and δ subunits and were sill processed through the ER, all other ER mediated folding events would still occur and the oligomerisation of mutant subunits may have been stabilised by the presence of the wild type subunits. These experiments showed that sisulphide bridge formation is not an absolute requirement for assembly of nACh receptor subunits, but greatly stabilise the process.

In the lumen of the ER, through which receptors are normally trafficked, disulphide bond formation is catalysed by protein disulphide isomerase (PDI). The folding process involved in forming these linkages requires a kinetically complex series of oxidation/reduction reactions to ensure that the correct disulphides are linked (Schwaller *et al.*, 2003). It was thought that the reducing conditions of the yeast cytoplasmic environment would inhibit these disulphide linking reactions. However, some proteins which contain disulphide bonds that are essential for the formation of their native structure, e.g. prolactin, growth hormone (GH) and vascular endothelial growth factor (VEGF), have been successfully shown to interact with their respective ligands in yeast (Ozenberger and Young, 1995), suggesting that in some cases, disulphide bond formation in the cytoplasm is possible.

The thiol-disulphide redox buffer, glutathione, which is found in the cytoplasm, is competent to mediate correct disulphide linkage formation (Gilbert, 1990). The standard laboratory conditions under which the cells are maintained e.g. acidic, may cause an oxidative stress within the cytoplasm that would cause a decrease in the concentration of glutathione found in its reduced state, making the yeast cytoplasm more oxidising and hence more conducive to disulphide bonds formation than was previously thought. In addition, Vallejo and Serrano (1989) showed that whatever the pH surrounding the cells, the yeast cytoplasm remains neutral. This is due to the proton pumping activity of a membrane ATPase. The increased efflux of positive ions out of the cell may cause localised changes in redox potential within the cytoplasm, making disulphide bond formation more likely. However, PDI mediated disulphide bond formation is much faster and more efficient than when mediated by the glutathione redox buffer alone (Gilbert, 1990). The complexity of receptor subunit folding and the sub-optimal redox conditions in the cytosol may mean that the peptides studied here were incorrectly or incompletely folded. Therefore the yeast two-hybrid system may not be amenable to the study of $GABA_A$ receptor subunit assembly, using subunit N-terminal domains.

FIGURE 3.1.1. THE GENETIC BASIS OF THE GAL4 YEAST TWO-HYBRID ASSAY

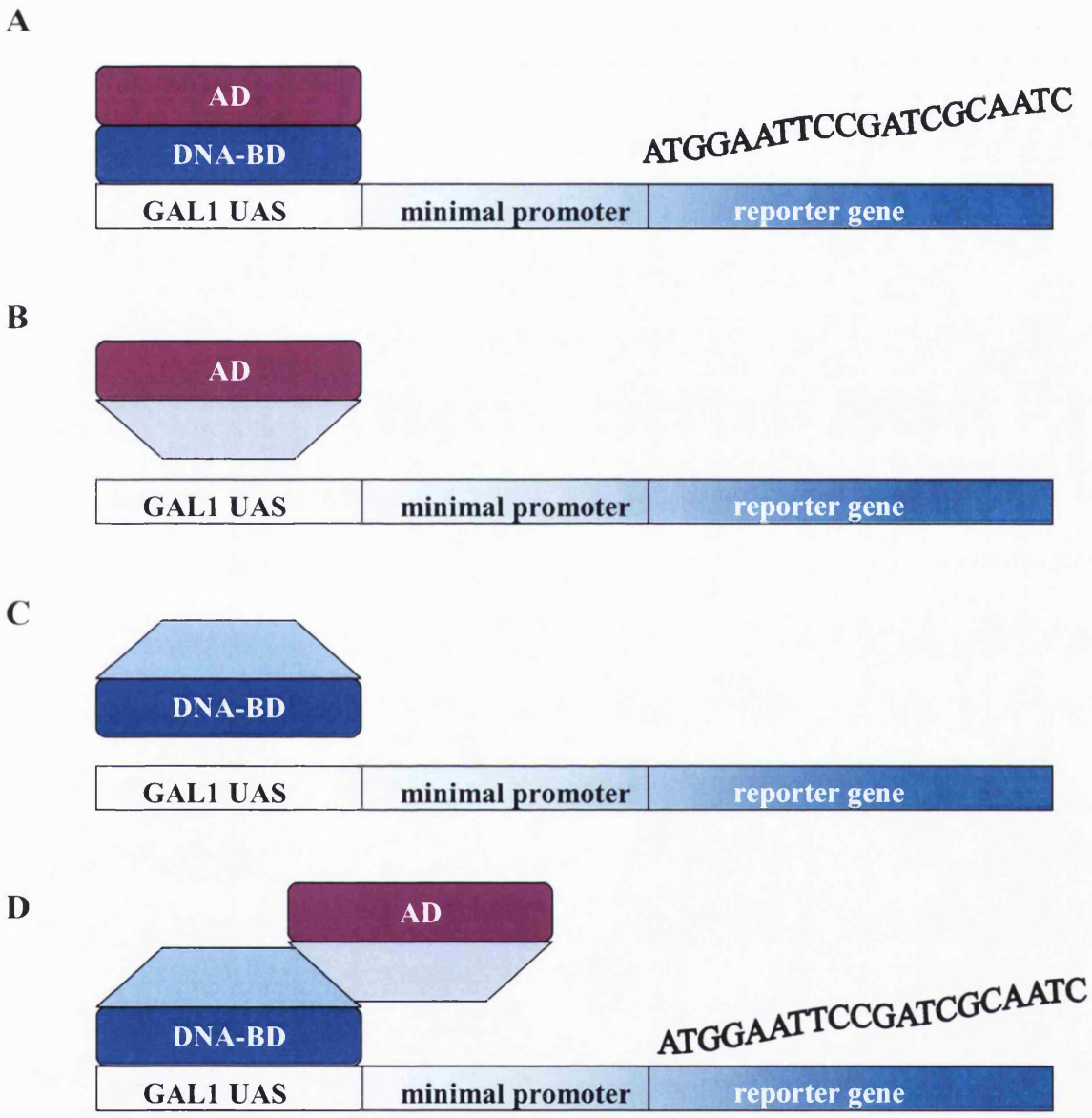

Figure 3.1.1 is a schematic representation showing the mechanism of activation of reporter genes in the GAL4 yeast two-hybrid system. A shows reporter gene transcription activated by the complete GAL4 transcription factor. B and C show that the DNA-BD-test protein 1 fusion construct or the AD-test protein 2 fusion construct alone is unable to activate transcription. D shows that an interaction between test proteins 1 and 2 bring the two TF domains together, thus restoring transcription activation.

FIGURE 3.1.2. THE REPORTER GENES UNDER THE CONTROL OF THE GAL4 TRANSCRIPTION FACTOR IN THE GAL4 YEAST TWO-HYBRID SYSTEM

The diagram represents the four reporter genes integrated into the GAL4 yeast two-hybrid system. The His and Ade nutritional markers are both under the control of the GAL1 UAS, but differ in their promoter sequences. The lacZ and MEL1 reporter genes encode the β- and α-Galactosidase enzymes, respectively and expression of each is controlled by the MEL1 UAS.

FIGURE 3.1.3. VECTOR DIAGRAMS OF THE MATCHMAKER GAL4 YEAST TWO-HYBRID SYSTEMS 2 AND 3

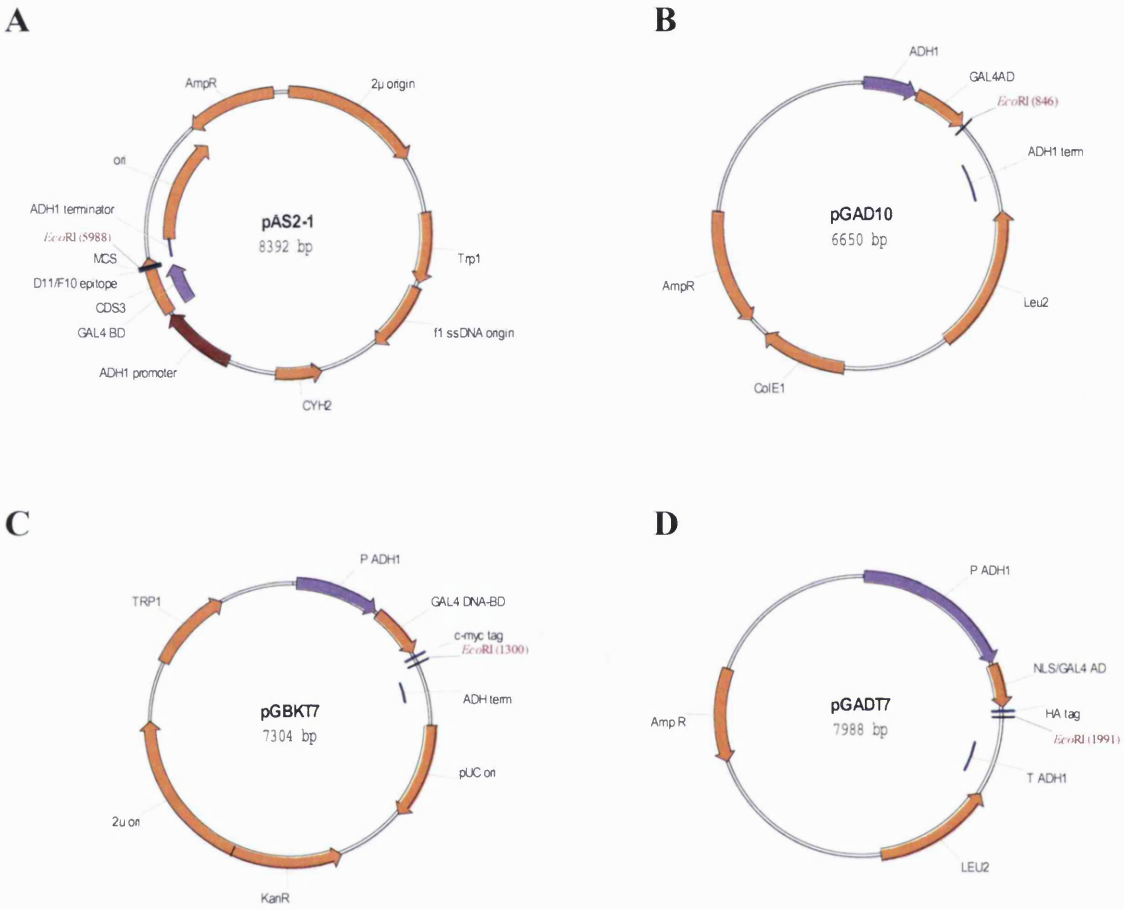

The pAS2-1 (A) and pGAD10 (B) plasmids encode the GAL4 DNA-BD and AD, respectively. Each of these genes is followed by a multiple cloning site for insertion of test sequences. Both plasmids also contain an Amp^r gene that allows growth on media containing ampicillin. pAS2-1 contains a Trp marker that allows the plasmid to grow on media lacking tryptophan, while pGAD10 contains a Leu marker that allows yeast to grow on media lacking leucine. These are the MATCHMAKER system 2 plasmids. pGBKT7 (C) and pGADT7 (D) vectors are the MATCHMAKER system 3 plasmids. The Amp^r gene of pAS2-1 is replaced by a Kan^r gene in pGBKT7 to allow bacterial cells to discriminate between BD and AD vectors. pGBKT7 and pGADT7 also contain compatible multiple cloning sites to allow ease of transfer of inserts between vectors.

FIGURE 3.1.4. VECTOR DIAGRAM FOR THE MODIFIED LEXA YEAST TWO-HYBRID PLASMID

A

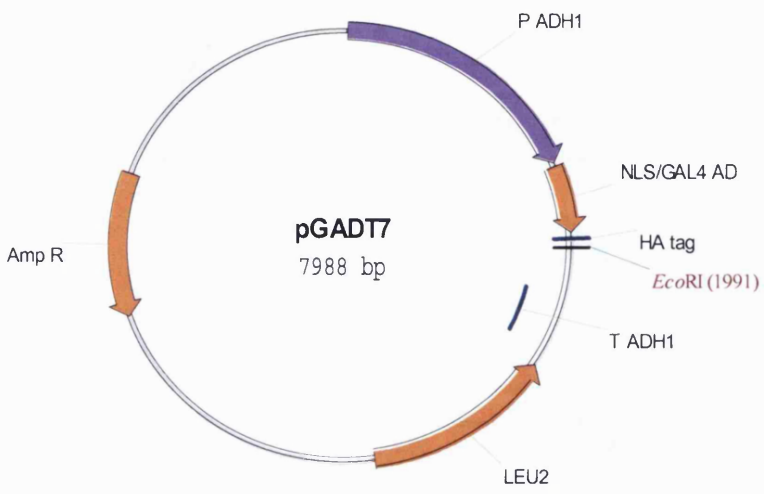

B

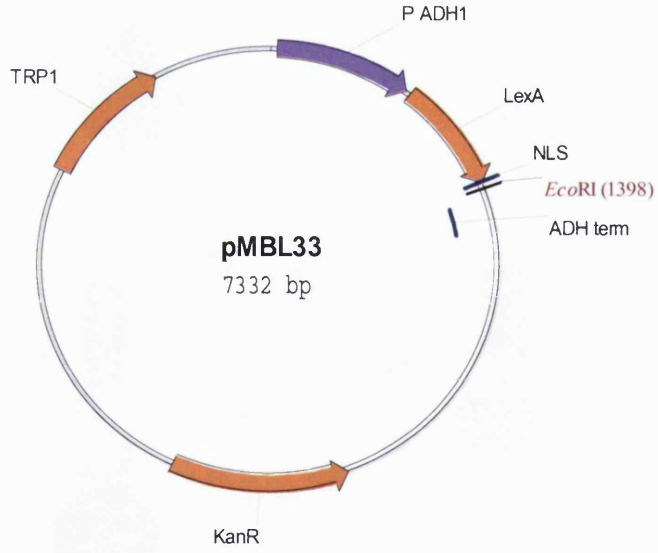

The modified yeast two-hybrid system uses the pGADT7 (A) vector of the GAL4 system with the hybrid vector, pMBL33 (B). The pMBL33 vector was created from the GAL4 plasmid, pGBKT7, and the LexA plasmid, pEG202-NLS. The hybrid vector contains the prokaryotic LexA DNA-BD and multiple cloning site of pEG202-NLS, vector fused to the backbone of the pGBKT7 vector i.e. contains the bacterial selection gene, Kan^r, for kanamycin selection and the yeast selection gene, Trp, to allow growth on media lacking tryptophan.

FIGURE 3.1.5. SCHEMATIC DIAGRAM SHOWING THE BASIS OF THE CYTOTRAP® YEAST TWO-HYBRID ASSAY

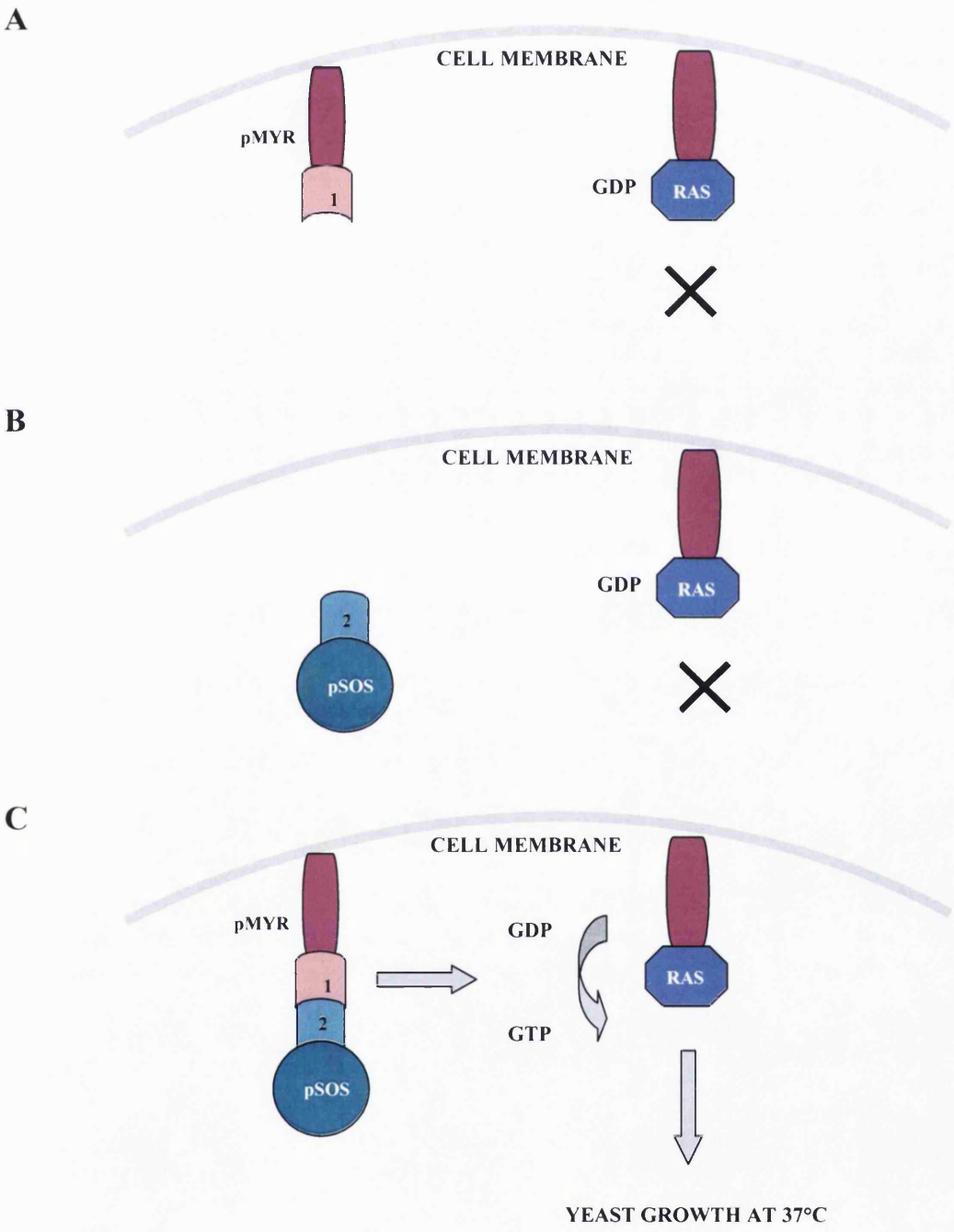

Figure 3.1.5 shows the basis of the CytoTrap® assay. A and B show that either the pMyr or pSos fusion construct alone will not activate the Ras signalling pathway. Only the presence of both constructs, brought together by an interaction between two test proteins, leads to the activation of Ras and yeast growth at 37°C.

FIGURE 3.1.6. VECTOR DIAGRAMS OF THE CYTOTRAP® PLASMIDS pMYR AND pSOS

A

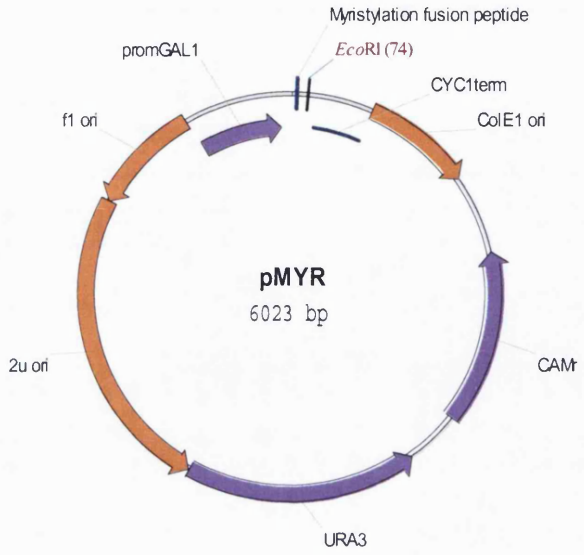

B

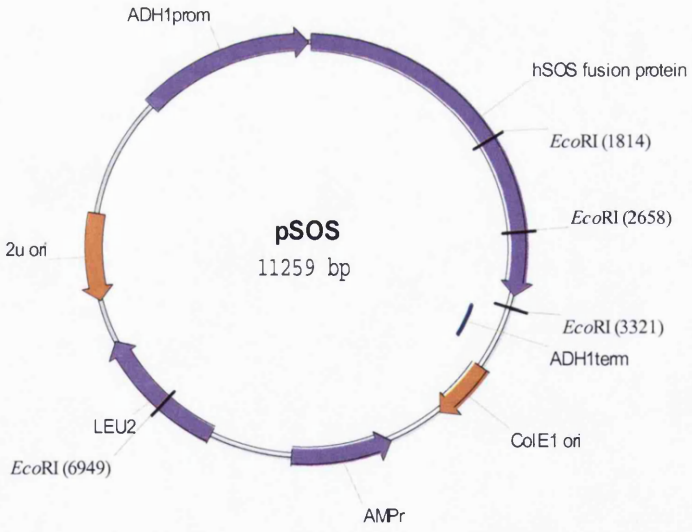

The pMyr vector (A) encodes the v-Src myristylation signal to direct the fusion protein product to the cell surface. Downstream of this is the multiple cloning site. The bacterial selection marker, Cam^r, allows growth on media containing chloramphenicol and the yeast selection marker, Ura, allows growth on media lacking uracil. The pSos vector (B) encodes the human Sos gene for activation of the Ras signalling pathway. pSos carries the bacterial selection marker, Amp^r, for growth on media containing ampicillin and the yeast selection marker, Leu, for growth on media lacking leucine.

FIGURE 3.2.1 AN AGAROSE GEL SHOWING AMPLIFIED PCR PRODUCTS FOR THE $GABA_A$ RECEPTOR SUBUNIT N-TERMINAL DOMAIN SEQUENCES, α1(1-224) AND β2(1-220)

100bp DNA ladder fragment sizes (bp):

1000, 900, 800, 700, 600, **500**, 400, 300, 200, 100, 80

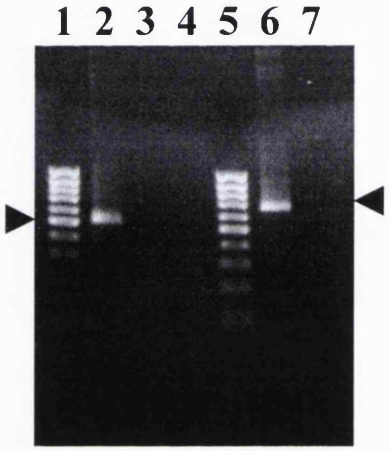

Lane	Sample	Predicted Sizes (bp)	Observed Sizes (bp)
1	100 bp DNA ladder	See above	-
2	α1(1-220) PCR product	660	~650
3	"No DNA" negative control	-	-
4	No sample	-	-
5	100 bp DNA ladder	See above	-
6	β(1-224) PCR product	672	~680
7	"No DNA" negative control	-	-

The $GABA_A$ receptor subunit N-terminal domain sequences α1(1-224) and β2(1-220) were amplified by PCR from rat brain cDNA. The "No DNA" negative control samples contained no template for amplification and demonstrated that no contaminating DNA was present in either reaction. All samples were electrophoresed on a 1% agarose gel. Arrowheads indicate the positions of PCR products.

FIGURE 3.2.2. ANALYSIS OF THE $GABA_A$ RECEPTOR SUBUNIT N-TERMINAL DOMAIN SEQUENCES, α1(1-224) AND β2(1-220), BY DIAGNOSTIC RESTRICTION ENZYME DIGESTION

100bp DNA ladder fragment sizes (bp):

1000, 900, 800, 700, 600, **500**, 400, 300, 200, 100, 80

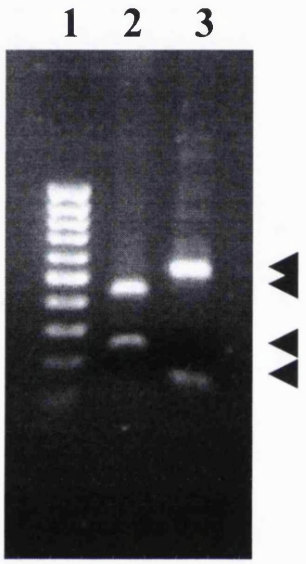

Lane	Sample	Predicted Sizes (bp)	Observed Sizes (bp)
1	100 bp DNA ladder	See above	-
2	α1(1-220)	436, 236	~250, 450
3	β(1-224)	532, 128	~150, 550

Diagnostic digests were performed on the amplified $GABA_A$ receptor α1 and β2subunit N-terminal domains to verify that the correct sequences had been amplified. α1(1-224) was digested by *Nco*I and β2(1-220) was digested with *Eco*RV. Both samples were electrophoresed on a 1% agarose gel along with a 100 bp DNA ladder. Arrowheads indicate the positions of restriction digestion products. It can be seen from the gel that the expected fragment sizes were produced.

FIGURE 3.2.3. DIAGNOSTIC RESTRICTION ENZYME DIGESTION OF pGADT7α1(1-224), pGADT7β2(1-220), pGBKT7α1(1-224) AND pGBKT7β2(1-220) FUSION CONSTRUCTS

1kb DNA ladder fragment sizes (bp):

10000, 8000, 6000, 5000, 4000, 3500, **3000**, 2500, 2000, 1500, 1000, 750, 500, 250

A **B**

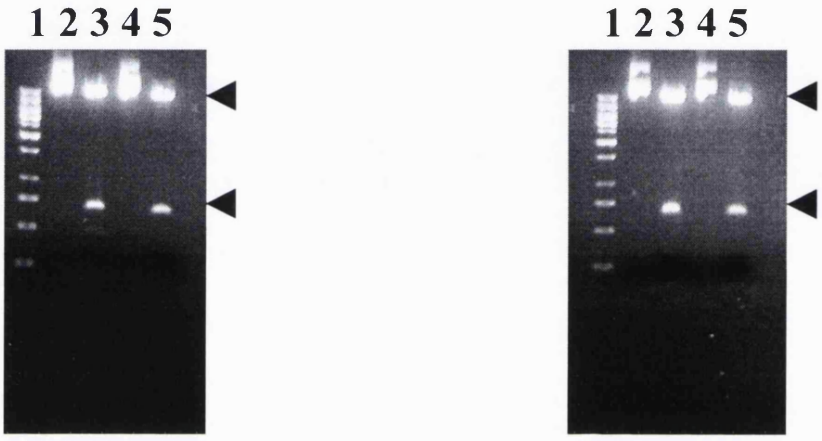

A

Lane	Sample	Predicted Sizes (bp)	Observed Sizes (bp)
1	1 kb DNA ladder	See above	-
2	Undigested pGADT7α1(1-224)	8638	~9000
3	Digested pGADT7α1(1-224)	7960, 672	~8000, 700
4	Undigested pGADT7β2(1-220)	8626	~8500
5	Digested pGADT7β2(1-220)	7960, 660	~8000, 650

B

Lane	Sample	Predicted Sizes (bp)	Observed Sizes (bp)
1	1 kb DNA ladder	See above	-
2	Undigested pGBKT7α1(1-224)	7972	~10000
3	Digested pGBKT7α1(1-224)	7300, 672	~8000, 650
4	Undigested pGBKT7β2(1-220)	7960	~10000
5	Digested pGBKT7β2(1-220)	7300, 660	~8000, 650

Purified pGADT7α1(1-224), pGADT7β2(1-220), pGBKT7α1(1-224) and pGBKT7β2(1-220) fusion constructs were digested by *Eco*R1 and *Bam*H1. Each digest was electrophoresed on a 1% agarose gel together with a sample of each non-digested construct. Arrowheads indicate the positions of restriction digestion products.

FIGURE 3.2.4. DNA SEQUENCING RESULTS FOR GAL4 YEAST TWO-HYBRID DNA-BD AND AD VECTOR FUSION CONSTRUCTS

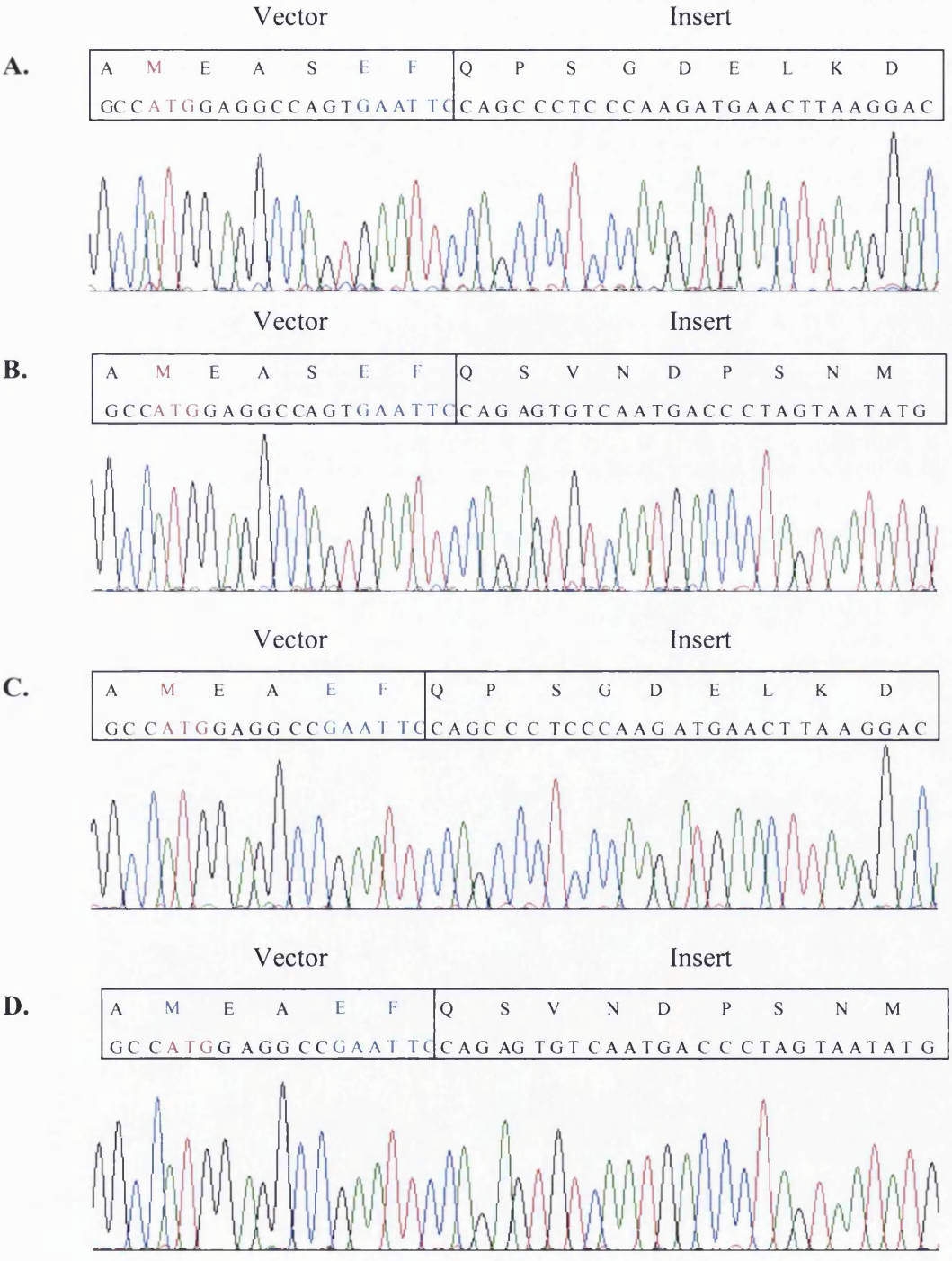

Nucleotide sequencing was carried out on the ABI PRISM 310 Genetic Analyser to confirm each insert was present and in-frame with the vector fusion protein. **A-D** represent pGADT7α1(1-224), pGADT7β2(1-220), pGBKT7α1(1-224) and pGBKT7β2(1-220) respectively. The insert start codon, within the vector, is highlighted in Red and the *Eco*RI restriction site is highlighted in Blue.

FIGURE 3.2.5. VECTOR DIAGRAMS OF THE GAL4 SYSTEM CONSTRUCTS USED TO STUDY THE INTERACTIONS BETWEEN α1 AND β2 N-TERMINALS

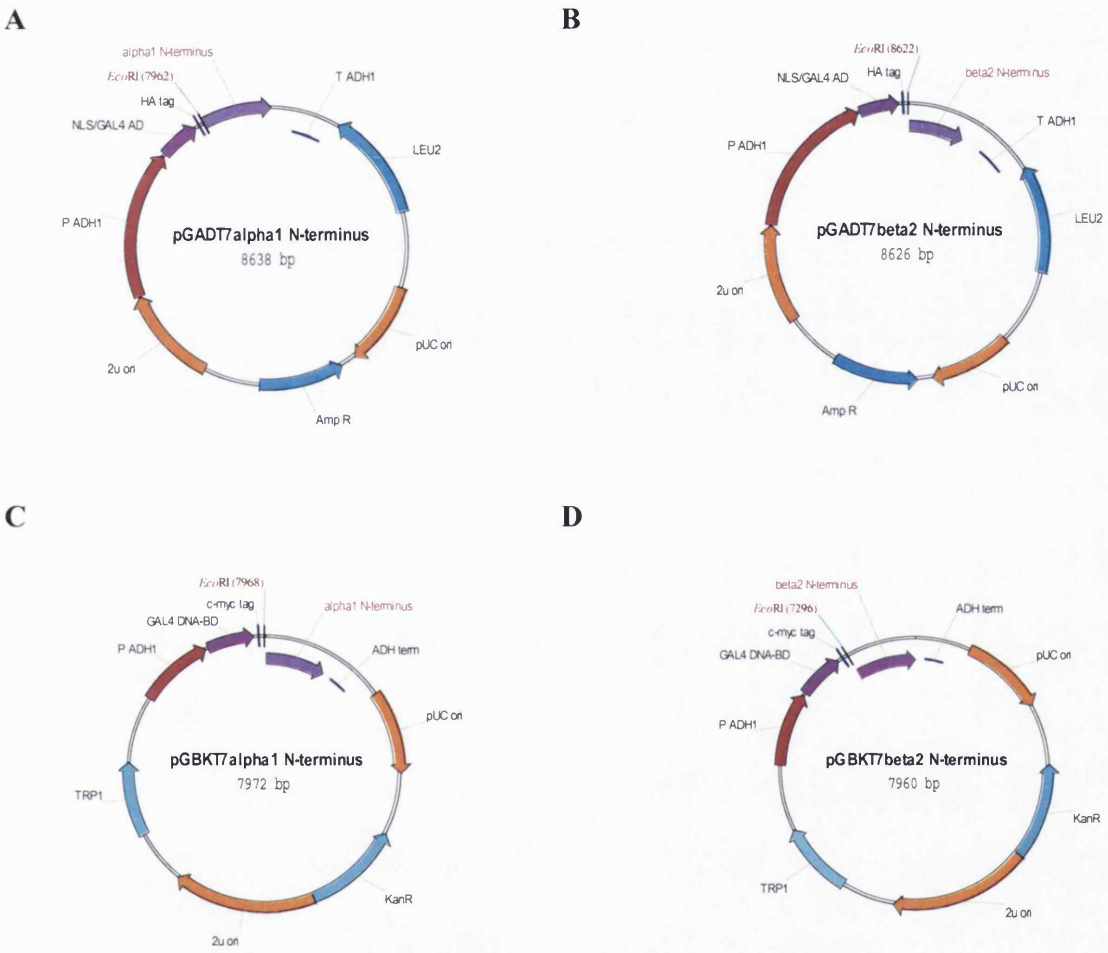

The $GABA_A$ receptor subunit N-terminal sequences α1(1-224) and β2(1-220) were cloned into the GAL4 yeast two hybrid AD and DNA-BD vectors.

FIGURE 3.2.6. AN IMMUNOBLOT SHOWING THE EXPRESSION OF THE GAL4 DNA-BD FUSION PROTEINS CONTAINING A $GABA_A$ RECEPTOR α1 OR β2 SUBUNIT N-TERMINAL DOMAIN IN THE YEAST STRAIN, AH109

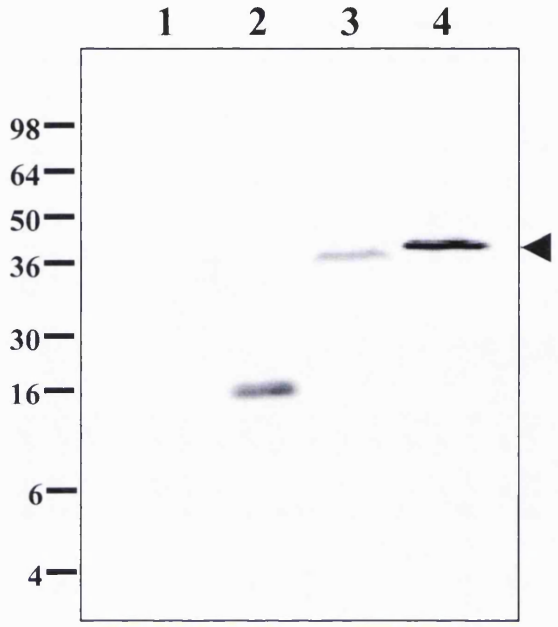

Lanes:

1. Untransformed AH109 cells
2. GAL4 DNA-BD
3. GAL4 DNA-BD α1(1-224)
4. GAL4 DNA-BD β2(1-220)

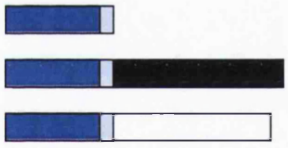

Key: = GAL4-DNA-BD = β2(1-220)
= C-myc epitope = α1(1-224)

Construct	Predicted M_r (kDa)	Observed M_r (kDa)
GAL4 DNA-BD	17	~14
GAL4 DNA-BD α1(1-224)	43	~39
GAL4 DNA-BD β2(1-220)	43	~43

The GAL4 DNA-BD vector containing a $GABA_A$ receptor α1 or β2 subunit N-terminal domain sequence was transformed into the yeast strain, AH109. Fusion proteins were extracted from yeast and analysed by immunoblotting using a monoclonal anti- c-myc antibody. The arrowhead indicates the positions of the α and β N-terminus fusion proteins.

FIGURE 3.2.7. AN IMMUNOBLOT SHOWING THE EXPRESSION OF THE GAL4 AD FUSION PROTEINS CONTAINING A $GABA_A$ RECEPTOR α1 OR β2 SUBUNIT N-TERMINAL DOMAIN IN THE YEAST STRAIN, AH109

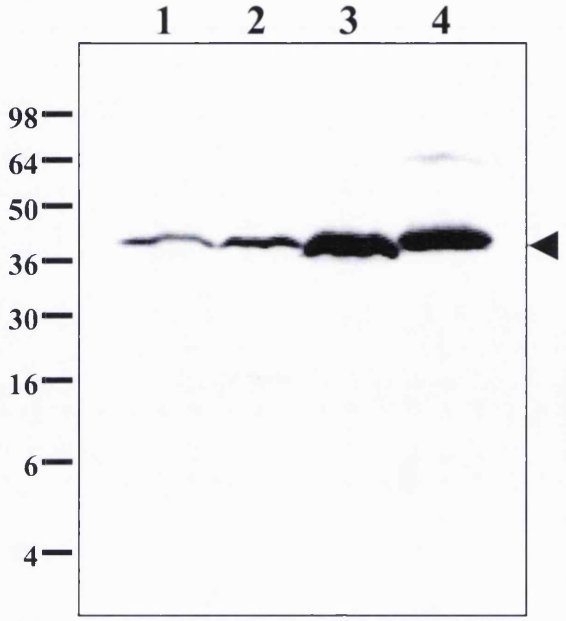

Lanes:

1. Untransformed AH109 cells
2. GAL4 AD
3. GAL4 AD α1(1-224)
4. GAL4 AD β2(1-220)

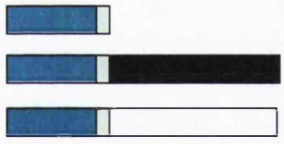

Key: = GAL4-AD = α1(1-224) = HA epitope = β2(1-220)

Construct	Predicted M_r (kDa)	Observed M_r (kDa)
pGADT7 vector	15	~15
pGADT7α1(1-224)	41	~39
pGADT7β2(1-220)	41	~41

The GAL4 AD vector containing a $GABA_A$ receptor α1 or β2 subunit N-terminal domain sequence was transformed into the yeast strain, AH109. Fusion proteins were extracted from yeast and analysed by immunoblotting using a monoclonal anti-HA antibody. The arrowhead indicates the position of α1 and β2 N-terminus fusion constructs.

FIGURE 3.2.8. AN EXAMPLE OF A β-GALACTOSIDASE ASSAY FOR LacZ REPORTER GENE ACTIVITY IN YEAST TRANSFORMED WITH $GABA_A$ RECEPTOR α1 AND β2 N-TERMINAL DOMAINS

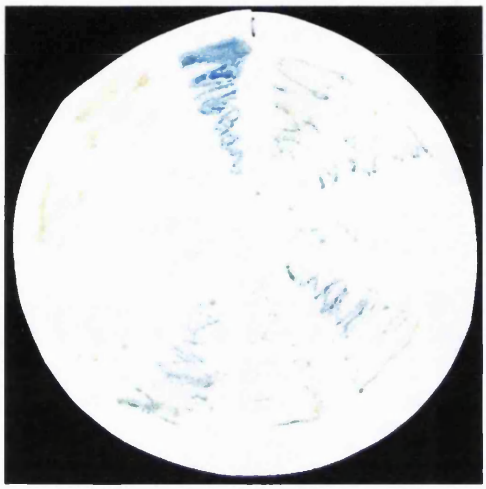

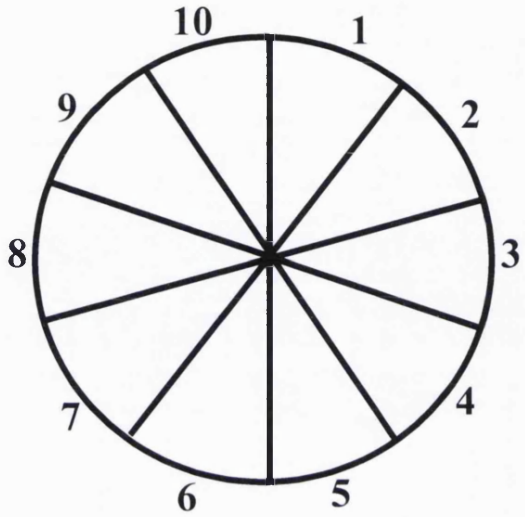

Plasmid combinations

1. pGADT7α1-N (1-224)/pGBKT7β2-N(1-220)
2. pGADT7β2-N(1-220)/pGBKT7α1-N(1-224)
3. pGADT7α1-N(1-224)/pGBKT7α1-N(1-224)
4. pGADT7β2-N(1-220)/pGBKT7β2-N(1-220)
5. pGADT7α1-N(1-224)/pGBKT7
6. pGADT7β2-N (1-220)/pGBKT7
7. pGADT7/pGBKT7β2-N(1-220)
8. pGADT7pGBKT7α1-N(1-224)
9. pGADT7/pGBKT7
10. pTD1-1/pVA3-1

A β-galactosidase assay was carried out on yeast co-transformed with combinations of α1 and β2 subunit N-termini to test for *LacZ* reporter gene activity which results in a blue colour.

FIGURE 3.2.9. VECTOR DIAGRAMS OF THE MODIFIED LEXA SYSTEM CONSTRUCTS USED TO STUDY THE INTERACTIONS BETWEEN α1 AND β2 N-TERMINALS

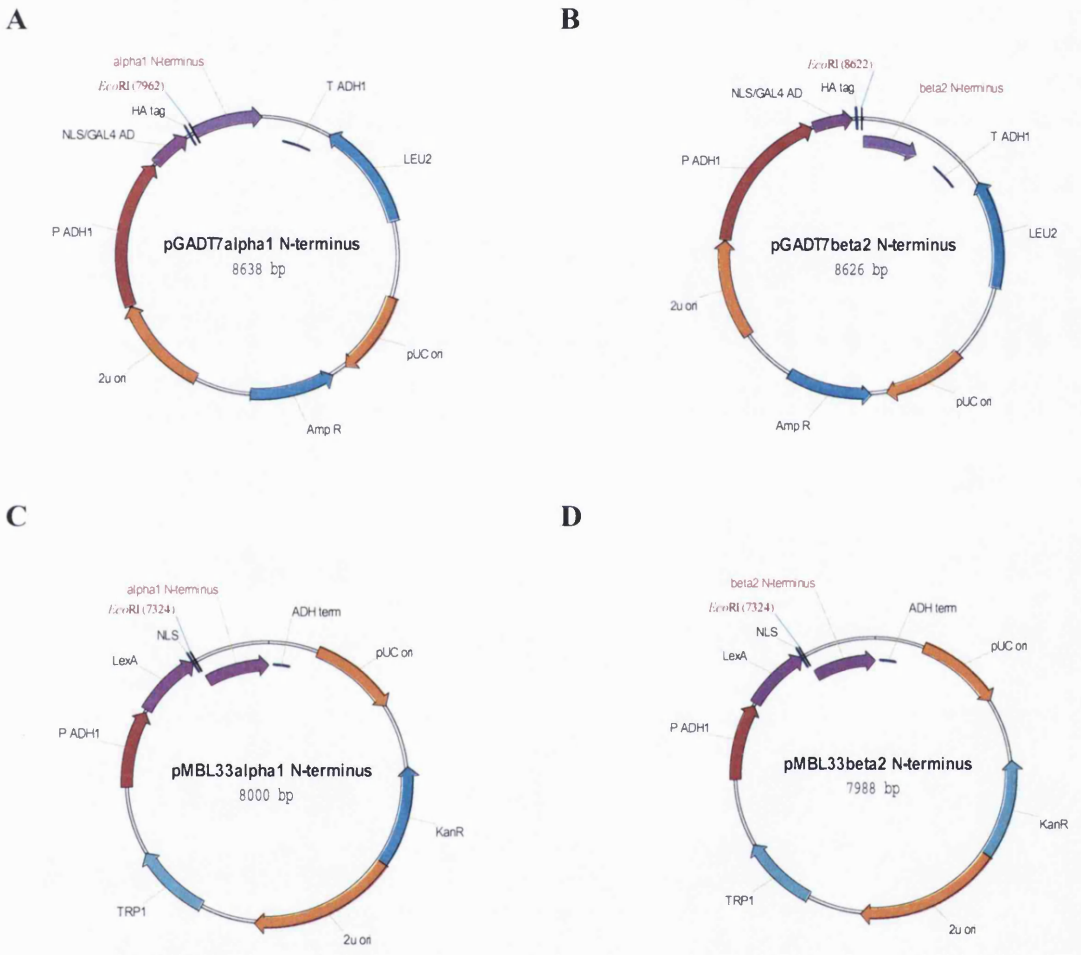

The $GABA_A$ receptor subunit sequences α1(1-224) and β2(1-220) were each sub-cloned into the modified LexA system DNA-BD vector, pMBL33.

FIGURE 3.2.10. VECTOR DIAGRAMS OF THE CYTOTRAP® SYSTEM CONSTRUCTS USED TO STUDY THE INTERACTIONS BETWEEN α1 AND β2 N-TERMINALS

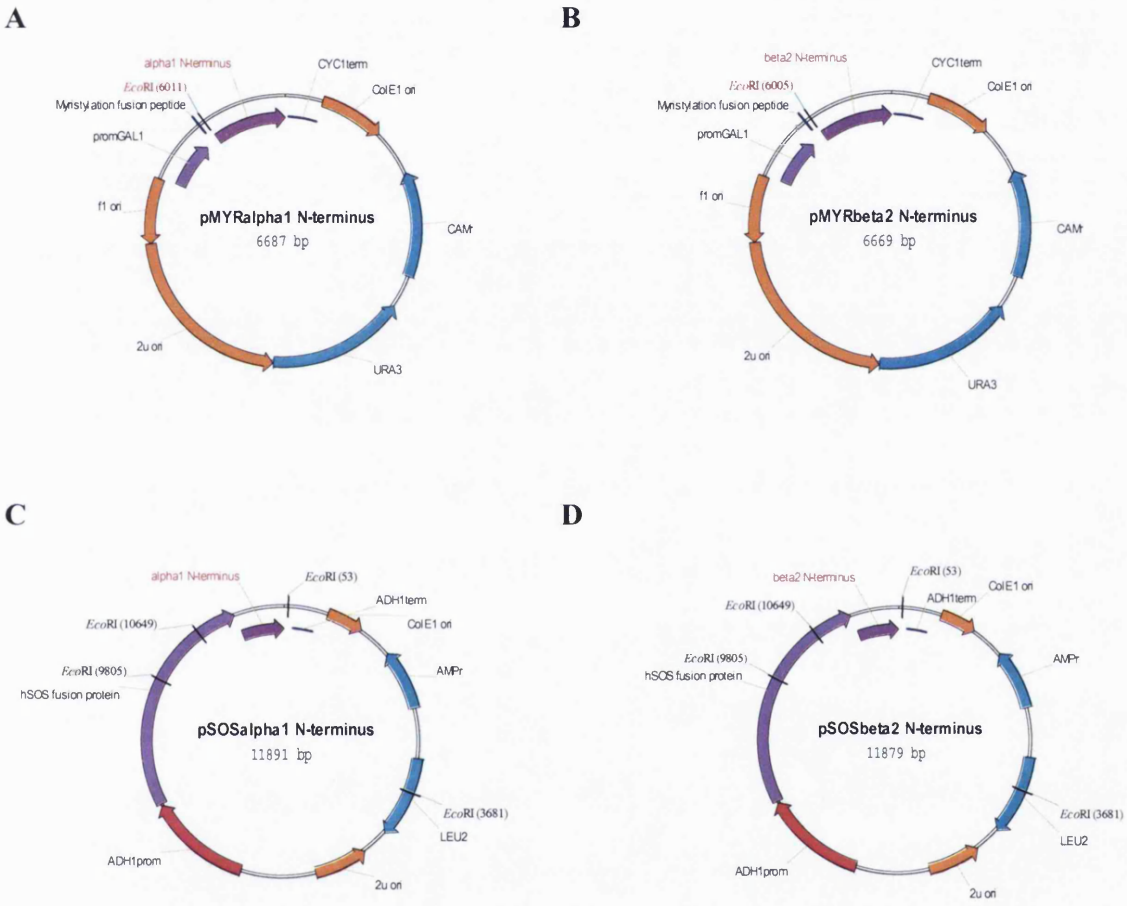

The $GABA_A$ receptor subunit sequences α1(1-224) and β2(1-220) were each sub-cloned into the CytoTrap® vectors, pMyr and pSos.

FIGURE 3.2.11. AN EXAMPLE OF COLONY GROWTH ON -U/-L GLUCOSE-BASED MEDIA AFTER CO-TRANSFORMATION OF CYTOTRAP® YEAST STRAIN, CDC25H, WITH α1 AND β2 N-TERMINAL DOMAINS

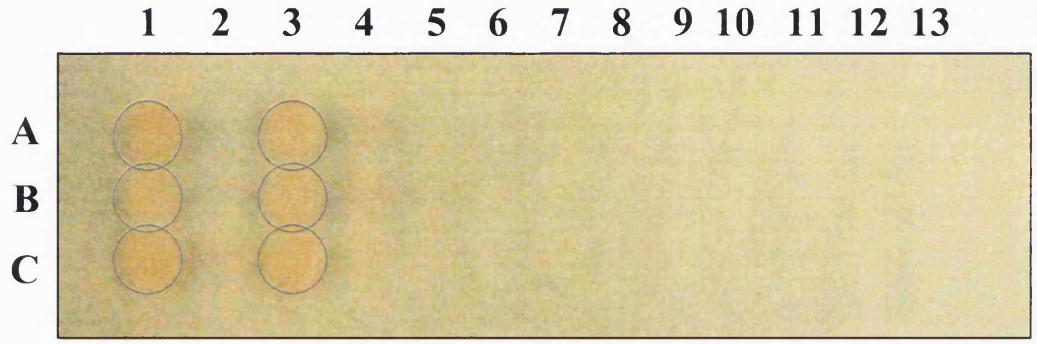

Patch	SOS CONSTRUCT	MYR CONSTRUCT
1 A-C	pSOSMAFB	pMYRMAFB
2 A-C	pSOSCOLL	pMYRMAFB
3 A-C	pSOSMAFB	pMYRSB
4 A-C	pSOSMAFB	pMYRLAMIN C
5 A-C	pSOSα1-N(1-224)	pMYRβ2-N(1-220)
6 A-C	pSOSβ2-N(1-220)	pMYRα1-N(1-224)
7 A-C	pSOSα1-N(1-224)	pMYRα1-N(1-224)
8 A-C	pSOSβ2-N(1-220)	pMYRβ2-N(1-220)
9 A-C	pSOSα1-N(1-224)	pMYR
10 A-C	pSOSβ2-N(1-220)	pMYR
11 A-C	pSOS	pMYRα1-N(1-224)
12 A-C	pSOS	pMYRβ2-N(1-220)
13 A-C	pSOS	pMYR

The CytoTrap® yeast strain, cdc25H, was co-transformed with combinations of $GABA_A$ receptor α1 and β2 subunit N-termini. Protein interactions were detected by growth on galactose-based selection media, lacking leucine and uracil and incubated at 37°C. Grey circles indicate areas of yeast growth after 5 days at 37°C.

FIGURE 3.2.12. SCHEMATIC REPRESENTATION OF THE RELATIVE SIZES OF FUSION PROTEIN CONSTRUCT DOMAINS USED IN EACH YEAST TWO-HYBRID SYSTEM

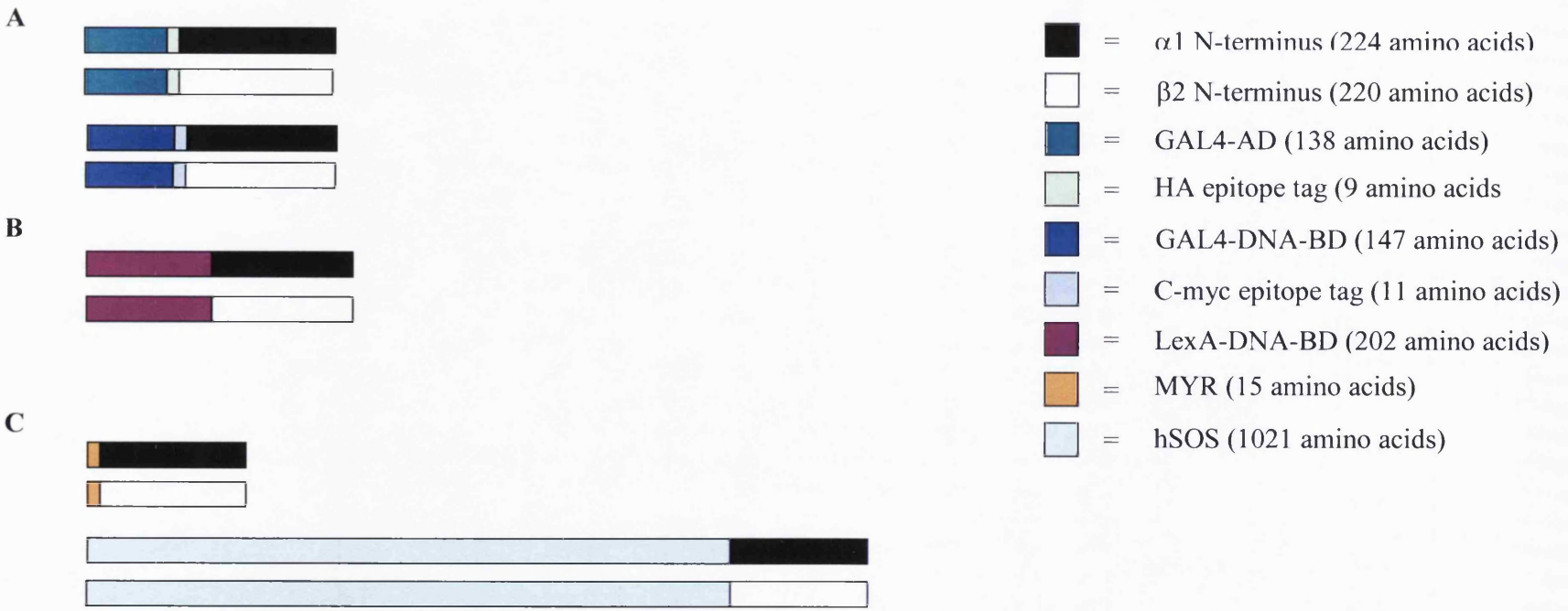

The diagram shows the relative sizes of the components of the fusion proteins used in each yeast two-hybrid system. The GAL4 system constructs, (A), produced from pGADT7 and pGBKT7 vectors, contain HA or c-myc epitope tags, respectively, for detection of expression in yeast by immunoblotting. The modified LexA system uses the same AD construct to the GAL4 system, but a different DNA-BD, (B). The CytoTrap® system, (C), uses two fusion proteins of very different sizes to the other two systems and to each other.

FIGURE 3.2.13. SCHEMATIC REPRESENTATION OF THE $GABA_A$ RECEPTOR SUBUNIT N-TERMINAL DOMAINS SHOWING SEQUENCES IMPORTANT FOR ASSEMBLY

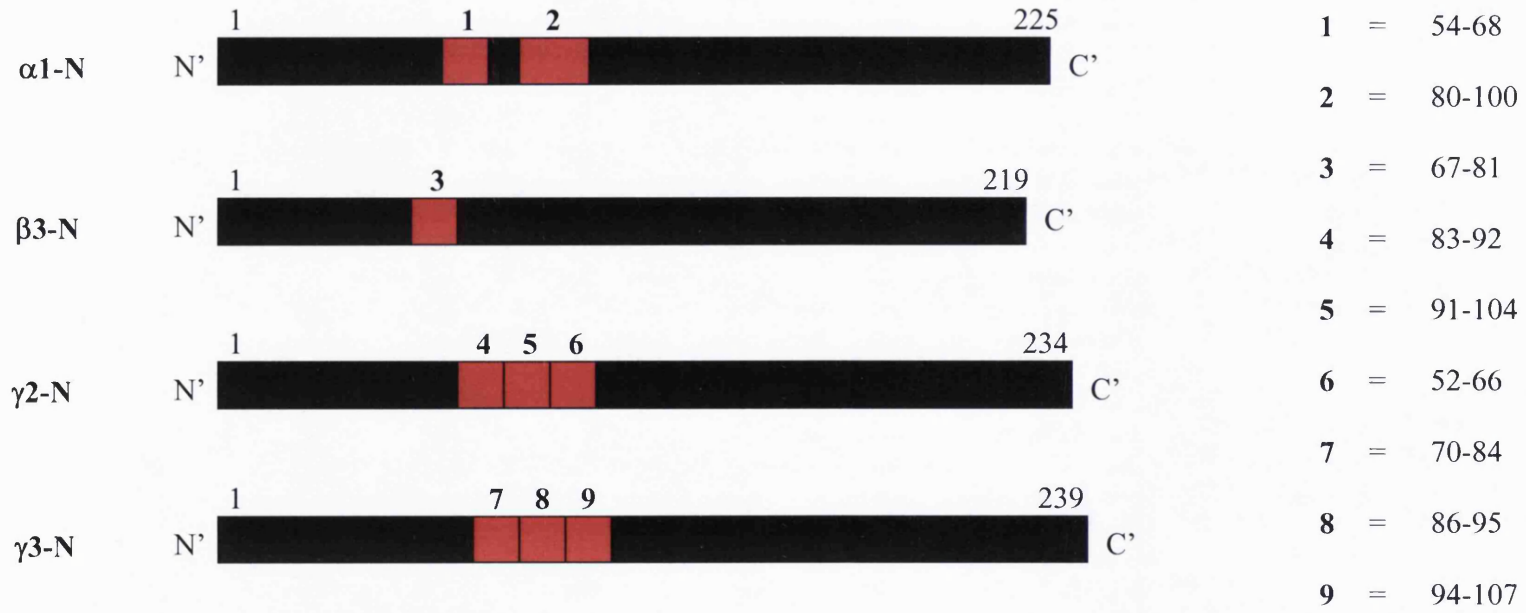

The diagram shows a schematic representation of the α1, β3, γ2 and γ3 $GABA_A$ receptor subunit N-terminal domains. The numbered red boxes represent the positions of sequences identified as important for subunit assembly and specific amino acid numbers are indicated on the right.

TABLE 3.1.1. COMPARISON OF THE GAL4, LEXA AND MODIFIED LEXA YEAST TWO-HYBRID SYSTEMS

Yeast Two-Hybrid System	GAL4	LexA	mLexA
Transcription Factor Type	Eukaryotic	Prokaryotic	Prokaryotic
Yeast Strain	AH109	EGY48	L40
AD Vector	pGADT7	pJG4-5	pGADT7
DNA-BD Vector	pGBKT7	pEG202-NLS	pMBL33
Reporter Genes	Adenine Histidine	Leucine	Histidine

The table shows a comparison between the GAL4, LexA and mLexA yeast two-hybrid systems, showing the features of each system that have been incorporated into the modified hybrid system.

TABLE 3.2.1. CO-TRANSFORMATION OF THE $GABA_A$ RECEPTOR α1 AND β2 N-TERMINALS IN THE GAL4 YEAST TWO-HYBRID SYSTEM

Activation Domain Construct	DNA-Binding Domain Construct	-2 Selective Media	-4 Selective Media	β-Galactosidase Activity
pGADT7 α1-N(1-224)	pGBKT7 β2-N(1-220)	++	(+)	+
pGADT7 β2-N(1-220)	pGBKT7 α1-N(1-224)	++	+	+
pGADT7 α1-N(1-224)	pGBKT7 α1-N(1-224)	++	(+)	+
pGADT7 β2-N(1-220)	pGBKT7 β2-N(1-220)	++	++	+
pGADT7 α1-N(1-224)	pGBKT7-	++	+	+
pGADT7 β2-N(1-220)	pGBKT7-	++	++	+
pGADT7-	pGBKT7 α1-N(1-224)	++	-	-
pGADT7-	pGBKT7 β2-N(1-220)	++	-	-
pGADT7-	pGBKT7-	++	-	-
pTD1-1	pVA3-1	+	+	+

The results are representative of n = 4 independent co-transformations

Key: -2 Selective media lacks leucine and tryptophan
-4 Selective media lacks adenine, histidine, leucine and tryptophan
For nutritional selection - = no growth, (+) = 1-10 colonies, + = 11-100 colonies, ++ = 101-200 colonies
For β-galactosidase assay + = enzyme activity observed, - = no enzyme activity observed

$GABA_A$ receptor α1 and β2 subunit N-terminal domains were cloned into the GAL4 AD and DNA-BD vectors to produce in frame fusion constructs. Combinations of these constructs were co-transformed into AH109 yeast and assayed for reporter gene activity, i.e. for growth on selective media and for β-galactosidase activity.

TABLE 3.2.2. CO-TRANSFORMATION OF THE $GABA_A$ RECEPTOR α1 AND β2 N-TERMINALS IN THE (m) LEXA YEAST TWO-HYBRID SYSTEM

Activation Domain Construct	DNA-Binding Domain Construct	-2 Selective Media	-3 Selective Media	β-galactosidase Activity
pGADT7 α1-N(1-224)	pMBL33 β2-N(1-220)	+++	(+)	+
pGADT7 β2-N(1-220)	pMBL33 α1-N(1-224)	+++	+	+
pGADT7 α1-N(1-224)	pMBL33 α1-N(1-224)	+++	(+)	+
pGADT7 β2-N(1-220)	pMBL33 β2-N(1-220)	+++	+	+
pGADT7 α1-N(1-224)	pMBL33-	+++	++	+
pGADT7 β2-N(1-220)	pMBL33-	+++	+++	+
pGADT7-	pMBL33 α1-N(1-224)	+++	–	-
pGADT7-	pMBL33 β2-N(1-220)	+++	–	-
pGADT7-	pMBL33-	+++	-	-
pGAD10 GRIF-1(8-633)	pMBL33 β2-IL(303-427)	+++	++	+

The results are representative of n = 3 independent co-transformations.

Key: -2 Selective media lacks leucine and tryptophan.
-3 Selective media lacks histidine, leucine and tryptophan and contains 2.5 mM 3-amino triazole
For nutritional selection - = no growth, (+) = 1-10 colonies, + = 11-100 colonies, ++ = 101-200, colonies, +++ = >200
For β-galactosidase assay + = enzyme activity observed, - = no enzyme activity observed

$GABA_A$ receptor α1 and β2 subunit N-terminal domains were sub-cloned in frame into the (m) LexA DNA-BD vector. Combinations of AD and DNA-BD constructs were co-transformed into L40 yeast and assayed for reporter gene activity, i.e. for growth on selective media and for β-galactosidase activity.

TABLE 3.2.3. CO-TRANSFORMATION OF THE POSITIVE AND NEGATIVE CYTOTRAP® YEAST TWO-HYBRID SYSTEM CONTROL PLASMIDS

pSOS Construct	pMYR Construct	-UL Glucose at 25°C	-UL Galactose at 25°C	-UL Glucose at 37°C	-UL Galactose at 37°C
pSOSMAFB	pMYRMAFB	+	+	-	+
pSOSCOL1	pMYRMAFB	+	+	-	-
pSOSMAFB	pMYRLamin C	+	+	-	-
pSOSMAFB	pMYRSB	+	+	-	+
pSOS-	pMYR-	+	+	-	-

The results are representative of n = 3 independent co-transformations.

Key: -UL media lacks uracil and leucine.
+ = cell growth, - = no cells growth

The CytoTrap® yeast strain, cdc25H, was co-transformed with double combinations of positive and negative control plasmids. The table shows that the positive control co-transformants pMyrMAFB/pSosMAFB and pMyrSB/pSosMAFB grew at 37°C on galactose-based media whereas pMyrMAFB/pSosCol1, pMyrLaminC/pSosMAFB and pMyr/pSos combinations show no growth.

TABLE 3.2.4. CO-TRANSFORMATION OF THE $GABA_A$ RECEPTOR α1 AND β2 N-TERMINALS IN THE CYTOTRAP® YEAST TWO-HYBRID SYSTEM

pSOS Construct	pMYR Construct	-UL Glucose at 25°C	-UL Galactose at 25°C	-UL Glucose at 37°C	-UL Galactose at 37°C
pSOSMAFB	pMYRMAFB	+	+	-	+
pSOSCOL1	pMYRMAFB	+	+	-	-
pSOSMAFB	pMYRLamin C	+	+	-	-
pSOSMAFB	pMYRSB	+	+	-	+
pSOS-	pMYR-	+	+	-	-
pSOS α1-N(1-224)	pMYR β2-N(1-220)	+	+	-	-
pSOS β2-N(1-220)	pMYR α1-N(1-224)	+	+	-	-
pSOS α1-N(1-224)	pMYR α1-N(1-224)	+	+	-	-
pSOS β2-N(1-220)	pMYR β2-N(1-220)	+	+	-	-
pSOS α1-N(1-224)	pMYR-	+	+	-	-
pSOS β2-N(1-220)	pMYR-	+	+	-	-
pSOS-	pMYR α1(1-224)	+	+	-	-
pSOS-	pMYR β2-N(1-220)	+	+	-	-

The results are representative of n = 3 independent co-transformations.

Key: -UL media lacks uracil and leucine.
+ = cell growth, - = no cells growth

$GABA_A$ receptor subunit domains α1(1-224) and β2(1-220) were sub-cloned into the CytoTrap® pSos and pMyr vectors. Combinations of Myr and Sos constructs were co-transformed into cdc25Hα yeast and assayed for reporter gene activity, i.e. growth at 37°C on galactose-based media lacking uracil and leucine.

CHAPTER 4:
RESULTS 2

4.1. RATIONALE FOR THE USE OF THE $GABA_A$ RECEPTOR β2 N-TERMINUS AND β3-IL TO SCREEN A YEAST TWO-HYBRID cDNA LIBRARY TO IDENTIFY INTERACTING PROTEINS

In parallel with the α1/β2 N-terminal domain interaction co-transformations, a yeast two-hybrid rat brain cDNA library was screened to try to identify novel proteins interacting with $GABA_A$ receptor subunits that may be involved in receptor assembly, trafficking and stabilisation at the synapse. The first consideration was which $GABA_A$ receptor subunit to use to screen the library.

4.1.1. THE $GABA_A$ RECEPTOR β3-IL

The $GABA_A$ receptor β2 subunit IL was used in a previous yeast two-hybrid library screen in this laboratory. It resulted in the identification of the novel protein, $GABA_A$ receptor interacting factor, GRIF-1 (Beck *et al.*, 2002), a putative trafficking factor (Section 1.2.6.5.2 and Chapter 5). Particular $GABA_A$ receptor subtypes are localised to distinct regions of neuronal membranes e.g. δ subunit-containing receptors are always found extra-synaptically (Nusser *et al.*, 1998). The $GABA_A$ receptor β subunits were shown to play a role in receptor targeting in polarised, MDCK cells (Connolly *et al.*, 1996a). The β1 subunit-containing receptors showed a non-polarised distribution, whereas β2 subunit- and β3 subunit-containing receptors were localised to the basolateral membrane. The β2 and β3 subunits differed in their transport mechanisms in that β2 subunits were targeted directly to the basolateral membrane, whereas the β3 subunits were firstly localised to the apical membrane, reaching the basolateral membrane by transcytosis over time. Of the β subunits β2 and β3 are the most abundantly expressed in rat brain, i.e. the β2 subunit is present in 55-60% of all $GABA_A$ receptors in rat brain membranes, the β3 subunit is present in 19-25% and the β1 subunit in 16-18% of these receptors (Benke *et al.*, 1994). Both the β2 and β3 subunits are good candidates for yeast two-hybrid baits to identify trafficking proteins. The β3 subunit isoform, the second most common form of β subunit, is widely expressed throughout the brain and displays a specific receptor trafficking function. Therefore, this subunit was chosen for use as the bait in the first yeast two-hybrid cDNA library screen. The intracellular loop (IL) of $GABA_A$ receptor subunits shows the most sequence variability among members of the same subunit subclass. The IL region is known to

contain binding domains for intracellular regulatory proteins such as kinases. Indeed, the serine kinase, $GABA_A$ receptor-tubulin complex-associated protein of molecular mass 34 kDa (GTAP-34), was identified by co-immunoprecipitation as interacting specifically with the IL of the β3 subunit (Kannenberg *et al.*, 1999). $GABA_A$ receptor subunit ILs have also been shown to interact selectively amongst themselves (Nymann-Andersen *et al.*, 2002) i.e. γ2-ILs will interact with γ1-3 subunit ILs and β1-3 subunit ILs, but not with the α subunit ILs. The same region of the γ2-IL that interacts with itself is also the binding motif for the $GABA_A$ receptor-associated protein, GABARAP, suggesting that IL interactions may be involved in receptor transport and clustering. Therefore, on the basis of abundance the IL of the $GABA_A$ receptor β3 subunit was chosen to screen the rat brain cDNA library for interacting proteins.

4.1.2. THE $GABA_A$ RECEPTOR β2 N-TERMINUS

A second library screen was carried out in an attempt to identify proteins involved in $GABA_A$ receptor assembly and synapse formation.

The formation of an intricate matrix of intracellular and extracellular proteins is involved in the development, stabilisation and plasticity of synapses. At the neuromuscular junction, for example, the extracellular protein, agrin, a synaptogenic factor secreted from the nerve terminal, indirectly mediates clustering of acetylcholine receptors at the synapse (Moransard *et al.*, 2003). Agrin binds its postsynaptic membrane receptor which contains a muscle specific kinase (MuSK) that clusters at synaptic sites. The extracellular domain of MuSK then interacts with acetylcholine receptor associated protein, rapsyn (Apel *et al.*, 1997). Since rapsyn is entirely intracellular, an as yet unidentified membrane spanning linker protein must also be involved in this interaction. Activated MuSK phosphorylates ACh receptors which initiates receptor clustering at the synapse. In this way, a series of protein-protein interactions is involved in the formation of synaptic specialisations.

Another example of protein interactions with neurotransmitter receptor extracellular domains is the interaction between the EphrinB receptor, EphB, and the NMDA receptor NR1 subunit. (Dalva *et al.*, 2000). EphrinB is a transmembrane signalling protein found on the pre-synapse. The interaction between EphrinB and its receptor, EphB, which is found on the post-synapse, causes the extracellular domain of EphB to interact with the extracellular domain of the NMDA receptor NR1 subunit. This

interaction suggests that EphrinB signalling causes clustering of EphB receptors with NMDA receptors at newly forming synaptic junctions. The association could also be indicative of cross-talk between the two receptor signalling pathways and could be important in synaptic plasticity.

The N-terminal domain of each assembled $GABA_A$ receptor subunit, when expressed at the cell surface, is located outside the cell where it interacts with the ligands that activate $GABA_A$ receptor activity, e.g. GABA, benzodiazepines and neurosteroids. This also leaves the extracellular N-termini open for interactions with proteins found in the synaptic cleft. The N-terminal domain of the AMPA receptor subunit GluR2 has been shown, through the use of deletion and chimeric constructs, to be important for dendritic spine formation in hippocampal neurones (Passafaro *et al.*, 2003). Chimeric constructs of NMDA receptor subunits expressed in HEK 293 cells have also been used to identify two domains of the NR2 subunits that are involved in the glycine-independent desensitisation of NMDA receptors (Krupp *et al.*, 1998).

It was therefore decided that a $GABA_A$ receptor subunit N-terminal domain would be used to screen a yeast two-hybrid rat brain cDNA library, to identify proteins that may be involved in the formation, stabilisation or plasticity of $GABA_A$ receptor synaptic specialisations. The rat β2 subunit N-terminus was chosen for use as a bait since, as discussed above, along with the α1 and γ2 subunits, it forms the most common receptor subtype in adult brain and it is widely distributed in both perinatal brain (when synaptogenesis begins) and in adult brain (Fritschy *et al.*, 1994).

4.2. RESULTS

4.2.1. CONSTRUCTION OF THE DNA-BD BAIT PLASMIDS

Construction and characterisation of the $GABA_A$ receptor β2(1-220) N-terminal domain DNA-BD plasmid is described in Section 3.3.1.

The $GABA_A$ receptor β3 subunit IL construct was prepared by direct cloning into the pGBKT7 vector (method summarised in Figure 2.1). The β3 subunit sequence, 306-425, was amplified by PCR from a previously prepared $GABA_A$ receptor β3 subunit plasmid construct, using specific oligonucleotide primers listed in Table 2.1, and specific thermocycling parameters, detailed in Table 2.1.4. This sequence was used to generate the construct pGBKT7β3-IL(306-425). The insertion and orientation of each sequence was confirmed by oligonuceotide sequencing, as shown for the GAL4 AD and DNA-BD fusion constructs in Figure 3.2.4. Plasmid maps for the bait constructs are shown in Figure 4.1. Figure 4.2 shows an immunoblot demonstrating expression of the β3-IL fusion protein, GAL4 DNA-BD β3-IL(306-425), in yeast. From the figure it can be seen that a band representing the β3-IL sequence was detected at ~26 kDa.

4.2.2. SMALL-SCALE LIBRARY TRANSFORMATION

A sequential transformation protocol was employed for the cDNA library screen to ensure that the availability of DNA-BD plasmid would not limit potential interactions with library clones. In this procedure the GAL4 yeast strain, AH109, was initially transformed individually with either the $GABA_A$ receptor β2-N(1-220) or the β3-IL(306-425) DNA-BD construct using a small-scale transformation procedure (Sections 2.2.3.2 and 2.2.3.3). Colonies were selected on dropout media lacking tryptophan to ensure that the resulting yeast contained the DNA-BD plasmid.

A small-scale test screen was carried out for each DNA-BD construct by transformation of yeast already containing the DNA-BD vector, with 1 μg of library cDNA. The transformation efficiency of the library was determined from this screen. A rat brain cDNA library with a complexity of ~1 x 10^6 independent clones was used. To screen 1 x 10^6 clones on 50 large plates would require 20000 clones screened per plate. Test transformations using 1 μg of library DNA produced approximately 5000 clones on 1 plate, therefore 4 x the amount of DNA per plate was needed to achieve 1 x library coverage (i.e. 200 μg DNA per screen).

4.2.3. LARGE-SCALE LIBRARY TRANSFORMATION

Rat brain mRNA for the MATCHMAKER yeast two-hybrid cDNA library was obtained from Clontech Laboratories UK Ltd. Each library contains genomic DNA from approximately one-hundred 10-12 week old male Sprague-Dawley rats (MATCHMAKER library user manual, Clontech). mRNA is reverse transcribed using oligo d(T) primers. Adaptor sequences are added to each clone to aid excision from the vector and cDNAs smaller than 400 bp are removed before the remaining clones are ligated into the AD plasmid. Libraries are guaranteed to have at least 1 x 10^6 independent clones. The library titre was 10^8 colony forming units (cfu)/ml, which is greater than 10-fold the number of independent clones in the library, therefore the library was suitable for screening.

Large-scale library transformations were carried out using AH109 yeast cells pre-transformed with a DNA-BD construct (Section 2.2.3.4). For each screen, cells were transformed with 200 μg of library cDNA. Colonies were selected on 50 x 140 mm -4 (-W, -L, -H, -Ade) dropout agar plates after 1 week at 30°C.

4.2.4. LIBRARY SCREENING USING THE $GABA_A$ RECEPTOR β3-IL(306-425) AS THE BAIT

For the $GABA_A$ receptor β3-IL(306-425) cDNA library screen, 7 putative interacting colonies were obtained. Each colony was re-streaked onto -4 dropout agar to allow time for the excess plasmids to dropout of the cells, since yeast cells containing interacting library clones may also contain extra AD plasmids which are not involved in the interaction. If kept under continuous selection, yeast tend to lose these plasmids leaving only the true interactor. Re-streaked cells were then tested for β-galactosidase reporter gene activity. Each putative positive clone showed β-galactosidase activity after 4 h. AD plasmids were extracted from yeast (Section 2.2.3.7) and amplified by electroporation transformation of bacteria. Selection for yeast AD plasmids from DNA isolated from yeast library transformants containing both AD and DNA-BD plasmids is possible because pGAD10 and pGBKT7 vectors contain different antibiotic resistance genes and DH5α bacteria cannot accommodate both of these plasmids simultaneously. Therefore, selection on LB-AMP agar caused selection of AD vectors and expulsion of DNA-BD vectors i.e. those containing a KAN^r gene. Each isolated library plasmid was purified from bacteria and digested by the restriction enzyme, *Eco*RI, to excise the clone

fragment and thus determine its size. Figure 4.3 shows the digestion products for each of the clones. Three bacterial clones were analysed for each putative interacting clone isolated from yeast. Clones 1, 4, and 7 contained no insert and were disregarded as false positives. Clone 2 contained an insert of ~740 bp. Clone 3 contained an insert of ~915 bp. Bacterial clones for yeast clone 5 each contained a different profile, i.e. the first contained 2 insert fragments of ~650 and ~315 bp, the second contained no insert and the third contained a fragment of ~2950 bp. Clone 6 contained an insert of ~350 bp. Each of the purified plasmids was co-transformed in yeast with the β3-IL(306-425) DNA-BD to confirm their interaction. Table 4.1. shows the results of these co-transformations. On re-co-transformation with the β3-IL(306-425), only clone 2 showed a positive interaction after 1 week under selection on -4 media, therefore clones 3, 5 and 6 were disregarded as false positives from the original screen. Clone 2 was next tested for its interaction specificity with the β3-IL(306-425). However, inclusion of a single negative control containing clone 2 co-transformed with an empty DNA-BD vector showed it to auto-activate reporter gene activity, therefore clone 2 was also disregarded.

4.2.5. LIBRARY SCREENING USING THE $GABA_A$ RECEPTOR β2-N(1-220) AS THE BAIT

For the β2-N(1-220) cDNA library screen 200μg DNA was used for screening and 10 putative interacting colonies were obtained. Each colony was re-streaked onto -4 dropout agar and tested for β-galactosidase reporter gene activity. All clones were positive for β-galactosidase reporter gene activity, therefore AD plasmids were extracted from yeast and amplified by electroporation transformation of bacteria, as in Section 4.2.4. Restriction enzyme digestion by *Eco*RI was carried out on each clone to determine the insert size. Figures 4.4 and 4.5 show the results of each digestion. Clones 1 and 9 contained no insert and were disregarded. Clones 2-8 and 10 all contained inserts. Clone 2 contained an insert of ~400 bp. Clone 3 contained an insert of ~600bp. Each bacterial clone from clone 4 contained a different insert, i.e. the first contained a ~480 bp insert, the second contained a ~290 bp insert and the third contained a ~375 bp insert. Clone 5 contained a 430 bp insert. One of the 3 bacterial clones for clone 6 contained an insert of ~2900 bp, whereas the remaining 2 contained no insert. Clone 7 contained an insert of ~1000 bp. Clone 8 contained an insert of ~2650 bp and clone 10 contained an insert of ~1420 bp. Each bacterial clone was re-co-transformed with the

original β2-N(1-220) DNA-BD construct to verify their interactions together with positive and negative controls i.e. the pTD1-1 and pVA3-1 plasmids and empty AD and DNA-BD plasmids, respectively. The results of the co-transformations are shown in Table 4.2. The pTD1-1/pVA3-1 positive control showed colony growth on -4 dropout media. The empty vector double negative control showed no growth. Clones 3 and 7 showed colony growth and α-galactosidase activity on co-transformation with the β2-N(1-220). Clones 2, 4-6, 8 and 10 showed no reporter gene activity and were disregarded. Co-transformations to test interaction specificity were carried out for clones 3 and 7. Each clone was co-transformed with a variety of DNA-BD constructs. The $GABA_A$ receptor constructs tested were β2-IL(303-427), β2TM3/IL/TM4(282-450), β2-IL/TM4(303-450), α1-IL(304-384), α1-N(1-224) and the original $GABA_A$ receptor construct β2-N(1-220). Positive and negative controls were also included. Clone 7 co-transformed with an empty DNA-BD vector showed it to auto-activate reporter genes, therefore it was disregarded. The results of the specificity test co-transformations for Clone 3 are shown in Table 4.3. The pTD1-1/pVA3-1 positive control showed reporter gene activity. The double empty vector negative control showed no reporter gene activity. The single negative control containing Clone 3 co-transformed with an empty DNA-BD vector also showed no reporter gene activity. Clone 3 showed reporter gene activity when co-transformed with either α1-N(1-224) or β2-N(1-220), but not with β2-IL(303-427), β2TM3/IL/TM4(282-450), β2-IL/TM4(303-450) or α1-IL(304-384).

4.2.5.1. NUCLEOTIDE SEQUENCE ANALYSIS AND DATABASE SEARCHING OF CLONE 3

Having confirmed the interaction of clone 3 with the $GABA_A$ receptor β2-N(1-220), oligonucleotide sequencing, using the ABI PRISM 310 Genetic Analyser, was carried out in order to identify the insert. The 504 bp oligonucleotide sequence was determined for clone 3 using a vector specific primer that hybridised upstream of the multiple cloning site. A second primer (shown in Table 2.1.3) was designed from initial sequencing results to hybridise within the clone 3 sequence and was used to determine the remainder of the sequence. The compiled sequence is shown in Figure 4.6. Translation of the nucleotide sequence was performed using a Translator program available at www.justbio.com. This translation revealed an open reading frame (ORF) in the +2 frame of the inserted sequence, which extended throughout the clone (Figure

4.7.). The ORF was also in frame with the GAL4 AD of the pGAD10 vector. Frames +1 and +3 contained stop codons near the beginning of the sequence. A nucleotide BLAST search of GenBank, RefSeq Nucleotides, EMBL, DDBJ and PDB databases, available via the National Centre for Biotechnology Information (NCBI) website (www.ncbi.nlm.nih.gov) was carried out and the search showed clone 3 to be 99% homologous to the cDNA sequence of the computationally predicted rat gene, TID1L, similar to the tumorous imaginal discs protein (Tid56-like protein), which is a DnaJ homologue. Greater than 90% nucleotide sequence homology was also found to numerous other DnaJ-domain-containing proteins.

4.2.5.2. AMINO ACID SEQUENCE DATABASE SEARCHING AND SEQUENCE ANALYSIS OF CLONE 3

A protein BLAST search of the Swissprot database was carried out on the deduced amino acid sequence of clone 3. This search found the protein to be 98% identical to a mouse tumorous imaginal discs protein. The search also showed clone 3 to be ~40% identical to the DnaJ chaperone protein of several species.

The protein sequence of clone 3 was analysed by the Simple Modular Architecture Research Tool program at smart.embl-heidelberg.de and by comparison to the DnaJ-like protein, TID1L. This analysis revealed the presence of DnaJ-like protein motifs. Clone 3 contains part of a J-domain motif, a glycine/phenylalanine-rich motif and a cysteine-rich zinc finger-like motif. An amino acid sequence alignment between TID1L and clone 3 is shown in Figure 4.8. The functional domains mentioned above are indicated on the alignment. Also indicated on the TID1L sequence is the HPD motif, which is conserved across all DnaJ homologous proteins. This motif lies outside the range of the clone 3 partial sequence.

4.2.5.3. SUB-CLONING OF CLONE 3 AND THE β2 N-TERMINAL DOMAIN INTO MAMMALIAN EXPRESSION VECTORS

Clone 3 and β2-N(1-220) sequences were each sub-cloned into a mammalian expression vector for transfection into HEK 293 cells. Clone 3 was sub-cloned into pCMV4a which yields a protein product with an N-terminal c-myc tag and the β2-N(1-220) was sub-cloned into pcDNA4a which yields a protein product with an N-terminal His tag. HEK 293 cells were transfected with the respective constructs and analysed by immunoblotting. Uridine diphospho-*N*-acetylglucosamine: polypeptide β-*N*-

acetyglucosaminyl transferase (OGT) was used as a positive control for the anti-his antibody and C-myc-tagged GRIF-1(1-913) was used as a control for the anti C-myc antibody. Figure 4.9 shows that both clone 3 and β2-N(1-220) were expressed with the correct molecular sizes. Time limitations prevented further use of these constructs to validate their interaction.

4.3. DISCUSSION

The library screen of the $GABA_A$ receptor β3-IL produced 7 potential interactors, but all of these were eventually proven to be false positive colonies. The screen of the $GABA_A$ receptor β2 N-terminal domain produced 10 potential interactors; 9 of these were proven to be false positives, but the 1 remaining clone, clone 3, was found to be a novel protein, 99% identical to the rat DnaJ-like protein, TID1L. Protein motifs identified within the sequence suggested that it was a class I DnaJ homologue. The library clone is an incomplete sequence that contains a J-domain, a G/F-rich domain and a cysteine-rich domain. The nucleotide sequence of clone 3 is 99% identical to the corresponding region of the computationally derived rat gene, TID1L sequence. The protein sequence is 100% identical over this region.

4.3.1. THE DnaJ PROTEINS

DnaJ (a homologue of hsp40) is a co-chaperone protein, which is involved in the DnaJ, DnaK (hsp70), GrpE (hsp105) heat-shock response where it aids refolding of unfolded proteins, by recruiting them to DnaK (Cyr *et al.*, 1994). Under normal cellular conditions the heat-shock proteins are involved in a variety of functions such as gene expression, translation initiation, protein folding and protein translocation. Different combinations of DnaK and DnaJ proteins are found in different sub-cellular compartments.

DnaJ homologues fall into three classes (Linke *et al*, 2003). Class I DnaJ homologues contain four domains. The first is the J-domain which contains 4 α-helical regions with a conserved HPD motif between helices 2 and 3 and this region forms a binding site for the chaperone protein, DnaK. Next, there is a G/F-rich domain that is involved in ATPase activation. This is followed by a cysteine-rich domain which forms zinc binding centres I and II. Zinc binding centre I is involved in the autonomous activity of DnaJ i.e. binding of substrate proteins to prevent their irreversible aggregation, whereas zinc centre II is involved in the co-chaperone functions by providing a second binding site between DnaJ and DnaK (Linke *et al.*, 2003). Finally, there is a poorly conserved C-terminal domain. Class II DnaJ homologues lack the zinc binding centre domains and class III DnaJ homologues contain only the DnaJ domain.

It is thought that those DnaJ homologues that contain the zinc centre domains are involved in recruiting a variety of substrate proteins to DnaK, whereas those that lack this region may have developed a more specific function (Kelly, 1998). DnaJ is also able to bind and recruit proteins that contain secondary or tertiary structures to DnaK, whereas DnaK itself binds only unfolded proteins.

4.3.2. TID1 PROTEINS

The human TID1 gene encodes two splice variants (long and short forms) of the hTid-1 protein. These proteins are the human homologues of the Drosophila tumour suppressor protein, Tid56, which is a DnaJ homologue. The long and short forms of hTid-1 were shown to have opposing effects on apoptosis induced by tumour necrosis factor α (TNFα) and mitomycin C in human U20S cells (Syken *et al.*, 1999). hTid-1_L increased apoptosis, while hTid-1_S suppressed apoptosis induced by TNFα and mitomycin C. This study also suggested that Tid-1 proteins were predominantly localised to the mitochondrial matrix. However, both long and short forms of hTid-1 have been found to interact with Jak2 which has a nucleocytoplasmic localisation (Sarker *et al.*, 2001). HTid-1 proteins were also shown to interact with cytoplasmic hsp70. Analysis of nuclear and cytoplasmic cellular fractions of Hep2 cells in this study detected mature hTid1 proteins.

More recently three rat isoforms of the Tid-1 protein (rTid-1 long, intermediate and short isoforms) were identified (Fujita *et al.*, 2004) however these sequences have not yet been published. The intermediate isoform of rTid-1 was found to interact with the hsp70 chaperone protein, mortalin. Mortalin is predominantly found in mitochondria, but has also been detected in the ER, cytoplasm, cytoplasmic vesicles and at perinuclear sites (Ran et al., 2000 and reviewed by Wadhwa *et al.*, 2002). Mortalin has been implicated in various cellular functions outside of mitochondria including receptor trafficking and internalisation (Sacht *et al.*, 1999; Mizakoshi *et al.*, 1999), inactivation of the tumour suppressor, p53 (Wadhwa *et al.*, 1998) and unfolding of proteins outside of mitochondria (reviewed by Wadhwa *et al.*, 2002) suggesting that the function of mortalin is dependent on its subcellular location.

4.3.3. POSSIBLE FUNCTION OF CLONE 3

Figure 4.10 shows a schematic diagram showing an alignment of a typical DnaJ protein and the isolated β2-N(1-220) screen library clone 3. In chapter 3 it was concluded that

the $GABA_A$ receptor α1 and β2 subunit N-termini do not fold correctly in yeast. Therefore, in this study it is likely that the isolated DnaJ homologue is involved in rescuing inappropriately folded proteins by recruitment of the polypeptides to a DnaK protein for folding. One way to test this theory would be by co-expression of the DnaJ clone in mammalian cells with the full-length β2 subunit, which would be expected to fold correctly, and testing for an association by co-immunoprecipitation

The results from chapters 3 and 4 suggest that, although it is possible to use the yeast two-hybrid system to study some proteins which require complex folding or post-translational modifications (Section 3.4.3), it is not a good strategy for the study of $GABA_A$ receptor subunit N-termini. Therefore, an alternative method would need to be employed for further studies. Some possibilities are discussed in Section 3.1.1.

FIGURE 4.1. VECTOR DIAGRAMS OF THE GAL4 SYSTEM CONSTRUCTS USED TO SCREEN A RAT BRAIN cDNA LIBRARY

A

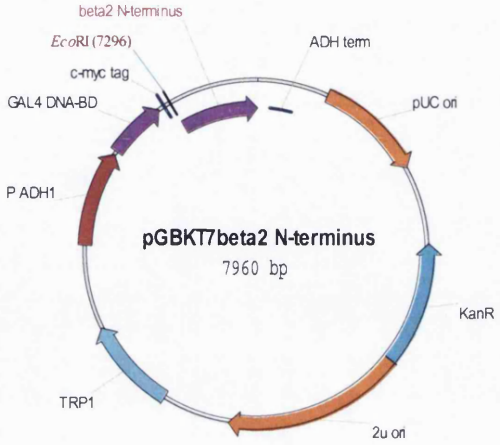

B

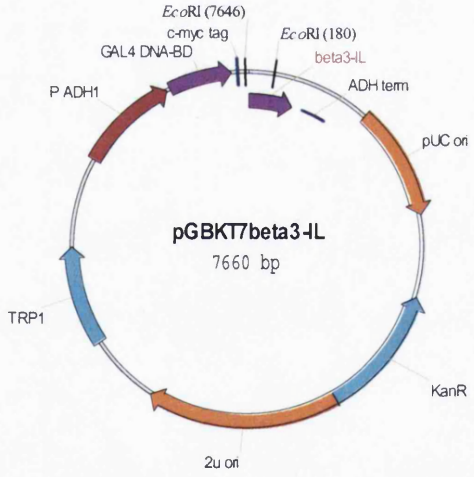

The $GABA_A$ receptor sequences β2(1-220) and β3(306-425) were cloned into the GAL4 yeast two-hybrid DNA-BD vector, pGBKT7, for use as bait constructs to screen a rat brain cDNA library for interacting proteins.

FIGURE 4.2. IMMUNOBLOT SHOWING THE EXPRESSION OF THE $GABA_A$ RECEPTOR GAL4 DNA-BD β3-IL(306-425) FUSION PROTEIN YEAST STRAIN, AH109

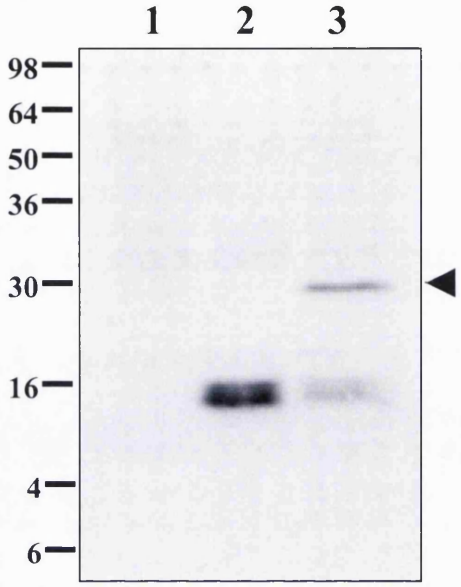

Lanes:

1. Untransformed AH109 cells
2. GAL4-DNA-BD
3. GAL4-DNA-BD β3-IL(306-425)

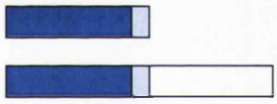

Key:

= GAL4-DNA-BD

= C-myc epitope

= β3-IL(306-425)

Construct	Predicted M_r (kDa)	Observed M_r (kDa)
GAL4-DNA-BD	17	~12
GAL4-DNA-BDβ3-IL(306-425)	31	~26

The GAL4 DNA-BD vector containing a $GABA_A$ receptor β3 subunit IL sequence, 306-425, was transformed into the yeast strain AH109. The fusion protein was extracted from yeast and analysed by immunoblotting using a monoclonal anti-c-myc antibody. The arrowhead indicates te position of the β3-IL fusion protein. Bands seen at ~16 kDa represent theC-myc epitope tagged GAL4 DNA-BD.

FIGURE 4.3. RESTRICTION ENZYME DIGESTION ANALYSIS OF CLONES 1-7 RESULTING FROM A $GABA_A$ RECEPTOR β3-IL(306-425) YEAST TWO-HYBRID cDNA LIBRARY SCREEN

1kb DNA ladder fragment sizes (bp):

10000, 8000, 6000, 5000, 4000, 3500, **3000**, 2500, 2000, 1500, 1000, 750, 500, 250

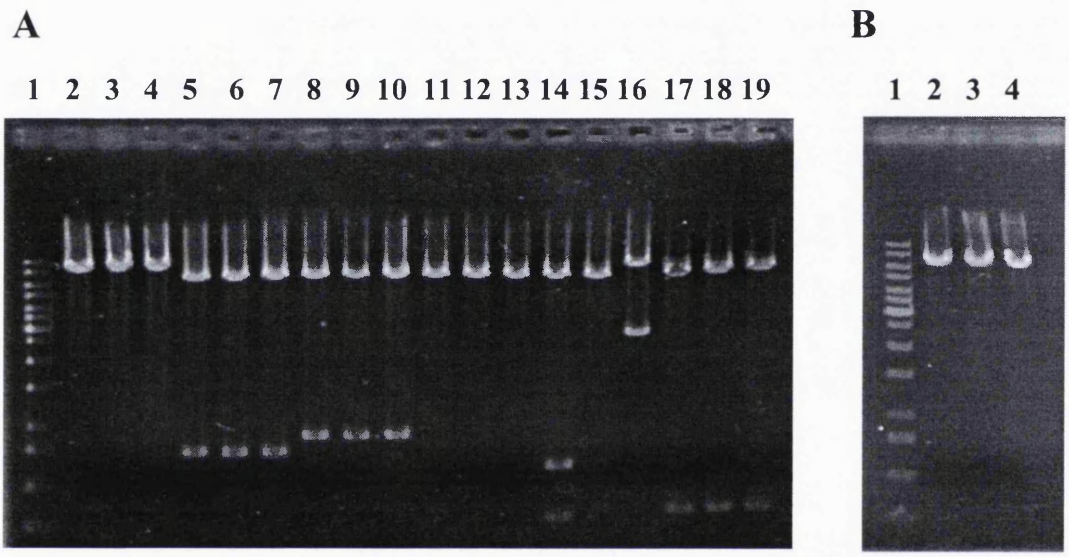

A

Lane	Sample	Calculated Insert Sizes (bp)
1	1kb DNA ladder	-
2-4	β3-IL screen clone 1	-
5-7	β3-IL screen clone 2	~740
8-10	β3-IL screen clone 3	~915
11-13	β3-IL screen clone 4	-
14-16	β3-IL screen clone 5	(315, 650, 2950)
17-19	β3-IL screen clone 6	~350

B

Lane	Sample	Calculated Insert Sizes (bp)
1	1kb DNA ladder	-
2-4	β3-IL screen clone 7	-

Plasmid DNA extracted from each β3-IL(306-425) yeast two-hybrid library screen clone was used to transform electrocompetent DH5α cells. Three bacterial clones were isolated for each yeast clone. Library plasmids were purified from each bacterial clone and digested by the restriction enzyme *Eco*RI. The digestion products for clones 1-7 are shown on the 1% agarose gel.

FIGURE 4.4. RESTRICTION ENZYME DIGESTION ANALYSIS OF CLONES 1-5 RESULTING FROM A $GABA_A$ RECEPTOR β2-N(1-220) YEAST TWO-HYBRID cDNA LIBRARY SCREEN

1kb DNA ladder fragment sizes (bp):

10000, 8000, 6000, 5000, 4000, 3500, **3000**, 2500, 2000, 1500, 1000, 750, 500, 250

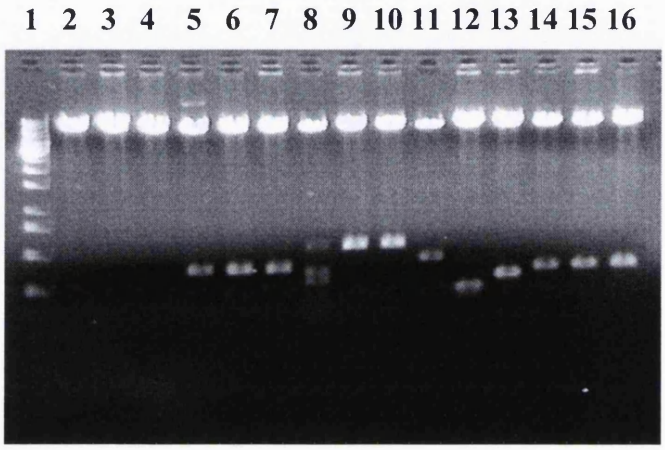

Lane	Sample	Calculated Insert Sizes (bp)
1	1kb DNA ladder	-
2-4	β2-N screen clone 1	-
5-7	β2-N screen clone 2	~400
8-10	β2-N screen clone 3	~615
11-13	β2-N screen clone 4	~(480, 290, 375)
14-16	β2-N screen clone 5	~430

Plasmid DNA extracted from each β2-N(1-220) yeast two-hybrid library screen clone was used to transform electrocompetent DH5α cells. Three bacterial clones were isolated for each yeast clone. Library plasmids were purified from each bacterial clone and digested by the restriction enzyme *Eco*RI. The digestion products for clones 1-5 are shown on the 1% agarose gel.

FIGURE 4.5. RESTRICTION ENZYME DIGESTION ANALYSIS OF CLONES 6-10 RESULTING FROM A $GABA_A$ RECEPTOR β2-N(1-220) YEAST TWO-HYBRID cDNA LIBRARY SCREEN

1kb DNA ladder fragment sizes (bp):

10000, 8000, 6000, 5000, 4000, 3500, **3000**, 2500, 2000, 1500, 1000, 750, 500, 250

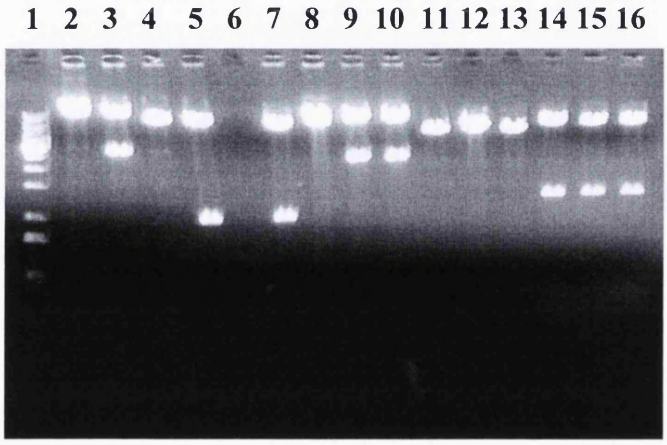

Lane	Sample	Calculated Insert Sizes (bp)
1	1kb DNA ladder	-
2-4	β2-N screen clone 6	~2900
5-7	β2-N screen clone 7	~1000
8-10	β2-N screen clone 8	~2650
11-13	β2-N screen clone 9	-
14-16	β2-N screen clone 10	~1420

Each library clone was excised from its vector by *Eco*RI restriction enzyme digestion of the extracted AD constructs. The digestion products for clones 6-10 are shown on the 1% agarose gel.

FIGURE 4.6. COMPILED NUCLEOTIDE SEQUENCE OF THE $GABA_A$ RECEPTOR β2-N(1-220) INTERACTING CLONE, CLONE 3

```
5'-GGATGATCCCAAAGCCAAGGAGAAGTTTTCCCAGCTGGCAGAAGC 45
   TTATGAGGTGTTGAGTGACGAGGTGAAGAGGAAGCAGTATGATGC 90
   TTACGGCTCCGCTGGCTTTGACCCTGGAGCCAGCAGCTCTGGGCA 135
   GGGCTACTGGAGAGGAGGTCCTTCTGTTGACCCCGAGGAGCTATT 180
   CAGGAAGATCTTTGGAGAGTTCTCATCTTCTCCTTTTGGTGATTT 225
   CCAGAATGTGTTTGATCAGCCTCAGGAGTACATCATGGAGTTGAC 270
   ATTCAATCAAGCCGCCAAGGGTGTCAACAAAGAGTTCACCGTGAA 315
   TATCATGGACACCTGTGAGCGCTGCGATGGCAAGGGGAACGAGCC 360
   TGGAACCAAAGTGCAGCATTGTCACTACTGCAGCGGCTCAGGCAT 405
   GGAAACCATCAATACAGGGCCTTTTGTGATGCGTTCCACGTGTCG 450
   GAGATGTGGTGGACGGGGCTCCATCATCACAAACCCTTGTGTGGT 495
   CTGCAGAGG-3' 504
```

Purified plasmid DNA, encoding library clone 3, was extracted from yeast and sequenced using the ABI PRISM 310 Genetic Analyser in order to identify the sequence. The compiled sequence is shown above.

FIGURE 4.7. TRANSLATION OF THE β2-N(1-220) INTERACTING CLONE, CLONE 3 INTO PROTEIN

```
Frame
        pGAD10 insert adaptor sequence
        GAA TTC GCG GCC GCG TCG ACG GAT GAT CCC AAA GCC AAG GAG AAG TTT TCC CAG
+1                                  STOP
+2      E   F   A   A   A   S   T   D   D   P   K   A   K   E   K   F   S   Q
+3

        CTG GCA GAA GCT TAT GAG GTG TTG AGT GAC GAG GTG AAG AGG AAG CAG TAT GAT
+2      L   A   E   A   Y   E   V   L   S   D   E   V   K   R   K   Q   Y   D
+3          STOP

+2      GCT TAC GGC TCC GCT GGC TTT GAC CCT GGA GCC AGC AGC TCT GGG CAG GGC TAC
        A   Y   G   S   A   G   F   D   P   G   A   S   S   S   G   Q   G   Y

        TGG AGA GGA GGT CCT TCT GTT GAC CCC GAG GAG CTA TTC AGG AAG ATC TTT GGA
+2      W   R   G   G   P   S   V   D   P   E   E   L   F   R   K   I   F   G

        GAG TTC TCA TCT TCT CCT TTT GGT GAT TTC CAG AAT GTG TTT GAT CAG CCT CAG
+2      E   F   S   S   S   P   F   G   D   F   Q   N   V   F   D   Q   P   Q

        GAG TAC ATC ATG GAG TTG ACA TTC AAT CAA GCC GCC AAG GGT GTC AAC AAA GAG
+2      E   Y   I   M   E   L   T   F   N   Q   A   A   K   G   V   N   K   E

        TTC ACC GTG AAT ATC ATG GAC ACC TGT GAG CGC TGC GAT GGC AAG GGG AAC GAG
+2      F   T   V   N   I   M   D   T   C   E   R   C   D   G   K   G   N   E

        CCT GGA ACC AAA GTG CAG CAT TGT CAC TAC TGC AGC GGC TCA GGC ATG GAA ACC
+2      P   G   T   K   V   Q   H   C   H   Y   C   S   G   S   G   M   E   T

        ATC AAT ACA GGG CCT TTT GTG ATG CGT TCC ACG TGT CGG AGA TGT GGT GGA CGG
+2      I   N   T   G   P   F   V   M   R   S   T   C   R   R   C   G   G   R

        GGC TCC ATC ATC ACA AAC CCT TGT GTG GTC TGC AGA GG
+2      G   S   I   I   T   N   P   C   V   V   C   R
```

Protein translation of the $GABA_A$ receptor β2-N(1-220) library clone 3, using the Translator program available at www.justbio.com, revealed an open reading frame in the +2 frame. This corresponds to the reading frame set by insertion into the pGAD10 vector. Frames +1 and +3 contain stop codons near the beginning of the sequence.

FIGURE 4.8. PROTEIN SEQUENCE ALIGNMENT BETWEEN THE RAT TUMOROUS IMAGINAL DISCS PROTEIN, TID1L, AND THE $GABA_A$ RECEPTOR β2-N(1-220) INTERACTING CLONE, CLONE 3

```
TID1L MAARCSPRWFRVAVGTPRLPAAAGRGVQQPQGGVVAASLCRKLCVSAFGL
      ---------------------------------------------------

TID1L SMGAHGPRALLTLRPGVRLTGTKSFPFVCTASFHTSASLAKDDYYQILGV
      ---------------------------------------------------

TID1L PRNASQKDIKKAYYQLAKKYHPDTNKDDPKAKEKFSQLAEAYEVLSDEVK
C3    ---------------------------DDPKAKEKFSQLAEAYEVLSDEVK

TID1L RKQYDAYGSAGFDPGASSSGQGYWRGGPSVDPEELFRKIFGEFSSSPFGD
C3    RKQYDAYGSAGFDPGASSSGQGYWRGGPSVDPEELFRKIFGEFSSSPFGD

TID1L FQNVFDQPQEYIMELTFNQAAKGVNKEFTVNIMDTCERCDGKGNEPGTKV
C3    FQNVFDQPQEYIMELTFNQAAKGVNKEFTVNIMDTCERCDGKGNEPGTKV

TID1L QHCHYCSGSGMETINTGPFVMRSTCRRCGGRGSIITNPCVVCRGAGQAKQ
C3    QHCHYCSGSGMETINTGPFVMRSTCRRCGGRGSIITNPCVVCR-------

TID1L KKRVTVPVPAGVEDGQTVRMPVGKREIFVTFRVQKSPVFRRDGADIHSDL
      ---------------------------------------------------

TID1L FISIAQAILGGTAKAQGLYETINVTIPAGIQTDQKIRLTGKGIPRINSYG
      ---------------------------------------------------

TID1L YGDHYIHIKIRVPKRLSSRQQNLILSYAEDETDVEGTVNGVTHTSTGGRT
      ---------------------------------------------------

TID1L MDSSTGSKDRREAGEDNEGFLSKLKKIFTS
      -------------------------------
```

An alignment of the protein sequences of the $GABA_A$ receptor β2-N(1-220) library screen clone 3 and the tumorous imaginal discs protein, TID1L, which was identified from the BLAST search of clone 3. The alignment highlights the features of the DnaJ-like protein that are present in the library clone. The J-domain motif is highlighted in blue, the glycine/phenylalanine-rich domain is highlighted in yellow and the cysteine-rich domain is highlighted in red.

FIGURE 4.9. IMMUNOBLOT SHOWING EXPRESSION OF THE GABA$_A$ RECEPTOR β2 SUBUNIT N-TERMINUS AND CLONE 3 IN HEK 293 CELLS

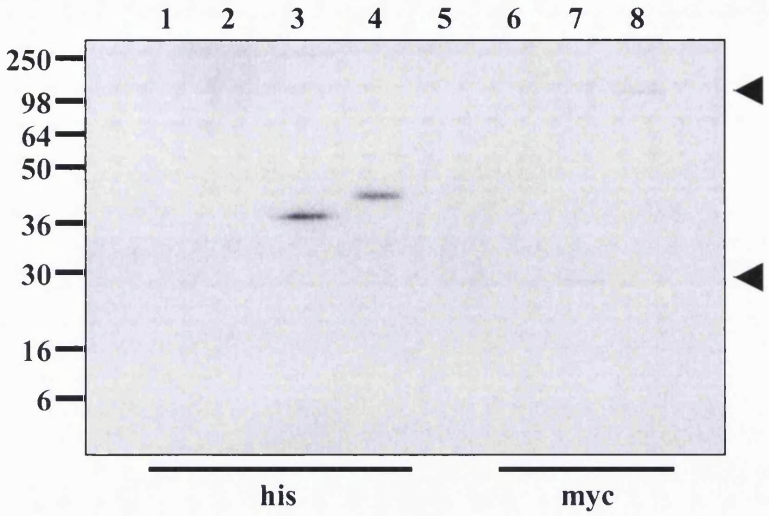

Lanes:

1. Untransfected HEK293 cells
2. β2(1-449) (untagged)
3. β2-N(1-220)
4. OGT (335 aa)
5. Empty lane
6. Untransfected HEK293 cells
7. Clone 3
8. GRIF-1(1-913)

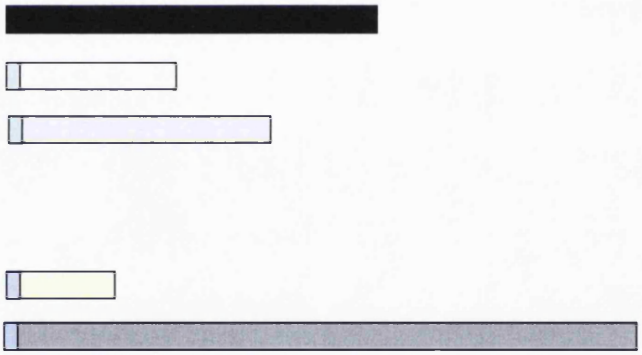

Key:

- = his epitope
- = c-myc epitope
- = β2(1-450)
- = β2-N(1-220)
- = OGT(335 aa)
- = clone 3(167 aa)
- = GRIF-1(1-913)

Construct	Predicted M_r (kDa)	Observed M_r (kDa)
β2(1-449) (untagged)	55	not detected in this assay
His-β2-N(1-220)	27	~38
His-OGT (335aa)	37	~48
C-myc-clone 3	20	~21
C-myc-GRIF-1(1-913)	102	~133

pCMVβ2-N(1-220) and pCMVclone 3 were each transfected into HEK 293 cells. Expressed proteins were analysed by immunoblotting. Arrowheads indicate the positions of Clone 3 (lanes 7) and GRIF-1 (lane 8) . His-tagged OGT and C-myc tagged GRIF-1(1-913) were used as positive controls for their respective antibodies.

FIGURE 4.10. SCHEMATIC DIAGRAM SHOWING A COMPARISON BETWEEN A TYPICAL TYPE I DNAJ-LIKE PROTEIN AND THE GABA$_A$ RECEPTOR β2-N(1-220) INTERACTING CLONE, CLONE 3

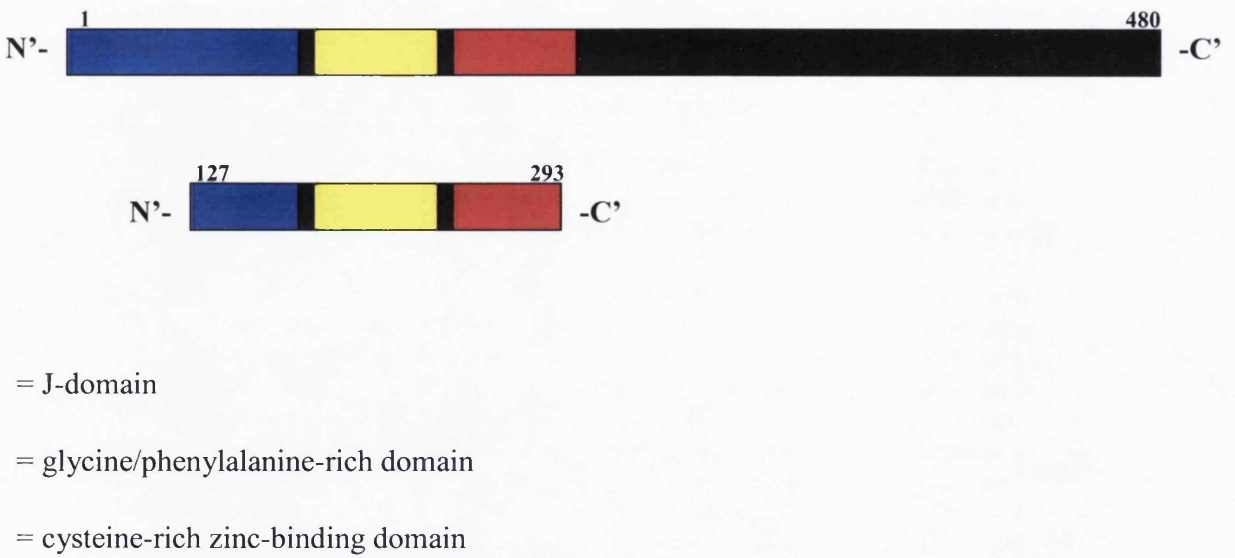

The figure shows an alignment between a typical DnaJ domain-like protein and the GABA$_A$ receptor β2-N interacting clone, clone 3. Clone 3 contains motifs for the 3 main features of a type I DnaJ homologue i.e. part of the J-domain motif, a glycine/phenylalanine-rich linker domain and a cysteine-rich domain.

TABLE 4.1. RESULTS OF THE CO-TRANSFORMATION OF THE $GABA_A$ RECEPTOR β3-IL(306-425) WITH PURIFIED PLASMIDS OF PUTATIVE INTERACTING LIBRARY SCREEN CLONES

Activation Domain Construct	DNA-Binding Domain Construct	-2 Selective Media	-4 Selective Media
pGAD10 Clone2	pGBKT7 β3-IL(306-425)	+++	++
pGAD10 Clone3	pGBKT7 β3-IL(306-425)	+++	-
pGAD10 Clone5	pGBKT7 β3-IL(306-425)	+++	-
pGAD10 Clone6	pGBKT7 β3-IL(306-425)	+++	-
pGAD10	pGBKT7 β3-IL(306-425)	+++	-
pTD1-1	pVA3-1	+	+

The results are representative of n = 3 independent co-transformations

Key: -2 Selective media lacks leucine and tryptophan
-4 Selective media lacks adenine, histidine, leucine and tryptophan
For nutritional selection - = No growth, + = 11-100 colonies, ++ = 101-200 colonies, +++ = >200 colonies.

Each potential β3-IL(305-425) interacting clone, identified from the library screen and found to contain an insert sequence, was used to co-transform yeast along with the pGBKT7β3-IL(306-425) to confirm the interaction.

TABLE 4.2. RESULTS OF THE CO-TRANSFORMATION OF THE β2-N(1-220) WITH PURIFIED PLASMIDS OF PUTATIVE INTERACTING LIBRARY SCREEN CLONES

Activation Domain Construct	DNA-Binding Domain Construct	-2 Selective Media	-4 Selective Media	α-galactosidase Activity
pGAD10 Clone2	pGBKT7 β2-N(1-220)	++	-	-
pGAD10 Clone3	pGBKT7 β2-N(1-220)	++	++	+
pGAD10 Clone4	pGBKT7 β2-N(1-220)	++	-	-
pGAD10 Clone5	pGBKT7 β2-N(1-220)	++	-	-
pGAD10 Clone6	pGBKT7 β2-N(1-220)	++	-	-
pGAD10 Clone7	pGBKT7 β2-N(1-220)	++	++	+
pGAD10 Clone8	pGBKT7 β2-N(1-220)	++	-	-
pGAD10 Clone10	pGBKT7 β2-N(1-220)	++	-	-
pGAD10	pGBKT7	-	-	-
pVA3-1	pTD1-1	++	++	+

The results are representative of n = 3 independent co-transformations

Key: -2 Selective media lacks leucine and tryptophan
-4 Selective media lacks adenine, histidine, leucine and tryptophan
For nutritional selection - = No growth, + = 11-100 colonies, ++ = 101-200 colonies.
For α-Galactosidase assay + = Enzyme activity observed, - = No enzyme activity observed.

Each potential β2-N(1-220) interacting clone, identified from the library screen and found to contain an insert sequence, was used to co-transform yeast together with the pGBKT7β2-N(1-220) to confirm the interaction.

TABLE 4.3. RESULTS OF THE TEST FOR SPECIFICITY OF INTERACTION OF LIBRARY SCREEN CLONE 3 WITH THE β2-N(1-220)

Activation Domain Construct	DNA-Binding Domain Construct	-2 Selective Media	-4 Selective Media
pGAD10 Clone3	pAS2-1 β2-IL(303-427)	+	-
pGAD10 Clone3	pAS2-1 β2TM3/IL/TM4(282-450)	++	-
pGAD10 Clone3	pGBKT7-MB2 β2-IL/TM4(303-450)	++	-
pGAD10 Clone3	pAS2-1 α1-IL(304-384)	++	-
pGAD10 Clone3	pGBKT7 α1-N(1-224)	++	+
pGAD10 Clone3	pGBKT7 β2-N(1-220)	++	++
pGAD10 Clone3	pAS2-1-	++	-
pVA3-1	pTD1-1	+	+
pGAD10-	pAS2-1-	++	-

The results are representative of n = 3 independent co-transformations

Key: -2 Selective media lacks leucine and tryptophan
-4 Selective media lacks adenine, histidine, leucine and tryptophan
For nutritional selection - = No growth, + = 11-100 colonies, ++ = 101-200 colonies.

Library screen clone 3, which was found to activate reporter genes on re-co-transformation with the $GABA_A$ receptor β2(1-220) DNA-BD construct, was tested for interaction specificity, by co-transformation with $GABA_A$ receptor constructs, as shown.

CHAPTER 5:
RESULTS 3

5.1. INTERACTIONS OF GRIF-1 AND KIAA1042 WITH THE $GABA_A$ RECEPTOR β2 SUBUNIT IL AND THE KINESIN HEAVY CHAIN, KIF5C

The aims of this chapter were (i) to investigate the specificity of interaction between the novel $GABA_A$ receptor interacting factor, GRIF-1 and the $GABA_A$ receptor β2-IL (ii) to compare binding of the $GABA_A$ receptor β2-IL to GRIF-1 and to the human GRIF-1 homologue, KIAA1042 (iii) to compare binding of the kinesin heavy chain clone, KIF5C, to GRIF-1 and to KIAA1042 and (iv) to test for dimerisation of KIAA1042.

5.1.1. RATIONALE

The $GABA_A$ receptor interacting factor, GRIF-1, was identified in a yeast two-hybrid library screen of a rat brain cDNA library, through its specific interaction with the human $GABA_A$ receptor β2 subunit intracellular loop (IL). As discussed earlier in this thesis, it is thought to be a $GABA_A$ receptor trafficking factor (Beck *et al.*, 2002). GRIF-1 was found to share approximately 47% similarity, over 297 amino acids, with Huntingtin-associated protein, HAP-1, which has been shown to play a role in vesicular trafficking from early to late endosomes, via its interaction with Hrs, a hepatocyte growth factor regulated tyrosine kinase substrate (Li *et al.*, 2002). The *Drosophila melanogaster* orthologue of GRIF-1 is Milton (Stowers *et al.*, 2002). Milton was identified by genetic mutation screening in the *Drosophila* retina and was shown to colocalise with mitochondria in HEK293 cells and *Drosophila* nerves. Co-immunoprecipitaion showed that Milton also associates with kinesin heavy chains. Axons from mutant *Drosophila* lacking Milton contained no mitochondria. These experiments suggested that Milton acts as a kinesin-associated adaptor protein involved in localisation of mitochondria to synapses. GRIF-1 shares approximately 40% amino acid similarity over 848 residues with Milton. Apart from these two proteins, GRIF-1 has no homology with proteins of known function. However, it does share approximately 86% homology over 468 amino acids with its human orthologue, ALS2CR3/KIAA0549, whose function is unknown, but which also interacts with the $GABA_A$ receptor β2-IL (Beck *et al.*, 2002). A second human gene, KIAA1042, whose function is also unknown, shares approximately 60% similarity, over 857 amino acids, with GRIF-1. KIAA1042 was also identified as a uridine diphospho-*N*-acetylglucosamine: polypeptide β-*N*-acetyglucosaminyl transferase (OGT) interacting protein and is also known as OIP106 (Iyer *et al.*, 2003). Each of these proteins contains

predicted coiled-coil motifs in their N-terminal domains, shown in Figure 5.1. Coiled-coil domains are found in many proteins throughout the cell and in the extracellular matrix and are important for mediating protein-protein interactions (Beck and Brodsky, 1998). The $GABA_A$ receptor β2-IL interacting domain of GRIF-1 was localised to residues 124-283. This region of GRIF-1 also corresponds to the end of the first, and the beginning of the second, predicted coiled-coil region. The peptide sequence in KIAA1042 which is homologous to the β2-IL binding domain identified in GRIF-1, i.e. residues 124-283, has a similarity of nearly 80% with GRIF-1 over this region, compared to ~60% for the full-length sequence. This similarity is also found within a coiled-coil domain of KIAA1042.

The first part of this investigation was the further characterisation of the interaction between GRIF-1 and the $GABA_A$ receptor β2-IL in the yeast two-hybrid system using a series of $GABA_A$ receptor subunit constructs. Secondly, since there was such a high degree of sequence homology between GRIF-1 and KIAA1042, an investigation was carried out to compare the binding of these two proteins to the β2-IL. Next, due to the similarity of GRIF-1 to Milton, which is known to bind kinesin heavy chains, both GRIF-1 and KIAA1042 were tested for an interaction with kinesin heavy chain, KIF5C. Finally, since GRIF-1 has been shown to form dimers in the yeast two-hybrid system and in mammalian cells (Ojla, G., Beck, M., Brickley, K. and Stephenson, F. A., unpublished results), KIAA1042 was tested for dimer formation with itself and with GRIF-1.

5.2. RESULTS

5.2.1. CONSTRUCTION OF THE TM3/β2-IL/TM4, α1-IL AND β2-IL/TM4 DNA-BD PLASMIDS

An initial project was undertaken to substantiate the interaction between the putative trafficking factor $GABA_A$ receptor interacting factor (GRIF-1) with the $GABA_A$ receptor β2 subunit IL and, further, to investigate the $GABA_A$ receptor subunit binding specificity and conformational dependence. These were investigated in the GAL4 yeast two-hybrid system, using yeast two-hybrid constructs, the $GABA_A$ receptor α1-IL, $GABA_A$ receptor β2-IL with transmembrane domains TM3 and TM4 (TM3/β2-IL/TM4) and $GABA_A$ receptor β2-IL with TM4 only (β2-IL/TM4). Plasmid maps for each fusion construct are shown in Figure 5.2.

The $GABA_A$ receptor β2 subunit intracellular loop with both transmembrane domains 3 and 4 i.e. TM3/β2-IL/TM4(282-450) was cloned into the yeast two-hybrid DNA-BD vector pAS2-1 indirectly, using the method outlined in Figure 2.2. The sequence TM3/β2-IL/TM4(282-450) was amplified by PCR from rat brain cDNA using the specific oligonucleotide primers shown in Table 2.1.3. These primers were designed to incorporate the restriction enzyme sites *Eco*RI and *Bam*HI to facilitate directional cloning. Specific parameters for PCR are shown in Table 2.1.4. Oligonucleotide sequencing was used to verify the construct and to show that the insert was in frame with the GAL4 DNA-BD.

DNA-BD plasmids containing $GABA_A$ receptor α1-IL(304-384) or $GABA_A$ receptor β2-IL/TM4(303-450) were constructed in a similar way to the $GABA_A$ receptor TM3/β2-IL/TM4(282-450) sequence, but were cloned non-directionally using only one restriction enzyme site. The $GABA_A$ receptor α1-IL(304-384) insert was cloned into the *Eco*RI restriction site of the pAS2-1 vector. The β2-IL/TM4(303-450) sequence was sub-cloned into the *Bam*HI restriction site of the vector, pGBKT7-MB2 (pGBKT7 vector engineered to ensure the *Bam*HI restriction site is in frame). Template DNA for amplification of $GABA_A$ receptor β2-IL/TM4(303-450) was the previously prepared TM3/β2-IL/TM4 DNA-BD construct. In this way, the fusion constructs pAS2-1TM3/β2-IL/TM4(282-450), pAS2-1α1-IL(304-384) and pGBKT7-MB2β2-IL/TM4(303-450) were generated. Oligonucleotide sequencing was used to ensure the inserts were in the correct orientation and were in frame with the GAL4 DNA-BD. Figure 5.3 shows immunoblots confirming expression of these fusion proteins in yeast.

Bands representing each fusion construct can be seen at ~41 kDa for GAL4 DNA-BD β2-IL(303-427) and GAL4 DNA-BD TM3/β2-IL/TM4(282-450), ~38 kDa for GAL4 DNA-BD β2-IL/TM4(303-450) and ~28 kDa for GAL4 DNA-BD α1-IL(304-384). These correspond to the calculated size of each fusion protein.

5.2.1.1. SUBSTANTIATION OF THE INTERACTION OF GRIF-1(8-633) WITH THE $GABA_A$ RECEPTOR SUBUNIT β2-IL(303-427) IN THE GAL4 YEAST TWO-HYBRID SYSTEM

The GAL4 DNA-BD construct pAS2-1β2-IL(303-427) and the AD library fusion clone pGAD10GRIF-1(8-633) were used to substantiate previous results showing an interaction between GRIF-1 and the $GABA_A$ receptor β2-IL(303-427) (Beck *et al.*, 2002). The GAL4 yeast strain, AH109, was co-transformed with the two yeast two-hybrid fusion proteins. The plasmids, pTD1-1 and pVA3-1, were used as a positive control for interacting proteins and the empty vectors, pAS2-1 and pGAD10, were used as a double negative control. pAS2-1β2-IL(303-427) was co-transformed with an empty AD vector and pGAD10GRIF-1(8-633) was co-transformed with an empty DNA-BD vector as single negative controls to ensure that neither fusion construct caused auto-activation of reporter gene activity. Colony growth on -W/-L selective medium showed that the transformation had been successful. Colony growth on -W/-L/-H/-Ade selective medium demonstrated an interaction between GRIF-1(8-633) and the $GABA_A$ receptor β2-IL(303-427). The results of these co-transformations are summarised in Table 5.1. where it can be seen that the positive control plasmids, pTD1-1 and pVA3-1 showed reporter gene activity and the negative control plasmids, empty pAS2-1 and empty pGAD10 showed no reporter gene activity. However, reporter gene activity was seen for the GRIF-1(8-633)/β2-IL(303-427) co-transformation, confirming that GRIF-1(8-633) does indeed associate with the $GABA_A$ receptor β2-IL(303-427).

5.2.1.2. SUBUNIT SPECIFICITY OF THE ASSOCIATION OF GRIF-1(8-633) WITH $GABA_A$ RECEPTORS

AH109 competent yeast cells were co-transformed with the constructs pAS2-1α1-IL(304-384) and pGAD10GRIF-1(8-633) to investigate the $GABA_A$ receptor subunit specificity of the GRIF-1(8-633) interaction. The full-length protein sequences for α1 and β2 subunits are 34% identical; however, the intracellular loops of these subunits do

not show any significant homology. pTD1-1 co-transformed with pVA3-1 was used as a positive control. Negative controls contained pAS2-1α1-IL(304-384) co-transformed with an empty AD vector or both an empty AD vector with an empty DNA-BD vector. The results of these co-transformations are shown in Table 5.2. It can be seen that the pTD1-1/pVA3-1 positive control showed reporter gene activity on selective media and for β-galactosidase activity. Neither of the negative controls showed any reporter gene activity. Co-transformation of GRIF-1(8-633) with the $GABA_A$ receptor α1-IL(304-384) did not result in reporter gene activation. This shows that GRIF-1(8-633) does not interact with the $GABA_A$ receptor α1-IL(304-384).

5.2.1.3. SPECIFICITY OF THE CONFORMATION OF THE $GABA_A$ RECEPTOR β2-IL NECESSARY FOR ASSOCIATION WITH GRIF-1(8-633)

The constructs pAS2-1TM3/β2-IL/TM4(282-450) and pGBKT7-MB2β2-IL/TM4(303-450) were used to test whether inclusion of both TM domains 3 and 4 which flank the β2-IL sequence, or of TM4 alone, affects the interaction of GRIF-1(8-633) with the $GABA_A$ receptor β2-IL(303-427) i.e. whether a specific $GABA_A$ receptor β2-IL conformation is important for the interaction. The pTD1-1 and pVA3-1 plasmids were used for a positive control. Empty AD and DNA-BD vectors were used as a double negative control. Single negative controls contained either pAS2-1TM3/β2-IL/TM4 or pGBKT7-MB2β2-IL/TM4 with an empty AD vector. The results for these co-transformations are shown in Table 5.3 where it can be seen that the pTD1-1/pVA3-1 positive control co-transformation showed both colony growth on -4 selective media and β-galactosidase activity. The double negative control, containing two empty vectors showed no reporter gene activity. Single negative controls showed no activation of reporter genes. However, neither of the constructs containing flanking TM domains activated reporter genes on co-transformation with GRIF-1(8-633). These results demonstrate that neither construct interacts with GRIF-1(8-633), indicating that introduction of the transmembrane domains influences the association of the $GABA_A$ receptor β2-IL(303-427) with GRIF-1(8-633). This may be due to a change in the conformation of the protein.

5.2.2. CONSTRUCTION OF THE KIAA1042 PLASMIDS

A full-length cDNA clone of KIAA1042(1-953) in the vector pBluescript II SK+ was obtained from Professor T. Nagase, Kazusa Research Institute, Chiba, Japan. The clone was excised from its vector by restriction enzyme digestion. KIAA1042(1-953) was excised using *Sal*I and *Not*I. The digestion products were used as template DNA for PCR amplification. Specific oligonucleotide primers used for amplification reaction are shown in Table 2.1.3 and specific PCR parameters are shown in Table 2.1.4. The KIAA1042 sequence was cloned into the mLexA yeast two-hybrid vectors at their *Eco*RI/*Bam*HI restriction sites to generate the constructs pGADT7KIAA1042(1-953) and pMBL33KIAA1042(1-953). The sequence KIAA1042(124-283) was obtained by PCR amplification using the full-length clone in pGADT7 as template DNA and cloned into the *Eco*RI/*Xho*I restriction sites of pGADT7 to generate the construct pGADT7KIAA1042(124-283) All constructs were verified by oligonucleotide sequencing using the ABI PRISM 310 Genetic Analyser. Plasmid maps representing each KIAA1042 and GRIF-1 fusion construct are shown in Figure 5.4. Figure 5.5 shows an immunoblot confirming the expression of the KIAA1042 construct in yeast. A band can be seen at ~96 kDa representing the KIAA1042(1-953) construct and a band at ~45 kDa represents the KIAA1042(124-283) construct.

5.2.2.1. COMPARISON BETWEEN THE INTERACTION OF THE β2-IL WITH GRIF-1 AND WITH KIAA1042 SEQUENCES

The GRIF-1 constructs, pGADT7GRIF-1(1-913), pGAD10GRIF-1(8-633) and pGADT7GRIF-1(124-283), have each been shown to interact with the $GABA_A$ receptor β2 subunit IL and were, therefore, each co-transformed into the mLexA yeast strain L40 along with the bait construct pMBL33β2-IL(303-427) as positive controls (Beck *et al.*, 2002). Expression of these constructs in yeast is shown in Figure 5.3. The KIAA1042 constructs pGADT7KIAA1042(1-953) and pGADT7KIAA1042(124-283) were each co-transformed with the $GABA_A$ receptor β2-IL(303-427) to test for direct interactions. Single negative control co-transformations were carried out for each GRIF-1 and KIAA1042 construct with an empty DNA-BD plasmid and a double negative control contained both an empty AD and an empty DNA-BD plasmid.

From the results shown in Table 5.4 it can be seen that each of the GRIF-1 fusion constructs GAL4 AD GRIF-1(1-913), GAL4 AD GRIF-1(8-633) and GAL4 AD GRIF-

1(124-283) interacted with the $GABA_A$ receptor β2-IL(303-427). Colony growth on –3 dropout media and β-galactosidase activity were seen for each co-transformation. No reporter gene activity was seen for any of the single negative co-transformations containing pGADT7GRIF-1(1-913), pGAD10GRIF-1(8-633), pGADT7GRIF-1(124-283), pGADT7KIAA1042(1-953) or pGADT7KIAA1042(124-283) with an empty DNA-BD plasmid or for the pMBL33β2-IL(303-427) co-transformed with an empty AD plasmid, demonstrating that no auto-activation had occurred for any construct. No reporter gene activity was detected for the double negative control co-transformations. However, no reporter gene activity was detected for either KIAA1042 construct, indicating that despite being 60-80% homologous to GRIF-1, they do not interact with the $GABA_A$ receptor β2-IL(303-427).

5.2.3. CONSTRUCTION OF THE KIF5C PLASMID

A full-length cDNA clone of KIF5C(1-957) in the vector pBluescript II SK+ was obtained from Professor T. Nagase, Kazusa Research Institute, Chiba, Japan. The clone was excised from its vector by restriction enzyme digestion using *Eco*RI. The digestion products were used as template DNA for PCR amplification. Specific oligonucleotide primers used for the amplification reaction are shown in Table 2.1.3 and specific PCR parameters are shown in Table 2.1.4. The KIF5C(1-957) sequence was cloned into the mLexA DNA-BD yeast two-hybrid vector at the *Eco*RI/*Sal*I restriction sites to generate the construct pMBL33KIF5C(1-957). The construct was verified by oligonucleotide sequencing using the ABI PRISM 310 Genetic Analyser. The KIF5C plasmid map is shown in Figure 5.6. Figure 5.7 shows an immunoblot confirming the expression of the KIF5C construct in yeast. The LEXA DNA-BD was Two bands can be seen for the KIF5C(1-957) construct at ~143 kDa and ~117 kDa. The band at ~143 kDa corresponds closely with the predicted size of the fusion protein. A faint band of the same size as the lower in the KIF5C lane is present in the untransformed cells lane and may therefore represent non-specific binding of the anti-KHC antibody.

5.2.3.1. COMPARISON BETWEEN THE INTERACTION OF THE KINESIN HEAVY CHAIN CONSTRUCT, KIF5C, WITH GRIF-1 AND WITH KIAA1042

The three GRIF-1 constructs pGADT7GRIF-1(1-913), pGAD10GRIF-1(8-633) and pGADT7GRIF-1(124-283) and the KIAA1042 constructs pGADT7KIAA1042(1-953)

and pGADT7KIAA1042(124-283) were each co-transformed with the kinesin heavy chain construct pMBL33KIF5C(1-957) in the mLexA yeast strain L40. Single negative controls contained an AD plasmid containing one of the GRIF-1 or KIAA1042 sequences, co-transformed with an empty DNA-BD vector or the KIF5C(1-957) construct co-transformed with an empty AD vector. A double negative control contained an empty AD and an empty DNA-BD vector. The pMBL33β2-IL(303-427) co-transformed with pGAD10GRIF-1(8-633) was used as a positive control.

As shown by the results in Table 5.5 reporter gene activity was seen for the GRIF-1(8-633)/β2-IL(303-427) positive control co-transformation. No reporter gene activity was seen for the double negative control. None of the single negative controls for GRIF-1 or KIAA1042 sequences in the AD vector co-transformed with an empty DNA-BD vector showed any reporter gene activity. For each of the GRIF-1 constructs pGADT7GRIF-1(1-913), pGAD10GRIF-1(8-633) and pGADT7GRIF-1(124-283) co-transformed with KIF5C(1-957), colony growth and β-galactosidase activity were detected with a stronger interaction for the shorter sequences. Neither of the KIAA1042 sequences, i.e. KIAA1042(1-953) or KIAA1042(124-283), showed any reporter gene activity when co-transformed with the kinesin heavy chain clone.

5.2.3.2. TEST FOR DIMERISATION INTERACTIONS OF FULL-LENGTH KIAA1042 WITH GRIF-1 AND KIAA1042 CONSTRUCTS

Since it is now known that GRIF-1 can form dimers (Ojla, G., Beck, M., Brickley, K. and Stephenson, F. A., unpublished results) it was of interest to determine if the yeast two-hybrid system could be used to investigate if KIAA1042 formed dimers with itself or indeed with GRIF-1. The full-length KIAA1042 sequence was sub-cloned from the pGADT7 vector into pMBL33 and the resulting construct used to test for homodimerisation. The plasmid map for KIAA1042 in the DNA-BD vector is shown in Figure 5.6. The three GRIF-1 AD constructs containing GRIF-1(1-913), GRIF-1(8-633) or GRIF-1(124-283) were each co-transformed with KIAA1042(1-953) in the DNA-BD vector. Single negative controls were also carried out for each construct. The positive control contained pMBL33β2-IL(303-427) co-transformed with pGAD10GRIF-1(8-633). The double negative control contained an empty AD and an empty DNA-BD vector. Table 5.6 shows the results for these co-transformations.

The double negative control containing two empty vectors showed no reporter gene activity. The GRIF-1(8-633)/β2-IL(303-427) positive control showed both colony growth and β-galactosidase activity. All single negative control reactions for the GRIF-1 and KIAA1042 constructs contained in the AD vector were negative for reporter gene activity. However, the single negative control for the KIAA1042(1-953) contained within the DNA-BD vector showed both colony growth and strong β-galactosidase activity, indicating that this construct is capable of auto-activation of reporter genes. Therefore, although each of the dual combinations of GRIF-1 and KIAA1042 in the AD vector with KIAA1042 in the DNA-BD vector showed reporter gene activity, it was not possible to know whether this represented a true interaction and thus evidence for dimer formation.

5.3. DISCUSSION

5.3.1. SPECIFICITY OF THE INTERACTION BETWEEN THE NOVEL PROTEIN, GRIF-1, AND THE $GABA_A$ RECEPTOR β2 SUBUNIT IL

Here, a series of yeast two-hybrid co-transformations were carried out in order to characterise further the novel $GABA_A$ receptor interacting factor, GRIF-1. Firstly, the subunit and conformational specificity necessary for the interaction between GRIF-1(8-633) with $GABA_A$ receptors was tested. The GAL4 yeast two-hybrid assay showed that GRIF-1(8-633) does not interact with the α1-IL(304-384). It has also been shown that GRIF-1 does not interact with the $GABA_A$ receptor β1-IL, β3-IL or γ2-IL (Beck *et al.*, 2002). The conformation of the β2-IL is also important for the interaction as the β2-IL sequences that either included both flanking TM domains 3 and 4 or TM4 alone did not interact with GRIF-1. Since TM3 and TM4 are hydrophobic, they may tend to cluster together in the cytoplasmic environment, where they are not supported by insertion into the cell membrane, resulting in incorrect folding of the β2-IL compared to folding in the absence of TM domains. Addition of TM4 alone will not cluster in the same way as when both TMs are present, but may still confer conformational distortions that prevent association of the β2-IL with GRIF-1(8-633). In addition, these loop constructs containing hydrophobic domains may be excluded from the yeast nuclei as they may not easily be able to cross the nuclear membrane.

5.3.2. INTERACTIONS OF THE $GABA_A$ RECEPTOR β2-IL WITH GRIF-1 AND KIAA1042

Having determined the interaction specificity of GRIF-1 with the $GABA_A$ receptor β2-IL, studies were next carried out to determine any structural and functional homologies between GRIF-1 and the human homologue, KIAA1042. First the possible association between KIAA1042 and β2-IL(303-427) was investigated. Three GRIF-1 constructs were used as positive controls: the original library clone, GRIF-1(8-633), full-length GRIF-1(1-913) and the identified β2-IL interacting domain, GRIF-1(124-283). All three of these fusion proteins associated with β2-IL in yeast two-hybrid assays. However, neither the full-length KIAA1042(1-953), nor KIAA1042(124-283), the domain homologous to the β2-IL interacting site of GRIF-1, interacted with the β2-IL despite sharing ~45% and ~60% amino acid sequence identity, respectively, with the corresponding GRIF-1 sequences.

Since GRIF-1 and its human orthologue, KIAA0549, both bind the $GABA_A$ receptor β2-IL whereas KIAA1042 does not, it may be that KIAA1042, as part of the same gene family, has a similar function to GRIF-1 and KIAA0549, but with a different protein binding specificity. A single amino acid change is enough to cause a difference in protein-protein binding interactions. Figures 5.8 and 5.9 show amino acid sequence alignments between GRIF-1 and KIAA1042. Figure 5.8 shows a comparison of the two full-length sequences, while Figure 5.9 is focussed on amino acids 124-283, i.e. the identified GRIF-1 $GABA_A$ receptor β2-IL interacting domain. There are 43 conservative and 26 non-conservative amino acid changes between residues 124-283 of GRIF-1 and KIAA1042. The region of greatest dissimilarity between the two sequences that occurs within this domain is located at the short gap between the two coiled-coil domains of each protein. Slight differences in sequence between GRIF-1 and KIAA1042 could change residues that are necessary for binding, or lead to a difference in the overall protein conformation, thus preventing an association between KIAA1042 and the $GABA_A$ receptor β2-IL.

It was shown previously that both the first coiled-coil domain and the first half of the second coiled-coil domain of GRIF-1 are necessary for binding to the $GABA_A$ receptor β2-IL. Each coiled-coil domain alone was not sufficient for an interaction (Beck *et al.*, 2002). Figure 5.10 shows a schematic diagram showing the localisation of the $GABA_A$ receptor β2-IL interaction domain of GRIF-1. Neither construct GRIF-1(8-206), containing coiled-coil domain 1, nor GRIF-1(207-633), containing coiled-coil domain 2, interacted with the β2-IL (Beck *et al.*, 2002). Interestingly, the construct GRIF-1(135-633), which contains both coiled-coil domains, but not the sequence 124-134, also did not interact with the β2-IL. These findings suggest that residues outside the coil domains are important for the interaction and that more than one site is involved in the association. The results from this chapter show that, although KIAA1042 shares a high degree of homology with GRIF-1, the differences between them are great enough to prevent an interaction between KIAA1042 and the β2-IL(303-427).

5.3.3. THE KINESINS

The *Drosophila melanogaster* orthologue of GRIF-1, Milton, was shown to aid mitochondrial transport to synapses via an association with a kinesin heavy chain (Stowers *et al.*, 2002). Kinesins are molecular motor proteins involved in the

anterograde transport of vesicles along microtubules (Verhey and Rapaport, 2001). Conventional kinesin molecules contain four subunits, two light chains (KLC) and two heavy chains (KHC). The light chains contain α-helical heptad repeats, responsible for interacting with the KHCs and six tetratricopeptide repeats involved in protein-protein interactions with cargoes. The KHCs contain the catalytic motor domains used to power the movement of kinesin along microtubules and a stalk domain that contains two coiled-coil domains that interact with KLCs and are responsible for dimerisation of KHCs. The KHC tail domain is also thought to bind cargo proteins. The overall strength of binding between kinesin and its vesicular cargoes is energy dependent and involves more than one interaction domain on both the heavy and light chains (Tsai *et al.*, 2000). There are more than 30 members of the kinesin family of proteins (KIFs). The KIF5s are the KHCs of conventional kinesin. There are three KIF5s, KIF5A, KIF5B and KIF5C (Kanai *et al.*, 2000). KIF5A and C are both neurone specific. KIF5A is pan-neuronal, whereas KIF5C is localised to motor neurones. KIF5B is found in both neuronal and non-neuronal cells.

GRIF-1 binds to both KIF5C and the β2-IL which may support the role for GRIF-1 as a trafficking factor. However both proteins bind to the same stretch of sequence i.e. between residues 124-283, which means that they would be competing for the same binding site. This may suggest a role for GRIF-1 in the loading or unloading of $GABA_A$ receptor containing vesicles to kinesin. The AMPA receptor interacting protein, GRIP1, has been found to interact with all 3 KIF5 isoforms (A-C) (Setou *et al.*, 2002; see Section 1.2.6.2.1). Therefore, it may be expected that GRIF-1 would also associate with KIF5A and B. Since KIF5C was seen to interact with GRIF-1, but not KIAA1042, it could be that KIAA1042 has a separate function in the cell, or alternatively a different KIF binding specificity.

5.3.3.1. INTERACTIONS OF KIF5C WITH GRIF-1 AND KIAA1042

To investigate the functional similarity of GRIF-1 and KIAA1042 with Milton, both were investigated for an interaction with a KHC. The KHC, KIF5C was chosen for investigation since it is neurone specific (Kanai *et al.*, 2000) and has a similar size to the KHCs detected in co-immunoprecipitation studies with GRIF-1 in HEK 293 cells and rat forebrain (Brickley, K., Smith, M., Beck, M. and Stephenson, F. A., results in preparation). The full-length KIF5C clone was available from the Kazusa Research

Institute, Japan. The sequences GRIF-1(1-913), GRIF-1(8-633) and GRIF-1(124-283) were all shown to interact with KIF5C. The interaction with full-length GRIF-1 was very weak, whereas the strength of interaction was stronger for each of the shorter sequences. The shortest fragment i.e. 124-283 was expressed at a significantly higher level compared with GRIF-1(8-633) and GRIF-1(1-913) (Figure 5.5.). This explanation may account for the stronger interaction with KIF5C. Neither full-length KIAA1042(1-953), nor KIAA1042(124-283) showed any interaction with KIF5C, despite showing strong expression in yeast.

5.3.4. DIMERISATION INTERACTIONS OF FULL-LENGTH KIAA1042 WITH GRIF-1 AND KIAA1042

Full-length KIAA1042 was investigated for dimer formation both with itself and with GRIF-1. The three GRIF-1 sequences, GRIF-1(1-913), GRIF-1(8-633) and GRIF-1(124-283) and the two KIAA1042 sequences, KIAA1042(1-953) and KIAA1042(124-283), were each co-transformed with the full-length KIAA1042(1-953). Unfortunately, as has been seen previously for full-length GRIF-1 and the original library clone, GRIF-1(8-633), full-length KIAA1042 shows strong auto-activation of reporter genes when transformed into yeast in the DNA-BD vector. This meant that the yeast two-hybrid system is inappropriate for the study of KIAA1042 homo- and heterodimer formation.

FIGURE 5.1. SCHEMATIC DIAGRAM COMPARING COILED-COIL MOTIFS IN GRIF-1, KIAA1042, MILTON AND HAP-1

A

Sequence comparison	Similarity over full-length sequence	Similarity over homologous GRIF-1-β2-IL binding domain
GRIF-1 + KIAA1042	~60	~80
GRIF-1 + MILTON	~40	~54
GRIF-1 + rHAP-1	~47	~51

B

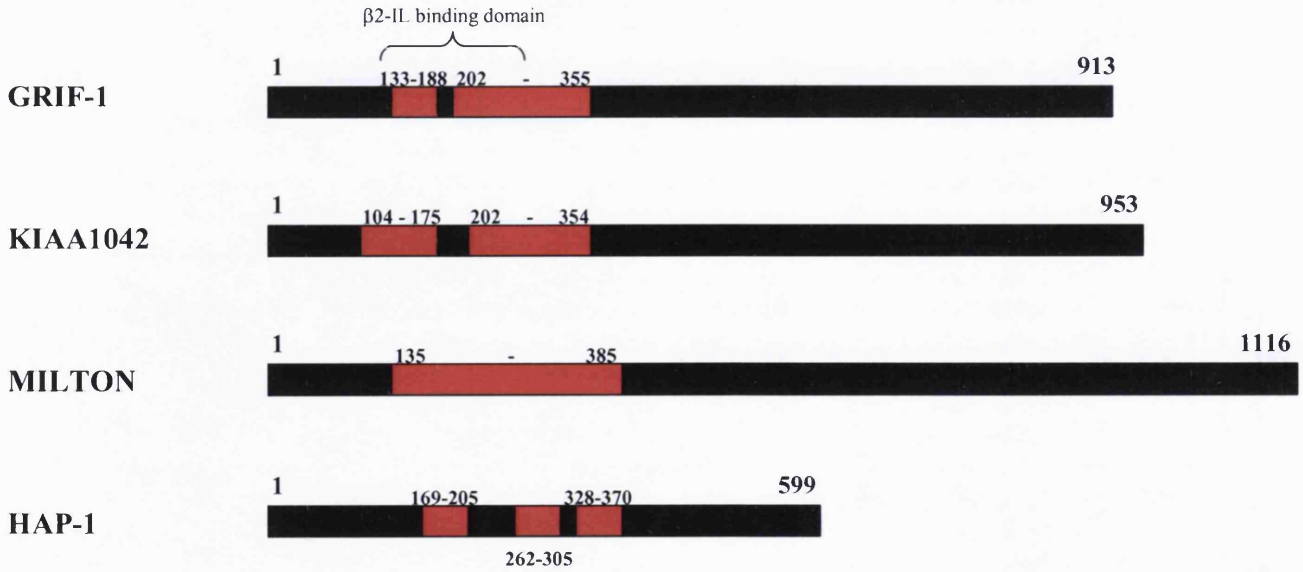

The figure shows a comparison between the coiled-coil domains ( ) of the $GABA_A$ receptor interacting factor, GRIF-1, family of proteins.

FIGURE 5.2. VECTOR DIAGRAMS OF THE GAL4 SYSTEM CONSTRUCTS USED TO TEST THE SPECIFICITY OF INTERACTION BETWEEN GRIF-1(8-633) AND THE β2-IL(303-427)

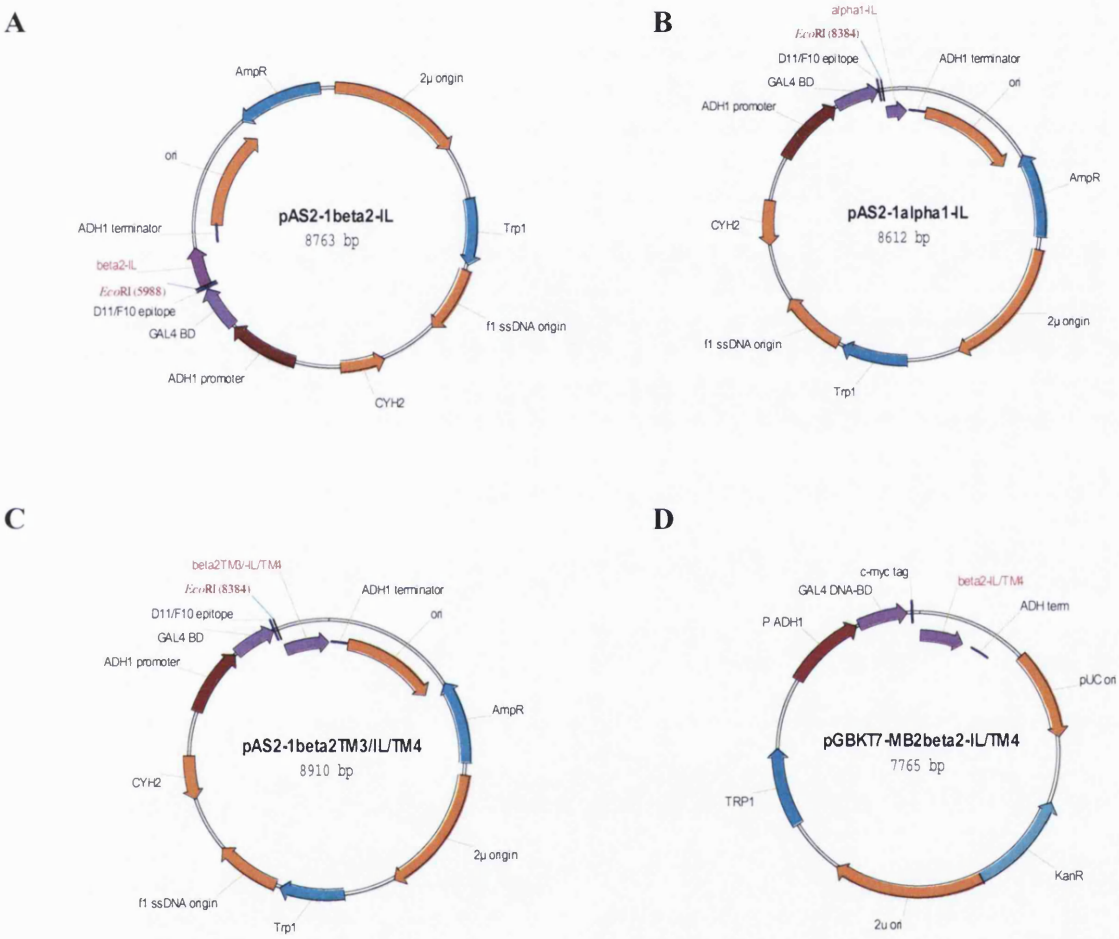

The $GABA_A$ receptor subunit sequences A, β2-IL(303-247), B, α1-IL(304-384), C, β2/TM3-IL/TM4(282-450) and D, β2-IL/TM4(303-450) were each cloned into a GAL4 DNA-BD vector to produce in frame fusion proteins for use in the GAL4 yeast two-hybrid system.

FIGURE 5.3. AN IMMUNOBLOT SHOWING THE EXPRESSION OF THE GAL4 DNA-BD FUSION PROTEINS CONTAINING $GABA_A$ RECEPTOR β2-IL OR α1-IL SEQUENCES IN THE IN THE YEAST STRAIN, AH109

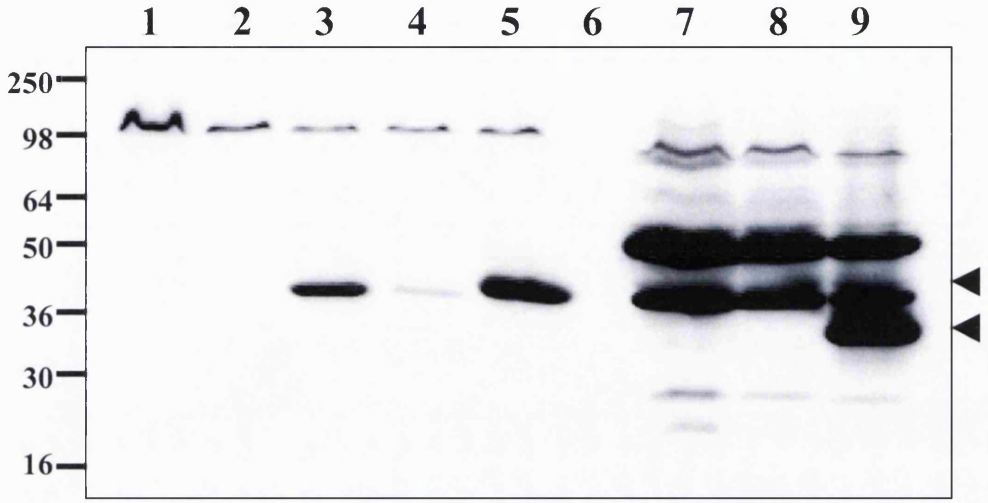

Lanes:

1. Untransformed AH109 cells
2. GAL4 DNA-BD
3. GAL4 DNA-BD β2-IL(303-427)
4. GAL4 DNA-BD β2-IL (282-450)
5. GAL4 DNA-BD β2-IL303-450)
6. Empty lane
7. Untransformed AH109 cells
8. GAL4 DNA-BD
9. GAL4 DNA-BD α1-IL(304-384)

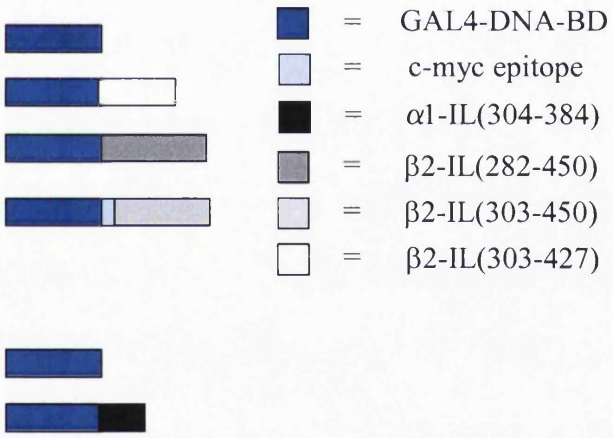

Construct	Predicted M_r (kDa)	Observed M_r (kDa)
GAL4 DNA-BD	17	Not observed
GAL4 DNA-BD β2-IL(303-427)	31	~41
GAL4 DNA-BD β2TM3-ILTM4(282-450)	37	~41
GAL4 DNA-BD β2-ILTM4(303-450)	34	~38
GAL4 DNA-BD α1-IL(304-384)	26	~28

The $GABA_A$ receptor subunit peptides β2-IL(303-427), β2TM3-ILTM4(282-450) and β2-ILTM4(303-450) and α1-IL(304-384) were transformed into AH109 yeast. Fusion proteins were extracted from yeast and analysed by immunoblotting using polyclonal antibodies against the $GABA_A$ receptor β2-IL(381-395) or α1-IL(324-341). The upper arrowhead indicates B2 loop constructs in lanes 3, 4 and 5. The lower arrowhead indicates the α1 loop in lane 9. Other bands on the immunoblot are also found in untransformed cells and represent non-specific antibody binding.

FIGURE 5.4. VECTOR DIAGRAMS OF THE MODIFIED LEXA AD VECTOR CONSTRUCTS USED TO TEST THE FUNCTIONAL HOMOLOGIES BETWEEN GRIF-1 AND KIAA1042

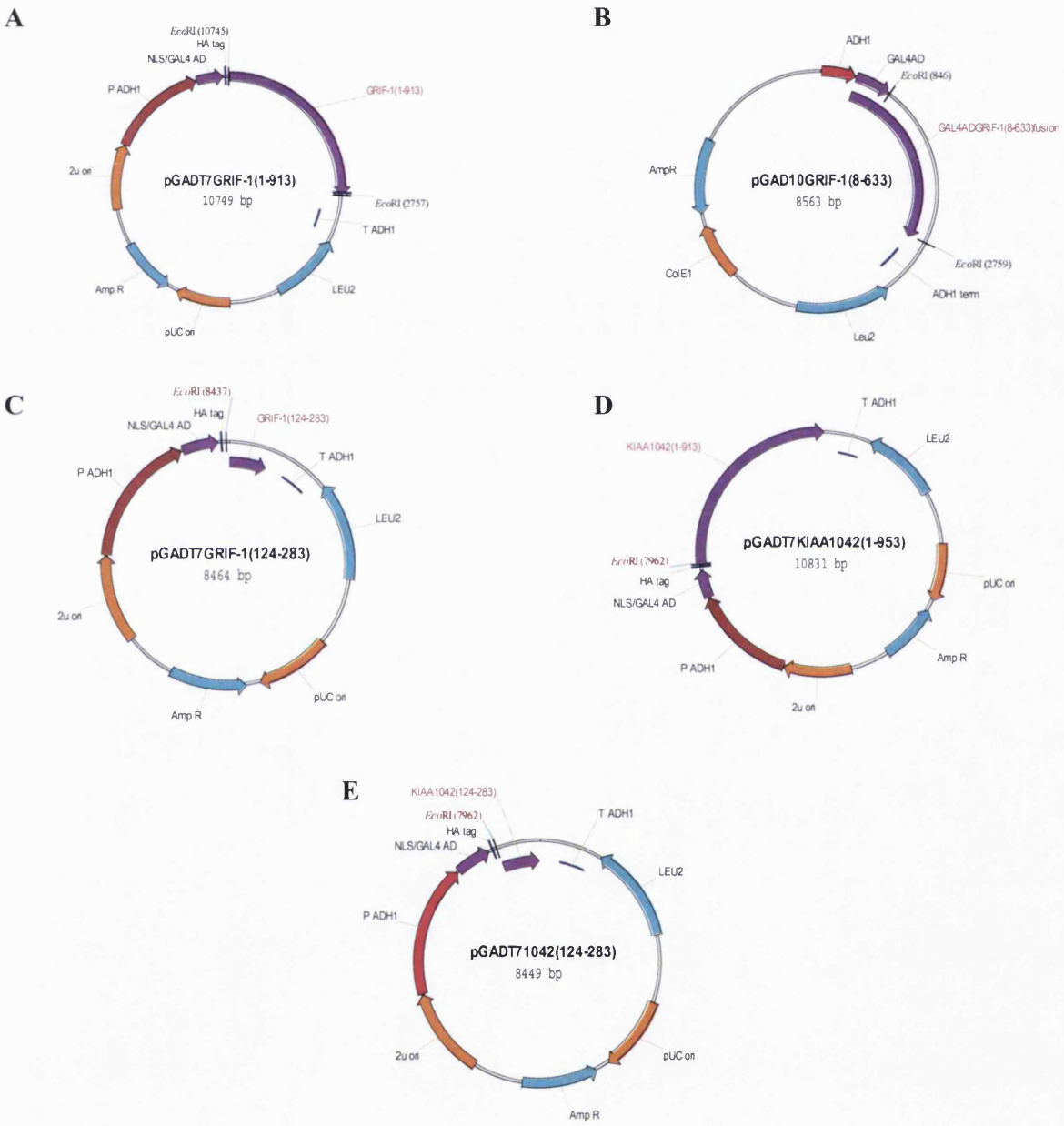

The GRIF-1 sequences A, GRIF-1(1-913), B, GRIF-1(8-633) and C, GRIF-1(124-283) and the KIAA1042 sequences D, KIAA1042(1-953) and E, KIAA1042(124-283) were each cloned into a GAL4 yeast two-hybrid AD vector to be tested for an interaction with the $GABA_A$ receptor β2-IL(303-427), KIF5C(1-957) and with KIAA1042(1-953).

FIGURE 5.5. AN IMMUNOBLOT SHOWING THE EXPRESSION OF THE GAL4-AD FUSION PROTEINS CONTAINING GRIF-1 OR KIAA1042 SEQUENCES IN THE YEAST STRAIN, L40

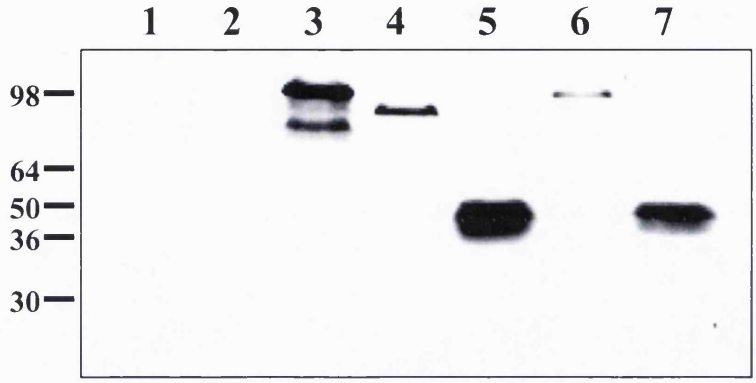

Lanes:

1. Untransformed L40 cells
2. GAL4-AD
3. GAL4-AD GRIF-1(1-913)
4. GAL4-AD GRIF-1(8-633)
5. GAL4-AD GRIF-1(124-283)
6. GAL4-AD KIAA1042(1-953)
7. GAL4-AD KIAA1042(124-283)

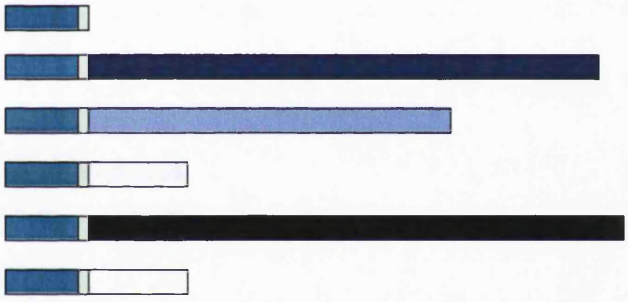

Key:

= GRIF-1(1-913)
= GRIF-1(8-633)
= GRIF-1(124-283)
= KIAA1042(1-953)
= KIAA1042(124-283)
= HA epitope
= GAL4-AD

Construct	Predicted M_r (kDa)	Observed M_r (kDa)
GAL4-AD	15	N/A
GAL4-AD GRIF-1(1-913)	117	~96, 78
GAL4-AD GRIF-1(8-633)	86	~86
GAL4-AD GRIF-1(124-283)	34	~41
GAL4-AD KIAA1042(1-953)	121	~96
GAL4-AD KIAA1042(124-283)	33	~45

The GAL4 AD vector containing a GRIF-1 or a KIAA1042 sequence was transformed into the yeast strain, L40. Fusion proteins were extracted from yeast and analysed by immunoblotting using the anti-GRIF-1(8-633) polyclonal antibody that recognises both GRIF-1 and KIAA1042.

FIGURE 5.6. VECTOR DIAGRAMS OF THE MODIFIED LEXA DNA-BD VECTOR CONSTRUCTS USED TO TEST THE FUNCTIONAL HOMOLOGIES BETWEEN GRIF-1 AND KIAA1042

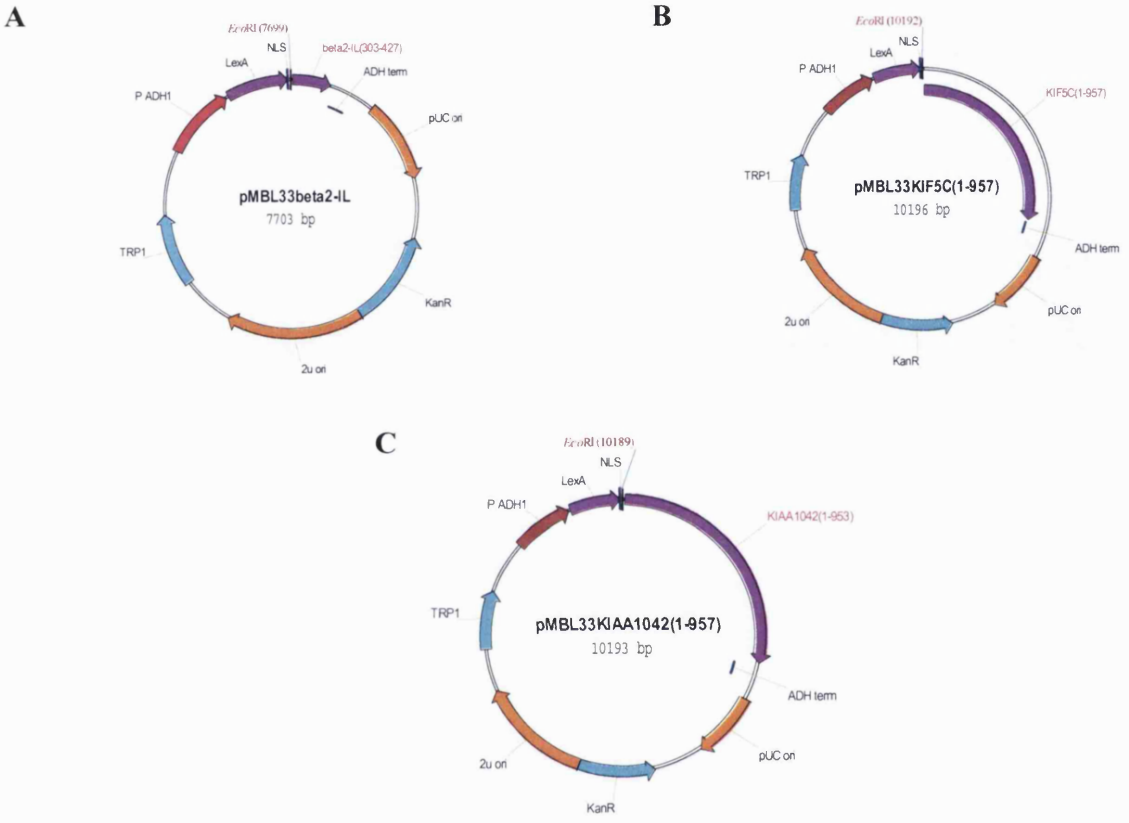

The sequences A, β2-IL(303-427), B, KIF5C(1-957) and C, KIAA1042(1-953) were each cloned into the mLexA yeast two-hybrid DNA-BD vector to test for interactions with GRIF-1 and KIAA1042 constructs.

FIGURE 5.7. AN IMMUNOBLOT SHOWING THE EXPRESSION OF THE LEXA DNA-BD FUSION PROTEIN CONTAINING KIF5C(1-957) IN THE YEAST STRAIN, L40

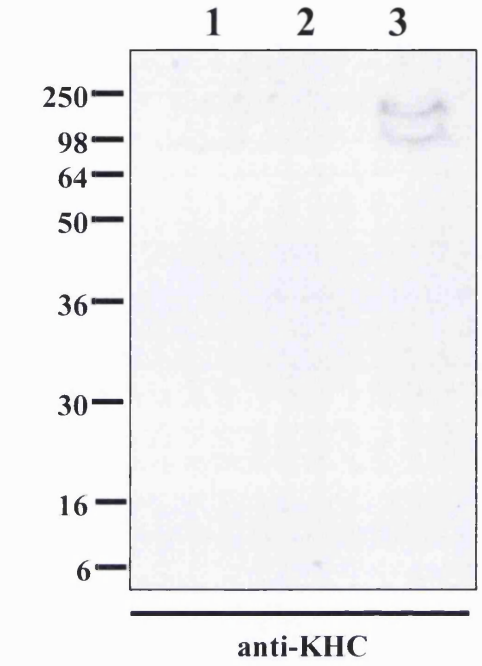

Lanes:

1. Untransformed AH109 cells
2. LEXA DNA-BD
3. LEXA DNA-BD KIF5C(1-957)

Key: □ = KIF5C(1-957)
■ = GAL4-DNA-BD

Construct	Predicted M_r (kDa)	Observed M_r (kDa)
LEXA DNA-BD	23	Not detected
LEXA DNA-BD KIF5C(1-957)	133	~143, ~117

The modified LexA DNA-BD vector pMBL33 containing the kinesin heavy chain clone KIF5C was transformed into the yeast strain, L40. The fusion protein was extracted from yeast and analysed by immunoblotting using the monoclonal anti-KHC antibody, AKIN02. Two bands can be seen in lane 3. The lower band correcponds to a faint band in the untransformed cells and may represent non-specific antibody binding. The upper band corresponds clsely to the expected size of the KIF5C fusion peptide.

FIGURE 5.8. AMINO ACID SEQUENCE ALIGNMENT BETWEEN GRIF-1(1-913) AND KIAA1042(1-953)

```
grif-1   MSLS-QN-AIFKSQTGEENLMSSNHRDSESITDVCSNEDLPEVELVNLLEEQLPQYKLRV   58
1042     MALVFQFGQPVRAQPLPGLCHGKLIRTN--ACDVCNSTDLPEVEIISLLEEQLPHYKLRA   58

grif-1   DSLFLYENQDWSQSSHQQQDASETLSPVLAEETFRYMILGTDRVEQMTKTYNDIDMVTHL   118
1042     DTIYGYDHDDWLHTPLISPDANIDLTTEQIEETLKYFLLCAERVGQMTKTYNDIDAVTRL   118

grif-1   LAERDRDLELAARIGQALLKRNHVLSEQNESLEEQLGQAFDQVNQLQHELSKKEELLRIV   178
1042     LEEKERDLELAARIGQSLLKKNKTLTERNELLEEQVEHIREEVSQLRHELSMKDELLQFY   178

grif-1   SIASEESETDSSCSTPLRFNESFSLSQGLLQLDMMHEKLKELEEENMALRSKACHIKTET   238
1042     TSAAEESEPESVCSTPLKRNESSSSVQNYFHLDSLQKKLKDLEEENVVLRSEASQLKTET   238

grif-1   FTYEEKEQKLINDCVNELRETNAQMSRMTEELSGKSDELLRYQEEISSLLSQIVDLQHKL   298
1042     ITYEEKEQQLVNDCVKELRDANVQIASISEELAKKTEDAARQQEEITHLLSQIVDLQKKA   298

grif-1   KEHVIEKEELRLHLQASKDAQRQLTMELHELQDRNMECLGMLHESQEEIKELRNKAGPSA   358
1042     KACAVENEELVQHLGAAKDAQRQLTAELRELEDKYAECMEMLHEAQEELKNLRNKTMPNT   358

grif-1   HLCFSQAYGVFAGESLAAEIEGTMRKKLSLDEESVFKQKAQQKRVFDTVKVANDTRGRSV   418
1042     TSRRYHSLGLFPMDSLAAEIEGTMRKELQL-EEAESPDITHQKRVFETVRNINQVVKQRS   417

grif-1   TFPVLLPIPGSNRSSVIMTAKPFESGVQQT----EDK---TLPNQGSS----TEVP--GN   465
1042     LTPSPMNIPGSNQSSAMNSLLSSCVSTPRSSFYGSDIGNVVLDNKTNSIILETEAADLGN   477

grif-1   SHP-RDP--PGLPEDSDLATALHRLSLRRQNYLSEKQFFAEEWERKLQILAEQEEEVSSC   522
1042     DERSKKPGTPGTPGSHDLETALRRLSLRRENYLSERRFFEEEQERKLQELAEKGELRSGS   537

grif-1   EALTENLASFCTDQ--SETTEL-GSAGCLRGFMPEKLQIVKPLEGSQTLHHWQQLAQPNL   579
1042     LTPTESIMSLGTHSRFSEFTGFSGMSFSSRSYLPEKLQIVKPLEGSATLHHWQQLAQPHL   597

grif-1   GTILDPRPGVITKGFTQMPK--DAVYHISDLEEDEEVGITFQVQQPLQLEQKPAPPPPVT   637
1042     GGILDPRPGVVTKGFRTLDVDLDEVYCLNDFEEDD-TGD--HISLP-RL----ATSTPVQ   649

grif-1   GIFLPPMTSAGGPVSVATSNPGKCLSFTNSTFTFTTCRILHPSD-ITQVTPSS-GFPSLS   695
1042     ----HPETSA--------HHPGKCMSQTNSTFTFTTCRILHPSDELTRVTPSLNSAPTPA   697

grif-1   CGSSAGSASNTAVNSPAASYRLSIGESITNRRDSTITFSSTRSLAKLLQERGISAKVYHS   755
1042     CGSTSHLKS-TPVATPCTPRRLSLAESFTNTRESTTTMSTSLGLVWLLKERGISAAVYD-   755

grif-1   PASEN-----PLLQ-LRPKALATPSTPPNSPSQSPCSSP--VPFEPRVHVSENFLASRPA   807
1042     PQSWDRAGRGSLLHSYTPKMAVIPSTPPNSPMQTPTSSPPSFEFKCTSPPYDNFLASKPA   815

grif-1   ETFLQEMY--GLRPSRAPPDVGQLKMNLVDRLKRLGIARVVKT---PVP---RENGKSRE   859
1042     SSILREVREKNVRSSESQTDVSVSNLNLVDKVRRFGVAKVVNSGRAHVPTLTEEQGPLLC   875

grif-1   AEMG-----LQK---PD------SAVYLNSGGSLLG-GLRRNQSLPVMMGS---FGAPVC   901
1042     GPPGPAPALVPRGLVPEGLPLRCPTVTSAIGGLQLNSGIRRNRSFPTMVGSSMQMKAPVT   935

grif-1   TTS-PKMG--ILKED---   913
1042     LTSGILMGAKLSKQTSLR   953
```

= sequence identity

= conservative amino acid changes

The figure shows an amino acid alignment between full-length GRIF-1(1-913) and KIAA1042(1-953). Coiled-coil domains are indicated in grey.

FIGURE 5.9. AMINO ACID SEQUENCE ALIGNMENT BETWEEN GRIF-1(124-283) AND KIAA1042(124-283)

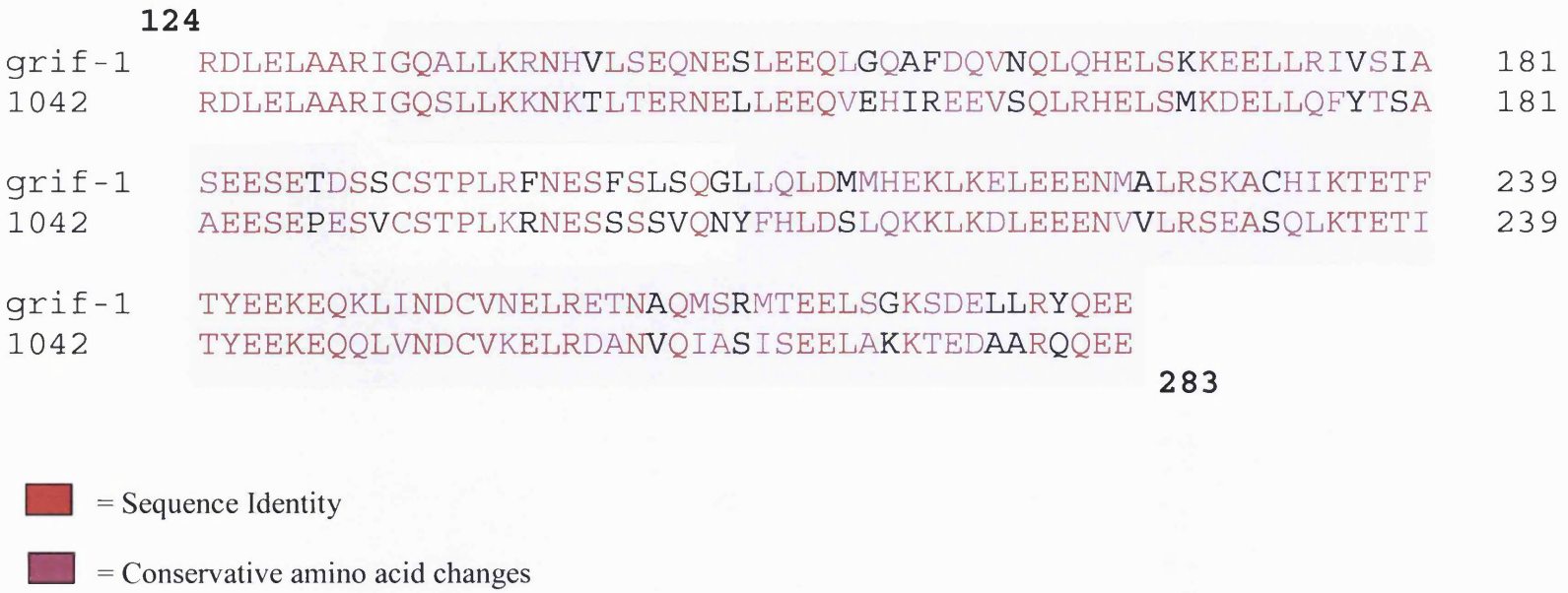

The figure shows an amino acid sequence alignment between GRIF-1 and KIAA1042, focussing on the region 124-283. This region corresponds to the first coiled-coil domain and the first half of the second coiled-coil domain GRIF-1(highlighted in grey) and has been identified as the GRIF-1/β2-IL interacting domain. Over these 160 amino acids, GRIF-1 and KIAA1042 show an amino acid sequence identity of 58%.

FIGURE 5.10. SCHEMATIC DIAGRAM SHOWING THE LOCALISATION OF THE β2-IL INTERACTION DOMAIN OF GRIF-1

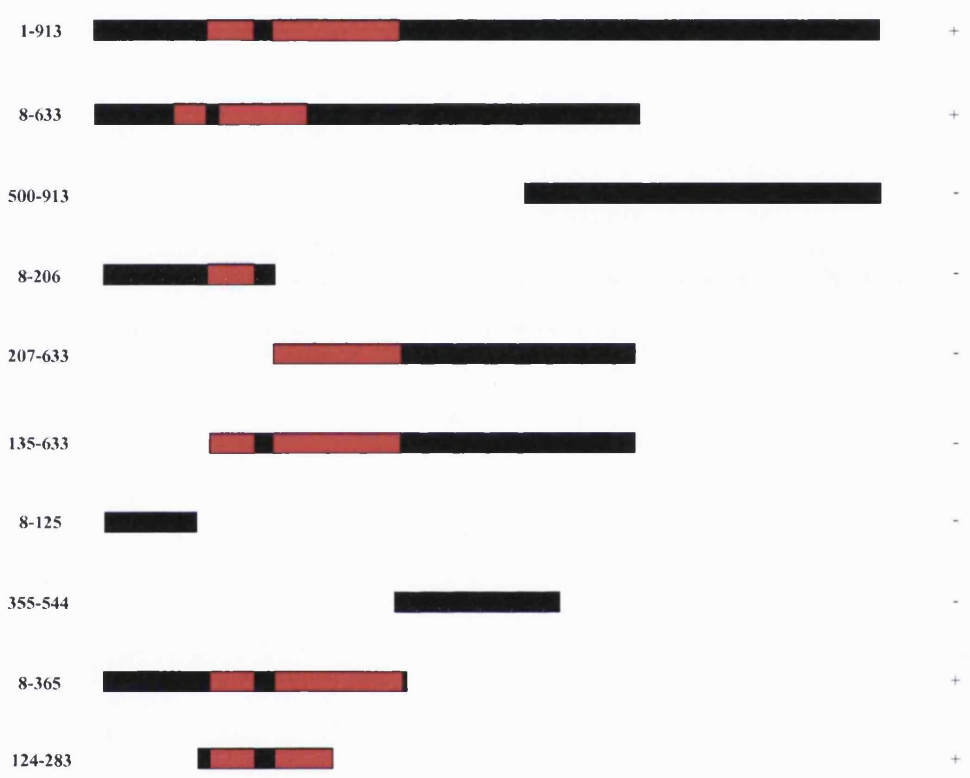

The diagram shows a series of full-length and truncated GRIF-1 constructs tested for their interaction with the $GABA_A$ receptor β2-IL. Red boxes indicate the positions of coiled-coil domains within GRIF-1. Adapted from Beck *et al.* (2002)

TABLE 5.1. RESULTS FOR THE CO-TRANSFORMATION OF YEAST WITH GRIF-1(8-633) AND THE $GABA_A$ RECEPTOR β2-IL(303-427) IN THE GAL4 YEAST TWO-HYBRID SYSTEM

AD Construct	DNA-BD Construct	-2 Selective Media	-4 Selective Media	β-Galactosidase assay
pVA3-1	pTD1-1	++	++	+
pGAD10 GRIF-1(8-633)	pAS2-1 β2-IL(303-427)	++	+	+
pGAD10	pAS2-1 β2-IL(303-427)	++	-	-
pGAD10 GRIF-1(8-633)	pAS2-1	++	-	-
pGAD10	pAS2-1	++	-	-

The results are representative of n = 4 independent co-transformations.

Key: -2 Selective media lacks leucine and tryptophan
-4 Selective media lacks adenine, histidine, leucine and tryptophan
For nutritional selection - = no growth, + = 11-100 colonies, ++ = 101-200 colonies
For β-galactosidase assay + = enzyme activity observed, - = No enzyme activity observed

The GAL4 yeast strain, AH109, was co-transformed with the cloned pAS2-1β2-IL(303-427) and pGAD10GRIF-1(8-633) two-hybrid constructs as described in section 2.2.3.2. and 2.2.3.3., to substantiate the positive interaction shown in previous experiments (Beck *et al.*, 2002). Growth on -2 selective medium shows that the transformation has been successful. Colony growth on -4 selective medium shows an interaction between the two proteins of interest.

TABLE 5.2. RESULTS FOR THE CO-TRANSFORMATION OF YEAST WITH GRIF-1(8-633) AND THE $GABA_A$ RECEPTOR α1-IL(304-384) IN THE GAL4 YEAST TWO-HYBRID SYSTEM

Activation Domain Construct	DNA-Binding Domain Construct	-2 Selective Media	-4 Selective Media	β-Galactosidase assay
pGAD10 GRIF-1(8-633)	pAS2-1 β2-IL(303-427)	++	+	+
pGAD10 GRIF-1(8-633)	pAS2-1 α1-IL(304-384)	++	-	-
pGAD10	pAS2-1 α1-IL(304-384)	++	-	-
pVA3-1	pTD1-1	++	++	+
pGAD10	pAS2-1	++	-	-

The results are representative of n = 3 independent co-transformations.

Key: -2 Selective media lacks leucine and tryptophan
-4 Selective media lacks adenine, histidine, leucine and tryptophan
For nutritional selection - = no growth, + = 11-100 colonies, ++ = 101-200 colonies
For β-galactosidase assay + = enzyme activity observed, - = no enzyme activity observed

The construct pAS2-1α1-IL(304-384) was transformed into yeast with pGAD10GRIF-1(8-633) to investigate the subunit specificity of the interaction between GRIF-1 and the $GABA_A$ receptor ILs.

TABLE 5.3. RESULTS FOR THE CO-TRANSFORMATION OF YEAST WITH GRIF-1(8-633) AND THE $GABA_A$ RECEPTOR TM3/β2-IL-TM4(282-450) AND β2-IL/TM4(303-450) IN THE GAL4 YEAST TWO-HYBRID SYSTEM

Activation Domain Construct	DNA-Binding Domain Construct	-2 Selective Media	-4 Selective Media	β-Galactosidase assay
pGAD10 GRIF-1(8-633)	pAS2-1 β2-IL(303-427)	++	+	(+)
pGAD10 GRIF-1(8-633)	pAS2-1 TM3/β2-IL-TM4 (282-450)	++	-	-
pGAD10	pAS2-1 TM3/β2-IL/TM4 (282-450)	++	-	-
pGAD10 GRIF-1(8-633)	pGBKT7_MB2 β2-IL/TM4(303-450)	+	-	-
pGAD10	pGBKT7_MB2 β2-IL/TM4(303-450)	+	-	-
pVA3-1	pTD1-1	++	+	+
pGAD10	pAS2-1	++	-	-

The results are representative of n = 3 independent co-transformations.

Key: -2 Selective media lacks leucine and tryptophan
-4 Selective media lacks adenine, histidine, leucine and tryptophan
For nutritional selection - = no growth, 1-10 colonies, + = 11-100 colonies, ++ = 101-200 colonies
For β-galactosidase assay (+) = weak enzyme activity observed + = enzyme activity observed, - = no enzyme activity observed

The constructs pAS2-1TM3/β2-IL/TM4(282-450) and pGBKT7_MB2β2-IL/TM4(303-450) were each co-transformed into yeast along with pGAD10GRIF-1(8-633) to test for the conformational specificity of the GRIF-1/β2-IL interaction by inclusion of either both TM3 and TM4 flanking the β2-IL sequence or, of TM4 alone.

TABLE 5.4 RESULTS FOR THE CO-TRANSFORMATION OF YEAST WITH THE $GABA_A$ RECEPTOR β2-IL(303-427) AND GRIF-1 OR KIAA1042

AD Vector	DNA-BD Vector	-2 Dropout Media	-3 (2 mM 3-AT) Dropout Media	β-Galactosdase Activity
pGADT7 GRIF-1(1-913)	pMBL33 β2-IL(303-427)	++	++	+
pGAD10 GRIF-1(8-633)	pMBL33 β2-IL (303-427)	++	++	+
pGADT7 GRIF-1(124-283)	pMBL33 β2-IL(303-427)	++	++	+
pGADT7 KIAA1042(1-953)	pMBL33 β2-IL(303-427)	++	-	-
pGADT7 KIAA1042(124-283)	pMBL33 β2-IL(303-427)	++	-	-
pGADT7	pMBL33 β2-IL(303-427)	++	-	-
pGADT7 GRIF-1(1-913)	pMBL33	++	-	-
pGAD10 GRIF-1(8-633)	pMBL33	++	-	-
pGADT7 GRIF-1(124-283)	pMBL33	++	-	-
pGADT7 KIAA1042(1-953)	pMBL33	++	-	-
pGADT7 KIAA1042(124-283)	pMBL33	++	-	-
pGADT7	pMBL33	++	-	-

The results are representative of n = 3 independent co-transformations.

Key: -2 Selective media lacks leucine and tryptophan
-3 Selective media lacks histidine, leucine and tryptophan and contains 2.5 mM 3-amino triazole
For nutritional selection - = no growth, colonies, ++ = 101-200 colonies
For β-galactosidase assay + = enzyme activity observed, - = no enzyme activity observed

Functional homologies between KIAA1042 and GRIF-1 were investigated by co-transformation of the yeast strain, L40, by each of the AD constructs containing GRIF-1(1-913), GRIF-1(8-633), GRIF-1(124-283), KIAA1042(1-953) or KIAA1042(124-283) along with the β2-IL in the DNA-BD plasmid pMBL33.

TABLE 5.5. RESULTS FOR THE CO-TRANSFORMATION OF YEAST WITH KIF5C AND GRIF-1 OR KIAA1042

AD Vector	DNA-BD Vector	-2 Dropout Media	-3 (2 mM 3-AT) Dropout Media	β-Galactosdase Activity
pGADT7 GRIF-1(1-913)	pMBL33 KIF5C(1-957)	++	(+)	(+)
pGAD10 GRIF-1(8-633)	pMBL33 KIF5C(1-957)	++	++	+
pGADT7 GRIF-1(124-283)	pMBL33 KIF5C(1-957)	++	+++	+
pGADT7 KIAA1042(1-953)	pMBL33 KIF5C(1-957)	++	-	-
pGADT7 KIAA1042(124-283)	pMBL33 KIF5C(1-957)	++	-	-
pGADT7 GRIF-1(1-913)	pMBL33	++	-	-
pGADT7 GRIF-1(8-633)	pMBL33	++	-	-
pGAD10 GRIF-1(124-283)	pMBL33	++	-	-
pGADT7 KIAA1042(1-953)	pMBL33	++	-	-
pGADT7 KIAA1042(124-283)	pMBL33	++	-	-
pGADT7	pMBL33 KIF5C(1-957)	++	-	-
pGADT7	pMBL33 β2-IL(303-427)	++	-	-
pGADT7	pMBL33	++	-	-
pGAD10 GRIF-1(8-633)	pMBL33 β2-IL(303-427)	++	+	+

The results are representative of n = 3 independent co-transformations.

Key: -2 Selective media lacks leucine and tryptophan
-3 Selective media lacks histidine, leucine and tryptophan and contains 2.5 mM 3-amino triazole
For nutritional selection - = no growth, (+) = 1-10 colonies, + = 11-100 colonies, ++ = 101-200 colonies, +++ = >200 colonies
For β-galactosidase assay + = enzyme activity observed, - = no enzyme activity observed

The yeast strain L40 was co-transformed with the kinesin heavy chain clone, KIF5C, along with a GRIF-1 or KIAA1042 sequence to determine functional homologies with each other and with the *drosophila* protein, Milton.

TABLE 5.6. RESULTS FOR THE CO-TRANSFORMATION OF YEAST WITH KIAA1042 AND GRIF-1 OR KIAA1042

AD Vector	DNA-BD Vector	-2 Dropout Media	-3 (2 mM 3-AT) Dropout Media	β-Galactosdase Activity
pGADT7 GRIF-1(1-913)	pMBL33 KIAA1042(1-953)	++	++	++
pGAD10 GRIF-1(8-633)	pMBL33 KIAA1042(1-953)	++	++	++
pGADT7 GRIF-1(124-283)	pMBL33 KIAA1042(1-953)	++	++	++
pGADT7 KIAA1042(1-953)	pMBL33 KIAA1042(1-953)	++	++	++
pGADT7 KIAA1042(124-283)	pMBL33 KIAA1042(1-953)	++	++	++
pGADT7 GRIF-1(1-913)	pMBL33	++	-	-
pGADT7 GRIF-1(8-633)	pMBL33	++	-	-
pGAD10 GRIF-1(124-283)	pMBL33	++	-	-
pGADT7 KIAA1042(1-953)	pMBL33	++	-	-
pGADT7 KIAA1042(124-283)	pMBL33	++	-	-
pGADT7	pMBL33 KIAA1042(1-953)	++	++	++
pGADT7	pMBL33 β2-IL(303-427)	++	-	-
pGADT7	pMBL33	++	-	-
pGAD10 GRIF-1(8-633)	pMBL33 β2-IL(303-427)	++	+	+

The results are representative of n = 3 independent co-transformations.

Key: -2 Selective media lacks leucine and tryptophan.
-3 Selective media lacks histidine, leucine and tryptophan and contains 2.5 mM 3-amino triazole
For nutritional selection - = no growth, + = 11-100 colonies, ++ = 101-200
For β-galactosidase assay + = enzyme activity observed, - = no enzyme activity observed

The yeast strain L40 was co-transformed with full-length KIAA1042(1-953), along with a GRIF-1 or KIAA1042 sequence to test for dimerisation interactions.

CHAPTER 6:
GENERAL DISCUSSION

6. GENERAL DISCUSSION

6.1. REGULATION OF GABAERGIC INHIBITION IN THE BRAIN

GABAergic inhibition is important for the regulation of excitatory synaptic potentials in the brain. In turn, GABAergic inhibition is controlled by several factors including the number of transmitter release sites, transporter activity, the pharmacological properties and cellular localisation of receptor subtypes and modulation of receptor activity by both endogenous and exogenous mechanisms (Cherubini and Conti, 2001). Figure 6.1 shows a schematic diagram representing the pathway from receptor subunit transcription to receptor cell surface expression at synapses and indicates some of the factors regulating the process.

The overall aim of this thesis was to identify factors involved in $GABA_A$ receptor subunit oligomerisation and cellular processing and, ultimately, in the regulation of receptor diversity.

6.1.1. $GABA_A$ RECEPTOR DIVERSITY

The pharmacological properties of $GABA_A$ receptors are dependent on subunit composition. Receptor diversity is limited by selective subunit expression in particular neurones, as well as the need for correct subunit folding and post-translational modifications for exit from the ER, and specificity of subunit oligomerisation. These factors ensure that receptors with the necessary pharmacological properties are expressed in particular neurones.

The first aim of this thesis was to identify residues in the N-terminal domains of the $GABA_A$ receptor α1 and β2 subunits that are important for subunit oligomerisation and to assess the usefulness of the yeast two-hybrid assay for these investigations. The subunit sequences α1(1-224) and β2(1-220) were cloned into the plasmid vectors of three different yeast two-hybrid systems to create in frame fusion constructs for each assay. Various combinations of $GABA_A$ receptor subunit N-terminal domains fused to yeast two-hybrid transcription factor GAL4 AD or DNA-BD domains were co-transformed into the GAL4 yeast strain, AH109. However, N-termini fused to the GAL4 AD were found to cause auto-activation of yeast reporter genes in the absence of a DNA-BD fusion sequence. The same result was found for co-transformation of N-termini, fused to the GAL4 AD and mLexA DNA-BD, into the mLexA system. A third two-hybrid system, the CytoTrap® system, which is not reliant on TF activation was

also established in the laboratory and the receptor sequences were tested using this assay. This system detects protein-protein interactions via reconstitution of the Ras signalling pathway, which is found in the cytoplasm. Therefore, false positive results due to TF activation by test proteins should not affect this assay. In this system, no interactions were observed between any combination of the α1 and/or β2 N-termini. Since other techniques have shown the $GABA_A$ receptor subunit N-termini to contain sequences that are important for subunit oligomerisation, these results suggest that the subunit sequences are not folded properly in yeast and, therefore, that yeast two-hybrid system was not useful for the study of $GABA_A$ receptor subunit N-terminal assembly domains.

6.1.2. $GABA_A$ RECEPTOR LOCALISATION AND STABILISATION AT THE SYNAPSE

Targeting of receptors to the cell surface and stabilisation of receptors in the plasma membrane are controlled by various interacting proteins. Trafficking proteins direct receptors through the exocytic pathway, via the ER, Golgi apparatus and in vesicles. Once inserted into the membrane, anchoring proteins stabilise receptor clusters. Extracellular proteins are also involved in stabilising receptor position e.g. the agrin-MuSK-rapsyn complex interaction with nACh receptors (discussed in Section 4.1.2). These extracellular interactions provide a physical link to the presynaptic neurone and are important for synaptogenesis and synaptic plasticity. However, evidence of this type of interaction is lacking for GABAergic synapses. Hence, the second aim of this thesis was to identify proteins that may be involved in $GABA_A$ receptor trafficking and the formation and plasticity of GABAergic synapses. The IL of the β3 subunit was used to screen a yeast two-hybrid cDNA library for trafficking proteins and the N-terminus of the β2 subunit was used to screen a rat brain cDNA library for proteins involved in synapse formation and plasticity. The β2 N-terminus screen isolated a putative novel chaperone protein which shares 99% cDNA sequence identity and 100% amino acid identity with the rat DnaJ-like protein, TID1L. Protein motifs within the sequence suggest that it is a class I DnaJ homologue. As mentioned earlier, chaperone proteins have been found to play a role in the trafficking (Mizukoshi *et al.*, 1999) and assembly (Sacht *et al.*, 1999) of receptors. However, since the data from Chapter 3 suggests that the N-termini of $GABA_A$ receptors may not be properly folded in yeast, the DnaJ-like

protein may be involved in the folding of incompletely folded receptor subunits, or in the re-folding of incorrectly folded subunits.

The β3-IL cDNA library screen did not identify any new $GABA_A$ receptor interacting partners. Several clustering and anchoring molecules have been identified for the glutamate receptors (discussed in Section 1.2.6). An equivalent protein scaffolding complex to the glutamate receptor post-synaptic density has not been found for the nACh receptor superfamily. The only clustering/anchoring proteins identified for these receptors are nACh receptor interacting protein, rapsyn, and the glycine receptor interacting protein, gephyrin. Studies carried out to identify a similar molecule for $GABA_A$ receptors have been unsuccessful. The intracellular loops of the nACh family of receptors are more conformationally restricted in comparison with the free C-termini of glutamate receptors. This may limit the number of proteins that can interact with this domain. Gephyrin has been shown to play a role in $GABA_A$ receptor clustering, but has not been shown to interact directly with $GABA_A$ receptors. GABARAP has been shown to bind directly to $GABA_A$ receptors, but its function at the synapse remains uncertain. This lack of $GABA_A$ receptor clustering/anchoring proteins may mean that use an alternative mechanism of clustering and anchoring at the synaptic membrane, or that an equivalent $GABA_A$ receptor clustering molecule exists that has not yet been identified.

6.1.3. CHARACTERISATION OF THE NOVEL $GABA_A$ RECEPTOR INTERACTING FACTOR, GRIF-1

The $GABA_A$ receptor interacting factor, GRIF-1, was identified as a $GABA_A$ receptor interacting protein in a yeast two-hybrid screen of a rat brain cDNA library, using the β2 subunit as a bait (Beck *et al.*, 2002). It was found to share amino acid sequence similarity with several proteins of unknown function (discussed in Section 5.1.1). The third aim of this thesis was to characterise further the GRIF-1 family of coiled-coil proteins. The interaction of GRIF-1 with the $GABA_A$ receptor was found to be specific for the β2 subunit IL. The conformation of the loop was also shown to be important, as the interaction was abolished by addition of one or both of the flanking transmembrane domains. Structural and functional homologies were assessed between GRIF-1 and the human homologue, KIAA1042, by comparison of their interactions with the $GABA_A$ receptor β2 subunit IL. KIAA1042 did not interact with the β2-IL, despite sharing a high degree of amino acid sequence homology with GRIF-1.

The possible role of GRIF-1 and KIAA1042 as $GABA_A$ receptor trafficking factors was also investigated by testing for interactions with the kinesin heavy chain clone, KIF5C. Full-length GRIF-1 showed a weak interaction with KIF5C. Shorter sequences of GRIF-1, each containing the coiled-coil domain, i.e. GRIF-1 (8-633) and GRIF-1(124-283), displayed a stronger interaction with KIF5C. Both full-length KIAA1042 and KIAA1042(124-283) did not interact with KIF5C. These results support the role of GRIF-1 as a β2 subunit-containing $GABA_A$ receptor trafficking factor and suggest a high specificity of function since the homologous protein, KIAA1042 did not display the same characteristic interactions. An investigation into the dimerisation of KIAA1042 and GRIF-1 proteins proved inconclusive, as KIAA1042 transformed into yeast as a DNA-BD fusion protein results in auto-activation of reporter gene activity. Similar auto-activation has been shown for GRIF-1.

6.2. FUTURE WORK

6.2.1. YEAST TWO-HYBRID SYSTEM MODIFICATIONS

The limitations of the yeast two-hybrid assay were discussed in section 3.1.13. In both the study of assembly domains for the $GABA_A$ receptor α1 and β2 subunit N-terminal domains (Chapter 3), and in the β2 N-terminus screening of the yeast two-hybrid cDNA library (Chapter 4), it is likely that the N-terminal fusion proteins were not folded correctly in yeast cells. This is possible because the sequences would have been manufactured in the yeast cytoplasm rather than in a mammalian cell ER as would be expected for normal membrane protein processing through the exocytic pathway (discussed in Section 3.2.11.3). The yeast cytoplasm lacks the particular folding proteins and modifying enzymes necessary for proper processing of receptor subunits such as BiP and PDI. Although it has been shown that certain proteins which do require these factors can be properly processed in the yeast cytoplasm (Ozenberger and Young, 1995), the results described here suggest that the $GABA_A$ receptor N-termini are mis-folded.

In some cases it is possible to produce the correct structural conformation of complex proteins by co-expression of the required modifying factors (Sobhanifar, 2003). Therefore, further studies of $GABA_A$ receptor N-termini in yeast may be possible if the lacking factors are introduced in parallel. Another problem encountered here which may be overcome by proper folding of the subunit sequences, is the auto-activation observed

in both GAL4 and LexA TF based assays. In some cases it is possible to prevent auto-activation by truncating the test proteins until a fragment is found that does not activate reporter genes. However, a drawback of this is that it may involve removing a part of the peptide that is necessary for the interactions being studied or for the 3 dimensional stability of the protein. An alternative method of studying the $GABA_A$ receptor assembly motifs therefore may be preferable.

The DnaJ-like protein (clone 3) isolated from the yeast two-hybrid library screen (Chapter 4) appears to be involved in re-folding of incorrectly folded proteins. It may be useful to obtain the full length sequence using rapid amplification of cDNA ends (RACE). It would be interesting to test the $GABA_A$ receptor β2(1-224) interaction with clone 3 in mammalian cells to determine whether it represents a physiological interaction. It would also be interesting to compare the interaction of the β2 N-terminus to that of a full-length β2 subunit which is more likely to be correctly folded.

6.2.2. RECEPTOR TRAFFICKING FUNCTIONS OF GRIF-1

Further work on the characterisation of GRIF-1 to elucidate the physiological significance of this protein in neurones is ongoing. Interactions between KIF5A, KIF5B and KIF5C are being screened for association with GRIF-1 in brain tissue (Brickley *et al.*, in preparation). Kanai *et al.* (2000) have shown that KIF5C knockout mice are non-lethal and KIF5B knockout mice, while not viable, can be rescued by injection of KIF5A, KIF5B or KIF5C, suggesting some functional redundancy between the isoforms. Therefore, it may be expected that GRIF-1 will interact with all three isoforms. It would also be interesting to determine whether KIF5A and KIF5B interact directly with GRIF-1 in the yeast two-hybrid system. The AMPA receptor trafficking protein, GRIP1, was shown to associate with all three KIF5C isoforms (Setou *et al.*, 2002) and the AMPA receptor GluR2 subunit. It was thus found to play a role in the trafficking of AMPA receptors (discussed in Section 1.2.6.2.1). GRIF-1 may have a similar role to GRIP1 in the trafficking of $GABA_A$ receptors, although no significant amino acid or DNA sequence homology exists between GRIF-1 and GRIP1. Similar studies could also be carried out to determine the functional significance of the interaction between GRIF-1 and kinesin, as were carried out for GRIP1 and kinesin, such as determination of the GRIF-1 binding domain in KIF5s and the subcellular colocalisation of GRIF-1 and $GABA_A$ receptors in neurones.

FIGURE 6.1. REGULATION OF $GABA_A$ RECEPTOR ASSEMBLY THROUGH THE EXOCYTIC PATHWAY

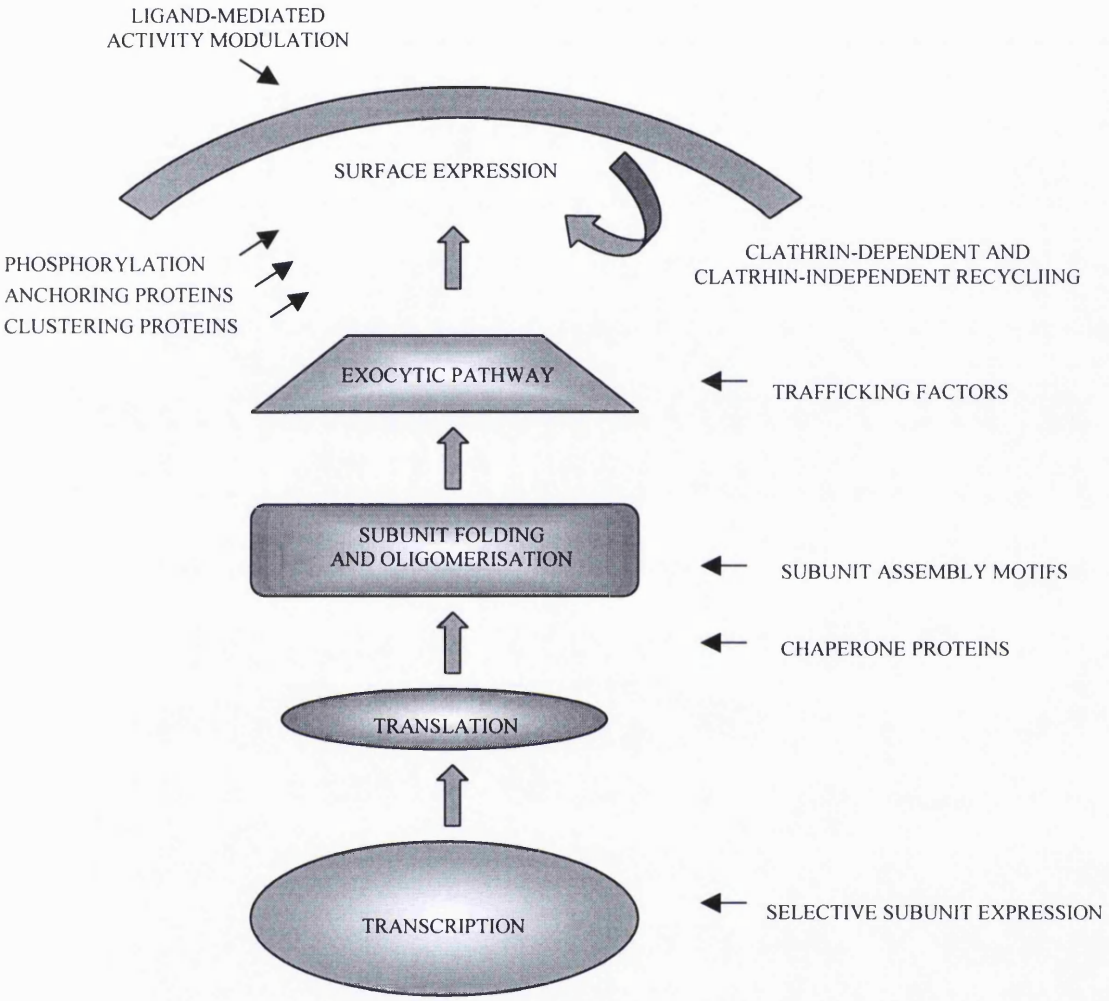

Figure 6.1 shows a schematic representation of the $GABA_A$ receptor exocytic pathway from gene expression to membrane insertion, indicating factors involved in regulating the process.

REFERENCES

Agatep, R., Kirkpatrick, R. D., Parchaliuk, D. L., Woods, R. A. and Gietz, R. D. (1998) *Elsevier Trends Journals Technical Tips Online* Transformation of *Saccharomyces cerevisciae* by Lithium Acetate/Single-stranded Carrier DNA/Polyethylene Glycol Protocol.

Akk, G., Bracamontes, J. and Steinbach, J. H. (2004) *J. Physiol.* **556**, 387-99. Activation of GABA(A) Receptors Containing the Alpha4 Subunit by GABA and Pentobarbital.

Akyol, Z., Bartos, J. A., Merrill, M. A., Faga, L. A., Jaren, O. R., Shea, M. A. and Hell, J. W. (2004) *J. Biol. Chem.* **279**, 2166-2175. Apo-Calmodulin Binds with its C-Terminal Domain to the N-Methyl-D-Aspartate Receptor NR1 C0 Region.

Amin, J. and Weiss, D. S. (1993) *Nature.* **366**, 565-569. $GABA_A$ Receptor Needs Two Homologous Domains of the β-Subunit for Activation by GABA but not by Pentobarbital.

Apel, E. D., Glass, D. J., Moscoso, L. M., Yancopoulos, G. D. and Sanes, J. R. (1997) *Neuron.* **18**, 623-635. Rapsyn is Required for MuSK Signalling and Recruits Synaptic Components to a MuSK-Containing Scaffold.

Araki, T., Kiyama, H. and Tohyama, M. (1992) *Neuroscience.* **51**, 582-591. $GABA_A$ Receptor Subunit Messenger RNAs Show Differential Expression During Cortical Development in the Rat Brain.

Aronheim, A., Zandi, E., Hennemann, H., Elledge, . J. and Karlin, M. (1997) *Mol. and Cell. Biol.* **17**, 3094-3102. Isolation of an AP-1 Repressor by a Novel Method for Detecting Protein-Protein Interactions.

Awapara, J., Landau, A. J., Fuerat, R. and Seale, B. (1950) *J. Biol. Chem.* **187**, 35-39. Free γ-Aminobutyric Acid in the Brain.

Bateson, A. N., Lasham, A. and Darlison, M. G. (1991) *J. Neurochem.* **56**, 1437-1440. γ-Aminobutyric $Acid_A$ Receptor Heterogeneity is Increased by Alternative Splicing of a Novel β-Subunit Gene Transcript.

Baumann, S. W., Baur, R. and Sigel, E. (2002) *J. Biol. Chem.* **277**, 46020-46025. Forced Subunit Assembly in α1β2γ2 GABA Receptors: Insight into the Absolute Arrangement.

Baur, R. and Sigel, E. (2003) *J. Neurochem.* **87**, 325-332. On High- and Low-Affinity Agonist Sites in $GABA_A$ Receptors.

Bazemore, A. W., Elliott, K. A. C. and Florey, E. (1957) *J. Neurochem.* **1**, 334-339. Isolation of Factor I.

Beck, K. and Brodsky, B. (1998) *J. Struct. Biol.* **122**, 17-29. Supercoiled Protein Motifs: the Collagen Triple-Helix and the Alpha-Helical Coiled Coil.

Beck, M., Brickley, K., Wilkinson, H. L., Sharma, S., Smith, M., Chazot, P. L., Pollard, S. and Stephenson, F. A. (2002) *J. Biol. Chem.* **277**, 30079-30090. Identification, Molecular Cloning, and Characterization of a Novel $GABA_A$ Receptor-Associated Protein, GRIF-1.

Bedford, F. K., Kittler, J. T., Muller, E., Thomas, P., Uren, J. M., Merlo, D., Wisden, W., Triller, A., Smart, T. G. and Moss, S. J. (2001) *Nat. Neurosci.* **4**, 908-916. $GABA_A$ Receptor Cell Surface Number and Subunit Stability are Regulated by the Ubiquitin-Like Protein Plic-1.

Beg, A. A. and Jorgensen, E. M. (2003) *Nat. Neurosci.* **6**, 1145-1152. EXP-1 is an Excitatory GABA-Gated Cation Channel.

Benke, D., Mertens, S., Trzeciak, A., Gillessen, D. and Mohler, H. (1991) *J. Biol. Chem.* **266**, 4478-4483. $GABA_A$ Receptors Display Association of γ2-Subunit with α1- and β2/3-Subunits.

Beranger, F., Aresta, S., de Gunzburg, J. and Camonis, J. (1997) *Nucleic Acids Research.* **25**, 2035-2036. Getting More from the Two-Hybrid System: N-Terminal Fusions to LexA are Efficient and Sensitive Baits for Two-Hybrid Studies.

Benke, D., Fritschy, J-M., Trzeciak, A., Bannwarth, W. and Mohler, H. (1994) *J. Biol. Chem.* **269**, 27100-27107. Distribution, Prevalence and Drug Binding Profile of γ-Aminobutyric Acid Type A Receptor Subtypes Differing in the β Subunit Variant.

Bettler, B., Kaupmann, K. and Bowery, N. (1998) *Curr. Opin. Neurobiol.* **8**, 345-354. $GABA_B$ Receptors: Drugs Meet Clones.

Bloom, F. E. and Iverson, L. L. (1971) *Nature.* **229**, 628-630. Localizing ^{3}H-GABA in Nerve Terminals of Rat Cerebral Cortex by Electron Microscopic Autoradiography.

Boileau, A. J., Evers, A. R., Davis, A. F. and Czajkowski, C. (1999) *J. Neurosci.* **19**, 4847-4854. Mapping the Agonist Binding Site of the $GABA_A$ Receptor: Evidence for a β-Strand.

Bohme, I., Rabe, H. and Luddens. (2004) *J. Biol. Chem.* **279**, 35193-35200. Four Amino Acids in the α Subunits Determine the γ-Aminobutyric Acid Sensitivities of $GABA_A$ Receptor Subtypes.

Bollan, K., King, D., Robertson, L. A., Brown, K., Taylor, P. M., Moss, S. J., and Connolly, C. N. (2003) *J. Biol. Chem.* **278,** 4747–4755. $GABA_A$ Receptor Composition is Determined by Distinct Assembly Signals within α and β Subunits.

Bormann, J. (2000) *Trends. Pharmacol. Sci.* **21**, 16-19. The 'ABC' of GABA Receptors.

Bonnert, T. P., McKernan, R. M., Farrar, S., le Bourdelles, B., Heavens, R. P., Smith, D. W., Hewson, L., Rigby, M. R., Sirinathsinghji, D. J. S., Brown, N., Wafford, K. A. and Whiting, P. J. (1999) *Proc. Acad. Natl. Sci. USA.* **96**, 9891-9896. θ, A Novel γ-Aminobutyric Acid Type A Receptor Subunit.

Boyd, G. W., Doward, A. I., Kirkness, E. F., Millar, N. S. and Connolly, C. N. (2003) *J. Biol. Chem.* **278**, 27681-27687. Cell Surface Expression of 5-Hydroxytryptamine Type 3 Receptors is Controlled by an Endoplasmic Reticulum Retention Signal.

Brandon, N. J., Uren, J. M., Kittler, J. T., Wang, H., Olsen, R., Parker, P. J. and Moss, S. J. (1999) *J. Neurosci.* **19**, 9228-9234. Subunit-Specific Association of Protein Kinase C and the Receptor for Activated C Kinase with GABA Type A Receptors.

Brejc, K., van Dijk, W. J., Klaasen, R. V., Schuurmans, M., van der Oost, J., Smit, A. B. and Sixma, T. K. (2001) *Nature.* **411**, 269-276. Crystal Structure of an Acetylcholine-Binding Protein Reveals the Ligand-Binding Domain of Nicotinic Receptors.

Brent, R. and Ptashne, M. (1985) *Cell.* **43**, 729-736. A Eukaryotic Transcriptional Activator Bearing the DNA Specificity of a Prokaryotic Repressor.

Brisson, A. and Unwin, P. N. T. (1985) *Nature.* **315**, 474-477. Quarternary Structure of the Acetylcholine Receptor.

Buhr, A. and Sigel, E. (1997) *Proc. Acad. Natl. Sci. USA.* **94**, 8824-8829. A Point Mutation in the γ2 Subunit of the γ-Aminobutyric Acid Type A Receptors Results in Altered Benzodiazepine Binding Site Specificity.

Changeux, J. P., Kasai, M. and Lee, C. Y. (1970) *Proc. Natl. Acad. Sci. USA.* **67**, 1241-1247. The Use of a Snake Venom Toxin to Characterise the Cholinergic Receptor Protein.

Chazot, P. L. and Stephenson. (1997) *J. Neurochem.* **69**, 2138-2144. Molecular Dissection of Native Mammalian Forebrain NMDA Receptors Containing the NR1 C2 Exon: Direct Demonstration of NMDA Receptors Comprising NR1, NR2A and NR2B Subunits within the same Complex.

Cherubini, E. and Conti, F. (2001) *Trends. Neurosci.* **24,** 155-162. Generating diversity at GABAergic synapses.

Cherubini, E., Gaiarsa, J. L. and Ben-Ari, Y. (1991) *Trends. Neurosci.* **14**, 515-519. GABA: An Excitatory Transmitter in Early Postnatal Life.

Chiara, D. C., Trinidad, J. C., Wang, D., Ziebell, M. R., Sullivan, D. and Cohen, J. B. (2003) *Biochemistry.* **42**, 271-283. Identification of Amino Acids in the Nicotinic Acetylcholine Receptor Agonist Binding Site and Ion Channel Photolabeled by 4-[(3-Trifluoromethyl)-3H-Diazirin-3-yl]Benzoylcholine, a Novel Photoaffinity Antagonist.

Clontech MATCHMAKER Library User Manual

Clontech MATCHMAKER GAL4 Two-Hybrid System 3 and Libraries User Manual

Clontech Yeast Protocols Handbook.

Cohen, A. S., Lin, D. D., Quirk, G. L. and Coulter, D. A. (2003) *Eur. J. Neurosci.* **17**, 1607. Dentate Granule Cell $GABA_A$ Receptors in Epileptic Hippocampus: Enhanced Synaptic Efficacy and Altered Pharmacology.

Collinson, N., Kuenzi, F. M., Jarolimek, W., Maubach, K. A., Cothliff, R., Sur, C., Smith, A., Otu, F. M., Howell, O., Atack, J. R., McKernan, R. M., Seabrook, G. R., Dawson, G. R., Whiting, P. J. and Rosahl, T. W. (2002) *J. Neurosci.* **22**, 5572-5580. Enhanced Learning and Memory and Altered GABAergic Synaptic Transmission in Mice Lacking the α5 Subunit of the $GABA_A$ Receptor.

Colonna, T. E., Huynh, L. and Fambrough, D. M. (1997) *J. Biol. Chem.* **272**, 12366-12372. Subunit Interactions in the Na, K-ATPase Explored with the Yeast Two-Hybrid System.

Connolly, C. N., Krishek, B. J., McDonald, B. J., Smart, T. G. and Moss, S. J. (1996a) *J. Biol. Chem.* **271**, 89-96. Assembly and Cell Surface Expression of Heteromeric and Homomeric γ-Aminobutyric Acid Type A Receptors.

Connolly, C. N., Wooltorton, J. R. A., Smart, T. G. and Moss, S. J. (1996b) *Proc Natl. Acad. Sci. USA* **93**, 9899-9904. Subcellular Localization of γ-aminobutyric Acid Type A Receptors is Determined by Receptor β Subunits.

Connolly, C. N., Kittler, J. T., Thomas, P., Uren, J. M., Brandon, N. J., Smart, T. G. and Moss, S. J. (1999) *J. Biol. Chem.* **274**, 36565-36572. Cell Surface Stability of γ-Aminobutyric Acid Type A Receptors: Dependence on Protein Kinase C Activity and Subunit Composition.

Corringer, J-P., Le Novere, N. and Changeux. (2000) *Ann. Rev. Pharmacol. Toxicol.* **40**, 431-458. Nicotinic Receptors at the Amino Acid Level.

Creikinge, W. V. and Bayaert, R. (1999) *Biological Procedures Online.* **2**, 1-38. Yeast Two-Hybrid: State of the Art.

Cyr, D. M., Langer, T. and Douglas, M. G. (1994) *Trends Biol. Sci.* **19**, 176-181. DnaJ-Like Proteins: Molecular Chaperones and Specific Regulators of Hsp70.

Dalva, M. B., Takasu, M. A., Lin, M. Z., Shamah, S. M., Hu, L., Gale, N. W. and Greenberg, M. E. (2000) *Cell.* **103**, 945-956. EphB Receptors Interact with NMDA Receptors and Regulate Excitatory Synapse Formation.

Dang, C. V., Barrett, J., Villa Garcia, ., Resar, L. M. S., Kato, G. J. Fearon, E. R. (1991) *Moll. Cell. Biol.* **11**, 954-962. Intracellular Leucine Zipper Interactions Suggest c-Myc Hetero-Oligomerization.

Das, S., Sasaki, Y. F., Rothe, T., Premkumar, L. S., Conner, D. A., Rayudu, P. V., Cheung, W., Chen, H-S. V., Lipton, S. A. and Nakashi, N. (1998) *Nature.* **393**, 377-381. Increased NMDA Current and Spine Density in Mice Lacking the NMDA Receptor Subunit NR3A.

Davies, C. H., Starkey, S. J., Pozzo, M. F. and Collingridge, G. L. (1991) *Nature.* **349**, 609-611. $GABA_B$ Autoreceptors Regulate the Induction of LTP.

Davies, P. A., Hanna, M. C., Hales, T. G. and Kirkness, E. F. (1997) *Nature.* **385**, 820-823. Insensitivity to Anaesthetic Agents Conferred by a Class of $GABA_A$ Receptor Subunit.

Dong, H., O' Brien, R. J., Fung, E. T., Lanahan, A. A., Worley, P. F. and Huganir, R. l. (1997) *Nature.* **386**, 279-284. GRIP: A Synaptic PDZ Domain-Containing Protein that Interacts with AMPA Receptors.

Duggan, M. J. and Stephenson, F. A. (1990) *J. Biol. Chem.* **265**, 3831-3835. Biochemical Evidence for the Existence of γ-Aminobutyrate$_A$ Receptor Iso-oligomers.

Duggan, M. J., Pollard, S. and Stephenson, F. A. (1991) *J. Biol. Chem.* **266**, 24778-24784. Immunoaffinity Purification of $GABA_A$ Receptor α-Subunit Iso-Oligomers: Demonstration of Receptor Populations Containing $\alpha1\alpha2$, $\alpha1\alpha3$ and $\alpha2\alpha3$ Subunit Pairs.

Ehlers, M. D., Zhang, S., Bernhardt, J. P. and Huganir, R. L. (1996) *Cell.* **84**, 745-755. Inactivation of NMDA Receptors by Direct Interaction of Calmodulin with the NR1 Subunit.

Ehlers, M. D., Fung, E. T., O' Brien, R. J. and Huganir, R. L. (1998) *J. Neurosci.* **18**, 720-730. Splice Variant-Specific Interaction of the NMDA Receptor Subunit NR1 with Neuronal Intermediate Filaments.

Enz, R. and Cutting, G. R. (1998) *Vision Research.* **38**, 1431-1441. Molecular Composition of $GABA_C$ Receptors.

Esserich, C., Lorez, M., Benson, J. A., Frischy, J-M. Luscher, B. (1998) *Nat. Neurosci.* **1**, 563-571. Postsynaptic Clustering of Major $GABA_A$ receptor Subtypes Requires the $\gamma2$ Subunit and Gephyrin.

Farrar, S. J., Whiting, P. J., Bonnert, T. P. McKernan, R. M. (1999) *J. Biol. Chem.* **274**, 10100-10104. Stoichiometry of a Ligand-Gated Ion Channel Determined by Fluorescence Energy Transfer.

Fields, S. and Song, O-K. (1989) *Nature.* **340**, 245-246. A Novel Genetic System to Detect Protein-Protein Interactions.

Fields, S. and Sternglanz, R. (1994) *Trends. Genet.* **10**, 286-292. The Two-Hybrid System: an Assay for Protein-Protein Interactions.

Fritschy, J-M., Benke, D., Mertens, S., Oertel, W. H., Bach, T. and Mohler, H. (1992) *Proc. Natl. Acad. Sci. USA.* **89**, 6726-6730. Five Subunits of Type A γ-Aminobutyric Acid Receptors Identified in Neurones by Double and Triple Immunofluorescence Staining with Subunit Specific Antibodies.

Fritschy, J-M., Paysan, J., Enna, A. and Mohler, H. (1994) *J. Neurosci.* **14**, 5302-5324. Switch in the Expression of Rat $GABA_A$-Receptor Subtypes During Postnatal Development: An Immunohistochemical Study.

Fritschy, J.M. and Mohler, H. (1995) *J. Comp. Neurol.* **359**, 154–194. $GABA_A$ Receptor Heterogeneity in the Adult Rat Brain: Differential Regional and Cellular Distribution of Seven Major Subunits.

Fujita, M., Nagai, Y., Sawada, T. and Heese, K. (2004) *Mol. Cell. Biochem.* **258**, 183-189. Identification of rTid-1, the Rat Homologue of the Drosophila Tumor Suppressor l(2)tid Gene.

Gilbert, H. (1990) *Adv. Enzymol.* **63**, 69-172. Molecular and Cellular Aspects of Thiol-Disulphide Exchange.

Goldmakher, G. V. and Moss, R. L. (2000) *Brain Res.* **871**, 7-15. A Subset of Periglomerular Neurons in the Rat Accessory Olfactory Bulb May be Excited by GABA Through a Na^+-Dependent Mechanism.

Golemis, E. (2002) Protein-Protein Interactions. Cold Spring Harbour Press.

Gorrie, G. H., Vallis, Y., Stephenson, A., Whitfield, J., Browning, B., Smart, T. G. and Moss, S. J. (1997) *J. Neurosci.* **17**, 6587-6596. Assembly of $GABA_A$ Receptors Composed of $\alpha 1$ and $\beta 2$ Subunits in Both Cultured Neurons and Fibroblasts.

Green, W. N. and Claudio, T. (1993) *Cell. 74*, 57-69. Acetylcholine Receptor Assembly: Subunit Folding and Oligomerization Occur Sequentially.

Green, W. N. and Wanamaker, C. P. (1998) *J. Neurosci.* **18**, 5555-5564. Formation of the Nicotinic Acetylcholine Receptor Binding Sites.

Hackman, A., Wang, T-L., Guggino, W. B. and Cutting, G. R. (1998) *J. Neurochem.* **70**, 40-46. Sequences in the Amino Terminal of GABA ρ and $GABA_A$ Subunits Specify their Interaction *In Vivo*.

Hedblom, E. and Kirkness, E. F. (1997) *J. Biol. Chem.* **272**, 15346-15350. A Novel Class of $GABA_A$ Receptor Subunit in Tissues of the Reproductive System.

Harvey, R. J., Kim, H-C. and Darlison, M. G. (1993) *FEBS.* **331**, 211-216. Molecular Cloning Reveals the Existence of a Fourth γ Subunit of the Vertebrate Brain $GABA_A$ Receptor.

Heim, R. and Tsien, R. Y. (1996) *Curr. Biol.* **6**, 178-182. Engineering Green Fluorescent Protein for Improved Brightness, Longer Wavelengths and Fluorescence Resonance Energy Transfer.

Herring, D., Huang, R., Singh, M., Robinson, L. C., Dillon, G. H. Leidenheimer, N. J. (2003) *J. Biol. Chem.* **278**, 24046-24052. Constitutive $GABA_A$ Receptor Endocytosis is Dynamin-Mediated and Dependent on a Dileucine AP2 Adaptin-Binding Motif within the $\beta 2$ Subunit of the Receptor.

Im, W. B., Pregenezer, J. F., Binder, J. A., Dillon, G. H. and Alberts, G. L. (1995) *J. Biol Chem.* **270**, 26063-26066. Chloride Channel Expression with the Tandem Construct of α6-β2 $GABA_A$ Receptor Subunit Requires a Monomeric Subunit of α6 or γ2.

Imoto, K., Busch, C., Sakmann, B., Mishina, M., Konno, T., Nakai, J., Bujo, H., Mori, Y., Fukuda, K. and Numa, S. (1988) *Nature.* **335**, 645-648. Rings of Negatively Charged Amino Acids Determine the Acetylcholine Receptor Channel Conductance.

Iyer, S. P., Akimoto, Y. and Hart, G. W. (2003) *J. Biol. Chem.* **278**, 5399-5409. Identification and Cloning of a Novel Family of Coiled-Coil Domain Proteins that Interact with O-GlcNAc Transferase.

Jechlinger, M., Pelz, M., Tretter, V., Klausberger, T. and Sieghart, W. (1998) *J. Neurosci.* **18**(7), 2449-2457. Subunit Composition and Quantitative Importance of Heterooligomeric Receptors: $GABA_A$ Receptors Containing α6 Subunits.

Kanai, Y., Okada, Y., Tanaka, Y., Harada, A., Terada, S. and Hirokawa, N. (2000) *J. Neurosci.* **20**, 6374-6384. KIF5C, a Novel Neuronal Kinesin Enriched in Motor Neurons.

Kannenberg, K., Baur, R. Sigel, E. (1997) *J. Neurochem.* **68**, 1352-1360. Proteins Associated with α1-Subunit-Containing $GABA_A$ Receptors from Bovine Brain.

Kannenberg, K., Schaerer, M. T., Fuchs, K., Sieghart, W. and Sigel, E. (1999) *J. Biol. Chem.* 274, 21257-21264. A Novel Serine Kinase with Specificity for β3-Subunits Is Tightly Associate with $GABA_A$ Receptors.

Karlin, A. (2002) *Nat. Rev. Neurosci.* **3**, 102-114. Emerging Structure of the Nicotinic Acetylcholine Receptors.

Kaupmann, K., Huggel, K., Heid, J., Flor, P. J., Bischoff, S., Mickel, S. J., McMaster, G., Angst, C., Bittiger, H., Froestl, W. and Bettler, B. (1997) *Nature.* **386**, 239-246. Expression Cloning of $GABA_B$ Receptors Uncovers Similarity to Metabotropic Glutamate Receptors.

Kaupmann, K., Malitschek, B., Schuler, V., Heid, J., Froestl, W., Beck, P., Mosbacher, J., Bischoff, S., Kulik, A., Shigemoto, R., Karschin, A. and Bettler, B. (1998) *Nature.* **396**, 683-687. $GABA_B$-Receptor Subtypes Assemble into Functional Heteromeric Complexes.

Kaupmann, K., Schuler, V., Mosbacher, J., Bischoff, S., Bittiger, H., Heid, J., Froestl, W., Leonhard, S., Pfaff, T., Karschin, A. and Bettler, B. (1998) *Proc. Natl. Acad. Sci. USA.* **95**, 14991-14996. Human γ-Aminobutyric Acid Type B Receptors are Differentially Expressed and Regulate Inwardly Rectifying K^+ Channels.

Kelley, W. L. (1998) *Trends Biol. Sci.* **23**, 222-227. The J-Domain Family and the Recruitment of Chaperone Power.

Keegan, L. Gill, G. and Ptashne, M. (1986) *Science.* **231**, 699-704. Separation of DNA Binding from the Transcription-Activating Function of a Eukaryotic Regulatory Protein.

Kim, E., Cho, K-O., Rothschild, A. and Sheng, M. (1996) *Neuron.* **17**, 103-113. Heteromultimerisation and NMDA Receptor-Clustering Activity of Chapsyn-110, a Member of the PSD-95 Family of Proteins.

Kins, S., Betz, H. and Kirsch, J. (2000) *Nat. Neurosci.* **3**, 22-29. Collybistin, A Newly Identified Brain-Specific GEF, induces Submembrane Clustering of Gephyrin.

Kirkness, E. F. and Fraser, C. M. (1993) *J. Biol. Chem.* **268**, 4420-4428. A Strong Promoter is Located Between Alternative Exons of a Gene Encoding the Human γ-Aminobutyric Acid-Type A Receptor β3 Subunit (GABRB3).

Kirsch, J., Langosch, D., Prior, P., Littauer, U. Z., Schmitt, B. and Betz, H. (1991) *J. Biol. Chem.* **266**, 22242-22245. The 93-kDa Glycine Receptor-Associated Protein Binds to Tubulin.

Kirsch, J. and Betz, H. (1993) *Brain Res.* **621**, 301-310. Widespread Expression of Gephyrin, A Putative Glycine Receptor-Tubulin Linker Protein, in Rat Brain.

Kistler, J. and Stroud. (1981) *Proc. Natl. Acad. Sci. USA.* **78**, 3678-3682. Crystalline Arrays of Membrane-Bound Acetylcholine Receptor.

Kittler, J. T., Delmas, P., Jovanovic, J. N., Brown, D. A., Smart, T. G. and Moss, S. J. (2000) *J. Neurosci.* **20**, 7972-7977. Constitutive Endocytosis of $GABA_A$ Receptors by an Association with the Adaptin AP2 Complex Modulates Inhibitory Synaptic Currents in Hippocampal neurons.

Klausberger, T., Fuchs, K., Mayer, B., Ehya, N. and Sieghart, W. (2000) *J. Biol. Chem.* **275**, 8921-8928. $GABA_A$ Receptor Assembly: Identification and Structure Prediction of γ2 Sequences Forming the Subunit Contacts with α1 and β3 Subunits.

Klausberger, T., Ehya, N., Fuchs, K., Fuchs, T., Ebert, V., Sarto, I. And Sieghart, W. (2001a) *J. Biol. Chem.* **276**, 16024-16032. Detection and Binding Properties of $GABA_A$ Receptor Assembly Intermediates.

Klausberger, T., Sarto, I., Ehya, N., Fuchs, K., Furtmuller., Mayer, B., Huck, S. and Sieghart, W. (2001b) *J. Neurosci.* **21**, 9124-9133. Alternate Use of Distinct Intersubunit Contacts Controls $GABA_A$ Receptor Assembly and Stoichiometry.

Kleizen, B. and Braakman, I. (2004) *Curr. Opin. Cell. Biol.* **16**, 343-349. Protein Folding and Quality Control in the Endoplasmic Reticulum.

Korpi, E. R., Kuner, T., Kristo, P., Kohler, M., Herb, A., Luddens, H. and Seeburg, P. H. (1994) *J. Neurochem.* **63**, 1167-1170. Small N-Terminal Deletion by Splicing in Cerebellar α6 Subunit Abolishes $GABA_A$ Receptor Function.

Kneussel, M., Haverkamp, S., Fuhrmann, J. C., Wang, H., Wassle, H. and Olsen, R. W. (2000) *Proc. Acad. Natl. Sci. USA.* **97**, 8594-8599. The γ-Aminobutyric Acid Type A

Receptor ($GABA_AR$)-Associated Protein GABARAP Interacts with Gephyrin but is not Involved in Receptor Anchoring at the Synapse.

Kornau, H-C., Schenker, L. T., Kennedy, M. B. and Seeburg, P. H. (1995) *Science.* **269**, 1737-1740. Domain Interaction Between NMDA Receptor Subunits and the Postsynaptic Density Protein PSD-95.
Korpi, E. R., Kleingoor, C., Kettenmann, H. and Seeburg, P. H. (1993) *Nature.* **361**, 356-359. Benzodiazepine-Induced Motor Impairment Linked to Point Mutation in Cerebellar $GABA_A$ Receptor.

Korpi, E. R., Kuner, T., Kristo, P., Kohler, M., Herb, A., Luddens, H. and Seeburg, P. H. (1994) *J. Neurochem.* **63**, 1167-1170. Small N-Terminal Deletion by Splicing in Cerebellar α6 Subunit Abolishes $GABA_A$ Receptor Function.

Krupp, J. J., Vissel, B., Heinemann, S. F. and Westbrook, G. L. (1998) *Neuron.* **20**, 317-327. N-Terminal Domains in the NR2 Subunit Control Desensitization of NMDA Receptors.

Kucken, A. M., Wagner, D. A., Ward, P. R., Teissere, J. A., Boileau, A. J. and Czajkowski, C. (2000) *Mol. Pharmacol.* **57**, 932-939. Identification of Benzodiazepine Binding Site Residues in the γ2 Subunit of the γ-Aminobutyric $Acid_A$ Receptor.

Lau, L-F., Mammen, A., Ehlers, M. D., Kindler, S., Chung, W J., Garner, C. C. and Huganir, R. L. (1996) *J. Biol. Chem.* **271**, 21622-21628. Interaction of the N-Methyl-D-Aspartate Receptor Complex with a Novel Synapse-Associated Protein, SAP102.

Laurie, D. J., Wisden, W. and Seeburg, P. H. (1992) *J. Neurosci.* **12**, 4151-4172. The Distribution of 13 $GABA_A$ Receptor Subunit mRNAs in the Rat Brain. III. Embryonic and Postnatal Development.

Laurie, D. J., Seeburg, P. H. and Wisden, W. (1992) *J. Neurosci.* **12**, 1063-1076. Distribution of 13 $GABA_A$ Receptor Subunit mRNAs in the Rat Brain. II. Olfactory Bulb and Cerebellum.

Le Novere, N. and Changeux, J. P. (1999) *Nucleic Acids Res.* **27**, 340-342. The Ligand Gated Ion Channel Database.
Leonard, A. S., Davare, M. A., Horne, M. C., Garner, C. C. and Hell, J. W. (1998) *J. Biol. Chem.* **273**, 19518-19524. SAP97 is Associated with the α-Amino-3-Hydroxy-5-Methylisoxazole-4-Propionic Acid Receptor GluR1 Subunit.

Li, M. and De Blas, A. L. (1997) *J. Biol. Chem.* **272**, 16564-16569. Coexistence of Two β Subunit Isoforms in the same γ-Aminobutyric Acid Type A Receptor.

Li, F., Wan, Q., Pristupa, Z. B., Yu, X-M., Wang, Y. T. and Niznik, H. B. (2000) *Nature.* **403**, 274-280. Direct Protein-Protein Coupling Enables Cross-Talk Between Dopamine D5 and γ-Aminobutyric Acid A Receptors.

Li, Y., Chin, L-S., Levey, A. I. and Li, Lian. (2002) *J. Biol. Chem. 277*, 28212-28221. Huntingtin-Associated Protein1 Interacts with Hepatocyte Growth Factor-Regulated Tyrosine Kinase Substrate and Functions in Endosomal Trafficking.

Lin, J. W., Wyszynski, M., Madhavan, R., Sealock, R., Kim, J. U. and Sheng, M. (1998) *J. Neurosci.* **18**, 2017-2027. Yotiao, a Novel Protein of Neuromuscular Junction and Brain that Interacts with Specific Splice Variants of NMDA Receptor Subunit NR1.

Lund, A. H., Duch, M. and Pederson, F. S. (1996) *Nucleic Acids Res.* **24**, 800-801. Increased Cloning Efficiency by Temperature-cycle Ligation.

Ma, J. and Ptashne, M. (1987) *Cell.* **51**, 113-119. A New Class of Yeast Transcriptional Activators.
Macdonald, R. L. and Olsen, R. W. (1994) *Ann. Rev. Neurosci.* **17**, 569-620. $GABA_A$ Receptor Channels.

McCormack, A. L., Schieltz, D. M., Goode, B., Yang, S., Barnes, G., Drubin, D. and Yates III, J. R. (1997) *Anal. Chem.* **69**, 767-776. Direct Analysis and Identification of Proteins in Mixtures by LC/MS/MS and Database Searching at the Low-Femtomole Level.

McKernan, R. M., Quirk, K., Prince, R., Cox, P. A., Gillard, N. P. Ragan, C. I. and Whiting, P. (1991) *Neuron.* **7**(4), 667-676. $GABA_A$ Receptor Subtypes Immunopurified from Rat Brain with Alpha Subunit-Specific Antibodies Have Unique Pharmacological Properties.

McKernan, R. M and Whiting, P. J. (1996) *Trends. Neurosci.* **19**, 139-143. Which $GABA_A$-Receptor Subtypes Really Occur in the Brain?

Merlie, J. P. and Lindstrom, J. (1983) *Cell.* **34**, 747-757. Assembly in vivo of Mouse Muscle Acetylcholine Receptor: Identification of an α Subunit Species that may be an Assembly Intermediate.

Michelson, H. B. and Wong, R. K. S. (1991) *Science.* **253**, 1420-1423. Excitatory Synaptic Responses Mediated by $GABA_A$ Receptors in the Hippocampus.

Middleton, R. E. and Cohen, J. B. (1991) *Biochemistry.* **30**, 6987-6997. Mapping of the Acetylcholine Binding Site of the Nicotinic Acetylcholine Receptor: [3H]Nicotine as an Agonist Photoaffinity Label.

Misgeld, U., Deisz, R. A., Dodt, R. A. and Lux, H. D. (1986) *Science.* **232**, 1413-1415. The Role of Chloride Transport in Postsynaptic Inhibition of Hippocampal Neurons.

Mitra, R. D., Silva, C. M. and Youvan, D. C. (1996) *Gene.* **173**, 13-17. Fluorescence Resonance Energy Transfer Between Blue-Emitting and Red-Shifted Excitation Derivatives of the Green Fluorescence Protein.

Mitra, M., Wanamaker, C. P. and Green, W. N. (2001) *J. Neurosci.* **21**, 3000-3008. Rearrangement of Nicotinic Receptor α Subunits During Formation of the Ligand Binding Sites.

Mizukoshi, E., Suzuki, M., Loupatov, A., Uruno, T., Hayashi, H., Misono, T., Kaul, S. C., Wadhwa, R. and Imamura, T. (1999) *Biochem. J.* **343**, 461-466. Fibroblast Growth Factor-1 Interacts with the Glucose-Regulated Protein GRP/Mortalin.

Moransard, M., Borges, L. S., Willman, R., Marangi, P. A., Brenner, H. R., Ferns, M. J. and Fuhrer, C. (2003) *J. Biol. Chem.* **278**, 7350-7359. Agrin Regulates Rapsyn Interaction with Surface Acetylcholine Receptors, and this Underlies Cytoskeletal Anchoring and Clustering.

Nayeem, N., Green, T. P., Martin, I. L. and Barnard, E. A. (1994) *J. Neurochem.* **62**, 815-818. Quarternary Structure of the Native $GABA_A$ Receptor Determined by Electron Microscopic Image Analysis.

Nehring, R. B., Horikawa, H. P. M., El Far, O., Kneussel, M., Brandstatter, J. H., Stamm, S., Wischmeyer, E., Betz, H. and Karschin, A. (2000) *J. Biol. Chem.* **275**, 35185-35191. The Metabotropic $GABA_B$ Receptor Directly Interacts with the Activating Transcription Factor 4.

Newell, J. G. and Dunn, S. M. J. (2002) *J. Biol Chem.* **277**, 21423-21430. Functional Consequences of the Loss of High Affinity Agonist Binding to γ-Aminobutyric Acid Type A Receptors.

Nishimune, A., Isaac, J. T. R., Molnar, E., Noel, J., Nash, S. R., Tagaya, M., Collingridge, G. L., Nakanishi, S. and Henley, J. (1998) *Neuron.* **21**, 87-97. NSF Binding to GluR2 Regulates Synaptic Transmission.

Nishimura, A., Morita, M., Nishimura, Y. and Sugino, Y. (1990) *Nucleic Acids Res.* **18**, 6169. A Rapid and Highly Efficient Method for Preparation of Competent *Escherichia coli* Cells.

Nusser, Z., Sieghart, W. and Somogyi, P. (1998) *J. Neurosci.* **18**, 1693-1703. Segregation of different $GABA_A$ receptors to synaptic and extrasynaptic membranes of cerebellar granule cells.

Nymann-Andersen, J., Wang, H., Sawyer, G. W. and Olsen, R. W. (2002) *J. Neurochem.* **83**, 1164-1171. Interaction Between $GABA_A$ Receptor Subunit Intracellular Loops: Implications for Higher Order Complex Formation.

Ortells, M. O. and Lunt, G. G. (1995) *Trends. Neurosci.* **18**, 121-127. Evolutionary History of the Ligand-Gated Ion-Channel Superfamily of Receptors.

Osborne, M. A., Dalton, S. and Kochan, J. P. (1995) *BioTechnology.* **13**, 1474-1478. The Yeast Tribrid System-Genetic Detection of *trans*-phosphorylated ITAM-SH2-Interactions.

Ozenberger, B. A. and Young, K. H. (1995) *Mol. Endocrinol.* **9**, 1321-1329. Functional Interaction of Ligands and Receptors of the Hematopoietic Superfamily in Yeast.

Passafaro, M., Nakagawa, T., Sala, C. and Sheng, M. (2003) *Nature.* **424**, 677-681. Induction of Dendritic Spines by an Extracellular Domain of AMPA Receptor Subunit GluR2.

Pei, L., Lee, F. J. S., Moszczynska, A., Vukusic, B. and Liu, F. (2004) *J. Neurosci.* **24**, 1149-1158. Regulation of Dopamine D1 Receptor Function by Physical Interaction with the NMDA Receptors.

Pfeiffer, F., Graham, D. Betz, H. (1982) *J. Biol. Chem.* **257**, 9389-9393. Purification by Affinity Chromatography of the Glycine Receptor of Rat Spinal Cord.

Phillips, W. D., Kopta, C., Blount, P., Gardner, P. d., Steinbach, J. H. Merlie, J. P. (1991) *Science.* **251**, 568-570. Acetylcholine Receptor-Rich Membrane Domains Organised in Fibroblasts by Recombinant 43 kDa Protein.

Pirker, S., Schwarzer, C., Wieselthaler, A., Sieghart, W. and Sperk, G. (2000) *Neuroscience.* **101**, 815-850. $GABA_A$ Receptors: Immunocytochemical Distribution of 13 Subunits in the Adult Rat Brain.

Pollard, S., Duggan, M. J. and Stephenson, F. A. (1993) *J. Biol. Chem.* **268**, 3753-3757. Further Evidence for the Existence of α Subunit Heterogeneity within Discrete γ-Aminobutyric $Acid_A$ Receptor Subpopulations.

Pollard, S., Thompson, C. L. and Stephenson, F. A. (1995) *J. Biol. Chem.* **270**, 21285-21292. Quantitative Characterization of α1 and α1α6 Subunit-Containing Native $GABA_A$ Receptors of Adult Rat Cerebellum Demonstrates 2α Subunits Per Receptor Oligomer.

Pollard, S. and Stephenson, F. A. (1997) *Biochem. Soc. Trans.* **25**, 547S Characterisation of Novel β2 and β3 γ-Aminobutyric $Acid_A$ Receptor Antibodies.

Pritchett, D. B., Sontheimer, H., Shivers, B. D., Ymer, S., Kettenmann, H., Schofield, P. R. and Seeburg, P. H. (1989) *Nature.* **338,** 582-585. Importance of a Novel $GABA_A$ Receptor Subunit for Benzodiazepine Pharmacology.

Pritchett, D. B., Luddens, H. and Seeburg, P H. (1989) *Science.* **341**, 1389-1392. Type I and Type II $GABA_A$ Benzodiazepine Receptors Produced in Transfected Cells.

Pritchett, D. B. and Seeburg, P. H. (1991) *Proc. Natl. Acad. Sci. USA.* **88**, 1421-1425. γ-Aminobutyric Acid Type A Receptor Point Mutation Increases the Affinity of Compounds for the Benzodiazepine Site.

Qiagen Qiaprep and Qiaquick protocol handbooks

Roberts, E. and Frankel, S. (1950) *J. Biol. Chem.* **187**, 55-63. γ-Aminobutyric Acid in Brain: its Formation from Glutamic Acid.

Ramarao, M. K. and Cohen, J. B. (1998) *Proc. Natl. Acad. Sci. USA.* **95**, 4007-4012. Mechanism of Nicotinic Acetylcholine Receptor Cluster Formation by Rapsyn.

Rivera, C., Voipio, J., Payne, J. A., Ruusuvuori, E., Lahtinen, H., Lamsa, K., Pirvola, U., Saarma, M. and Kaila, K. (1999) *Nature.* **397**, 251-255. The K+/Cl- Co-Transporter KCC2 Renders GABA Hyperpolarising During Neuronal Maturation.

Ran, Q., Wadhwa, R., Kawai, R., Kaul, S. C., Sifers, R. N., Bick, R. J., Smith, J. R and Pereira-Smith, O. M. (2000) *Biochem. Biophys. Res. Commun.* **275**, 174-179. Extramitochondrial Localisation of Mortalin/mthsp70/PBP74/GRP75.

Rivera, C., Voipio, J., Payne, J. A., Ruusuvuori, E., Lahtinen, H., Lamsa, K., Pirvola, U., Saarma, M. and Kaila, K. (1999) *Nature.* **397**, 251-255. The K+/Cl- Co-Transporter KCC2 Renders GABA Hyperpolarising During Neuronal Maturation.

Ross, A. F., Green, W. N., Hartman, D. S. and Claudio, T. (1991) *J. Cell Biol.* **113**, 623-636. Efficiency of Acetylcholine Receptor Subunit and its Regulation by cAMP.

Rutter, A. R. and Stephenson, F. A. (2000) *J. Neurochem.* **75**, 2501-2510. Coexpression of Postsynaptic Density-95 Protein with NMDA Receptors Results in Enhanced Receptor Expression Together with a Decreased Sensitivity to L-Glutamate.

Sacht, G., Brigelius-Flohe, R., Kiess, M., Sztajer, H. and Flohe, L. (1999) *Biofactors.* **9**, 49-60. ATP-Sensitive Association of Mortalin with the IL-1 Receptor Type I.

Saedi, M. S., Conroy, W. G. and Lindstrom, J. (1991) *J. Cell Biol.* **112**, 1007-1015. Assembly of *Torpedo* Acetylcholine Receptors in *Xenopus* Oocytes.

Sanger, F., Nicklen, S. and Coulson, A. R. (1977) *Proc. Natl. Acad. Sci. USA.* **74**, 5463-5467 DNA Sequencing with Chain Terminating Inhibitors.

Saras, J. and Heldin, C-H. (1996) *Trends Biochem. Sci.* **21**, 455-458. PDZ Domains Bind Carboxy-Terminal Sequences of Target Proteins.

Sarkar, S., Pollack, B. P., Lin, K-T., Kotenko, S. V., Cook, J. r., Lewis, A. and Pestka, S. (2001) *J. Biol. Chem.* **276**, 49034-49042. hTid-1, a Human DnaJ Protein, Modulates the Interferon Signaling Pathway.

Sarto, I., Wabnegger, L., Dogl, E. and Sieghart, W. (2002) Neuropharmacology. **43**, 482-491. Homologous Sites of $GABA_A$ Receptor $\alpha 1$, $\beta 3$ and $\gamma 2$ Subunits are important for Assembly.

Sarto, I., Klausberger, T., Ehya, N., Mayer, B., Fuchs, K. and Sieghart, W. (2002) *J. Biol. Chem.* **277**, 30656-30664. A Novel Site on $\gamma 3$ Subunits Important for Assembly of $GABA_A$ Receptors.

Saxena, N. C., MacDonald, R. L. (1996) *Mol. Pharmacol.* **49**, 567-579. Properties of Putative Cerebellar γ-Aminobutyric $Acid_A$ Receptor Isoforms.

Schaerer, M. T., Kannenberg, K., Hunziker, P., Baumann, S. W. and Sigel, E. (2001) *J. Biol. Chem.* **276**, 26597-26604. Interaction Between $GABA_A$ Receptor β Subunit and the Multifunctional Protein gC1q-R.

Schwaller, M., Wilkinson, B. and Gilbert, H. F. (2003) *J. Biol. Chem.* **278**, 7154-7159. Reduction/Reoxidation Cycles Contribute to Catalysis of Disulphide Isomerization by Protein Disulphide Isomerase.

Schwarzer, C., Tsunashima, K., Wanzenbock, C., Fuchs, K., Sieghart, W. and Sperk, G. (1997) *Neuroscience.* **80**, 1001-1017. $GABA_A$ Receptor Subunits in the Rat Hippocampus II: Altered Distribution in Kainic Acid-Induced Temporal Lobe Epilepsy.

SenGupta, D. J., Zhang, B., Kraemer, B., Pochart, P., Fields, S. and Wickens, M. (1996) *Proc. Natl. Acad. Sci. USA.* **93**, 8496-8501. A Three-Hybrid System to Detect RNA-Protein Interactions *In Vivo.*

Setou, M., Seog, D-H., Tanaka, Y., Kanai, Y., Takei, Y., Kawagishi, M. and Hirokawa, N. (2002) *Nature.* **417**, 83-87. Glutamate-Receptor-Interacting Protein GRIP1 Directly Steers Kinesin to Dendrites.

Shivers, B. D., Killisch, I., Sprengel, R., Sontheimer, H., Kohler, M., Schofield, P. R. and Seeburg, P. H. (1989) *Neuron.* **3,** 327-337. Two novel $GABA_A$ receptor subunits exist in distinct neuronal subpopulations.

Sieghart, W. (2000) *Trends Pharmacol. Sci.* **21**, 411-413. Unraveling the Function of $GABA_A$ Receptor Subtypes.

Smit, A. B., Syed, N. I., Schaap, D., van Minnen, J., Klumperman, J., Kits, K. S., Lodder, H., van der Schors, R. C., van Elk, R., Sorgedrager, B., Brejc, K., Sixma, T. K. and Geraerts, W. P. M. (2001) *Nature.* **411**, 261-268. A Glial-Derived Acetylcholine-Binding Protein that Modulates Synaptic Transmission.

Smith, G. B. and Olsen, R. W. (1994) *J. Biol. Chem.* **269**, 20380-20387. Identification of a [3H]Muscimol Photoaffinity Substrate Bovine γ-Aminobutyric $Acid_A$ Receptor α Subunit.

Sobhanifar, S. (2003) *BioTeach Journal.* **1**, 81-87. Yeast Two Hybrid Assay: A Fishing Tale

Srinivasan, S., Nichols, C. J., Lawless, G. M., Olsen, R. W. and Tobin, A. J. (1999) *J. Biol. Chem.* **274**, 26633-26638. Two Invariant Tryptophans on the α1 Subunit Define Domains Necessary for $GABA_A$ Receptor Assembly.

Staley, K. J., Soldo, B. L. and Proctor, W. R. (1995) *Science.* **269**, 977-981. Ionic Mechanisms of Neuronal Excitation by Inhibitory $GABA_A$ Receptors.

Staudinger, J., Zhou., Burgess, R., Elledge, S. J. and Olson, E. N. (1995) *J. Cell Biol.* **128**, 263-271. PICK1: A Perinuclear Binding Protein and Substrate for Protein Kinase C Isolated by the Yeast Two-Hybrid System.

Stephenson, F. A., Duggan, M. J. and Pollard, S. (1990) *J. Biol. Chem.* **265**, 21160-21165. The γ2 Subunit is an Integral Component of the γ-Aminobutyric $Acid_A$ Receptor but the α1 Polypeptide is the Principal Site of the Agonist Benzodiazepine Photoaffinity Labelling Reaction.

Stephenson, F. A. (1995) *Biochem. J.* **310**, 1-9. The $GABA_A$ Receptors.

Stephenson, F. A. (2001) *Curr. Drug Targets.* **2**, 233-239. Subunit Characterisation of NMDA Receptors.

Stowers, R. S., Megeath, L. J., Gorska-Andrzejak, J., Meinertzhagen, I. A. and Schwarz, T. L. (2002) *Neuron.* **36**, 1063-1077. Axonal Transport of Mitochondria to Synapses Depends on Milton, a Novel *Drosophila* Protein.

Stratagene CytoTrap Vector Kit Instruction Manual.

Sumikawa, K. and Gehle. (1992) *J. Biol. Chem.* **267**, 6286-6290. Assembly of Mutant Subunits of the Nicotinic Acetylcholine Receptor Lacking the Conserved Disulphide Loop Structure.

Sur, C., Fresu, L., Howell, O., McKernan, R. M. and Atack, J. R. (1999a) *Brain Res.* **822**, 265-270. Autoradiographic Localisation of α5 Subunit-Containing $GABA_A$ Receptors in Rat Brain.

Sur, C., Farrar, S. J., Kerby, J., Whiting, P. J., Atack, J. R. and McKernan, R. M. (1999b) *Mol. Pharmacol.* **56**, 110-115. Preferential Coassembly of α4 and δ Subunits of the γ-Aminobutyric $Acid_A$ Receptor in Rat Thalamus.

Syken, J., De-Medina, T. and Munger, K. (1999) *Proc. Acad. Natl. Sci. USA.* **96**, 8499-8504. *TID1*, a Human Homologue of the *Drosophila* Tumor Suppressor l(2)tid, Encodes Two Mitochondrial Modulators of Apoptosis with Opposing Functions.

Taylor, P., Thomas, P., Gorrie, G., Connolly, C., Smart, T. and Moss, S. J. (1999) *J. Neurosci.* **19**, 6360–6371. Identification of Amino Acids Residues within $GABA_A$ Receptor β Subunits which Mediate Both Homomeric and Heteromeric Receptor Expression.

Taylor, P. M., Connolly, C. N., Kittler, J. T., Gorrie, G. H., Hosie, A., Smart, T. G. and Moss, S. J. (2000) *J. Neurosci.* **20**, 1297-1306. Identification of Residues within $GABA_A$ Receptor α Subunits that Mediate Specific Assembly with Receptor β Subunits.

Teissere, J. A. and Czajkowski, C. (2001) *J. Neurosci.* **21**, 4977-4986. A β-Strand in the γ2 Subunit Lines the Benzodiazepine Binding Site of the $GABA_A$ Receptor: Structural Rearrangements Detected During Channel Gating.

Torres, R., Firestein, B. L., Dong, H., Staudinger, J., Olson, E. N., Huganir, R. L., Bredt, D. S., Gale, N. W. and Yancopoulos, G. D. (1998) *Neuron.* **21**, 1453-1463. PDZ Proteins Bind, Cluster, and Synaptically Colocalise with Eph Receptors and their Ephrin Ligands.

Tretter, V., Ehya, N., Fuchs, K. and Sieghart, W. (1997) *J. Neurosci.* **17**, 2728-2737. Stoichiometry and Assembly of a Recombinant $GABA_A$ Receptor Subtype.

Trudell, J. R. (2002) *Biochemica et Biophysica Acta.* **1565**, 91-96. Unique Assignment of Inter-Subunit Association in $GABA_A$ α1β3γ2 Receptors Determined by Molecular Modeling.

Tsai, M-Y., Morfini, G., Szebenyi, G. and Brady, S. T. (2000) *Mol. Biol. Cell.* **11**, 2161-2173. Release of Kinesin from Vesicles by hsc70 and Regulation of Fast Axonal Transport.

Udenfriend, S. (1950) *J. Biol. Chem.* **187**, 65-69 . Identification of γ-Aminobutyric Acid in Brain by the Isotope Derivative Method.

Vallejo, C. G. and Serrano, R. (1989) *Yeast.* **5**, 307-319. Physiology of Mutants with Reduced Expression of Plasma Membrane H^+-ATPase.

Vasavada, H. A., Ganguly, S., Germino, F. J., Wang, Z. X. and Weissman, S. M. (1991) *Proc. Acad. Natl. Sci. USA.* **88,** 10686-10690,. A Contingent Replication Assay for the Detection of Protein-Protein Interactions in Animal Cells.

Verhey, K. J. and Rapaport, T. A. (2001) *Trends Biochem. Sci.* **26**, 545-549. Kinesin Carries the Signal.

Vidal, M., Brachmann, R. K., Fattaey, A., Harlow, E. and Boeke, J. D. (1996a) *Proc. Acad. Natl. Sci. USA.* **93**, 10315-10320. Reverse Two-Hybrid and One-Hybrid Systems to Detect Dissociations of Protein-Protein and DNA-Protein Interactions.

Vidal, M., Braun, P., Chen, E., Boeke, J. D., and Harlow, E. (1996b) *Proc. Acad. Natl. Sci. USA.* **93**, 10321-10326. Genetic Characterization of a Mammalian Protein-Protein Interaction Domain by Using a Yeast Reverse Two-Hybrid System.

Wadhwa, R., Takano, S., Robert, M., Yoshida, A., Nomura, H., Reddel, R. R., Mitsui, Y. and Kaul, S. C. (1998) *J. Biol. Chem.* **273**, 29586-29591. Inactivation of Tumor Suppressor p53 by Mot-2, a Hsp70 Family Member.

Wadhwa, R., Taira, K., Kaul, S. C. (2002) *Cell Stress Chaperones.* **7**, 309-316. An Hsp70 Family Chaperone, Mortalin/mthsp70/PBP74.Grp75: What, When and Where?

Wagner, D. A. and Czajkowski, C. (2001) *J. Neurosci.* **21**, 67-74. Structure and Dynamics of the GABA Binding Pocket: A Narrowing Cleft that Constricts During Activation.

Wallace, R.B. Shaffer, J. Murphy, R.F. Bonner, J. Hirose, T. Itakura, K. (1979) *Nucleic Acids Res.* **6**, 3543-6357. Hybridization of Synthetic Oligodeoxyribonucleotides to Phi Chi 174 DNA: the effect of single base pair mismatch.

Wang, M. and Reed, R. R. (1993) *Nature.* **364**, 121-126. Molecular Cloning of the Olfactory Neuronal Transcription Factor Olf-1 by Genetic Selection in Yeast.

Wang, Z-Z., Mathias, A., Gautam, M. and Hall, Z. W. (1999) *J. Neurosci.* **19**, 1998-2007. Metabolic Stabilisation of Muscle Nicotinic Acetylcholine Receptor by Rapsyn.

Wang, H., Bedford, F. K., Brandon, N. J., Moss, S. J. and Olsen, R. W. (1999) *Nature.* **397**, 69-72. $GABA_A$-Receptor-Associated Protein Links $GABA_A$ Receptors and the Cytoskeleton.

Wang, H. Olsen, R. W. (2000) *J. Neurochem.* **75**, 644-655. Binding of the $GABA_A$ Receptor-Associated Protein (GABARAP) to Microtubules and Microfilaments Suggests Involvement of the Cytoskeleton in GABARAP-$GABA_A$ Receptor Interaction.

Wieland, H. A., Luddens, H. and Seeburg, P. H. (1992) *J. Biol. Chem.* **267**, 1426-1429. A Single Histidine in $GABA_A$ Receptors is Essential for Benzodiazepine Agonist Binding.

Wieland, H. A. and Luddens, H. (1994) *J. Med. Chem.* **37**, 4576-4580. Four Amino Acid Exchanges Convert a Diazepam-Insensitive, Inverse Agonist-Preferring $GABA_A$ Receptor into a Diazepam-Preferring $GABA_A$ Receptor.

Whiting, P., McKernan, R. M. and Iversen, L. L. (1990) *Proc. Natl. Acad. Sci. USA.* **87**, 9966-9970. Another Mechanism for Creating Diversity in γ-Aminobutyrate Type A Receptors: RNA Splicing Directs Expression of Two Forms of γ2 Subunit, One of which Contains a Protein Kinase C Phosphorylation Site.

Wisden, W., Laurie, D. J., Monyer, H. and Seeburg, P. H. (1992) *J. Neurosci.* **12**, 1040-1062. The Distribution of 13 $GABA_A$ Receptor Subunit mRNAs in the Rat Brain. I. Telencephalon, Diencephalon, Mesencephalon.

Wyszynski, M., Kharazia, V., Shanghvi, R., Rao, A., Beggs, A. H., Craig, A. M., Weinberg, R. and Sheng, M (1998) *J. Neurosci.* **18**, 1383-1392. Differential Regional Expression and Ultrastructural Localisation of α-Actinin-2, a Putative NMDA Receptor-Anchoring Protein, in Rat Brain.

Xia, J., Zhang, X., Staudinger, J. and Huganir, R. L. (1999) *Neuron.* **22**, 179-187. Clustering of AMPA Receptors by the Synaptic PDZ Domain-Containing Protein PICK1.

Xu, J., Yu, W., Jan, Y. N., Jan, L. Y. and Li, M. (1995) *J. Biol. Chem.* **270**, 24761-24768. Assembly of Voltage-Gated Potassium Channels.

Yamada, Y., Chochi, Y., Takamiya, K., Sobue, K. and Inui, M. (1999) *J. Biol. Chem.* **274**, 6647-6652. Modulation of the Channel Activity of the ε2/ξ1-Subtype N-Methyl-D-Aspartate Receptor by PSD-95.

Yates III, J. R. (2000) *Trends. Genet.* **16**, 5-8. Mass Spectrometry from Genomics to Proteomics.

Ymer, S., Draguhn, A., Wisden, W., Werner, P., Keinanen, K., Schofield, P. R. and Seeburg, P. H. (1990) *EMBO J*, **9**, 3261-3267. Structural and Functional Characterization of the γ1 Subunit of $GABA_A$/Benzodiazepine Receptors.

List of Publications

Posters

Brickley, K., Beck, M., Wilkinson, H. L., Sharma, S., Smith, M. J., Chazot, P. L., Pollard, S. and Stephenson, F. A.
Identification, Molecular Cloning, and Characterization of a Novel $GABA_A$ Receptor-Associated Protein, GRIF-1.
FENS Abstr. Vol 1, A078.5, 2002

Smith, M. J., Beck, M. and Stephenson, F. A.
British Neurosci. Assoc. Abstr. (2003) 17, p26.12.
Can the Yeast Two-Hybrid System be used to Study Assembly Domains of $GABA_A$ Receptor Subunits?

Smith, M. J., Beck, M., Brickley, K. and Stephenson, F. A.
Society for Neuroscience Program No. 569.3, 2003 Abstract Viewer an Itinerary Planner.
Washington, DC: Society for Neuroscience, 2003. Online
Does KIAA1042, a Member of the GRIF-1, Coiled-Coil Novel Gene Family, Associate with $GABA_A$ Receptors?

Research articles

Beck, M., Brickley, K., Wilkinson, H. L., Sharma, S., Smith, M., Chazot, P. L., Pollard, S. and Stephenson, F. A. (2002) *J. Biol. Chem.* **277**, 30079-30090. Identification, Molecular Cloning, and Characterization of a Novel $GABA_A$ Receptor-Associated Protein, GRIF-1.

Brickley, K., Smith, M. J., Beck, M. and Stephenson, F. A. GRIF-1 and KIAA1042, Members of a Novel Gene Family of Coiled-Coil Domain Proteins, Associate *in Vivo* and *in Vitro* with Kinesin (manuscript in preparation)

IDENTIFICATION, MOLECULAR CLONING AND CHARACTERIZATION OF A NOVEL GABA$_A$ RECEPTOR ASSOCIATED PROTEIN, GRIF-1

Kieran Brickley Mike Beck Helen Wilkinson Seema Sharma Miriam J. Smith Paul L. Chazot Simon Pollard

F. Anne Stephenson

School of Pharmacy, University of London, 29/39 Brunswick Square, London, WC1N 1AX, UK.

INTRODUCTION

GABA$_A$ receptors, major mediators of inhibitory neurotransmission in the central nervous system, are localized predominantly in the post-synaptic membrane. Compared to excitatory synapses, there is a paucity of information available regarding the trafficking, clustering and anchoring of GABA$_A$ receptors at synaptic sites. It has been shown that GABA$_A$ receptor β subunits selectively target assembled receptor complexes to distinct subcellular locations (1). This suggests that β subunits may be pivotal for appropriate cell surface receptor expression. In adult brain, of the β subunits, β2 and β3 are the most abundant. Therefore, we used the GABA$_A$ receptor β2 intracellular loop (β2-IL) as a bait in a yeast two-hybrid screen to identify GABA$_A$ receptor-associated proteins. We report here the cloning and characterization of a novel protein, GRIF-1, GABA$_A$ receptor interacting factor, that specifically associates with β2 subunits (2).

RESULTS

TABLE 1 A summary of the specificity of the GRIF-1/GABA$_A$ receptor subunit interactions in the yeast two-hybrid assay

GAL4 Binding domain fusion construct	Activation domain construct	HIS3 ARE2 Lac2 MEL1 reporter gene activities	Lac Z activity (%)
pAS2-1α1-IL	pGAD10GRIF-1$_{b-633}$	–	ND
pAS2-1β1-IL	pGAD10GRIF-1$_{b-633}$	–	ND
pAS2-1β2-IL	pGAD10GRIF-1$_{b-633}$	+	13 ± 0.4 (n=3)
pAS2-1β3-IL	pGAD10GRIF-1$_{b-633}$	–	ND
pAS2-1β2-TM-IL/TM	pGAD10GRIF-1$_{b-633}$	–	ND
pAS2-1β2-IL/TM4	pGAD10GRIF-1$_{b-633}$	–	ND
pAS2-1γ2-IL	pGAD10GRIF-1$_{b-633}$	–	ND
pAS2-1β2-IL	pGAD10GRIF-1$_{b-633}$	+	12 ± 0.4 (n=3)
pAS2-1β2-IL	pGAD7RIAA0549$_{full}$	+	14 ± 0.4 (n=3)
pAS2-1β2-IL	pGAD10RIAA0549$_{full}$	–	ND
–	pGAD10GRIF-1$_{b-633}$	–	ND
pVA3-1	pGAD10GRIF-1$_{b-633}$	–	ND
pVA3-1	pTD1-1	+++	100
–	pSE-1	+++	100

The yeast strain AH109 was co-transformed with bait and fish constructs and transformants grown on -W, -L, -H, -Ade (i.e. SD- 4) plates. -, +, +++, relative measure of colony growth; β-galactosidase activity was measured by filter lift assay and Mel 1 activity by growth on SD-4 plates with agarose X-α Gal overlay. The strength of the bait and fish interactions are expressed as a percentage of wild-type Gal4 protein transformants.

FIGURE 1 The deduced amino acid sequence of GRIF-1 aligned with the human orthologue KIAA0549/ALS2CR3

GRIF-1$_{b-633}$ was identified as a partial cDNA encoding a novel GABA$_A$ receptor β2 subunit interacting clone from a library screen of 1.5 x 10^6 independent transformants. The full length sequence was determined by 5' and 3' RACE. Amino acids identical between rat GRIF-1 and the human orthologue KIAA0549/ALS2CR3 are shown as •; sites of consensus sequences for protein kinase A and tyrosine kinase are shown as ▼ and ❖, respectively. The hatched areas show the position of two predicted coiled-coil regions. The C-terminal proline-rich region is marked with a round-edged rectangle. Grey open rectangles indicate the position of two regions that are highly conserved among members of the GRIF-1 family. The GenBank accesion number for GRIF-1 is AJ288898

FIGURE 2 Tissue distribution of GRIF-1a mRNA and GRIF-1a protein

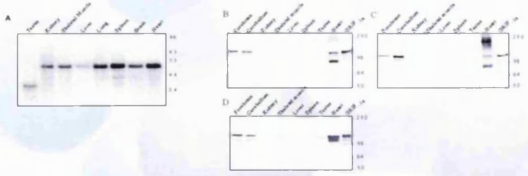

A is a northern blot probed with [^{32}P] GRIF-1$_{b-633}$ revealing a major transcript of 6.2 kb in all tissues except testes. B, C and D are immunoblots of P1 (nuclear), P2 (membrane) and S (soluble) fractions respectively. Blots were probed with affinity-purified anti-GRIF-1$_{b-633}$ antibodies. Major immunoreactive bands with M$_r$s 115 000 and 106 000 were found in brain, heart and skeletal muscle.

FIGURE 3 Demonstration of binding of native GABA$_A$ receptor α1 and β2 subunits to GRIF-1$_{b-633}$ using immobilized GRIF-1$_{b-611}$ affinity chromatography purification

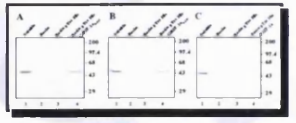

Triton X-100 extracts of P2 membrane fractions from rat brain were incubated with either Ni^{2+} agarose, pTrcHis-Ni^{2+} agarose or pTrcHisGRIF-1$_{b-633}$-Ni^{2+} agarose and the resultant agarose pellets analyzed by immunoblotting. A, probing with anti-GABA$_A$ receptor β2 381-395; B, anti-GABA$_A$ receptor α1 413-429 and C, anti-neuron specific enolase antibodies. It can be seen that GRIF-1$_{b-633}$-Ni^{2+} agarose specifically precipitates both α1 and β2 subunit immunoreactivities

FIGURE 4 Localization of GRIF-1 and GABA$_A$ receptor β2 subunits in HEK 293 cells transfected with GRIF-1a$_{FLAG}$ and α1β2γ2 GABA$_A$ receptors

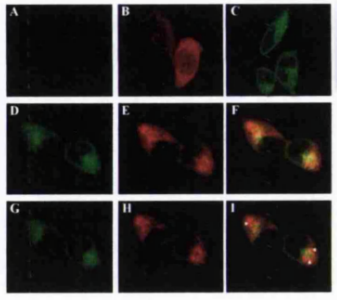

A, untransfected cells; B, transfected with GRIF-1a$_{FLAG}$; C, transfected with GABA$_A$ receptor α1β2γ2 subunits; D-I transfected with both GRIF-1a$_{FLAG}$ and GABA$_A$ receptor α1β2γ2 subunits. A, B probed with affinity-purified anti-GRIF-1$_{b-633}$ antibodies; C, probed with anti-GABA$_A$ receptor β2 subunit monoclonal antibody; D - I probed with both affinity-purified anti-GRIF-1$_{b-633}$ antibodies and the anti-GABA$_A$ receptor β2 subunit monoclonal antibody. A-F are projections of numerous confocal planes. G, H and I are single planes from the composites in D, E and F respectively. Arrow points indicate yellow colour where GRIF and β2 subunits co-localize.

FIGURE 5 Co-association of GRIF-1 and GABA$_A$ receptor β2 subunits in HEK 293 cells transfected with GRIF-1a$_{FLAG}$ and GABA$_A$ receptor β2 subunits as shown by immunoprecipitation

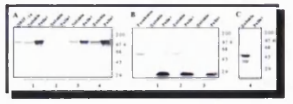

HEK 293 cells were transfected with either GRIF-1$_{FLAG}$ + GABA$_A$ receptor β2 subunit (1); GABA$_A$ receptor β2 alone (2); GRIF-1$_{FLAG}$ alone (3) or GRIF-1a$_{FLAG}$ + GABA$_A$ receptor α1 subunit (4). Immunoprecipitation assays with anti-FLAG agarose were carried out on detergent extracts of the various transfected cells and the resultant immune pellets analyzed by immunoblotting. A, probed with affinity-purified anti-GRIF-1$_{b-633}$; B, with anti-GABA$_A$ receptor β2 381-395 subunit and C, with anti-GABA$_A$ receptor α1 1-15 subunit antibodies. It is seen that GRIF-1$_{FLAG}$ specifically precipitated GABA$_A$ receptor β2 subunit immunoreactivity.

FIGURE 6 Schematic diagram showing the interaction between GRIF-1$_{b-633}$ and GABA$_A$ receptor β2-IL constructs and between GABA$_A$ receptor β2-IL and truncated GRIF-1 constructs using the yeast two-hybrid assay

CONCLUSIONS

- GRIF-1a, identified as interacting with the GABA$_A$ receptor β2-IL in a yeast two-hybrid screen, is a novel, soluble, 913 amino acid, M$_r$ 102 kDa protein. GRIF-1 exists in two splice forms, GRIF-1a and a C-terminal truncated form, GRIF-1b, with 672 amino acids.
- GRIF-1 mRNA has a wide tissue distribution with a major transcript size of 6.2 kb. GRIF-1 protein was detected only in excitable tissues.
- Co-expression of GRIF-1a and α1β2γ2 GABA$_A$ receptors in mammalian cells revealed some co-localization in the cell cytoplasm.
- Anti-FLAG agarose specifically precipitated GRIF-1$_{FLAG}$ and GABA$_A$ receptor β2 subunits from HEK 293 cells co-expressing GRIF-1$_{FLAG}$ and GABA$_A$ receptor β2 subunits.
- *In vitro* protein interactions demonstrated an association between GRIF-1$_{b-633}$ and assembled GABA$_A$ receptors.
- Amino acid similarities with Huntingtin associated protein suggest that GRIF-1 may fulfil a role in the transport or targeting of β2 subunit-containing GABA$_A$ receptors to the post-synaptic membrane of inhibitory synapse.

ACKNOWLEDGEMENTS

This work was supported by the BBSRC (UK). We thank Professor T Nagase, Kasuza Research Institute, Chiba, Japan for the gift of the partial KIAA0549 cDNA.

REFERENCES

1. Connolly, C.N., Wooltorton, J.R.A., Smart, T.G. & Moss, S.J. (1996) Proc. Natl. Acad. Sci. USA 93: 9899-9904. Subcellular localization of γ-aminobutyric acid type A receptors is determined by receptor β subunits
2. Beck, M., Brickley, K., Wilkinson, H.L., Sharma, S., Smith, M. J., Chazot, P.L., Pollard, S. & Stephenson, F.A. (2002) J. Biol. Chem. 277: 30079-30090. Identification, molecular cloning and characterization of a novel GABA$_A$ receptor-associated protein, GRIF-1.

CAN THE YEAST TWO-HYBRID SYSTEM BE USED TO STUDY ASSEMBLY DOMAINS OF $GABA_A$ RECEPTOR SUBUNITS?

Miriam J. Smith, Mike Beck and F. Anne Stephenson

School of Pharmacy, University of London, 29/39 Brunswick Square, London, WC1N 1AX, UK.

INTRODUCTION

The 16 γ-aminobutyric acid type A ($GABA_A$) receptor subunits found in the mammalian central nervous system, α1-6, β1-3, γ1-3, δ, ϵ, θ and π, give rise to potentially 16^5 receptor subtypes using all possible pentameric permutations. Relatively few of these combinations are actually found *in vivo*. Since multiple receptor subunits are often expressed at the same time in certain neurons, there must be mechanisms in the assembly process, other than transcriptional control, that regulate $GABA_A$ receptor subunit composition. Identifying assembly boxes in $GABA_A$ receptor subunits that dictate which subunits will associate may give an insight into the processes controlling receptor diversity. Assembly domains in K^+ channels[1] and the Na^+/K^+ ATPase[2] have been successfully studied using the yeast two-hybrid system offering an alternative approach to identify these sequences. Such an approach should be feasible for $GABA_A$ receptors since the soluble acetylcholine binding protein (AChBP)[3], the structural equivalent to the N-terminal domain of nicotinic acetylcholine receptors, is able to co-assemble to form a pentameric homo-oligomer i.e., assembly of N-terminal regions in the absence of transmembrane domains. Further, the N-terminal portions of $GABA_A$ receptor subunits have been implicated in receptor assembly from studies involving the expression of different combinations of full-length and truncated subunits in mammalian cells[4].

The aim of this study was to test the validity of the yeast two-hybrid system in the delineation of assembly motifs in $GABA_A$ receptor subunit N-terminal domains. The α1 and β2 subunit extracellular N-terminals were chosen for initial studies as they, together with the γ2 subunit, form the most abundant $GABA_A$ receptor subtype in adult brain.

A B

Figure 1: A. Typical $GABA_A$ receptor subunit topology. B. A model of the most abundant $GABA_A$ receptor subtype expressed in mammalian brain showing the predicted subunit stoichiometry and arrangement.

THE GAL 4 YEAST TWO-HYBRID SYSTEM

The $GABA_A$ receptor N-terminal sequences α1(1-224) and β2(1-220) were amplified by PCR from adult rat brain cDNA using specific oligonucleotide primers. The PCR products were cloned in-frame into the GAL4 plasmids pGADT7 (fish) and pGBKT7 (bait), to generate the fusion constructs pGADT7α1(1-224), pGADT7β2(1-220), pGBKT7α1(1-224) and pGBKT7β2(1-220). Combinations of α1(1-224) and β2(1-220) were co-transformed into the yeast strain AH109. Negative controls were empty fish or bait vectors co-transformed with α1(1-224) or β2(1-220) constructs. The $GABA_A$ receptor interacting factor (GRIF-1)[5] was co-transformed with the $GABA_A$ receptor β2 subunit intracellular loop as a positive control. Table 1 shows the results from n=3 independent co-transformations.

Table 1: $GABA_A$ receptor subunit N-terminal domain interactions in the GAL4 two-hybrid system

Fish	Bait	Selection Media Lacking W/L/H/Ade	β-Galactosidase Activity
pGADT7α1 (1-224)	pGBKT7β2 (1-220)	(+)	✓
pGADT7β2 (1-220)	pGBKT7α1 (1-224)	+	✓
pGADT7α1 (1-224)	pGBKT7α1 (1-224)	(+)	✓
pGADT7β2 (1-220)	pGBKT7β2 (1-220)	++	✓
pGADT7α1 (1-224)	pGBKT7-	+	✓
pGADT7β2 (1-220)	pGBKT7-	++	✓
pGADT7-	pGBKT7α1 (1-224)	-	×
pGADT7-	pGBKT7β2 (1-220)	-	×
pGADT7-	pGBKT7-	-	×
pGAD10GRIF-1(8-633)	pAS2-1β2-IL(303-427)	+	✓

Key: (+), +, ++, represent relative colony growth. ✓= β-galactosidase activity. × = no β-galactosidase activity. W = tryptophan, L= leucine, H = histidine, Ade = adenine

THE MODIFIED LEX A YEAST TWO-HYBRID SYSTEM

Since it was observed that the pGADT7α1(1-224) and pGADT7β2(1-220) sequences auto-activated reporter gene activity when co-transformed with an empty bait vector, an alternative yeast two-hybrid system was tested. The modified LexA system works on the same principle as the GAL4 system, except that it uses the prokaryotic LexA transcription factor (TF) rather than the eukaryotic GAL4 TF and hence, a different transcription apparatus. The $GABA_A$ receptor N-terminal sequences α1(1-224) and β2(1-220) were sub-cloned into the modified LexA plasmids pGADT7 (fish) and pMBL33 (bait) to generate the fusion constructs pGADT7α1(1-224), pGADT7β2(1-220), pMBL33α1(1-224) and pMBL33β2(1-220). Combinations of α1(1-224) and β2(1-220) constructs were co-transformed into the yeast strain, L40, together with positive and negative controls, as above for the GAL4 system. Table 2 shows the results from n=3 independent co-transformations.

Table 2: $GABA_A$ receptor subunit N-terminal domain interactions in the modified LexA two-hybrid system

Fish	Bait	Selection Media Lacking W /L /H	β-Galactosidase Activity
pGADT7 α1(1-224)	pMBL33 β2(1-220)	+	✓
pGADT7 β2(1-220)	pMBL33 α1(1-224)	++	✓
pGADT7 α1(1-224)	pMBL33 α1(1-224)	+	✓
pGADT7 β2(1-220)	pMBL33 β2(1-220)	++	✓
pGADT7 α1(1-224)	pMBL33-	+++	✓
pGADT7 β2(1-220)	pMBL33-	+++	✓
pGADT7-	pMBL33 α1(1-224)	-	×
pGADT7-	pMBL33 β2(1-220)	-	×
pGADT7-	pMBL33-	-	×
pGAD10GRIF-1(8-633)	pAS2-1β2-IL(303-427)	+++	✓

Key: +, ++, +++ represent relative colony growth. ✓= β-galactosidase activity. × = no β-galactosidase activity. W = tryptophan, L= leucine, H = histidine

THE CYTOTRAP® YEAST TWO-HYBRID SYSTEM

The CytoTrap® yeast two-hybrid system differs from both the GAL4 and the mLexA systems in that it is not dependent on transcription factor activation for detection of protein protein interactions. Instead, interactions are detected in the cytoplasm of the temperature-sensitive yeast strain, cdc25H.

The CytoTrap® assay is based on a mutation in the yeast cdc25 gene which encodes a guanyl nucleotide exchange factor (GNF). This leads to an inactive Ras signalling pathway that prevents cell growth at 37°C but not at the permissive temperature of 25°C. Bait and fish constructs for this assay each contain a protein of interest fused to either a myristylation signal to carry the first protein to the cell membrane or a functional copy of the human GNF, hSOS, which activates Ras, but is not targeted to the membrane. A positive interaction between the two test proteins results in transport of the GNF to the membrane where it initiates the Ras signalling pathway, thus restoring the ability to grow at 37°C. Thus, the $GABA_A$ receptor N-terminal sequences α1(1-224) and β2(1-220) have been cloned into the CytoTrap® vectors, pMYR and pSOS and initial control experiments are being carried out to validate this system for study of $GABA_A$ receptor inter-subunit contact sequences.

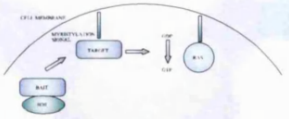

Figure 3: Schematic diagram of the CytoTrap® two-hybrid system.

CONCLUSIONS

- Reporter gene activity was produced following co-transformation of $GABA_A$ receptor N-terminal sequences α1(1-224) and β2(1-220) into GAL4 yeast strain AH109. Unfortunately colony growth and β-galactosidase reporter gene activity were also present when the fish construct containing either α1(1-224) or β2(1-220) was co-transformed with a bait plasmid that contained no insert sequence. This is indicative of auto-activation of reporter gene activity by both α1(1-224) and β2(1-220).
- The modified LexA system showed similar results to the GAL4 system, i.e. fish constructs containing either α1(1-224) and β2(1-220) sequences caused auto-activation of reporter gene transcription when co-transformed with a bait vector containing no insert sequence.
- The auto-activation seen in both the eukaryotic GAL4 and prokaryotic modified LexA assays means that neither is useful for the study of $GABA_A$ receptor subunit assembly domains.

ACKNOWLEDGEMENTS

I would like to acknowledge the Society for Experimental Biology (SEB) and the Company of Biologists (CoB) for the award of a travel grant to attend this meeting.

REFERENCES

1. Xu, J., Yu, W., Jan, Y. N., Jan, L. Y. and Li, M. (1995) J. Biol. Chem., 270, 24761-24768.
2. Colonna, T. E., Huynh, L. and Fambrough, D. M. (1997) J. Biol. Chem., 272, 12366-12372.
3. Smit, A. B., Brejc, K., van Dijk, W. J., Klaassen, R. V., Schuurmans, M., van der Oost, J., Smit, A. B. and Sixma, T. K. (2001) Nature, 411, 261-268.
4. Klausberger, T., Fuchs, K., Mayer, B., Ehya, N. And Werner, S. (2000) J. Biol. Chem., 275, 8921-8928.
5. Beck, M., Brickley, K., Wilkinson, H.L., Sharma, S., Smith, M. J., Chazot, P.L., Pollard, S. & Stephenson, F.A. (2002) J. Biol. Chem. 277. 30079-30090.

DOES KIAA1042, A MEMBER OF THE GRIF-1, COILED-COIL NOVEL GENE FAMILY, ASSOCIATE WITH $GABA_A$ RECEPTORS?

Miriam J. Smith Mike Beck Kieran Brickley and F. Anne Stephenson

School of Pharmacy, University of London, 29/39 Brunswick Square, London, WC1N 1AX, UK.

INTRODUCTION

$GABA_A$ receptor interacting factor-1 (GRIF-1) was identified as a $GABA_A$ receptor-associated protein in rat brain by virtue of its specific interaction with the $GABA_A$ receptor β2 subunit intracellular loop (β2-IL, Beck *et al.*, 2002). It has been proposed to function as a β2 subunit trafficking factor. GRIF-1 shares ~ 47% amino acid sequence similarity over a stretch of 297 amino acids with Huntingtin-associated protein (HAP-1), recently shown to be involved in the regulation of endosomal vesicular trafficking of hepatocyte growth factor-regulated tyrosine kinase substrate and $GABA_A$ receptors (Li *et al.*, 2002; Kittler *et al.*, 2002). Otherwise, GRIF-1 has no homology with proteins of known function. GRIF-1 is the rat orthologue of ALS2CR3/KIAA0549, a human gene of unknown function. A second human gene, KIAA1042, again of unknown function shares ~ 45% amino acid identity with GRIF-1, thus KIAA1042 and GRIF-1 potentially constitute members of a new gene family. The *Drosophila melanogaster* GRIF-1 orthologue is probably Milton, a kinesin-associated adaptor protein that shares ~ 40% homology with GRIF-1. Milton was shown to play a role in mitochondrial transport in the retina (Stowers *et al.*, 2002).

Here, we explored structural and functional homologies between GRIF-1 and KIAA1042, by comparing their sequences and investigating the possible association of KIAA1042 with the $GABA_A$ receptor β2 subunit IL.

Figure 1: Schematic diagram comparing the functional domains of GRIF-1, KIAA1042, Milton and HAP-1.

The schematic diagram shows the relative sizes of the proteins GRIF-1, KIAA1042, Milton, and HAP-1. Hatched boxes represent the positions of predicted coiled-coil regions, the only identified functional domain, for each protein. For HAP-1 the huntingtin binding domain (HB) is also shown.

Figure 2: Schematic diagram showing the interaction of the $GABA_A$ receptor β2-IL with truncated GRIF-1 constructs as determined using the yeast two-hybrid assay.

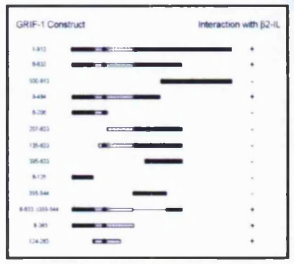

The truncated GRIF-1 constructs illustrated were co-expressed in yeast with the $GABA_A$ receptor β2-IL. Protein:protein interactions were detected by reporter gene activities. + = detectable interaction, - = no detectable interaction. Hatched areas indicate the positions of predicted coiled-coil domains.

The GRIF-1/β2-IL subunit binding domain maps to GRIF-1 (124-283), a region that coincides with the first predicted coiled-coil domain of GRIF-1 and the predicted coiled-coil domains of KIAA1042, Milton and HAP-1.

Figure 3: Amino acid sequence alignment of GRIF-1 with KIAA1042.

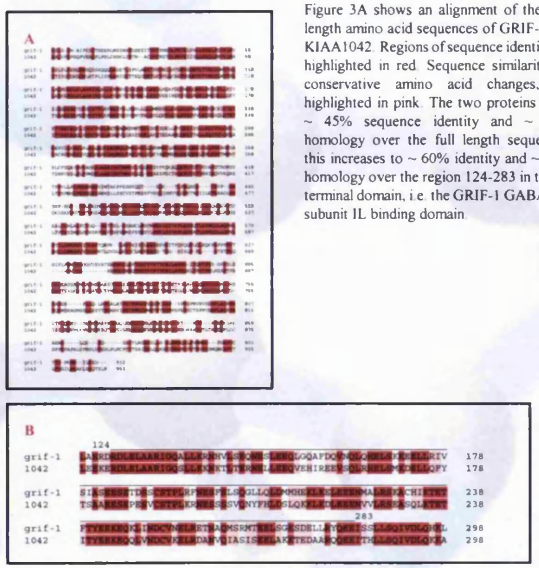

Figure 3A shows an alignment of the full-length amino acid sequences of GRIF-1 and KIAA1042. Regions of sequence identity are highlighted in red. Sequence similarity i.e. conservative amino acid changes, are highlighted in pink. The two proteins share ~ 45% sequence identity and ~ 60% homology over the full length sequences, this increases to ~ 60% identity and ~ 80% homology over the region 124-283 in the N-terminal domain, i.e. the GRIF-1 $GABA_A$ β2 subunit IL binding domain.

Figure 3B is an alignment of the GRIF-1/ $GABA_A$ receptor β2-IL binding domain (GRIF-1 124-283) with the equivalent domain of KIAA1042 (KIAA1042 124-283).

METHODS

The full-length KIAA1042 sequence KIAA1042 (1-953) and the region of KIAA1042 which is equivalent to the $GABA_A$ receptor β2-IL binding domain of GRIF-1, KIAA1042 (124-283), were tested for association with the $GABA_A$ receptor β2-IL in a modified version of the LexA yeast two-hybrid system (mLexA). The KIAA1042 gene in pBluescript II SK+ was used as a PCR template to amplify the KIAA1042 cDNA sequences encoding the amino acids 1-953 and 124-283. The amplified PCR products were cloned in frame into the modified LexA activation domain (AD) vector, pGADT7. These constructs were then co-transformed into L40 yeast with the $GABA_A$ receptor β2-IL which had been cloned into the mLexA DNA binding domain (DNA-BD) vector, pMBL33. Protein:protein interactions were detected by reporter gene activation of nutritional markers and β-galactosidase activity. Interactions between the $GABA_A$ receptor β2-IL and GRIF-1(1-913), (8-633) and (124-283) were used as positive controls.

Table 1: A summary of the results investigating the possible association between KIAA1042 and the $GABA_A$ receptor β2-IL using the yeast two-hybrid system.

AD VECTOR	DNA-BD VECTOR	REPORTER GENE ACTIVITY DETECTED
pMBL33/β2-IL	pGADT7/GRIF-1(1-913)	✓
pMBL33/β2-IL	pGAD10/GRIF-1(8-633)	✓
pMBL33/β2-IL	pGADT7/GRIF-1(124-283)	✓
pMBL33/β2-IL	pGADT7/KIAA1042(1-953)	×
pMBL33/β2-IL	pGADT7/KIAA1042(124-283)	×
pMBL33/β2-IL	pGADT7	×
pMBL33	pGADT7/GRIF-1(1-913)	×
pMBL33	pGAD10/GRIF-1(8-633)	×
pMBL33	pGADT7/GRIF-1(124-283)	×
pMBL33	pGADT7/KIAA1042(1-953)	×
pMBL33	pGADT7/KIAA1042(124-283)	×
pMBL33	pGADT7	×

✓ = Reporter gene activity detected, × = No reporter gene activity detected.
The results are representative of n = 3 independent co-transformations.

The results show that full-length GRIF-1 (1-913), GRIF-1 (8-633) and GRIF-1 (124-283) all produced reporter gene activity when co-transformed into the yeast strain L40 with the $GABA_A$ receptor β2-IL. Neither full-length KIAA1042 (1-953), nor KIAA1042 (124-283) produced reporter gene activity on co-transformation with the $GABA_A$ receptor β2-IL. Single negative controls containing either an empty DNA-BD vector co-transformed with an AD fusion construct of GRIF-1 or KIAA1042, or an empty AD vector co-transformed with the DNA-BD vector containing the $GABA_A$ receptor β2-IL produced no reporter gene activity. The double negative control containing empty AD and DNA-BD vectors also showed no reporter gene activity.

CONCLUSIONS

- The proteins GRIF-1 and KIAA1042 both contain coiled-coil domains within their N-terminal region and constitute a novel gene family of proteins by virtue of their conserved amino acid sequence homology.
- In a yeast two-hybrid assay, GRIF-1(124-283) was shown to encompass the $GABA_A$ receptor β2 subunit IL binding domain.
- Full length KIAA1042 (1-953) and KIAA1042 (124-283), the equivalent of the GRIF-1 $GABA_A$ receptor β2 subunit IL binding domain, despite sharing ~ 45% and ~ 60% sequence identity with GRIF-1, respectively, do not associate with the $GABA_A$ receptor β2 subunit IL in yeast two-hybrid assays.
- Comparing the amino acid sequences of GRIF-1 (124-283) and KIAA1042 (124-283) revealed four candidate regions where the two sequences were most divergent. Using this information studies are on-going to refine the GRIF-1 $GABA_A$ receptor β2 subunit IL binding domain.

Acknowledgements

References

THE JOURNAL OF BIOLOGICAL CHEMISTRY
Vol. 277, No. 33, Issue of August 16, pp. 30079–30090, 2002
Printed in U.S.A.

Identification, Molecular Cloning, and Characterization of a Novel $GABA_A$ Receptor-associated Protein, GRIF-1*

Received for publication, January 15, 2002, and in revised form, May 24, 2002
Published, JBC Papers in Press, May 28, 2002, DOI 10.1074/jbc.M200438200

Mike Beck‡§, Kieran Brickley§, Helen L. Wilkinson¶, Seema Sharma‖, Miriam Smith‖, Paul L. Chazot, Simon Pollard, and F. Anne Stephenson‡‡**

From the Department of Pharmaceutical and Biological Chemistry, School of Pharmacy, University of London, 29/39 Brunswick Square, London WC1N 1AX, United Kingdom

A novel 913-amino acid protein, γ-aminobutyric acid type A ($GABA_A$) receptor interacting factor-1 (GRIF-1), has been cloned and identified as a $GABA_A$ receptor-associated protein by virtue of its specific interaction with the $GABA_A$ receptor β2 subunit intracellular loop in a yeast two-hybrid assay. GRIF-1 has no homology with proteins of known function, but it is the rat orthologue of the human ALS2CR3/KIAA0549 gene. GRIF-1 is expressed as two alternative splice forms, GRIF-1a and a C-terminally truncated form, GRIF-1b. GRIF-1 mRNA has a wide distribution with a major transcript size of 6.2 kb. GRIF-1a protein is only expressed in excitable tissues, *i.e.* brain, heart, and skeletal muscle major immunoreactive bands of M_r ~ 115 and 106 kDa and, in muscle and heart only, an additional 88-kDa species. When expressed in human embryonic kidney 293 cells, GRIF-1a yielded three immunoreactive bands with M_r ~ 115, 106, and 98 kDa. Co-expression of GRIF-1a and α1β2γ2 $GABA_A$ receptors in mammalian cells revealed some co-localization in the cell cytoplasm. Anti-FLAG-agarose specifically precipitated $GRIF\text{-}1_{FLAG}$ and $GABA_A$ receptor β2 subunits from human embryonic kidney 293 cells co-transfected with $GRIF\text{-}1a_{FLAG}$ and β2 subunit clones. Further, immobilized GRIF-1-(8–633) specifically precipitated *in vitro* $GABA_A$ receptor α1 and β2 subunit immunoreactivities from detergent extracts of adult rat brain. The respective $GABA_A$ receptor β2 subunit/GRIF-1 binding domains were mapped using the yeast two-hybrid reporter gene assays. A possible role for GRIF-1 as a $GABA_A$ receptor β2 subunit trafficking factor is proposed.

γ-Aminobutyric acid type A ($GABA_A$)[1] receptors, fast-acting ligand-gated chloride ion channels, are the major inhibitory neurotransmitter receptors in the mammalian central nervous system. There are multiple $GABA_A$ receptor subunit genes encoding the α1–6, β1–3, γ1–3, δ, ϵ, θ, and π subunits. These subunits co-assemble in different pentameric combinations throughout development to form functional receptors (reviewed in, *e.g.*, Ref. 1). The major $GABA_A$ receptor subtype in adult brain is composed of α1, β2/3, and γ2 subunits with a probable stoichiometry of 2α1, 2β2/3, 1γ2. This subunit combination is expressed predominantly at the synapse, whereas other subunit combinations have different subcellular localizations, *e.g.* δ subunit-containing $GABA_A$ receptors are localized extrasynaptically in cerebellar granule cells (2) and α2 subunit-containing receptors are found uniquely at axon initial segments in hippocampal pyramidal cells (3). By analogy with other neurotransmitter receptor systems, it is thought that $GABA_A$ receptor-associated proteins exist that determine receptor subcellular localization, mediate receptor clustering, and regulate receptor activity. For example, Sigel and colleagues (4) reported co-purification of α1 subunit-containing $GABA_A$ receptors and several proteins including actin and tubulin. Some of these proteins were identified as $GABA_A$ receptor-tubulin complex-associated proteins, thus showing a link between the receptors and the cytoskeleton. One of these proteins, $GABA_A$ receptor-tubulin complex-associated protein 34, was shown to be a novel serine kinase with specificity for β3 subunits (5). More recently, the same group identified this protein as the mitochondrial, multifunctional protein, gC1q-R (6). The glycine receptor-associated protein, gephyrin, has also been implicated in the synaptic clustering of $GABA_A$ receptors, although a direct association between the two proteins has not been shown (reviewed in Refs. 7 and 8). Knock-out γ2 (−/−) mice have a parallel deficiency in both gephyrin and clustered post-synaptic $GABA_A$ receptors (9). More recently, the yeast two-hybrid system has been used to identify $GABA_A$ receptor-associated proteins. Proteins identified via this route include GABARAP ($GABA_A$ receptor-associated protein), Plic-1 ($GABA_A$ receptor-associated ubiquitin-like protein), and microtubule-associated protein 1B (MAP-1B). MAP-1B was shown to link $GABA_C$ receptors to the cytoskeleton at retinal synapses (10). GABARAP is a 13.9-kDa microtubule-associated protein that binds specifically to the γ2 subunit and promotes the clustering of $GABA_A$ receptors expressed in Qt-6 quail fibroblasts (11, 12). Differences in functional properties were reported between the clustered and unclustered receptors (12). It has also recently been reported to mediate intracellular transport of $GABA_A$ receptors by virtue of its specific interaction with *N*-ethylmaleimide-sensitive factor (13). Plic-1 (formerly GRUB1) is a

* This work was supported in part by the Biotechnology and Biological Sciences Research Council (BBSRC), United Kingdom. The costs of publication of this article were defrayed in part by the payment of page charges. This article must therefore be hereby marked "*advertisement*" in accordance with 18 U.S.C. Section 1734 solely to indicate this fact.

The nucleotide sequence(s) reported in this paper has been submitted to the DDBJ/GenBank™/EBI Data Bank with accession number(s) AJ288898.

‡ Recipient of a postdoctoral fellowship from the German Academic Exchange Service. Current address: Max Planck Inst. for Molecular Cell Biology and Genetics, D-01307 Dresden, Germany.

§ These authors contributed equally to this work.

¶ Recipient of a BBSRC earmarked studentship.

‖ Recipient of a School of Pharmacy funded Ph.D. studentship.

** Current address: School of Health Sciences, University of Sunderland, Sunderland, Tyne and Wear SR2 7EE, United Kingdom.

‡‡ To whom correspondence should be addressed. Tel.: 44-207-753-5877; E-mail: anne.stephenson@ams1.ulsop.ac.uk.

[1] The abbreviations used are: GABA, γ-aminobutyric acid; aa, amino acid(s); AD, activation domain; BD, binding domain; GRIF-1, γ-aminobutyric acid type A receptor interacting factor-1; HEK, human embryonic kidney; HAP-1, huntingtin-associated protein; IL, intracellular loop; NSE, neuron-specific γ,γ′-enolase; RACE, rapid amplification of cDNA ends; TM, transmembrane region; TBS, Tris-buffered saline; contig, group of overlapping clones.

$GABA_A$ receptor-associated ubiquitin-like protein that binds the α1 subunit and plays a role in the stabilization of cell surface receptors (14, 15).

We have used the yeast two-hybrid system to identify $GABA_A$ receptor-associated proteins. Using the $GABA_A$ receptor β2 intracellular loop (β2-IL) as a bait, we have discovered a novel protein $GABA_A$ receptor interacting factor (GRIF-1) that is expressed predominantly in excitable tissues. The characterization of this protein is reported in this paper.

EXPERIMENTAL PROCEDURES

Constructs

The IL of the $GABA_A$ receptor β2 subunit was selected as a bait in a yeast two-hybrid screen. The coding sequence of the human β2-IL (aa 301–426; Ref. 16) was amplified by the polymerase chain reaction (PCR) utilizing primers that contained *EcoR*I and *Bam*HI restriction enzyme sites. The product was subcloned into the *EcoR*I and *Bam*HI sites of the bait vector, pAS2–1 (Matchmaker Two-Hybrid System 2, CLONTECH, Palo Alto, CA). Likewise, constructs encoding Gal4 DNA binding domain (BD) fusion proteins of the rat $GABA_A$ receptor α1 (aa 304–384), β1 (aa 293–426), β3 (aa 293–426), and $\gamma 2_L$ (aa 317–411) subunit ILs and β2-TM3/IL/TM4 (aa 292–439) and β2-IL/TM4 (aa 272–439) in pAS2–1 were prepared. The authenticity of all constructs was verified by nucleotide sequencing utilizing ABI PRISM dye terminator chemistry on an ABI 310 Genetic Analyzer and immunoblotting of respective yeast protein extracts. All bait constructs tested negative for auto-activation of reporter gene activity in the yeast two-hybrid reporter strains, CG1945 and AH109.

Yeast Two-hybrid Screening

Yeast cultures were grown on standard solid or in liquid media using either YPAD (yeast, peptone, adenine, dextrose; 2% (w/v) peptone, 1% (w/v) yeast extract, 2% (w/v) glucose, 0.003% (w/v) adenine) or SD (synthetic dropout medium; 0.67% (w/v) yeast nitrogen base (BD PharMingen, Cowley, Oxford, UK), 2% (w/v) glucose, 1× dropout supplement (CLONTECH) as appropriate for the selection involved). All transformations were performed using the lithium acetate/polyethylene glycol method (17). *Saccharomyces cerevisiae* strain CG1945 (*MATa, ura3–52, his3–200, ade2–101, lys2–801, trp1–901, leu2–3, 112, gal4–542, gal80–538, cyh^r2, LYS2::GAL1$_{UAS}$-GAL1$_{TATA}$-HIS3, URA3::GAL4$_{17\text{-}mer\ (3x)}$-CYC1$_{TATA}$-lacZ*) was used to screen a rat brain cDNA library (in vector, pGAD10; CLONTECH) with pAS2–1β2-IL as a bait. Resulting colonies were assessed for reporter gene activation by initial nutritional selection (growth on SD −His) and subsequent *lacZ* activity assay. *lacZ* activity was determined by filter lift analysis, including appropriate positive and negative interaction controls. Clones encoding putative interacting proteins were isolated and analyzed following standard procedures (18). Their association with the $GABA_A$ receptor β2-IL was verified by reconstitution assays with a selection of different bait constructs introduced by both yeast mating assays and repeated co-transformation.

Quantification of β-Galactosidase Reporter Gene Activity

β-Galactosidase reporter gene activity was determined by liquid culture assays using *o*-nitrophenyl β-D-galactopyranoside as substrate according to protocols provided by CLONTECH. Briefly, double transformants of yeast strain AH109 expressing the appropriate GAL4 BD and AD fusions were grown overnight in selective medium followed by expansion to mid-log phase in YPAD medium. Cells were harvested, washed once with Z-buffer (0.1 M sodium phosphate, pH 7.0, 1 mM KCl, 1 mM $MgSO_4$), and resuspended in 0.2 of the original volume in Z-buffer. For each sample, 100 μl of cell suspension was subjected to three freeze-thaw cycles in liquid nitrogen, and then 0.96 ml of Z-buffer containing 38 mM β-mercaptoethanol and 0.16 mM *o*-nitrophenyl β-D-galactopyranoside was added. The mixture was incubated at 30 °C for 10 min to overnight depending on the time taken for color development. Reactions were stopped by the addition of 1 M Na_2CO_3 (0.4 ml), cellular debris removed by centrifugation, and OD at λ = 420 nm measured against Z-buffer blanks. Values of β-galactosidase activity were normalized to the cell density of the expansion culture and then expressed as a percentage of wild-type Gal4p.

Cloning of the Entire GRIF-1 cDNA and Sequence Analysis

The full-length GRIF-1 cDNA was obtained by a combination of cDNA library screening and rapid amplification of cDNA ends (RACE). The clone resulting from the initial yeast two-hybrid screen was labeled with α-^{32}P by the random primer method (19). It was used to screen a rat brain cDNA library by colony hybridization. DNA from positive clones were sequenced and used for subsequent screenings. In addition, 5′- and 3′-RACE was performed on rat brain cDNA using the Marathon cDNA amplification system (CLONTECH). RACE products were TA-subcloned into pCR2.1 (Invitrogen, Groningen, The Netherlands) for further analysis. Cloned fragments and RACE PCR products were sequenced as described. The GRIF-1 contig was assembled using Lasergene software (DNAstar Inc., Madison, WI). The assembled cDNA and deduced amino acid sequence were subjected to analysis by a variety of predictive algorithms. BLAST searches were conducted against GenBank™ and EMBL data bases. Procrustes (20) analysis and a selection of hits obtained by BLAST searches against the human subset of GenBank™ and EMBL sequences were used to assemble the cDNA sequence of the human homologue of GRIF-1. Sequence alignments were performed with CLUSTAL. Structure predictions used a variety of publicly available resources such as psort (Ref. 21; psort.nibb.ac.jp) and SMART (Ref. 22; smart.embl-heidelberg.de).

GRIF-1 mRNA Expression and mRNA Analysis

Northern Blotting—GRIF-1 cDNA fragments were radiolabeled with α-^{32}P by a standard random priming method and used to probe a rat multiple tissue Northern blot (CLONTECH). Hybridization was carried out using ExpressHyb solution according to the manufacturer's instructions. After final washing (0.1× SSC, 0.1% (w/v) SDS, 50 °C), the blot was exposed to imaging plates for 20 h. Plates were read with a PhosphorImager (Amersham Biosciences, Aylesbury, Bucks., UK) and analyzed using ImageQuant software.

Reverse Transcription-PCR Analysis—A set of PCR reactions with primers spanning the whole GRIF-1 coding region was employed to screen for alternative spliced isoforms in rat brain. Amplification was usually performed in a total volume of 25 μl containing 1× PCR buffer (10 mM Tris-HCl, pH 9.0, 50 mM KCl, 0.1% (v/v) Triton X-100; Promega Corp., Madison, WI), 1.5 mM $MgCl_2$, 0.5 mM each dNTP, 0.2 μM each primer, 0.5 unit of *Taq* DNA polymerase, and 0.5 μl of cDNA (CLONTECH). Reactions were cycled through a profile consisting of 5 min of initial denaturation at 94 °C, followed by 30 cycles consisting each of 25 s at 94 °C, 25 s at 55 °C, and 1 min at 72 °C, followed by a final extension step of 7 min at 72 °C on a Hybaid OmniGene thermal cycler. PCR products were separated by flatbed agarose gel electrophoresis, visualized by ethidium bromide staining, and analyzed using the EDAS120 imaging system (Eastman Kodak Co.).

Generation of Anti-GRIF-1 Antibodies

A fusion protein was used to generate anti-GRIF-1 polyclonal antibodies in rabbits. For the fusion protein, the DNA encoding GRIF-1-(8–633), *i.e.* the original library clone, was subcloned into the bacterial expression vector, pTrcHisB (Invitrogen). BL 21 *Escherichia coli* transformed with the recombinant pTrcHisBGRIF-1-(8–633) were cultured overnight, diluted 1:50 with LB and grown at 37 °C until mid-log phase (OD $\lambda_{=600\ nm}$ = 0.6). Expression of the poly(His)-GRIF-1-(8–633) fusion protein was induced by the addition of 1 mM isopropyl-β-D-thiogalactopyranoside for 3–5 h at 30 °C. The *E. coli* culture was centrifuged at 5000 × *g* for 10 min at 4 °C, the supernatant discarded, and the pellet resuspended in lysis buffer, which was 20 mM sodium phosphate, pH 7.8, 6 M guanidine hydrochloride, 500 mM sodium chloride (10 ml) at 37 °C. The lysate was stirred gently at room temperature for 10 min followed by sonication (three 5-s pulses at high intensity) on ice. The cleared suspension was centrifuged at 3000 × *g* for 15 min at 4 °C and the poly(His)-GRIF-1-(8–633) fusion protein purified from the supernatant by Ni^{2+} affinity chromatography using ProBond columns exactly as per the manufacturer's instructions (Invitrogen) followed by preparative sodium dodecyl sulfate-polyacrylamide gel electrophoresis (SDS-PAGE). The purified fusion protein, M_r ~ 70 kDa, was used to generate anti-GRIF-1-(8–633) polyclonal antibodies in rabbits. Anti-GRIF-1-(8–633) antibodies were affinity-purified by GRIF-1-(8–633)-Ni^{2+}-agarose affinity chromatography prior to use (23).

Immunoblotting

SDS-PAGE was carried out using 10% polyacrylamide slab gels under reducing conditions. Samples were prepared using the chloroform/methanol method of protein precipitation, and immunoblotting was carried out as previously described using affinity-purified anti-$GABA_A$ receptor α1 subunit (24), anti-β2 subunit (25), affinity-purified anti-GRIF-1-(8–633), and anti-neuron-specific γ,γ′-enolase (NSE) antibodies in conjunction with the enhanced chemiluminescence (ECL) Plus

TABLE I

A summary of the specificity of the GRIF-1/GABA$_A$ receptor subunit interactions in the yeast two-hybrid system

The yeast strain AH109 was co-transformed with bait and fish constructs and transformants grown on SD −Trp, −Leu, −His, −Ade, *i.e.* SD − 4 plates. Colonies were patched to either SD − 4 plates and β-galactosidase activity measured by filter lift assays or alternatively to − 4 plates with agarose X-α Gal overlay to measure Mel activity all as described under "Experimental Procedures." The strength of the bait and fish interactions are expressed as a percentage of wild-type Gal4 protein transformants which were determined using the yeast strain, AH109. ND, not determined.

Gal4 binding domain fusion construct	Activation domain construct	*HIS3, ADE2, lacZ, MEL1* reporter gene activities	*lacZ* activity
			%
pAS2–1α1-IL	pGAD10GRIF-1-(8–633)	−	ND
pAS2–1β1-IL	pGAD10GRIF-1-(8–633)	−	ND
pAS2–1β2-IL	pGAD10GRIF-1-(8–633)	+	1.5 ± 0.4 (n = 3)
pAS2–1β3-IL	pGAD10GRIF-1-(8–633)	−	ND
pAS2–1β2-TM3/IL/TM4	pGAD10GRIF-1-(8–633)	−	ND
pAS2–1β2-IL/TM4	pGAD10GRIF-1-(8–633)	−	ND
pAS2–1γ2-IL	pGAD10GRIF-1-(8–633)	−	ND
pAS2–1β2-IL	pGADT7GRIF-1-(1–913)	+	1.7 ± 0.4 (n = 3)
pAS2–1β2-IL	pGADT7KIAA0549-(1–483)	+	1.2 ± 0.4 (n = 3)
pAS2–1β2-IL	pGAD10KIAA0549-(446–914)	−	ND
	pGAD10GRIF-1-(8–633)	−	ND
pVA3–1	pGAD10GRIF-1-(8–633)	−	ND
pVA3–1	PTD1–1	+++	100
	PCL-1	+++	100

Western blotting detection system (Amersham Biosciences) for the detection of immunoreactive species. Anti-rabbit and mouse immunoglobulin horseradish peroxidase-linked whole antibodies (Amersham Biosciences) were used at a final dilution of 1:2000. Where applicable, immunoblots were quantified by densitometry using a Personal Densitometer and ImageQuant (Amersham Biosciences) in the linear range of the film.

Subcellular Fractionation of Rat Tissues

Tissues from rat forebrain, cerebellum, liver, kidney, heart, and spleen were each homogenized in nine volumes of homogenizing buffer (20 mM Tris-HCl, pH 7.4, 0.25 M sucrose, containing benzamidine (1 μg/ml), bacitracin (1 μg/ml), soybean trypsin inhibitor (1 μg/ml), chicken egg trypsin inhibitor (1 μg/ml), and phenylmethylsulfonyl fluoride (1 mM)) at 4 °C using a hand-held glass-glass homogenizer. Skeletal and cardiac muscle was removed, minced using scissors, and homogenized using an Ultra-Turrax (six 10-s pulses at medium speed) followed by homogenization as above. Homogenates were centrifuged at 600 × *g* for 10 min at 4 °C. The supernatants were collected and the P1 nuclear pellets re-homogenized in three volumes of homogenizing buffer and re-centrifuged at 600 × *g* for 10 min at 4 °C. Both supernatants were combined and centrifuged at 100,000 × *g* for 40 min at 4 °C to yield the soluble (S) and P2 membrane fractions. The P1 and P2 pellets were re-suspended in homogenizing buffer and stored at −20 °C until use.

Co-expression of GABA$_A$ Receptors and GRIF-1a in Human Embryonic Kidney (HEK) 293 Cells

The cDNA encoding the full-length GRIF-1a was obtained by PCR from rat brain cDNA and subcloned into both the mammalian expression vectors, pCIS and pCMV-Tag4 (Stratagene, La Jolla, CA). The latter yielded a C-terminal FLAG-tagged GRIF-1. HEK 293 cells were cultured and transfected in 250-ml flasks using the calcium phosphate method as described previously (26). Cells were transfected with pCIS GRIF-1a or pCMV-Tag4GRIF-1a alone (10 μg of DNA) or with the GABA$_A$ receptor clones pCDM8α1 (bovine), pCISβ2 (rat), pCDM8γ2L (bovine), and pCISGRIF-1 or pCMV-TagGRIF-1 in a 1:1:1:1 ratio with a total of 10 μg of DNA. Cells were harvested 24–48 h following transfection and analyzed by immunoblotting. For immunocytochemical studies, transfections were carried out by the calcium phosphate method on HEK 293 cells adhered to poly-L-lysine-coated cover slips. Transfected cells were cultured for 40 h, the cover slips washed three times for 5 min each at 20 °C with 20 mM Tris-HCl, pH 7.25, 145 mM NaCl (TBS), followed by fixation with 4% (w/v) paraformaldehyde in TBS for 10 min at 20 °C. Cells were washed three times for 5 min each with TBS containing 0.15% (v/v) Triton X-100 followed by three 5-min washes with TBS containing 20% (v/v) goat serum, 2% (w/v) bovine serum albumin, and 0.1% (w/v) DL-lysine. Transfected cells were incubated for 2 h at 20 °C with the primary antibody diluted appropriately in TBS containing 10% (v/v) goat serum, 1% (w/v) bovine serum albumin, and 0.1% (w/v) DL-lysine followed by five 5-min washes with TBS at 20 °C. Incubation with the secondary antibody, either goat anti-rabbit Ig-Alexa Fluor 594 or goat anti-mouse Ig-AlexaFluor 488 (Molecular Probes, Eugene, OR) diluted 1:150 in TBS. Finally, cells were washed five times for 5 min each time with TBS, mounted in UV-free mounting medium (H.D. Supplies, Muratech Scientific, Aylesbury, Bucks., UK), and viewed with a Leica TCSSP confocal microscope.

Co-immunoprecipitation Assays

HEK 293 cells were co-transfected with pCMV-Tag4GRIF-1a + pCISβ2; pCISβ2 + pCIS, pCMV-Tag4GRIF-1a + pCDM8α1, or pCMV-Tag4GRIF-1a + pCIS (1:1 ratio with 10 μg of total DNA). Cells were harvested 48 h after transfection and solubilized for 1 h at 4 °C with 10 mM HEPES, 150 mM NaCl, 5 mM EDTA, 5 mM EGTA, 1% (v/v) Triton X-100, and protease inhibitors as described above under "Subcellular Fractionation of Rat Tissues." The solubilized material was collected by centrifugation at 100,000 × *g*, diluted 1:3 in 10 mM HEPES, 50 mM NaCl, 16 mM KCl, 1 mM EDTA + protease inhibitors, and incubated (8 ml) with anti-FLAG M2-agarose (30 μl; Sigma, Poole, Dorset, UK) for 1 h at 37 °C. Samples were centrifuged for 20 s at 3000 × *g* and the pellet washed with two 0.5-ml (17 volumes) amounts of 10 mM HEPES, 75 mM NaCl, 12.5 mM KCl, 2 mM EDTA, 1.25 mM EGTA + protease inhibitors, 0.25% (v/v) Triton X-100, followed by 17 volumes of the same buffer but with a Triton X-100 concentration of 1% (v/v). The pellets were collected by centrifugation as above and analyzed by immunoblotting.

In Vitro Protein Interaction Assay

BL 21 cells were transformed with either pTrcHisBGRIF-1-(8–633) or the empty, pTrcHisB expression vector and the respective bacterial cell lysates prepared as detailed under "Generation of Anti-GRIF-1 Antibodies." ProBond resin (Invitrogen) was washed three times with seven volumes of distilled H_2O followed by seven volumes of denaturing binding buffer, which was 20 mM sodium phosphate, pH 7.8, 8 M urea, 500 mM NaCl. The resin (25 μl) was incubated with either the pTrcHis-GRIF-(8–633) lysate, the pTrcHis lysate or lysis buffer (1 ml) for 10 min at 20 °C. Each resin was then washed two times with 14-volumes native binding buffer, which was 20 mM sodium phosphate, pH 7.8, 500 mM NaCl. A detergent-solubilized rat forebrain P2 extract was prepared by re-suspension of a 100,000 × *g* P2 pellet in 10 mM HEPES, pH 7.5, 50 mM KCl, 1 mM EDTA, 1% (v/v) Triton X-100, benzamidine HCl (1 μg/ml), bacitracin (1 μg/ml), soybean trypsin inhibitor (1 μg/ml), chicken egg trypsin inhibitor (1 μg/ml), and phenylmethylsulfonyl fluoride (1 mM) to a concentration of 3 mg of protein. Solubilization was carried out for 1 h at 4 °C and the detergent extract cleared by centrifugation at 100,000 × *g* for 40 min at 4 °C. The derivatized resins were incubated with the solubilized P2 membrane proteins diluted 1:3 with 10 mM HEPES, pH 7.5, 17 mM KCl, with the protease inhibitors as above to give final concentrations of 0.25% (v/v) Triton X-100 and 25 mM KCl (1 ml of 1 mg/ml protein) overnight at 4 °C. The supernatant was removed by centrifugation of the resins at 200 × *g* for 10 s at 4 °C. Each resin was washed once with 40 volumes of 20 mM sodium phosphate, pH 7.8, 500 mM NaCl., 0.05% (v/v) Triton X-100. The bound proteins were extracted with SDS-PAGE sample buffer (50 μl), heated for 5 min at

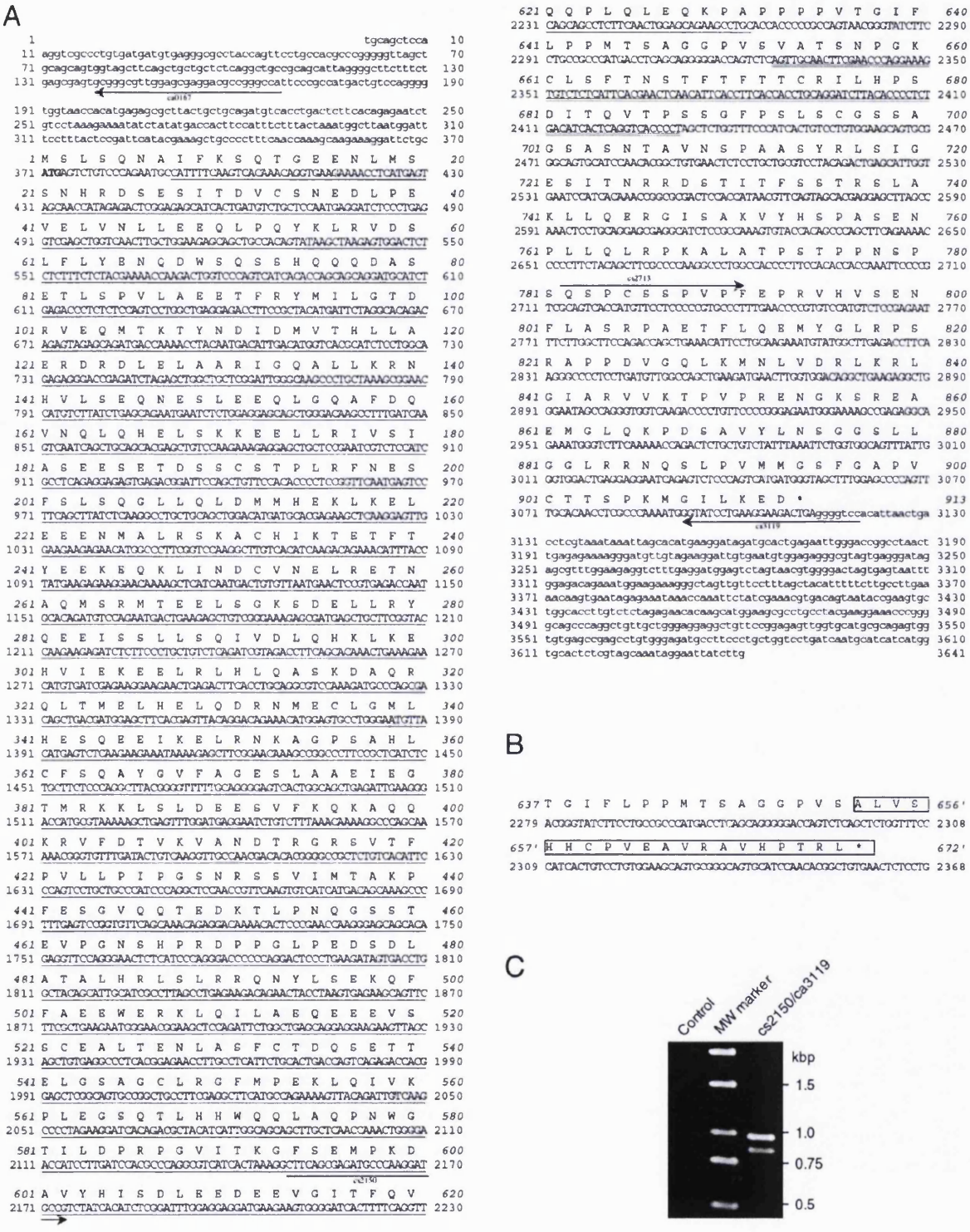

FIG. 1. **Nucleotide and deduced amino acid sequence of full-length GRIF-1a and the alternative splice variant, GRIF-1b.** *A*, the complete nucleotide and deduced amino acid sequence of GRIF-1a. The nucleotide sequence was compiled from the original clone isolated during the initial yeast two-hybrid screen (*underlined*), ~400 bp (nucleotides 1–400) derived from clone 1.2.B isolated by cDNA library screening and 5′- and 3′-RACE. The positions of the primers used for 5′- and 3′-RACE as well as for the reverse transcriptase PCR for detection of alternative splicing are shown as *arrows*. *Numbers* in *italics* are the amino acids of the full-length protein. *ATG* defines the start of the longest open reading frame. Alternative splicing resulted in a deletion of the nucleotide sequence double *underlined* in *A* yielding an altered and truncated protein of 672 aa. The amino acid sequence of the truncated protein, GRIF-1b, is shown in *B*. *C* shows the results of PCR amplification of rat brain cDNA using oligonucleotide primers cs2150 and ca3119. Flatbed agarose gel electrophoresis revealed two products of 970 and 860 bp, corresponding to two alternatively spliced transcripts. The sequence in *A* has been deposited in the EMBL/GenBank™/DDBJ data base with accession no. AJ288898.

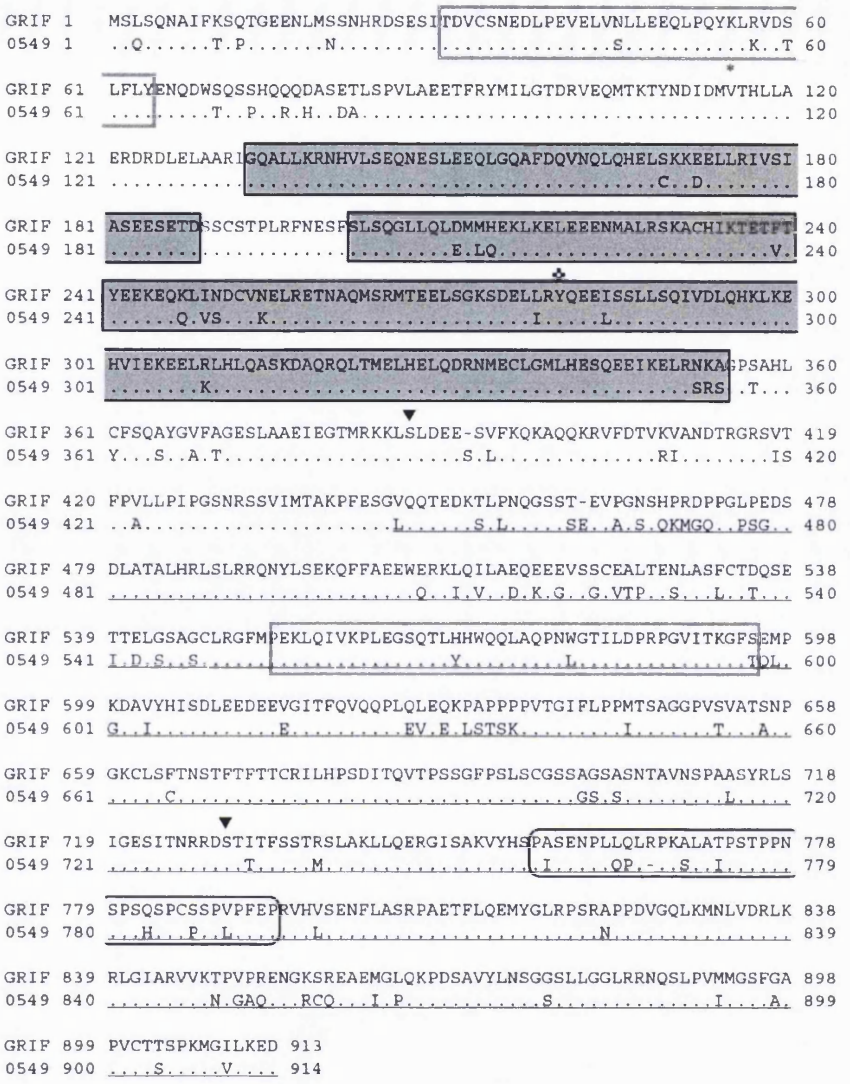

FIG. 2. **Alignment of the amino acid sequence of GRIF-1 and full-length KIAA0549.** The figure depicts the rat GRIF-1 deduced amino acid sequence aligned with that deduced for the human orthologue, labeled here as *0549*. Amino acids identical between the two sequences are shown as .; the original KIAA0549 sequence is *underlined*. *K**, the single amino acid difference (K55R) found between the deduced human sequence and that reported by Hadano *et al.* (37) for ALS2CR3; ▼, the sites of consensus sequences for protein kinase A; ✥, the site of the tyrosine kinase consensus sequence. The *hatched areas* show the positions of the two predicted coiled-coil regions in the N-terminal domain. The C-terminal proline-rich region is marked with a *round-edged rectangle*. *Gray open rectangles* indicate the position of two regions that are highly conserved among members of the GRIF-1 family.

100 °C, and the supernatants analyzed by quantitative immunoblotting using affinity-purified anti-β2 fragment 381–395 (25), anti-α1 fragment 413–429 (27), and anti-NSE antibodies (Affiniti Research Products Ltd., Mamhead, Exeter, UK). The results were analyzed by paired Student's *t* test.

Determination of the GRIF-1 and β2-IL Interacting Domains

A series of GRIF-1 fragments were constructed by either standard subcloning techniques from the isolated library clone, C3, or PCR amplification. These were subcloned into pGAD10, pACT2, or pGADT7 (CLONTECH) to yield Gal4 AD fusion proteins. Similarly, fragments of the β2-IL (aa 303–427, 303–370, 355–427, 371–427, 303–394, 324–394, and 324–427) were fused to the GAL4 BD in pAS2–1. The yeast strain AH109 (*MATa, trp1–901, leu2–3, 112, ura3–52, his3–200, gal4Δ, gal80D, LYS2::GAL1$_{UAS}$-GAL1$_{TATA}$-HIS3, GAL2$_{UAS}$-GAL2$_{TATA}$-ADE2, URA3::MEL1$_{UAS}$-MEL1$_{TATA}$-lacZ*; CLONTECH) was transformed with pair-wise combinations of β2-ILBD and GRIF-1AD fusions. The interaction between pairs of proteins was assayed by nutritional selection on SD −4 (−His, −Trp, −Ade, −Leu) plates as well as β-galactosidase and α-galactosidase (Mel1) activity. α-Galactosidase activity was determined by overlaying the plates with X-α Gal-top agar (0.4% (w/v) low melting point agarose, 0.001% (w/v) X-α Gal (Melford Laboratories, Cambridge, UK) in Z-buffer. Coloration usually occurred within 3–6 h.

RESULTS

Identification of a Novel Protein That Interacts with the GABA$_A$ Receptor β2 Subunit—The GABA$_A$ receptor β subunits have been reported to determine the subcellular localization of αβγ receptors (28). The β2 subunit is the most abundantly expressed of the β isoforms in adult brain (see, *e.g.*, Refs. 29 and 30). Therefore, the GABA$_A$ receptor β2-IL was selected as a bait to identify β subunit interacting proteins that may function as targeting or clustering molecules. A yeast two-hybrid cDNA library screen of 1.5×10^6 independent transformants with the GABA$_A$ receptor β2-IL as the bait yielded initially 36 positively growing clones of which one, C3, showed *lacZ* reporter gene activity. The plasmid isolated contained a 1.8-kb insert with an in-frame fusion encoding 626 aa. Re-transformation of this clone into yeast strain, AH109, with a variety of different GABA$_A$ receptor subunit IL bait constructs, *i.e.* α1, β1, β3, and γ2-ILs, showed that C3 interacted specifically with the β2-IL (Table I). Further, C3 did not yield reporter gene activity when alternative β2-IL constructs that incorporated either both TM3 and TM4, *i.e.* β2-TM3/ILTM4, or TM4 only, *i.e.* β2-IL/TM4, were used as baits (Table I). Quantification of *lacZ* reporter gene activity revealed a relative strength of the C3/β2-IL interaction of ~1.5% relative to 100% of the pCL-1 (Gal4p wild-type) positive control (Table I).

The cDNA Encodes a Novel Protein That Is Conserved in Mammalian Evolution—Nucleotide sequencing revealed that

C3 contained an open reading frame of novel sequence fused in-frame to the GAL4 activation domain. The full-length cDNA of the protein was obtained by cDNA library screening using the C3 probe in conjunction with 5′- and 3′-RACE. The assembled cDNA sequence (3641 bp) contains an open reading frame of 2739 bp predicting a protein of 913 aa residues, a calculated molecular mass of 102 kDa, and an acidic pI = 5.14. Within the protein, the original two-hybrid interacting fragment (C3) extends from aa 8 to 633. We have called the protein, GRIF-1, for GABA$_A$ receptor interacting factor. The nucleotide and deduced amino acid sequence of GRIF-1 are shown in Fig. 1. Expression of a transcript of the predicted sequence was verified by PCR amplification from adult rat brain cDNA utilizing a variety of oligonucleotide primers (results not shown). Using the primers cs2150 and ca3119, two PCR products were obtained (Fig. 1). Nucleotide sequencing of the PCR products revealed a deletion of 107 bp in the smaller product that altered the reading frame of GRIF-1. Thus, an alternative, C-terminally truncated splice form of GRIF-1 with 672 aa was identified and termed GRIF-1b, with the original 913-aa protein now denoted GRIF-1a. Both GRIF-1a and GRIF-1b were shown to associate with the GABA$_A$ receptor β2-IL in the yeast two-hybrid assay. Quantitative analysis of the resultant reporter gene activity showed that GRIF-1a and the original C3 clone yielded a similar strength of interaction with β2-IL (Table I).

Analysis of the GRIF-1 deduced amino acid sequence revealed a hydrophilic protein with no predicted transmembrane domains and no hydrophobic signal peptide. Structure prediction analysis indicated a high α-helical content (31) and the presence of a coiled-coil identified by both the Lupas and the paircoil algorithms (32, 33). The GRIF-1 aa sequence contains consensus sequences for protein kinase A phosphorylation at aa 384 and 726 and tyrosine kinase at aa 273, as well as 16 potential protein kinase C and 15 potential casein kinase II phosphorylation sites. There is also a proline-rich domain with 29% proline residues between aa 756 and 793 (Fig. 2).

Data base searches revealed that GRIF-1 has no significant homology with proteins of known function. However, amino acid sequence similarity was found between GRIF-1 and two human genes of unknown function identified in a brain gene cloning project, a chromosome 2 gene, KIAA0549 (~78% over 469 aa; Ref. 34) and KIAA1042 (~45% identity over 913 aa; Ref. 35). Homology of ~47% over 297 aa was also found with the rat huntingtin-associated protein (rHAP-1; Ref. 36). The similarity between GRIF-1, HAP-1 and the related protein, HAP-like protein, was restricted to the N terminus in a region that coincided with the first predicted coiled-coil domain (Fig. 2), whereas it became evident that GRIF-1 and KIAA0549 are species orthologues.

Procrustes analysis of GRIF-1 *versus* the draft human genome sequence of chromosome 2 predicted the existence of a gene comprising at least 15 exons and extended the reading frame of KIAA0549 toward its N terminus. From these results, in conjunction with a number of expressed sequence tag sequences (dbEST accession nos. AA338224, AA075951, AW952742, and BE070051), the full-length KIAA0549 cDNA sequence was assembled. The deduced cDNA encodes a 914-amino acid protein with an overall ~88% amino acid sequence identity to GRIF-1. The expression of this novel sequence was verified by its PCR amplification from human fetal brain cDNA (data not shown). This cDNA corresponds to one recently reported by Hadano *et al.* (37), ALS2CR3, with the exception of one conservative amino acid change, K55R (Fig. 2). ALS2CR3 was shown to contain 16 exons (37). Functional equivalence between GRIF-1 and full-length KIAA0549 was demonstrated by a similar strength of interaction with the GABA$_A$ receptor β2-IL in the yeast two-hybrid reporter strain, AH109 (Table I). Furthermore, the deletion found in the GRIF-1b isoform was found to be equivalent to exon 15 of the human ALS2CR3/KIAA0549 gene.

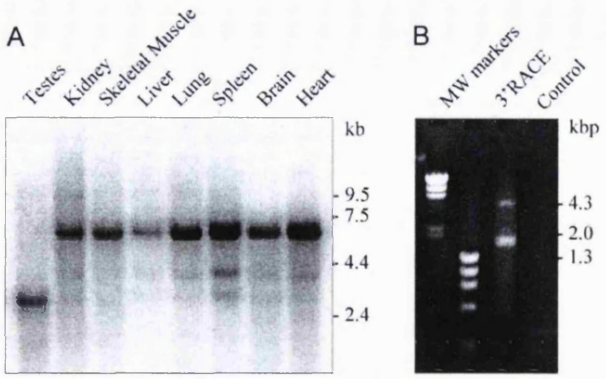

FIG. 3. **Tissue distribution and heterogeneity of GRIF-1 mRNA.** *A*, a multiple tissue Northern blot was probed with a 1.9-kb fragment of GRIF-1 labeled with ^{32}P by random priming as described under "Experimental Procedures." Major transcripts of 6.2 kb were present in all tissues except testes, where the major transcript was 2.9 kb. A minor 4.2-kb hybridizing species was also present, with the highest expression being found in the spleen. *B*, rat brain cDNA was subject to 3′-RACE using the oligonucleotide primer cs2150 and the Marathon adaptor AP1 as described under "Experimental Procedures." Flatbed agarose gel electrophoresis yielded two products of 1.9 and 4.2 kb.

More recently, similarity was found between GRIF-1 and the *Drosophila melanogaster* gene product, CG13777 (also known as LD313316p and mltLD8CG13777; GenBank™ accession nos. AE003616, AY051825, and AY038001, respectively) and the *Macaca fascicularis* hypothetical protein, BAB41149 (Genpept accession no. AB060210). Using expressed sequence tag data (AK014647) as well as the Celera discovery system, partial sequences of the mouse orthologues of both KIAA0549 (ALS2CR3)/GRIF-1 and KIAA1042 were identified. Blockmaker and MEME analysis (38) identified conserved regions and predicted a similar domain structure for all these proteins. The conserved domain structure includes the N-terminal coiled-coil region and two motifs outside this region, namely GRIF-1 aa 30–60, with a consensus sequence: TDVC(S/N)(N/S)EDLPEVE(I/L)(V/I)SLLEEQLPQYKLRVD(S/T)(L/I)(F/Y)(L/G)Y and aa 553–595, consensus sequence PEKLQIVKPLEGS(Q/A)TLHHWQQLAQP(H/N)LG(G/T)ILDPRRGV(I/V)TKGF(S/T) (Fig. 2). Thus GRIF-1 is a member of a new protein family with as yet, two known members in mammals and a single homologue in *D. melanogaster*. GRIF-1 (rat), KIAA0549 (ALS2CR3) (human), and mCP 20802/mCP20839 (mouse) are a group of species orthologues as are KIAA1042 (human), BAB41149 (*M. fascicularis*), and mCP13834 (mouse).

Tissue Distribution of GRIF-1 mRNA and GRIF-1 Protein—A rat multiple tissue Northern blot probed with [^{32}P]GRIF-1 revealed a major hybridizing transcript of 6.2 kb, which was present in all tissues tested except testis, where a transcript of 2.9 kb was found (Fig. 3). The rank order of expression was spleen > heart > lung > brain > kidney ~ skeletal muscle. A minor transcript of 4.2 kb was also detectable with highest expression in the spleen. Electrophoretic separation of 3′-RACE products revealed two major species of 4.2 and 1.9 kb, which correspond in size to the 6.2- and 4.2-kb transcripts identified in the Northern blot (Fig. 3). These two transcripts are most likely derived by alternative use of polyadenylation sites in the 3′-untranslated region.

Soluble, P1 nuclear fractions and P2 membrane fractions

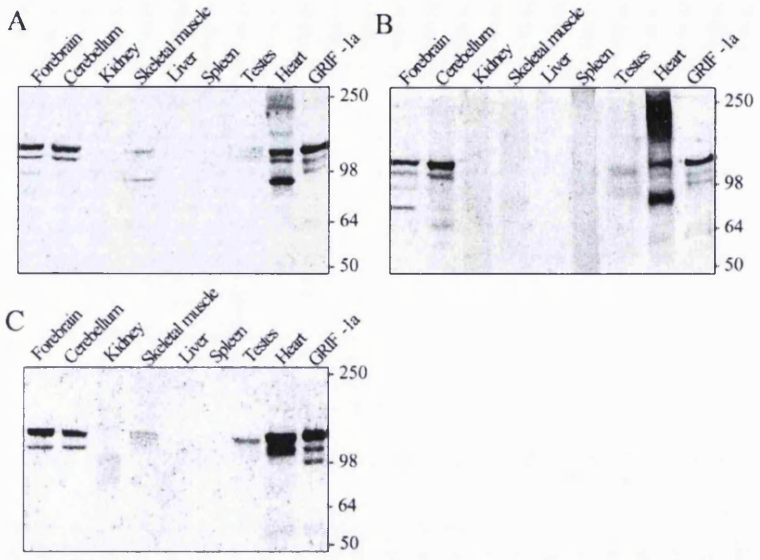

FIG. 4. **Subcellular and tissue distribution of GRIF-1 protein by immunoblotting.** Rat tissues were homogenized and subjected to subcellular fractionation to yield the P1 (nuclear fraction), the P2 (membrane fraction), and S (soluble) proteins. Samples (10 μg of protein/gel lane) were analyzed by immunoblotting using affinity-purified anti-poly(His)-GRIF-1-(8–633) fusion protein antibodies all as described under "Experimental Procedures." *A*, *B*, and *C* are immunoblots of P1, P2, and soluble fractions, respectively, with tissues as indicated. The last lane of each blot contains pCISGRIF-1-transfected HEK 293 cell homogenates. A major immunoreactive band with M_r ~ 115,000 was found in P1, P2, and S fractions for forebrain, cerebellum, heart, skeletal muscle, in HEK cells transfected with pCISGRIF-1a and in the S fraction of testes (n = 3–10). In P1 and P2 membrane preparations of rat forebrain, cerebellum, and heart, an additional band with M_r ~ 106,000 (n = 11) was found. HEK 293 cell homogenates transfected with GRIF-1a showed two additional bands with M_r values ~ 106,000 and 98,000. Heart and skeletal muscle P1 fractions both expressed a M_r ~ 88,000 immunoreactive species. Molecular size markers (× 10^3 kDa) are shown on the *right*.

were prepared from all tissues used in the Northern blot except lung. These were analyzed by immunoblotting using affinity-purified anti-GRIF-1-(8–633) antibodies. The results are shown in Fig. 4. It can be seen that, in all subcellular fractions of forebrain, cerebellum and heart, the antibodies recognized two bands with M_r ~ 115,000 (major) and M_r ~ 106,000 (n = 3). In skeletal muscle, a single immunoreactive species with M_r ~ 115,000 was found in the P1 and soluble fractions; this band was also present in the soluble fraction of testes. An additional immunoreactive band with M_r ~ 88,000 was observed in heart P1 and P2 fractions, in P1 for muscle and P2 for forebrain. A molecular weight of 115,000 is in the range of that predicted for a 913-aa protein. Importantly, the band is coincident with the major immunoreactive species obtained following expression of the full-length GRIF-1 in HEK 293 cells. The lower molecular mass M_r ~ 106,000 band, which is also observed in the transfected cells, may be a proteolytic product. The M_r ~ 88,000 immunoreactive species expressed predominantly in the heart has a molecular size consistent with the predicted size of the GRIF-1b variant.

In Vitro Protein Interaction Assay—To demonstrate that GRIF-1 can associate with β2 subunit-containing GABA$_A$ receptors, *in vitro* protein interaction assays were carried out. Thus, poly(His)-GRIF-1-(8–633) immobilized on Ni^{2+}-agarose, poly(His)-Ni^{2+}-agarose, or Ni^{2+}-agarose was each incubated with Triton X-100 detergent extracts of rat forebrain and associated proteins identified by precipitation followed by immunoblotting. The results are shown in Fig. 5. It can be seen that poly(His)-GRIF-1-(8–633)-Ni^{2+}-agarose specifically precipitated GABA$_A$ receptor β2 and α1 subunit immunoreactivities. No immunoreactivities were precipitated by the resin alone Some β2 and α1 immunoreactivity was always associated with the control poly(His)-Ni^{2+}-agarose, but the respective immunoreactivities were always greatest for precipitation by poly(His)-GRIF-1-(8–633)-Ni^{2+}-agarose. As an additional control, the agarose pellets were probed with anti-NSE antibodies. No anti-NSE immunoreactivity was detected in either the control poly-(His)-Ni^{2+}-agarose or the poly(His)-GRIF-1-(8–633)-Ni^{2+}-agarose pellets (Fig. 5*C*). The relative intensities of the α1 and β2 immune signals between the control poly(His)-Ni^{2+}-agarose and the test, poly(His)-GRIF-1-(8–633)-Ni^{2+}-agarose were found to vary with assay incubation conditions. Optimal results were obtained by reducing the concentration of Triton X-100 to 0.25% (v/v). The results of the pull-down assays in the presence of 0.5 and 0.25% (v/v) Triton X-100 were analyzed by quantitative immunoblotting with the following results, which are expressed as the -fold increase in immunoreactivity precipitated by poly(His)-GRIF-1-(8–633)-Ni^{2+}-agarose with respect to that precipitated by poly(His)-Ni^{2+}-agarose: 0.5% Triton X-100, 2.9 ± 0.5 (β2) (n = 5; $p < 0.01$) and 1.6 ± 0.2 (α1) (n = 4; $p < 0.05$); 0.25% Triton X-100, 4.0 ± 0.7 (β2) (n = 4; $p < 0.03$) and 1.9 (α1) (n = 2). The ratio for the -fold increase in immunoprecipitation for β2/α1 was 1.8 (0.5% Triton X-100) and 2.1 (0.25% Triton X-100). Thus, GRIF-1-(8–633) does interact with both α1 and β2 GABA$_A$ receptor subunits, suggesting co-association with assembled β2 subunit-containing GABA$_A$ receptors. It was noted, however, that the percentage of β2 subunit immunoreactivity precipitated was always significantly higher than that found in α1 (see "Discussion").

Expression of GRIF-1 in HEK 293 Cells—Untransfected HEK 293 cells showed no anti-GRIF-1 immunoreactivity when analyzed by either immunoblotting or immunocytochemistry (Fig. 6*A*). As described above, when HEK 293 cells were transfected with either pCISGRIF-1a or pCMVTag4GRIF-1a$_{FLAG}$, a major band with M_r ~ 115,000 was recognized in whole cell homogenates by both anti-GRIF-1-(8–633) or anti-FLAG antibodies (Fig. 4); two minor bands with M_r values of 105,000 and 98,000 were also detected. All three immunoreactive bands were detected in the P1, P2, and soluble cell cytoplasm fraction (results not shown). In permeabilized, transfected cells, GRIF-1 or GRIF-1$_{FLAG}$ expressed alone had a diffuse, intracellular localization (Fig. 6*B*). This was in contrast to the pattern ob-

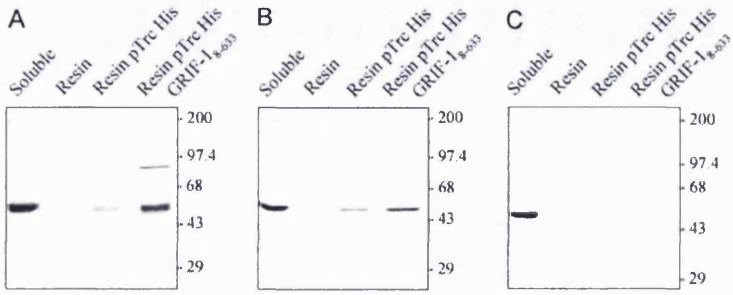

FIG. 5. **Demonstration of the binding of native $GABA_A$ receptor α1 and β2 subunits to GRIF-1-(8–633) using immobilized GRIF-1-(8–633) affinity chromatography purification.** The fusion proteins, pTrcHis and pTrcHis-GRIF-1-(8–633), were generated in *E. coli* and immobilized to washed and equilibrated Ni^{2+}-agarose. Triton X-100 extracts (1 mg of protein; 1 ml) of rat brain were incubated with Ni^{2+}-agarose, pTrcHis-Ni^{2+}-agarose, or pTrcHis-GRIF-1-(8–633) -Ni^{2+}-agarose overnight at 4 °C in the presence of 0.25% (v/v) Triton X-100 and 25 mM KCl. Agarose pellets were collected by centrifugation and analyzed by quantitative immunoblotting using anti-β2 381–395 (*A*), α1 413–429 (*B*), and neuron-specific enolase (*C*) antibodies all as described under "Experimental Procedures." The gel layout is identical for each blot. *Lane 1*, Triton X-100 extract of rat forebrain; *lane 2*, Ni^{2+}-agarose pellet; *lane 3*, pTrcHis-Ni^{2+}-agarose; *lane 4*, pTrcHis-GRIF-1-(8–633)-Ni^{2+}-agarose. The positions of molecular size standards are shown on the *right*.

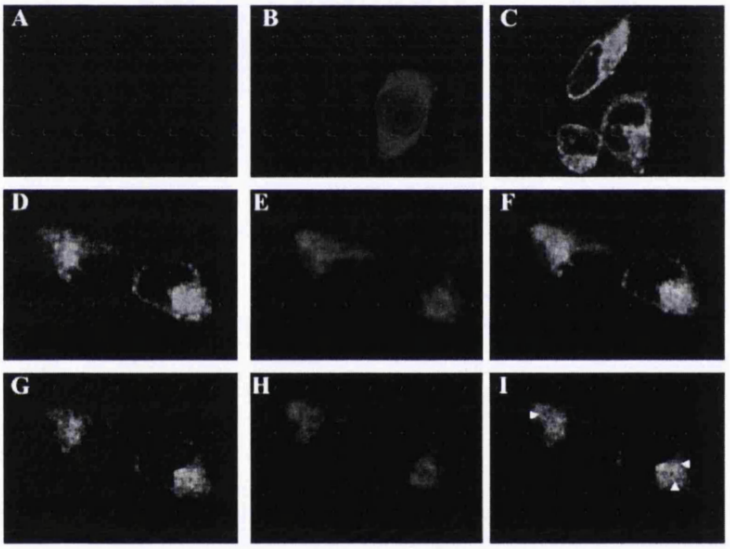

FIG. 6. **Localization of GRIF-1 and $GABA_A$ receptor β2 subunits in HEK 293 cells transfected with GRIF-1a$_{FLAG}$ and $\alpha1\beta2\gamma2$ $GABA_A$ receptors.** HEK 293 cells adhered to poly-L-lysine-coated cover slips were transfected with the appropriate clones by the calcium phosphate method. Cells were fixed 24–40 h after transfection, permeabilized with 0.15% Triton X-100, and immunolabeled with primary antibody, which was either monoclonal antibody bd-17 or affinity-purified anti-GRIF-1-(8–633) polyclonal antibodies, followed by the appropriate fluorescent secondary antibody and visualization by confocal microscopy all as described under "Experimental Procedures." *Panels A–F* are composites of multiple focal planes viewed at a magnification of 40,000 and zoom, 2. *A*, *B*, and *E*, staining was with anti-GRIF-1-(8–633) polyclonal antibodies and anti-rabbit-Ig Alexa Fluor 594; *C* and *D*, staining was with monoclonal antibody bd-17 and goat anti-mouse-Ig AlexaFluor 488. *A*, untransfected HEK cells; *B*, HEK 293 cells transfected with pCMVTag4GRIF-1a$_{FLAG}$; *C*, HEK 293 cells transfected with $GABA_A$ receptor $\alpha1\beta2\gamma2$ clones; *D–F*, HEK 293 cells transfected with pCMVTag4GRIF-1a$_{FLAG}$ and $GABA_A$ receptor $\alpha1\beta2\gamma2$ clones. *F* is *D* and *E* merged, where *yellow* shows areas of co-localization. *G* and *H* shows a section of a *z* series for *D*, *E*, and *F*, respectively; *arrowheads* in *H* show areas of co-localization. The results shown are representative of observations found for $n = 6$ independent transfection experiments.

served for HEK 293 cells expressing $\alpha1\beta2\gamma2$ $GABA_A$ receptors probed with the anti-$GABA_A$ receptor $\beta2/\beta3$ subunit monoclonal antibody, bd-17. Here, the immunoreactivity showed a punctate, plasma membrane localization in addition to some cytoplasmic staining (Fig. 6*C*). Fig. 6 (*D–F*) shows the distribution of GRIF-1a and $\beta2$ subunit immunoreactivity when GRIF-1$_{FLAG}$ was co-expressed with the $GABA_A$ receptor $\alpha1$, $\beta2$, and $\gamma2$ subunit clones. The $\beta2$ subunit is again localized predominantly to the plasma membrane, but some intracellular staining is evident. For GRIF-1a, immunoreactivity is still mostly distributed in the cell cytoplasm. Merging of the GRIF-1a and $\beta2$ subunit immunoreactivities revealed some areas of co-localization within the cell cytoplasm (Fig. 6*F*).

Co-immunoprecipitation Assays—To substantiate co-association of GRIF-1 and $GABA_A$ receptor $\beta2$ subunits, HEK 293 cells were co-transfected with pCMVTag4GRIF-1a$_{FLAG}$ and pCIS$\beta2$ and immunoprecipitation assays carried out. The results are shown in Fig. 7. In Fig. 7*A*, it can be seen that GRIF-1, $M_r \sim 115{,}000$, is present in the immune pellets following incubation with anti-FLAG M2-agarose only when cells were transfected with the GRIF-1 clone. This confirms the immunocytochemical studies, *i.e.* HEK 293 cells have no detectable endogenous GRIF-1. $GABA_A$ receptor $\beta2$ subunit immunoreactivity was also precipitated by anti-FLAG M2-agarose in the presence of GRIF-1 (Fig. 7*B*). Anti-$\beta2$ 381–395 antibodies recognized four molecular weight species with M_r in the range of 48–58 kDa in cells co-transfected with GRIF-1 and $GABA_A$ receptor $\beta2$ subunit clones and precipitated with anti-FLAG M2-agarose. An additional immunoreactive band with $M_r \sim$ 26,000 was detected by the anti-$\beta2$ antibodies; however, this

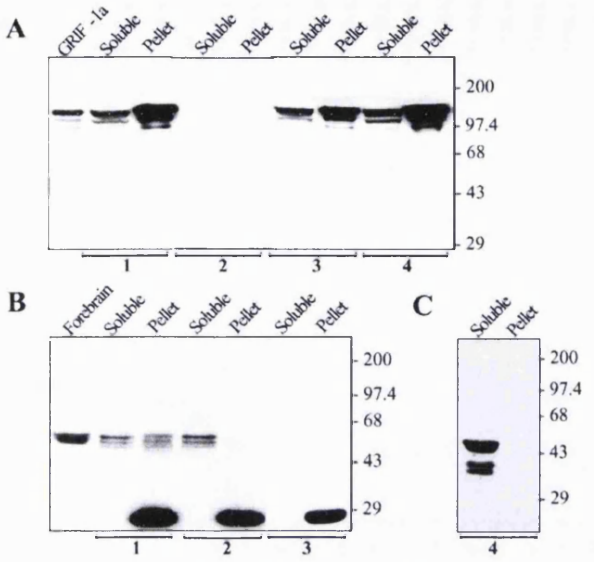

FIG. 7. **Co-association of GRIF-1 and GABA$_A$ receptor β2 subunits in HEK 293 cells transfected with GRIF-1a$_{FLAG}$ and GABA$_A$ receptor β2 subunits as shown by immunoprecipitation.** HEK 293 cells were co-transfected with the appropriate clones by the calcium phosphate method. Cells were harvested after 48 h, Triton X-100 detergent extracts prepared, immunoprecipitation carried out using anti-FLAG M2-agarose, and the resultant immune pellets analyzed by immunoblotting all as described under "Experimental Procedures." *A*, immunoblotting with affinity-purified anti-GRIF-1a-(8–633); *B*, with anti-β2 381–395; *C*, with anti-α1 1–15 antibodies. In *A–C*, *1* is co-transfection with pCMVTag4GRIF-1a$_{FLAG}$ + pCISβ2; *2*, co-transfection with pCISβ2 + pCIS; *3*, pCMVTag4GRIF-1a$_{FLAG}$ + pCIS; *4*, HEK 293 cells co-transfected with pCMVTag4GRIF-1a$_{FLAG}$ + pCDM8α1. The immunoblots are representative of $n = 3$ independent co-transfection experiments. The positions of molecular size standards are shown on the *right*.

was the result of the anti-FLAG monoclonal antibody because it was present in control experiments when immunoprecipitation was carried out from buffer solution (Fig. 7*B*). Further specificity controls showed that β2 subunit immunoreactivity was not precipitated in the absence of GRIF-1 (Fig. 7*B*). HEK 293 cells co-transfected with GRIF-1 and GABA$_A$ receptor α1 subunits did not result in the precipitation of α1 subunits by anti-FLAG-agarose (Fig. 7*C*). Anti-β2 subunit antibodies recognized only two bands with M_r 56,000 and 58,000 in forebrain but three to four bands in solubilized preparations of transfected HEK 293 cells. Deglycosylation of native GABA$_A$ receptor β2 subunits yielded two additional immunoreactive bands (39). Thus, because the β2 subunit is overexpressed in the HEK 293 cells, it is probable that the two additional bands are non-*N*-glycosylated forms of the β2 subunit. It is relevant to compare the intensities of the immunoreactive signals. The solubilized sample (Fig. 7*B*, *1*) is ~0.25% of the total β2 immunoreactivity applied for the resultant immune pellet (Fig. 7*B*), suggesting, in accord with the immunocytochemical observations, a weak or transient interaction between GRIF-1 and the GABA$_A$ receptor β2 subunit.

Determination of the GRIF-1 and GABA$_A$ Receptor β2-IL Interacting Domains—The GRIF-1/GABA$_A$ receptor β2-IL interacting domains were determined by the creation of a series of both GRIF-1-(8–633) and GABA$_A$ receptor β2-IL truncation mutants followed by the analysis of protein:protein association using the yeast two-hybrid assay. These studies were all carried out with the GRIF-1 constructs subcloned into the GAL4 AD fish vectors because several N-terminal fragments from aa 1 to 543 of GRIF-1 fused to the GAL4 BD all yielded strong auto-activation of reporter genes without requirement for the GAL4 BD (data not shown). The results are summarized in Figs. 8 and 9. For the β2-IL truncation mutants, it can be deduced that the binding site for GRIF-1 is located between amino acids 324 and 394 (Fig. 8). Quantitative analysis showed that the relative strength of the interaction between β2-IL-(324–394) and GRIF-1 was 1.4 ± 0.1% ($n = 3$) of wild-type Gal4p in the yeast strain AH109. This value is similar to that found for the complete β2-IL (Table I). For the GRIF-1 truncation mutants, GRIF-1-(124–283) was the smallest fragment that still resulted in reporter gene activity following co-expression with the GABA$_A$ receptor β2-IL-Gal4 BD fusion protein. This 124–283 region largely coincides with the first coil of the predicted coiled-coil region (Fig. 2). Interestingly, the Lupas algorithm predicts three coil regions within the β2 subunit intracellular loop. One of these, β2 348–361, is completely contained within the region of the β2 subunit intracellular loop that retains an interaction with GRIF-1; a second, β2 316–339, is partially within the β2 324–394 interacting domain (Fig. 8).

DISCUSSION

In this paper, we have characterized a novel 913-amino acid protein, GRIF-1, which was identified by virtue of its specific interaction with the GABA$_A$ receptor β2-IL in the yeast two-hybrid assay system. GRIF-1 mRNA has a wide distribution with major transcripts of 6.2 kb being detected in all tissues analyzed except testis, where a major 2.9-kb transcript was found. GRIF-1 protein, however, is expressed only in excitable tissues, where it was detected in soluble, nuclear, and P2 membrane subcellular fractions of brain, heart, and skeletal muscle by immunoblotting. Overexpression of GRIF-1 or GRIF-1$_{FLAG}$ in mammalian cells yielded an intracellular localization. Some intracellular co-localization of GRIF-1 and GABA$_A$ receptor β2 subunits was evident following co-expression of GRIF-1 and α1β2γ2 receptors in mammalian cells. GRIF-1 affinity purification showed *in vitro* association with β2 subunit-containing GABA$_A$ receptors in detergent extracts of rat brain. Further, GRIF-1 co-immunoprecipitated GABA$_A$ receptor β2 subunits, albeit at low efficiency, following co-expression in HEK 293 cells.

Functional Motifs Yielding Insights into the Putative Function of GRIF-1—GRIF-1 and the human orthologue, ALS2CR3, are novel protein sequences. Neither GRIF-1 nor ALS2CR3 have distinguishing amino acid sequence motifs that may have helped to reveal insights into their respective functions. ALS2CR3 was cloned by virtue of its being located in the critical region for juvenile amyotrophic lateral sclerosis on chromosome 2q33-q34. However, no evidence was found to suggest that ALS2CR3 was a causative gene for this form of amyotrophic lateral sclerosis (37). Secondary structure analyses for both GRIF-1 and the full-length KIAA0549, *i.e.* ALS2CR3, does predict the presence of two coiled regions within their respective N-terminal regions. These could form a coiled-coil domain that is recognized as being implicated in protein-protein interactions and oligomerization of proteins (reviewed in Ref. 40). Interestingly, one of the coil regions was found to coincide with a region of GRIF-1 that was homologous to HAP-1A and -1B (Fig. 2). HAP-1A and -1B are neuronal cytoplasmic proteins that bind to the protein huntingtin and to microtubules. Their subcellular localization is consistent with a role in intracellular transport (36, 41). Indeed more recently, HAP-1 proteins were found to bind to dynactin p150^{Glued} (P150), an accessory protein for cytoplasmic dynein that participates in microtubule-dependent retrograde transport of membranous organelles (42). HAP-1A was also found to associate in a yeast two-hybrid screen with GRIP, a PDZ domain-containing protein that is thought to be involved in the target-

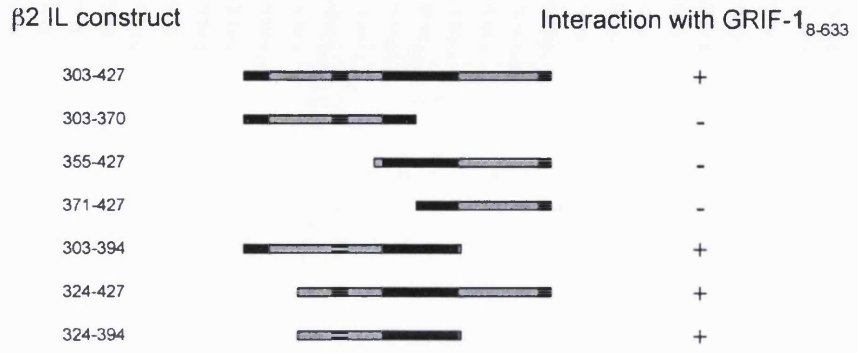

FIG. 8. **Schematic diagram showing the interaction between GRIF-1-(8–633) with truncated GABA$_A$ receptor β2-IL constructs as determined using the yeast two-hybrid assay.** GRIF-1-(8–633) and the depicted truncated GABA$_A$ receptor β2-IL constructs were co-expressed in the yeast strain AH109 as fusions to the GAL4 AD and BD, respectively. Protein-protein interactions were determined by nutritional selection and reporter gene activities as under "Experimental Procedures." −, no detectable interaction; +, detectable interaction. The *hatched areas* show the positions of coiled-coil domains predicted by the Lupas algorithm.

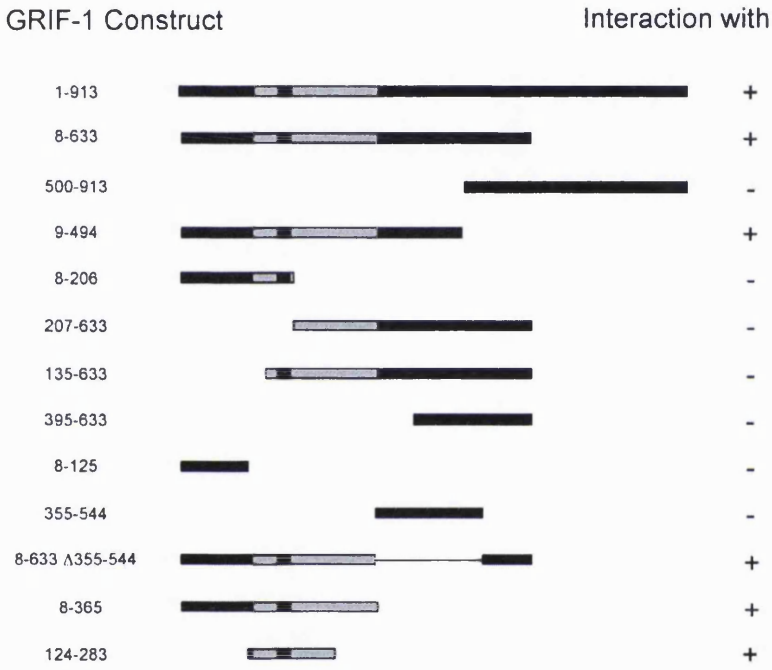

FIG. 9. **Schematic diagram showing the interaction of the GABA$_A$ receptor β2-IL with truncated GRIF-1 constructs as determined using the yeast two-hybrid assay.** The GABA$_A$ receptor β2-IL and the depicted truncated GRIF-1 constructs were co-expressed in the yeast strain AH109 as fusions to the GAL4 BD and AD, respectively. Protein-protein interactions were determined by nutritional selection and reporter gene activities as under "Experimental Procedures." −, no detectable interaction; +, detectable interaction. The *hatched* areas show the positions of coiled-coil domains predicted by the Lupas algorithm.

ing of AMPA glutamate receptors (43). The alignment of all the GRIF-1-related protein sequences revealed the presence of two highly conserved motifs; however, the functional significance of these remains unknown.

Tissue Distribution of GRIF-1—GRIF-1 mRNA, like other GABA$_A$ receptor-associated proteins such as gephyrin and GABARAP, has a wide tissue distribution. GRIF-1 protein, however, was expressed only in excitable tissues. This mismatch between mRNA and protein distribution may be a result of the long cDNA probe used for the Northern blot. It is possible that the GRIF-1-(8–633) cDNA probe also hybridized to mRNA transcripts of the rat homologue of KIAA1042. In brain, heart, and skeletal muscle, GRIF-1 immunoreactivity was found in all subcellular fractions. Overexpression of GRIF-1a in HEK 293 cells yielded an intracellular, non-nuclear distribution. The method used for the subcellular fractionation studies does not generate pure organelles; thus, the ubiquitous presence of GRIF-1 is probably a result of the fact that it is a soluble protein. Interestingly, an M_r 88,000 immunoreactive band was found in the nuclear fraction of both smooth and skeletal muscle. This molecular size corresponds to that predicted for the C-terminal truncated variant, GRIF-1b. GRIF-1 does contain a weak leucine zipper motif.

Heterogeneity of GRIF-1—Two alternative splice forms of GRIF-1 were discovered, GRIF-1a and GRIF-1b. The short variant, GRIF-1b, was found to have a deletion that corresponded to exon 15 of the ALS2CR3 gene (37). There is only a weak splice acceptor site at the intron/exon boundary for exon 15; thus, it may be readily skipped to yield GRIF-1b. GRIF-1b has 672 amino acids and thus a predicted molecular mass of ~70–80 kDa. As described above, a 88-kDa species was recognized by anti-GRIF-1-(8–633) antibodies in P1 from muscle. In some immunoblots of adult brain, this 88-kDa species was sometimes detected but it was always less abundant than the 115- and 106-kDa species; thus, GRIF-1a is the most prevalent of the expressed splice variants in brain. Heterogeneity of GRIF-1 mRNA because of possible alternative polyadenylation sites in the 3′-untranslated region was also apparent in the Northern blot and RACE experiments. Again, analysis of the human KIAA0549/ALS2CR3 gene revealed several strong polyadenylation sites within exon 16 that could give rise to transcripts differing by ~2 kb in size. In the Northern blot, the smaller less abundant 4.4-kb transcript is clearly visible, but, because GRIF-1 mRNA has qualitatively the highest expression level in spleen, this may just be a reflection of the overall abundance of GRIF-1 expression.

Specificity of Interaction between GRIF-1 and the GABA$_A$ Receptor β2-IL—The interaction of GRIF-1-(8–633), the origi-

nal isolated interacting clone, was specific to the β2-IL of the $GABA_A$ receptor subunits tested (Table I). The GRIF-1-(8–633) binding domain was localized to a region of 70 amino acids toward the N-terminal end of the bait, *i.e.* the intracellular loop of the β2 subunit (Fig. 8). It is notable that, when the TM3 and TM4 regions or the TM4 domain alone were included as part of the β2-IL bait, no reporter gene activity was detected (Table I). This suggests, not surprisingly, that the presence of the hydrophobic transmembrane domains affects the conformation of the fusion protein and thus its association with putative interacting partners. GRIF-1-(124–283), which coincides with the first predicted coil domain of GRIF-1, was the smallest fragment that still interacted with the β2-IL-GAL4 BD fusion protein. Full-length GRIF-1 and the N-terminal domain of the human orthologue, KIAA0549, which includes the 124–283 β2-IL binding site, both associated with the β2-IL (Table I). Quantification of the strength of GRIF-1/β2-IL binding showed that the interaction was weak, being ~1–2% of positive control samples. This may reflect either a low affinity of association or a transient interaction. Alternatively, we have recently shown that, in the yeast two-hybrid screen, GRIF-1-(8–633) associates with high affinity with itself.[2] Thus, within the co-transformed yeast, there may be competitive interaction between GRIF-1-(8–633)/GRIF-1-(8–633) and GRIF-1-(8–633)/β2-IL.

Association of GRIF-1 with $GABA_A$ Receptors —The association between $GABA_A$ receptor β2 subunits and GRIF-1 was demonstrated by two different experimental paradigms. *In vitro* protein interaction assays demonstrated that GRIF-1-(8–633) specifically associated with β2 and α1 $GABA_A$ receptor subunits in detergent extracts of rat brain, implying that GRIF-1 can associate with assembled $GABA_A$ receptors. Co-immunoprecipitation of GRIF-1 and $GABA_A$ receptor β2 subunits from HEK 293 cells transfected with the respective clones showed that the two proteins do indeed co-associate. For the *in vitro* protein interaction assays, interestingly, the percentage of β2 subunit immunoreactivity specifically precipitated by poly(His)-GRIF-1-(8–633)-Ni^{2+}-agarose was always higher than that found for the α1 subunit. This may be explained by the co-association of β2 with other α subunits in the brain detergent extracts. Alternatively, Tehrani *et al.* (44) reported that, in clathrin-coated vesicles, $GABA_A$ receptors appear to be uncoupled with respect to the GABA modulation of [^{3}H]flunitrazepam binding activity. This is accompanied by a reduction of the α1/β2 subunit ratio in clathrin-coated vesicles compared with synaptic membranes. It was suggested that a selective decline of the α1 subunits could account for the uncoupling (44). The higher percentage of β2 compared with α1 subunits precipitated by poly(His)-GRIF-1-(8–633)-Ni^{2+}-agarose may be explained by an association with unassembled β2 subunits as found in clathrin-coated vesicles; thus, GRIF-1 may play a role in the intracellular trafficking or sequestration of β2 subunits.

Although GRIF-1 and β2 subunits were co-immunoprecipitated from transfected cells, it is important to note that the association between the two proteins was not stoichiometric. This again suggests a low affinity or a transient association in agreement with the quantitative yeast two-hybrid assays, the *in vitro* protein interaction studies, and the HEK 293 co-localization studies.

Co-immunoprecipitations have also been attempted using native tissue as the source of GRIF-1 and $GABA_A$ receptor β2 subunits. These experiments have been unsuccessful so far, a major technical difficulty being the presence of the IgG heavy chain in immunoprecipitates. IgG heavy chains have a similar molecular weight to the β2 subunit; thus, detection of the latter is masked.

[2] M. Beck and F. A. Stephenson, unpublished observations.

Conclusions—Neurotransmitter receptors are targeted predominantly to the post-synaptic membrane. Although it is recognized that the transport of these proteins to these sites is mediated via molecular motors, it is not yet known how this sorting process occurs. Recently, Setou *et al.* (45) reported that the neuron-specific microtubule-associated protein, KIF17, forms a complex with mLin-10 to transport vesicles containing the NR2B-containing NMDA receptors to excitatory post-synaptic membranes. It is thus speculated from the homology found to known proteins that the neuronal protein, GRIF-1, which may fulfill a similar function in the transport of β2 subunit-containing $GABA_A$ receptors to inhibitory post-synaptic membranes, may be a novel $GABA_A$ receptor trafficking factor.

Acknowledgments—We thank Jurgen Groet from the laboratory of Dr. Dean Nizetic (School of Pharmacy, University of London) for nucleotide sequencing, Professor T. Nagase (Kazusa Research Institute, Chiba, Japan) for the gift of the partial KIAA0549 cDNA, and Drs. L. M. Hawkins and A. F. Wilderspin (School of Pharmacy, University of London) for insightful discussions.

REFERENCES

1. Stephenson, F. A. (1998) in *Amino Acid Neurotransmission* (Stephenson, F. A., and Turner, A. J., eds) pp. 65–92, Portland Press, London
2. Nusser, Z., Sieghart, W., and Somogyi, P. (1998) *J. Neurosci.* **18,** 1693–1703
3. Nusser, Z., Sieghart, W., Benke, D., Fritschy, J.-M., and Somogyi, P. (1996) *Proc. Natl. Acad. Sci. U. S. A.* **93,** 11939–11944
4. Kannenberg, K., Baur, R., and Sigel, E. (1997) *J. Neurochem.* **68,** 1352–1360
5. Kannenberg, K., Schaerer, M. T., Fuchs, K., Sieghart, W., and Sigel, E. (1999) *J. Biol. Chem.* **274,** 21257–21264
6. Schaerer, M. T., Kannenberg, K., Hunziker, P., Baumann, S., and Sigel, E. (2001) *J. Biol. Chem.* **276,** 26597–266604
7. Betz, H. (1998) *Nat. Neurosci.* **1,** 541–543
8. Sassoe-Pognetto, M., and Fristchy, J.-M. (2000) *Eur. J. Neurosci.* **12,** 2205–2210
9. Essrich, C., Lorez, M., Benson, J. A., Fritschy, J.-M., and Luscher, B. (1998) *Nat. Neurosci.* **1,** 563–571
10. Hanley, J. G., Koulen, P., Bedford, F., Gordon-Weeks, P. R., and Moss, S. J. (1999) *Nature* **397,** 66–69
11. Wang, H., Bedford, F. K., Brandon, N. J., Moss, S. J., and Olsen, R. W. (1999) *Nature* **397,** 69–72
12. Chen, L., Wang, H., Vicini, S., and Olsen, R. W. (2000) *Proc. Natl. Acad. Sci. U. S. A.* **97,** 11557–11562
13. Kittler, J. T., Rostaing, P., Schiavo, G., Fritschy, J.-M., Olsen, R. W., Triller, A., and Moss, S. J. (2001) *Mol. Cell. Neurosci.* **18,** 13–25
14. Bedford, F. K., Kittler, J. T., Uren, J. M., Thomas, P., Smart, T. G., and Moss, S. J. (2000) *Eur. J. Neurosci. Suppl.* **12,** 016.14
15. Bedford, F. K., Kittler, J. T., Muller, E., Thomas, P., Uren, J. M., Merlo, D., Wisden, W., Triller, A., Smart, T. G., and Moss, S. J. (2001) *Nat. Neurosci.* **4,** 908–916
16. Ymer, S., Schofield, P. R., Draguhn, A., Werner, P., Kohler, M., and Seeburg, P. H. (1989) *EMBO J.* **9,** 1665–1670
17. Geitz, R. D., Schiestl, R. H., Willems, A. R., and Woods, R. A. (1995) *Yeast* **11,** 355–360
18. Bartel, P. L., and Fields, S. (1997) *The Yeast Two-hybrid System*, Oxford University Press, Oxford
19. Sambrook, J., and Russell, D. W. (2001) *Molecular Cloning: A Laboratory Manual*, Cold Spring Harbor Laboratory Press, Cold Spring Harbor, NY
20. Gelfand, M. S., Mironov, A. A., and Pevzner, P. A. (1996) *Proc. Natl. Acad. Sci. U. S. A.* **93,** 9061–9066
21. Nakai, K., and Horton, P. (1999) *Trends Biochem. Sci.* **24,** 34–35
22. Schultz, J., Copley, R. R., Doerks, T., Ponting, C. P., and Bork, P. (2000) *Nucleic Acids Res.* **28,** 231–234
23. Harlow, E., and Lane, D. (1999) *Using Antibodies: A Laboratory Manual*, Cold Spring Harbor Laboratory Press, Cold Spring Harbor, NY
24. Pollard, S., Thompson, C. L., and Stephenson, F. A. (1995) *J. Biol. Chem.* **270,** 21285–21290
25. Pollard, S., and Stephenson, F. A. (1997) *Biochem. Soc. Trans.* **25,** 547S
26. Hawkins, L. M., Chazot, P. L., and Stephenson, F. A. (1999) *J. Biol. Chem.* **274,** 27211–27218
27. Duggan, M. J., and Stephenson, F. A. (1989) *J. Neurochem.* **53,** 132–139
28. Connolly, C. N., Wooltorton, J. R. A., Smart, T. G., and Moss, S. J. (1996) *Proc. Natl. Acad. Sci. U. S. A.* **93,** 9899–9904
29. Li, M., and De Blas, A. L. (1997) *J. Biol. Chem.* **272,** 16564–16569
30. Sur, C., Wafford, K. A., Reynolds, D. S., Hadingham, K. L., Bromidge, F., Macaulay, A., Collinson, N., O'Meara, G., Howell, O., Newman, R., Myers, J., Atack, J. R., Dawson, G. R., McKernan, R. M., Whiting, P. J., and Rosahl, T. W. (2001) *J. Neurosci.* **21,** 3409–3418
31. Chou, P. Y., and Fasman, G. D. (1978) *Adv. Enzymol. Relat. Areas Mol. Biol.* **47,** 45–148
32. Lupas, A., Van Dyke, M., and Stock, J. (1991) *Science* **252,** 1162–1164
33. Berger, B., Wilson, D. B., Wolf, E., Tonchev, T., Milla, M., and Kim, P. S. (1995) *Proc. Natl. Acad. Sci. U. S. A.* **92,** 8259–8263
34. Nagase, T., Ishikawa, K., Miyajima, N., Tanaka, A., Kotani, H., Nomura, N., and Ohara, O. (1998) *DNA Res.* **5,** 31–39

35. Kikuno, R., Nagase, T., Ishikawa, K., Hirosawa, M., Miyajima, N., Tanaka, A., Kotani, H., Nomura, N., and Ohara, O. (1999) *DNA Res.* **6,** 197–205
36. Li, X., Li, S., Sharp, A. H., Nuclfora, F. C., Schilling, G., Lanahan, A., Worley, P., Snyder, S. H., and Ross, C. A. (1995) *Nature* **378,** 398–402
37. Hadano, S., Yoshiko, Y., Skaug, J., Fichter, K., Nasir, J., Martindale, D., Koop, B. F., Scherer, S. W., Nicholson, D. W., Rouleau, G. A., Ikeda, J.-E., and Hayden, M. R. (2001) *Genomics* **71,** 200–213
38. Bailey, T. L., and Elkan, C. (1994) *Proc. Intl. Conf. Intelligent Systems Mol. Biol.* **2,** 28–36
39. Mamalaki, C., Stephenson, F. A., and Barnard, E. A. (1987) *EMBO J.* **6,** 561–565
40. Beck, K., and Brodsky, B. (1998) *J. Struct. Biol.* **122,** 17–29
41. Gutekunst, C.-A., Li, S.-H., Yi, H., Ferrante, R. J., Li, X.-J., and Hersch, S. M. (1998) *J. Neurosci.* **18,** 7674–7678
42. Li, S.-H., Gutenkunst, C.-A., Hersch, S. M., and Li, X.-J. (1998) *J. Neurosci.* **18,** 1261–1269
43. Ye, B., Liao, D., Zhang, X., Zhang, P., Dong, H., and Huganir, R. L. (2000) *Neuron* **26,** 603–617
44. Tehrani, M. H. J., Baumgartner, B. J., and Barnes, E. M. (1997) *Brain Res.* **776,** 195–203
45. Setou, M., Nakagawa, T., Seog, D.-H., and Hirokawa, N. (2000) *Science* **288,** 1796–1802